Mechanisms and Substituent Effects of Metal-free Bioorthogonal Reactions

Titas Deb,† Julian Tu,† Raphael M. Franzini

Department of Medicinal Chemistry, University of Utah, 30 S 2000 E, Salt Lake City, Utah 84112, United States

KEYWORDS: Bioorthogonal reactions, pericyclic reactions, mechanistic analysis, click chemistry

ABSTRACT: Reactions that occur under physiological conditions find diverse uses in the chemical and biological sciences. However, the limitations that biological systems place on chemical reactions restrict the number of such bioorthogonal reactions. A profound understanding of the mechanistic principles and structure-reactivity trends of these transformations is therefore critical to access new and improved versions of bioorthogonal chemistry. The present article reviews the mechanisms and substituent effects of some of the principal metal-free bioorthogonal reactions based on inverse-electron demand Diels-Alder reactions, 1,3-dipolar cycloadditions, and the Staudinger reaction. Mechanisms of modified versions that link these reactions to a dissociative step are further discussed. The presented summary is anticipated to aid the advancement of bioorthogonal chemistry.

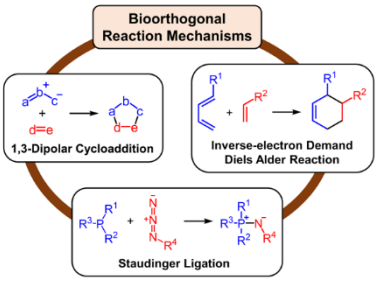

Contents

1. INTRODUCTION

The aspiration to study life processes on the molecular level has led to a convergence of biology and chemistry. As a result, the need to manipulate molecules of biological importance has emerged in the form of labeling specific biomolecules for imaging, generating bioconjugates, and site-specifically releasing bioactive agents. However, the required chemical capabilities have been developed only over the last two decades, and this chemistry has opened new

opportunities for elucidating fundamental biological questions. Considerable efforts have led to chemical reactions that work in the presence of biomolecules, in cells, and ultimately in higher organisms.[1, 2] Such chemical reactions are often referred to as "bioorthogonal". To qualify as bioorthogonal, two molecules need to readily react with each other without interfering with normal biological processes and at the same time must be inert to the functional groups present in living systems. In other words, a bioorthogonal reaction is highly chemoselective against the molecules that are typically encountered in a cell. Diverse and elaborate chemistry has been developed to access bioorthogonal reactions, and such transformations are having a lasting impact on biological, chemical, materials, and pharmaceutical sciences.[1-4]

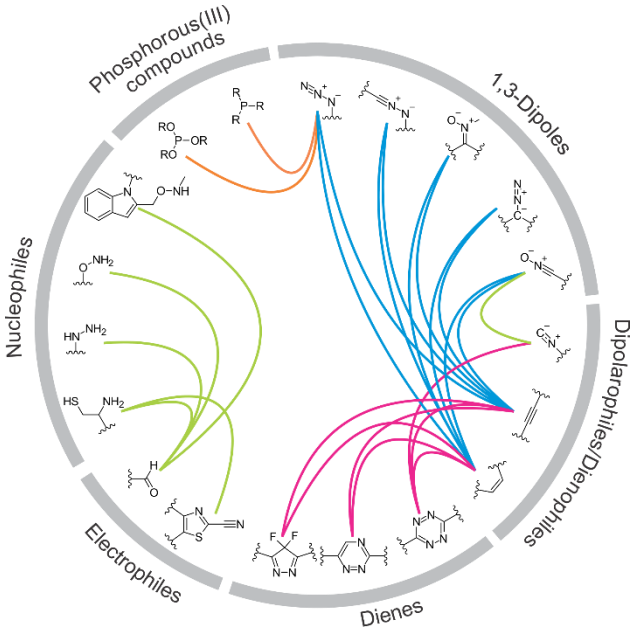

Figure 1. Overview of important bioorthogonal reactions. Lines correspond to a reaction between two bioorthogonal reactive groups. Colors indicate the type of reaction (magenta: inverse-electron demand cycloadditions; blue: 1,3-dipolar cycloaddition; orange: Staudinger reactions; green: polar reactions [not discussed in this review]). Reactions involving metals or photo-chemistry are not included.

Despite the many success stories, developing bioorthogonal chemistry remains challenging. Only a minute fraction of chemical reactions can be performed in the presence of biomolecules.[1] Whereas a synthetic chemist can increase reaction yields and rates by adjusting temperature, solvents, and acidity/b24asicity, the reaction conditions for bioorthogonal chemistry are set by what is physiologically relevant. Bioorthogonal reactions must be water-compatible, occur at ambient temperature, and at near-neutral pH. Organic chemists further have a plethora of catalysts at their disposition to promote reactions. While metal-catalyzed bioorthogonal reactions have been described,[5-7] it is typically preferable to have two reagents that react directly with each other.[8-11] To be useful for biological studies, reactions further need to go to completion in a defined time window at the low concentrations tolerated by living systems, and therefore need to occur at a practical rate.[11, 12]

These prerequisites critically restrict the scope of chemical reactions that can be performed in a biological context. The number of functional groups that at the same time are intrinsically reactive to xenobiotic molecules and inert to biomolecules is limited (**Fig. 1**). Accordingly, there are only a few types of reactions that occur chemoselectively under such circumstances. Nevertheless, a growing set of biocompatible reactions has been identified that provides scientists with a toolbox to work with, and chemists have found ingenious ways of combining these functional groups in different combinations (**Fig. 1**).[1, 2] Prominent examples of bioorthogonal groups are alkenes and alkynes.[13] Although the functional groups themselves are only modestly reactive, ring strain is highly effective in boosting the reactivity while maintaining the reagents' stability (see section 2.3).[13, 14] One type of molecules that react with alkenes/alkynes are 1,2,4,5-tetrazines and related dienes.[10, 15] These heterocycles undergo inverse electron-demand cycloaddition reactions with various dienophiles[10, 15, 16] that depending on the reagents can be very fast while the molecules are stable in cells.[10] Unsaturated C-C bonds can further react in cycloadditions with various 1,3-dipoles.[8] The most prominent example of an 1,3-dipole is the azide group. Azides are xenobiotic, highly stable in biological settings, and offer unique reactivity patterns.[17] In addition to participating in 1,3-dipolar cycloadditions,[8] azides also react with phosphines in the Staudinger reaction generating iminophosphoranes that depending on the reagents' structures and reaction conditions, can either be stable, hydrolyze to the amine, or act as nucleophiles.[18-20] In addition to the bioorthogonal functional groups and reactions mentioned here, there are numerous chemical transformations that have been proposed for use in biology. For example, polar reactions between nucleophiles and electrophiles are frequently used together with biomolecules and interested readers are directed to dedicated reviews.[21, 22]

In light of the limited number of bioorthogonal functional groups, an in-depth understanding of mechanisms and structural effects is essential for accessing new chemical capabilities.[23] The development of bioorthogonal chemistry typically starts from identifying reactions in the literature that have a high likelihood of functioning in biological settings followed by mechanistic rationalization on how to achieve tailor-made reactions for chemical biology. In this article, we review the current knowledge of the mechanisms of some of the most widely used bioorthogonal reactions. Given the extensive progress in this area, it is beyond the scope of this review to cover all bioorthogonal reactions. Instead, the review focuses on three classes of bioorthogonal reactions: inverse electron-demand Diels-Alder (IEDDA) cycloadditions (section 3),[9] 1,3-dipolar cycloadditions (section 4),[24] and the Staudinger reaction (section 5).[19, 20, 25] These three transformations are the foundation of bioorthogonal chemistry and have been studied in great detail. Other examples of bioorthogonal reactions include hydrazone/oxime formation,[21] Pictet-Spengler reaction,[26] reactions of aminothiols with electron-deficient nitriles,[27] and

many more. Readers interested in a comprehensive overview of the different types of bioorthogonal reactions are advised to consult the many excellent reviews on this topic.[1-4] Furthermore, the review is restricted to the mechanisms of metal-free reactions. Metal catalysis provides another dimension to bioorthogonal and click chemistry, and important breakthroughs have been achieved with the use of metal catalysis.[5-7] Foremost, Cu(I)-catalyzed azide-alkyne cycloadditions are ubiquitous in bioorganic chemistry and chemical biology. This reaction has been discussed in detail in dedicated reviews[28-30] and is outside the scope of the present article.

In recent years, there have been increasing efforts to develop "smart" bioorthogonal chemistry.[31] Such chemistry relates to reactions that link a bioorthogonal transformation to a conditional step or a downstream effect. For example, light-activated bioorthogonal reactions[32] and dissociative bioorthogonal reactions[12, 33, 34] are examples of such "smart" reactions. Important mechanistic considerations for these transformations are outlined here. By summarizing these mechanistic processes, we hope to contribute to the efforts of the scientific community to develop the next generation of bioorthogonal chemistry.

2. PHYSICAL ORGANIC CHEMISTRY CONCEPTS UNDERLYING BIOORTHOGONAL REACTIONS

In this section, we introduce selected physical organic chemistry principles that form the theoretical framework for the mechanistic understanding of bioorthogonal reactions. The section is intended to aid readers that are unfamiliar with these concepts in understanding the content of this review. A rigorous and critical discussion of these topics is beyond the scope of this article and can be found in the cited reviews and in standard physical organic chemistry textbooks.

2.1 Linear Free Energy Relationships

Substituents on the reactive groups often increase or decrease the rate of bioorthogonal reactions by several orders of magnitude. Understanding these effects is critical in designing new bioorthogonal chemistry and constitutes a central part of this review article. Organic chemists use electronic and steric properties to rationalize substituent effects on reactions, and it is possible to express these characteristics in linear free energy relationships.

The most widely adopted approach in analyzing electronic effects is the Hammett equation (1):

$$log\frac{k}{k_0} = \sigma \times \rho \quad (1)$$

The Hammett equation asserts that equilibrium constants and reaction rates depend linearly on the electronic properties of substituents that are reflected by the substituent constant σ. The slope of the correlation is determined by the reaction parameter ρ. The Hammett equation is mostly used with phenyl-derived substrates, and the electronic properties are a combination of inductive and mesomeric effects. As these parameters vary depending on the position, different σ constants have been compiled for the para and the meta position (σ_p and σ_m). Substituent coefficients vary from σ_p = 0.82 for the electron-withdrawing trimethylammonium group to σ_p = -0.77 for the electron-donating triphenylphosphane imine group, which assuming ρ = 1 corresponds to a 39-fold difference in reaction rates. Substituent coefficients have been compiled and a comprehensive table with such constants can be found in Ref. 391.

The reaction constant ρ is an inherent property of the implicated chemical transformation and provides valuable insight into its mechanism. A reaction with ρ > 0 is accelerated by electron-withdrawing groups, which indicates a buildup of negative charge (or decrease of positive charge) in the transition state. Conversely, a ρ < 0 indicates an increased positive charge (or decreased negative charge) in the transition state and a rate-accelerating effect by electron-donating substituents. The charge of the transition state remains constant relative to reactants in reactions with ρ = 0. The reaction constant ρ therefore provides valuable information both to elucidate a reaction's mechanism and to predict what substituents can accelerate it.

Taft modified the Hammett equation to take into account steric effects.[35] The Taft's equation is given as (2):

$$log\frac{k}{k_0} = \sigma^* \times \rho^* + \delta \times E_S \quad (2)$$

As for the Hammett equation, the Taft's equation describes electronic effects as the product of the polar sensitivity factor ρ* and the polar substituent constant σ*. The sensitivity factor ρ* is an inherent characteristic of the reaction reflecting buildup of charge in the transition state, whereas σ* mirrors the electronic nature of the substituent. Steric effects are taken into account by the product of steric sensitivity factor δ and the steric substituent constant E_s. As for the electronic effects, the sensitivity factor δ provides information on how sensitive the reaction is to steric bulk and the E_s constant is a descriptor of the size of a substituent.[35]

2.2 Orbital Symmetry and FMO Theory

Cycloaddition reactions are prominently employed in bioorthogonal chemistry. Concerted pericyclic reactions are controlled by conservation of orbital symmetry and frontier molecular orbital (FMO) theory has been used to accurately describe cycloadditions. We here provide a brief

introduction to concepts involving molecular orbitals (MOs) as the theoretical foundation for the discussion of IEDDA and 1,3-dipolar cycloaddition reactions. For interested readers, references that provide a more in-depth review of FMO theory are cited.[36-40]

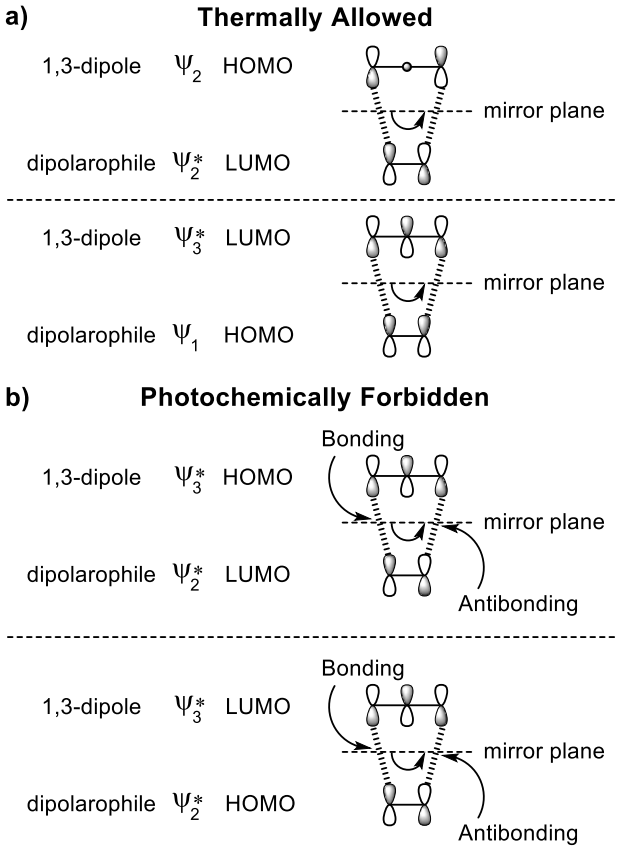

Figure 2. Interactions between the frontier orbitals. a) the reaction is thermally allowed as the interactions between the frontier orbitals are in a bonding orientation; b) the reaction is photochemically forbidden as not all the interactions between orbitals are symmetrical, leading to antibonding interactions

Woodward and Hoffmann developed the principles of orbital symmetry conservation,[38-40] which provide a theoretical basis for both the IEDDA and 1,3-dipolar cycloaddition reactions widely used in bioorthogonal chemistry. These principles, known as the Woodward-Hoffmann rules predict which concerted reactions are allowed and which ones are forbidden (**Fig. 2**). Allowed reactions maintain bonding along a concerted pathway (**Fig. 2a**) while forbidden reactions experience an antisymmetric overlap (**Fig. 2b**) of interacting orbitals along their reaction pathway. Both the Diels-Alder and 1,3-dipolar cycloaddition are symmetry allowed [$\pi^4s + \pi^2s$] reactions as described by their MO interactions. In principle, all MOs of one reactant will interact with the MOs of the other having the same symmetry. However, to simplify the understanding of these reactions, FMO theory considers only the interaction between the highest occupied molecular orbital (HOMO) and the lowest unoccupied molecular orbital (LUMO) of the reactants with the same symmetry, which are their frontier orbitals. In general, small HOMO-LUMO separations favor such reactions.

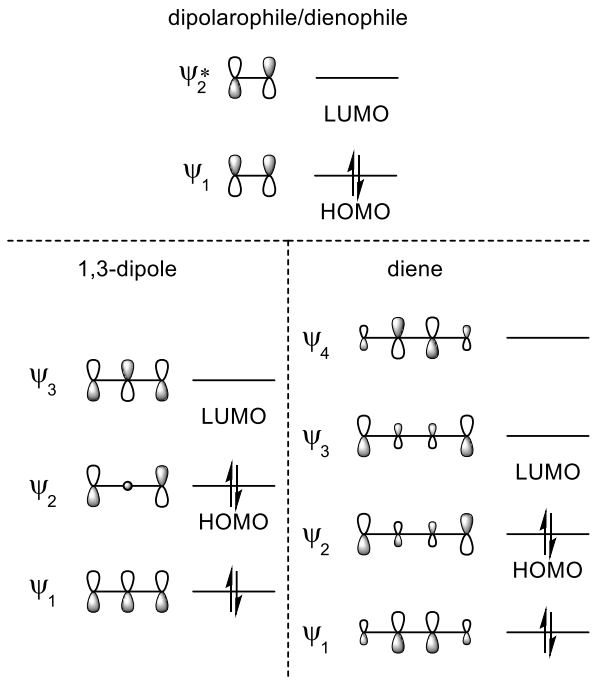

Figure 3. Molecular orbitals of an 1,3-dipole, diene, and dipolarophile/dienophile.

An example of how HOMO-LUMO interactions control pericyclic reactions is provided in **Fig. 2** considering the FMOs of a 1,3-dipole and a dipolarophile. The same type of analysis of orbital symmetry can be extended to describe the Diels-Alder reaction as the 1,3-dipole is a four π-electron component distributed over three atoms, representing a structural variant of the diene in a Diels-Alder with both having a two-fold axis symmetry (**Fig. 3**). Therefore, for both Diels-Alder and 1,3-dipolar cycloadditions, the $HOMO_{dipole}$ has the same symmetry as the $LUMO_{dipolarophile}$ of the reaction partner, both being antisymmetric with respect to mirror symmetry, resulting in symmetry-allowed maximum overlap of the orbitals (**Fig. 2a**). Likewise, when the $HOMO_{dipolarophile}$ interacts with the $LUMO_{dipole}$, they are symmetric with respect to the mirror plane or antisymmetric to their respective two-fold axis of symmetry, allowing again for maximum overlap (**Fig. 2a**). These reactions are thermally allowed according to the Woodward-Hoffmann rules. Importantly, Woodward-Hoffmann rules deem [$\pi^4s + \pi^2s$] photochemical reactions to be forbidden. To visualize such a forbidden reaction, the interaction between the HOMO in the excited state of one reactant and the LUMO in the ground state of the other is shown in **Fig. 2b**. In this case, antibonding orbital interactions occur, which disallows product formation.

Following the inception of FMO theory and orbital symmetry analysis in the context of cycloadditions, Sustmann classified both the Diels-Alder and the 1,3-dipolar cycloaddition reactions into three types based on the relative FMO energies between the dipole or diene and dipolarophile or dienophile (**Fig. 4**).[41-43] Type I reactions are dominated by

the interaction between the $HOMO_{dipole/diene}$ and the $LUMO_{dipolarophile/dienophile}$, which corresponds to normal electron-demand Diels-Alder reactions. Because of a similar FMO energy gap in both directions, type II reactions can proceed either dominated by the $HOMO_{dipole/diene}$—$LUMO_{dipolarophile/dienophile}$ interaction or the $HOMO_{dipolarophile/dienophile}$—$LUMO_{dipole/diene}$ interaction. Lastly, type III reactions are dominated by the interaction between the $LUMO_{dipole/diene}$ and the $HOMO_{dipolarophile/dienophile}$, which corresponds to an inverse electron-demand cycloaddition reaction. In the context of bioorthogonal chemistry, the 1,3-dipolar cycloaddition reactions generally fall under a type II classification and Diels-Alder reactions employed are of type III. We discuss factors that influence the rates of reaction for 1,3-dipolar cycloadditions and IEDDA reactions in their following respective sections and relate them back to how basic FMO theory explains such reactivities.

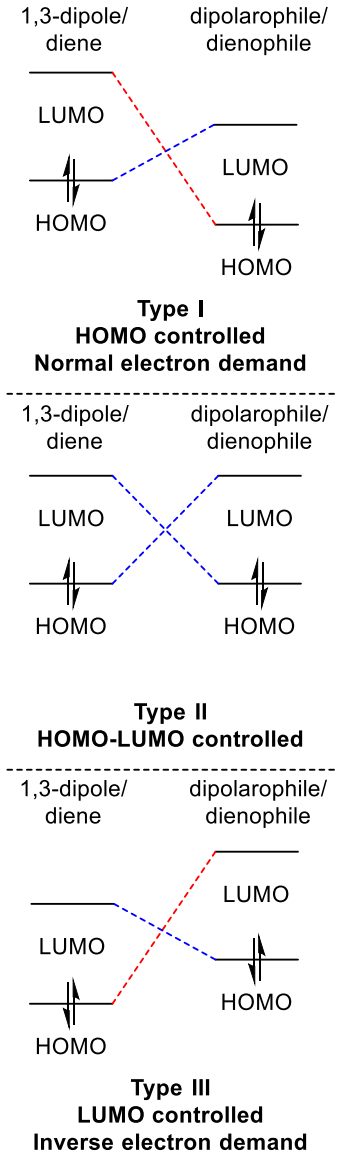

Figure 4. Classification of cycloaddition reactions based on the dominant interaction in the frontier molecule orbitals. The dashed blue line indicates the major interaction while the red dashed line shows a larger energy gap interaction.

2.3. Strain and Distortion in Pericyclic Reactions

The reactivity of pericyclic reactions depends largely on the HOMO/LUMO energy levels of the reactants. A higher ground state energy in either or both of the reactants corresponds to higher rate constants. Strain and distortion can play central roles in raising the internal energy of the reactants. Here we give a brief introduction to these concepts in the context of 1,3-dipolar cycloadditions and Diels-Alder reactions.

Strain refers to structural stress in a molecule that is absent in a relaxed reference compound, which results in an increase in its internal energy.[44, 45] In organic chemistry, strain is generally associated with a conformational distortion or nonoptimal bonding (bond angle or length) relative to a standard molecule. For instance, the chair conformation of cyclohexane, which is considered to have a strain energy of 0 kcal mol^{-1}, is often taken as the reference for other cycloalkanes. As a consequence of the increased energy, strained molecules are intrinsically more reactive than their relaxed counterparts. The energy difference linked to strain can be quantified from the heat of combustion or heat of atomization data.[46]

Strain can be classified into static strain, which is inherent in a molecule and is independent of molecular motion, and dynamic strain, which arises during conformational changes. In bioorthogonal chemistry, strain has a large impact over the reaction kinetics. A large fraction of the strain in ring systems arises from nonstandard bond angles, referred to as Baeyer strain (**Fig. 5**).[45] Baeyer strain can be further broken down into small-angle strain (bond angles smaller than the ideal values),[47] exemplified by 3- and 4-membered rings, and large-angle strain (bond angles larger than the ideal values),[48] which causes a substantial portion of the strain present in 8- to 12-membered rings. Such ring strain is sometimes partially relieved by the rehybridization effect. For example, in the case of cyclopropane, the orbitals involved in ring bonding have more *p* character than a typical sp^3 orbital. Therefore, they resemble *p* orbitals which have a preferred bond angle of 90° rather than 109.5° for sp^3 orbitals, and which relieves some of the small angle strain.[46, 49-51] Unsaturated bonds in a ring system typically increase ring strain and this effect can be quite significant (**Fig. 6**). Small angle strain is amplified in cyclic olefins since sp^2 carbons prefer larger angles than sp^3 carbons, resulting in larger angle compression.[44-46] In pericyclic reactions, the bond order of reactant decreases, which can be associated with a relaxation of ring strain. Therefore, ring-strain typically enhances the rate of such reactions.

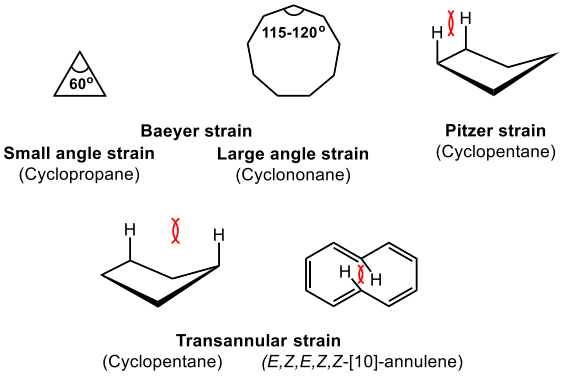

Figure 5. Types of strain in organic molecules.

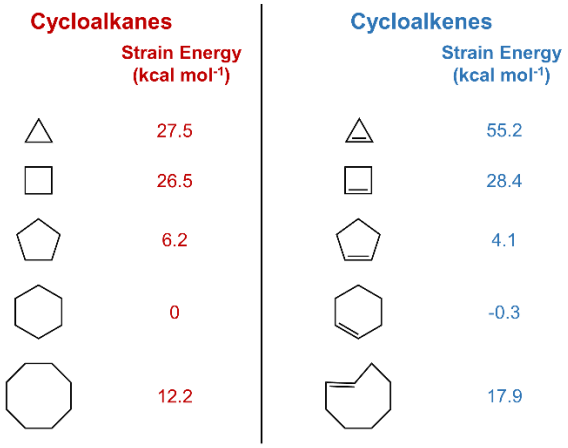

Figure 6. Strain energy of common cycloalkanes and cycloalkenes.

Smaller cycloalkenes always feature the double bond in a *cis* geometry.[46] The smallest ring system that forms a stable structure including a *trans* olefin is *trans*-cyclooctene (TCO).[45] The ring strain of TCO is approximately 17.9 kcal mol^{-1}, [52, 53] which is much higher than most cycloalkenes. Therefore, pericyclic reactions of TCO occur orders of magnitude faster than reactions with simple alkenes.[54, 55] The strain-enhancing effect of the endocyclic *trans*-olefin is widely utilized in bioorthogonal chemistry as the dienophile component in IEDDA reactions (see section 3).[12, 56, 57] Similarly, cyclooctyne is the smallest isolable carbocyclic alkyne and is considerably strained (19.9 kcal mol^{-1}).[45, 52, 53, 58] Cyclooctyne participates in both 1,3-dipolar cycloadditions and Diels-Alder reactions with rapid kinetics.[8, 9] Small angle strain is generally absent in rings with five or more atoms; however, transannular strain (Prelog strain),[59] which is caused by steric repulsions between atoms across the ring, and torsional strain (Pitzer strain), stemming from eclipsing interactions, can emerge (**Fig. 5**). Larger rings (>13 atoms) are almost strain-free due to a resemblance of the bond angles to open chains, although some transannular strain may exist.[60] For most cyclic structures, there exists at least one of the above types of strain. The relative contribution of each type to the total ring strain depends on the bonding and geometry of the molecule. For rings <5 atoms in size, small angle strain constitutes a major portion of the strain, which is replaced by Pitzer and transannular strains in 5-membered and 7-13-membered rings.[59, 61] For 9-10 membered rings, some of these two types of strain is relieved by large angle strain.[46]

Strain is a major factor in cycloaddition reactions, which are central to bioorthogonal chemistry. Rates of reaction of cycloalkenes with similar dipoles/dienes tend to increase with ring strain.[62] For instance, the high reactivity of 3- and 4-membered cycloalkenes in IEDDA reactions, and that of cyclooctyne in strain-promoted azide-alkyne cyclcoadditions (SPAAC), can be rationalized by the release of ring strain during these reactions as a result of a decrease in bond order. Similarly, the fast kinetics of the reaction between TCO and tetrazine is a direct consequence of the ring strain of the endocyclic *trans*-olefin.

While strain energy provides a simple explanation for overall reactivity trends of cyclic alkenes and alkynes, it fails to consistently correlate with rate constants.[53, 63] TCO reacts 2-3 orders of magnitude faster than cyclooctyne in a tetrazine cycloaddition, whereas strain release would predict an opposite trend. To rationalize these inconsistencies, the distortion/introduction model (also known as activation-strain model) was developed.[53, 63-67] This model proposes that the activation energy comprises of distortion energy ($\Delta E^{\ddagger}_{dist}$) and interaction energy ($\Delta E^{\ddagger}_{int}$) (**Fig. 7**). The distortion energy is the energy required to distort the reactants into their transition state geometries. In other words, the energy difference between the optimized ground state structures and the distorted transition-state structures is $\Delta E^{\ddagger}_{dist}$. An early transition state indicates that the transition state geometry is closer to that of the ground state, i.e. the ground state is pre-distorted towards the transition state, which results in a lower $\Delta E^{\ddagger}_{dist}$. There is noteworthy correlation between activation energy and distortion energy, which indicates that reactivity is mainly controlled by $\Delta E^{\ddagger}_{dist}$.[53, 63, 66, 67] When $\Delta E^{\ddagger}_{dist}$ is similar for a series of compounds, $\Delta E^{\ddagger}_{int}$ becomes the controlling factor.[66] This energy is the difference between the activation energy and the total distortion energy. Interaction energy is comprised of attractive electrostatic and charge-transfer stabilization interactions and repulsive closed shell (Pauli) interactions. A smaller HOMO-LUMO gap results in a stronger $\Delta E^{\ddagger}_{int}$.

Numerous studies using the distortion/interaction model have allowed describing cycloaddition reactions more accurately than analyses based solely on strain and FMO theory. For instance, the activation barriers of ethylene and acetylene are similar when reacting with a given 1,3-dipole, which is unexpected based on FMO interactions in light of the different FMO energies based on ionization potentials and electron affinity values.[66] The reaction exothermicities (ΔH_{rxn}) are also different for alkenes and alkynes. In contrast, the activation energies correlate remarkably well with distortion energies.[53, 66] The distortion/interaction model further takes into account the loss of aromaticity in the transition state of reactions that involve aromatic substrates. These interactions critically affect the rates of IEDDA reactions. The distortion/interaction model, therefore, provides a reliable method for explaining the reactivity trends in cycloaddition reactions.

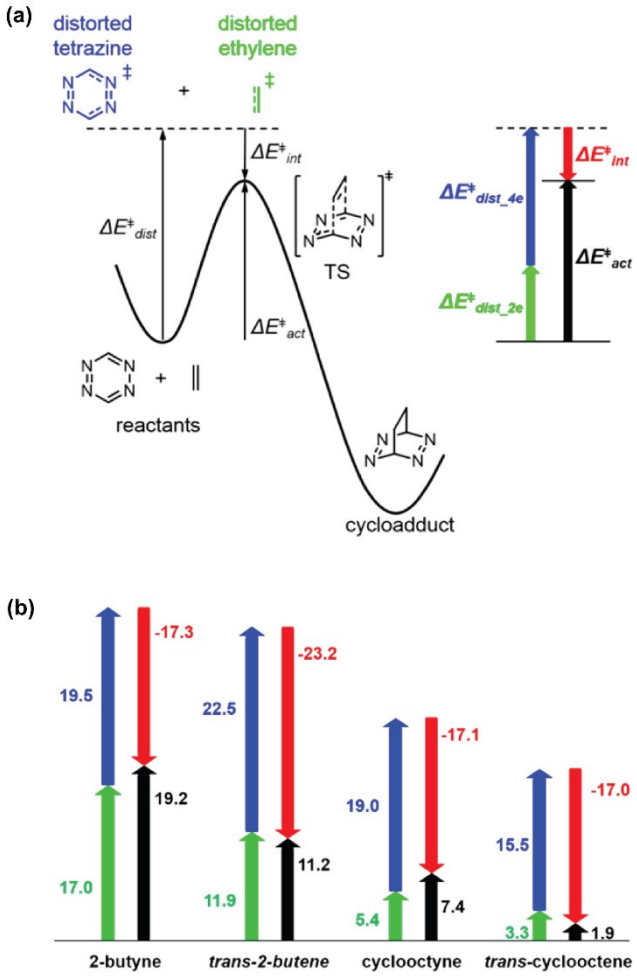

Figure 7. a) Schematic representation of the distortion/interaction model. b) Graph of distortion, interaction and activation energies for the transition states of reactions between 3,6-dimethyltetrazine and the dienophiles 2-butyne, *trans*-2-butene, cyclooctyne and TCO. (Adapted with permission from Ref. 53. Copyright 2014 American Chemical Society).

The discussion above highlights the importance of strain and distortion in cycloaddition reactivity. The following sections will go into more detail in the context of specific reactions and relate them to the general principles discussed here.

3. INVERSE-ELECTRON DEMAND DIELS-ALDER CYCLOADDITION REACTIONS

The Diels-Alder cycloaddition, the conjugate addition of a 1,3-diene to a 2π system, is one of the most widely used reactions in organic chemistry.[68, 69] The Diels-Alder reaction is a concerted [$\pi 4_s + \pi 2_s$] cycloaddition reaction with an orbital symmetry that makes it thermally permitted according to the Woodward-Hoffmann rules (see 2.2).[70] The cycloaddition occurs between a conjugated diene which acts as the 4π component, and an unsaturated compound, commonly known as the dienophile, which is the 2π component (**Fig. 8**).

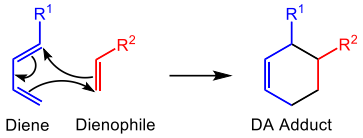

Figure 8. General concerted mechanism for Diels-Alder reaction. (Normal electron-demand Diels-Alder reaction: R^1 = EDG, R^2 = EWG; Inverse electron-demand Diels-Alder reaction: R^1 = EWG, R^2 = EDG)

FMO theory allows stratifying Diels-Alder reactions into three classes based on the relative HOMO/LUMO levels of the diene and the dienophile.[71, 72] In type I DA reactions, the primary interaction is between HOMO of the diene and LUMO of the dienophile (**Fig. 4**). Type I Diels-Alder reactions are often referred to as normal electron-demand Diels-Alder because they are the most prevalent such reactions. By virtue of being metal-free and rapid, type I reactions have been used in bioconjugations of proteins, carbohydrates and oligonucleotides.[73-75] In type II or neutral Diels-Alder reaction, both the $HOMO_{diene}$-$LUMO_{dienophile}$ and the $HOMO_{dienophile}$-$LUMO_{diene}$ separations are similar, and this class can be considered as a transition between types I and III (**Fig. 4**). In type III Diels-Alder reactions, the HOMO of the dienophile interacts with the LUMO of the diene. This type of Diels-Alder reaction is known as the inverse electron demand Diels-Alder (IEDDA) reaction and was first introduced by Bachmann and Deno.[76] Electron-acceptors which lower the LUMO of the diene, and electron-donors that elevate the HOMO of the dienophile accelerate IEDDA reactions as detailed in section 3.2. According to the Hammett equation, IEDDA reactions display positive reaction parameters ρ for variation of substituents in the diene, and negative ρ values for changes in the dienophile. IEDDA reactions have received much attention in bioorthogonal chemistry.[12, 56] The cycloaddition between 1,2,4,5-tetrazines as the archetypical electron-deficient diene and dienophiles such as *trans*-cyclooctene,[55, 77-81] cyclooctyne,[82, 83] norbornene,[84-87] cyclopropene[88-91] and isocyanide[92-95] are among the most widely used and fastest bioorthogonal reactions known. A

thorough understanding of the mechanism will help in designing diene-dienophile pairs with faster kinetics and enhanced stability *in vivo*.

3.1. IEDDA Mechanism

Depending on the nature of the substrates and solvents, IEDDA reactions can proceed through either stepwise or concerted mechanisms as shown for the example of the reaction of substituted ethylene and 1,2,3-triazine (**Fig. 9**).[96] The stepwise mechanism involves the formation of a zwitterionic intermediate followed by ring closure to yield the IEDDA adduct. The concerted mechanism, on the other hand, proceeds in a single step, and the bond formation may either be synchronous or asynchronous. The principles of stepwise and concerted mechanisms and their implication for the design of bioorthogonal reactions are outlined below.

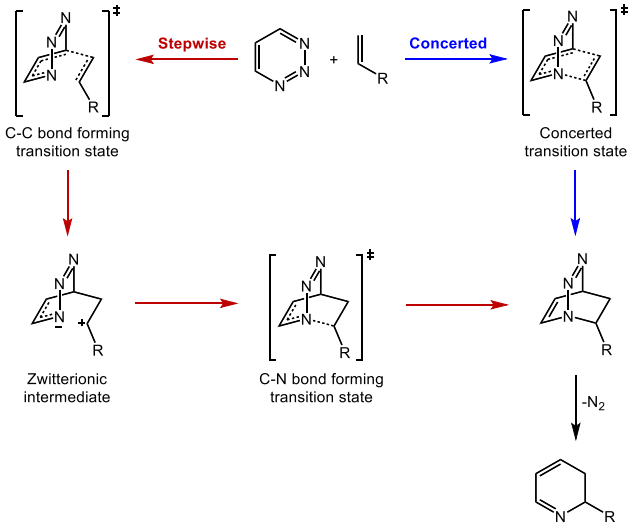

Figure 9. General scheme for concerted and stepwise mechanisms for the IEDDA reaction between 1,2,3-triazine and substituted ethylene.

3.1.1. Stepwise IEDDA Mechanism

The mechanism of the IEDDA reaction has been a subject of intensive investigation, and several groups have postulated and observed both the stepwise and concerted mechanisms. It has been shown that a substantial separation in the HOMO and LUMO of the reacting partners and steric hindrance to the cyclization step favor a stepwise mechanism.[97-100] Polar protic solvents also promote stepwise IEDDA reactions.[96] Theoretical calculations confirmed a switch in the mechanism from concerted to stepwise when changing the diene from an unsubstituted triazine to a highly electron-deficient one, with substituted enamines as the dienophile.[96-98]

Studies on the IEDDA reaction of 2,4,6-tris-(trifluoro)-1,3,5-triazine (**2**) and 4-aminopyrrole (**1**) were central in elucidating the stepwise IEDDA reaction mechanism (**Fig. 10**). De Rosa's group used multinuclear NMR experiments to identify five species in the IEDDA cascade reactions: four sequential intermediates (**4, 6, 6', 7**) and a dead-end product (**5**), with other potential tautomeric intermediates involved.[101] The stepwise IEDDA mechanism starts with the nucleophilic attack of the π-bond next to the amine substituent of 2-aminopyrrole on an electrophilic carbon of the triazine ring to yield the postulated zwitterionic intermediate **3**. The existence of **3** was inferred from the isolation of the zwitterionic tautomer **4**. Electron-withdrawing substituents on the diene stabilize the anionic σ-complex and electron-donating groups on the dienophile stabilize the cationic σ-complex in zwitterion **4**, facilitating a stepwise mechanism. Polar solvents stabilize the zwitterionic intermediate and polar transition states in this mechanism.[101] Formation of the zwitterion is followed by an intramolecular cyclization to give the tricyclic adduct **6**. This ring closure step has been shown to be dependent on the steric bulk of the diene substituents, and also controls the regioselectivity of the product with asymmetric dienes.

From the cyclic intermediate **6**, there are two paths that the reaction can take. The first is the elimination of NH_3, followed by a retro-Diels Alder reaction to lose CF_3CN and form the final aromatic product, known as the IER (IEDDA, Elimination, retro Diels-Alder) path (**Fig. 10**).[102] Conversely, the loss of NH_3 can come after the retro Diels-Alder step, known as the IRE (IEDDA, RDA, Elimination) pathway.[102] Energetically, the IEDDA cycloaddition step is highly endothermic, [100] which is intuitive considering that two aromatic molecules are being converted to one non-aromatic intermediate. The driving force for the reaction are the two subsequent cascade reactions.[100] Theoretical studies to compare the feasibility of the two reaction paths ruled out the IRE pathway based on energy calculations where they showed that the activation barrier for the RDA reaction is prohibitively high (ca. 50 kcal mol^{-1}).[102] In contrast, the elimination of NH_3 in the IER pathway is energetically favorable in terms of entropy and because of the formation of an aromatic pyrrole.[100] The subsequent retro Diels-Alder reaction is exothermic because it generates an aromatic system. However, the actual pathway may be a function of the reactants and reaction conditions.[101, 102] In the reaction between 2,4,6-tris-(trifluoro)-1,3,5-triazine and 2-aminopyrrole (**Fig. 10**), the reaction was proposed to go through an IRE pathway based on spectroscopic data which showed that all the intermediates contained the *exo*-nitrogen functional group. No evidence for either NH_3 or CF_3CN was detectable experimentally; instead, intermediate **7** was observed by NMR (**Fig. 10**).[101] The competition between the IER and IRE pathways is also of relevance to bioorthogonal chemistry. In case of 1,2,4,5-tetrazines, the elimination step can occur via either IER or IRE pathways depending on the reactants; however, the theoretical understanding is less well established for tetrazines than for 1,3,5-triazines.[102] On the basis of the Bell-Evans-Polanyi principle, the retro Diels-Alder reaction losing N_2 (for tetrazines) is more facile than losing RCN (for triazines; IRE pathway), which makes the retro

Diels-Alder reaction possible even without aromatization, as shown by Seitz and Kampchen.[100]

From the above discussion, it is clear that both electronic effects that stabilize the zwitterion and steric effects that hinder the cyclization play crucial roles in the stepwise mechanism of the IEDDA reaction. While only few studies have looked at both the stepwise and concerted mechanisms in the context of bioorthogonal chemistry, it is conceivable that varying sterics and electronics of the substituents and the reaction conditions leads to either stepwise or concerted IEDDA mechanisms. For instance, in the bioorthogonal reaction between tetrazines and isonitriles, an intriguing interplay between the stepwise and concerted

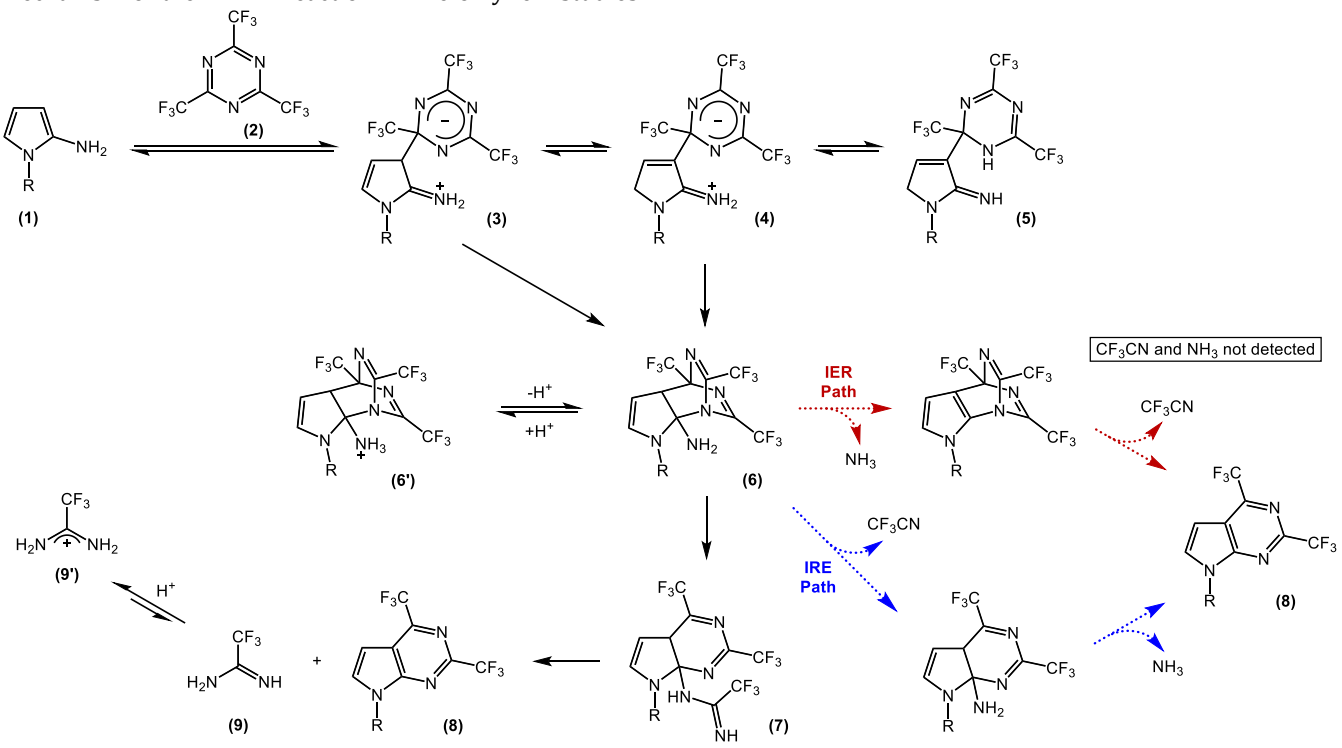

Figure 10. Proposed mechanism for stepwise IEDDA cycloaddition of 4-aminopyrroles with 2,4,6-*tris*-(trifluoro)-1,3,5-triazine.

mechanisms was observed.[93] According to DFT calculations, dimethyltetrazine, diethyltetrazine and diisopropyltetrazine react in a stepwise fashion with methylisocyanide. In contrast, the reaction with bis-*tert*-butyltetrazine was predicted to proceed through a single highly asynchronous transition state (see section 3.2.4.1).[93]

3.1.2. Concerted IEDDA Mechanism

Several studies have helped elucidate the mechanism of IEDDA reactions involving tetrazines, which is the most commonly used diene in bioorthogonal chemistry. Most reports have proposed a concerted mechanism for the IEDDA reaction of tetrazines. A concerted mechanism proceeds in a single step through a single transition state. This reaction step can have two variations: synchronous, where the two new bonds are formed to the same extent in the transition state, and asynchronous, where the bond formation is asymmetric in the transition state.[103]

Detailed computational studies on the IEDDA reaction of alkynylboronate as the dienophile with tetrazine and furan as the dienes served to illustrate the difference between the two variants (**Fig. 11**).[104] These theoretical studies predicted the reaction with tetrazine to be synchronous with the distances of the forming C-C bonds within the range of 2.1-2.3 Å in the transition state (**Fig. 11b**). In contrast, the reaction with the furan derivative bis-2,5-trimethylsilyloxyfuran was asynchronous with the distances of the forming bonds at 2.57 and 1.91 Å (**Fig. 11a**). The mechanistic analysis also showed dependence on the type of heteroatom attached to the boron center. The reaction was found to be concerted for alkynylboronate but stepwise for alkynylborondichloride.

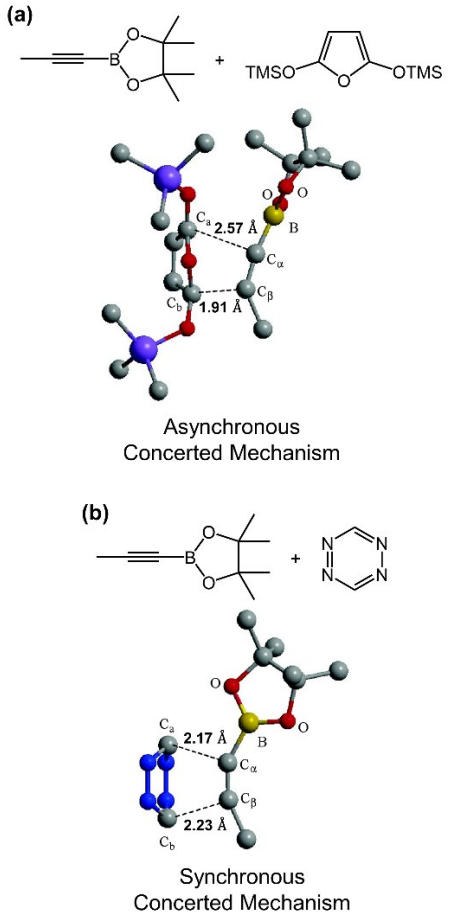

Figure 11. Synchronous and asynchronous concerted IEDDA mechanisms. a) transition state of the reaction between alkynylboronate and bis-2,5-trimethylsilyloxyfuran as an example of an asynchronous mechanism; b) transition state of the reaction between alkynylboronate and tetrazine as an example of a synchronous mechanism. Transition states were calculated by DFT. (Adapted with permission from Ref. 104. Copyright 2007 American Chemical Society).

To explain the extent of synchronism in concerted IEDDA reactions, the diradicaloid model for transition states was proposed (**Fig. 12a**).[105] The two main reaction coordinates taken into consideration are the C1···Cβ and the C4···Cα distances, from which two limiting diradicals (**A** and **B** in **Fig. 12a**) can form in the transition state. The transition states for the concerted mechanisms can be represented as a combination of **A** and **B**, their relative weights depending on their relative stability. For detailed discussions, the interested reader is directed to the excellent book authored by Vogel and Houk.[105]

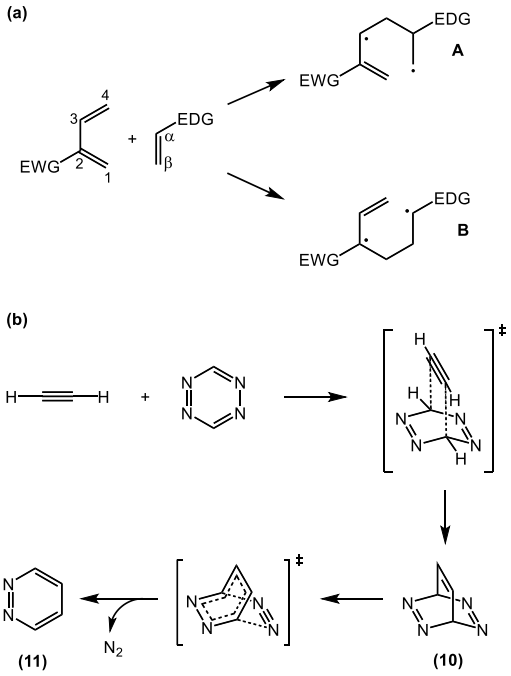

Figure 12. a) Diradicaloid model for transition states of concerted IEDDA cycloaddition. b) Proposed mechanism for concerted IEDDA reaction between tetrazine and acetylene.

The mechanism of the concerted reaction of tetrazines and alkynes used in bioorthogonal chemistry has been extensively studied. Using quantum mechanical calculations, Cioslowski *et al.* shed light on the IEDDA reaction between tetrazine and acetylene and the subsequent steps in the cascade (**Fig. 12b**).[106] They reported that the first step comprising of the cycloaddition reaction to give tetraazabarrelene **10** is the rate-determining step. This step is exothermic with an early transition state. The bond angles and lengths in the transition state are significantly distorted relative to those in the reactants. In particular, the intermolecular distances between the 1,4-carbon atoms of tetrazine and the carbon atoms of acetylene are reduced. The tetraazabarrelene intermediate has not been observed. Instead, pyridazine **11** that formed upon elimination of N_2 has been isolated.[106] The N_2-elimination step is rapid and highly exothermic. Although the expulsion of N_2 was proposed to be a separate step in the reaction cascade, Cioslowski et al. could not locate the transition state computationally.[106] Therefore, they hypothesized that the cycloaddition and elimination of nitrogen occured in a single asynchronous step, wherein the C–C bonds form and C – N bonds break simultaneously. However, calculations that showed that the activation energy of the one-step pathway is almost 50 kcal mol^{-1} higher than that for the stepwise pathway later dismissed this view and predicted that a stepwise mechanism was preferred.[107] More recently, it was computationally determined that the barrier for the loss of nitrogen from the tetraazabarrelene intermediate is essentially non-existent. Therefore, there are two sequential transition states, the first for the cycloaddition, and the second for the loss of N_2 to generate a pyridazine. The barrier for the loss of N_2 ranged from 0.1-1.5 kcal mol^{-1} depending of the structures of the tetrazine and alkyne reacting partners (**Fig. 13**).[108]

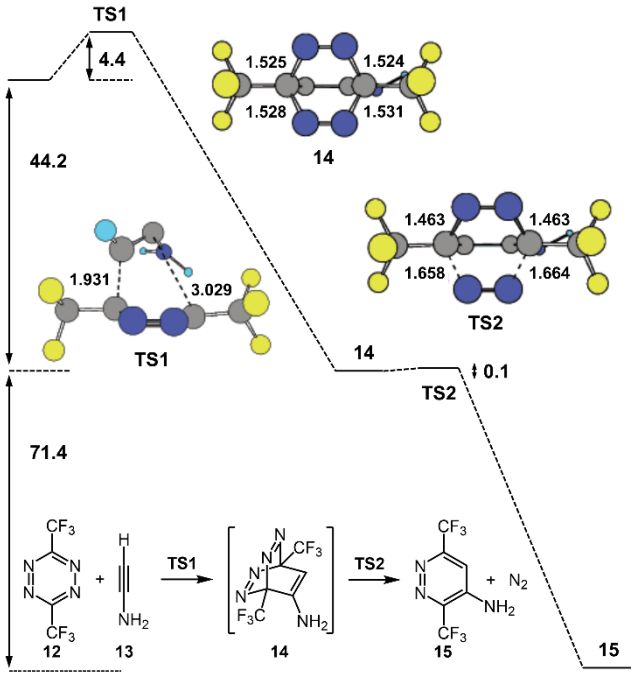

Figure 13. Relative energies and optimized geometries for the reaction between 3,6-*bis*-(trifluoromethyl)-1,2,4,5-tetrazine (**12**) and acetylenamine (**13**). (Adapted with permission from Ref. 108. Copyright 2006 American Chemical Society).

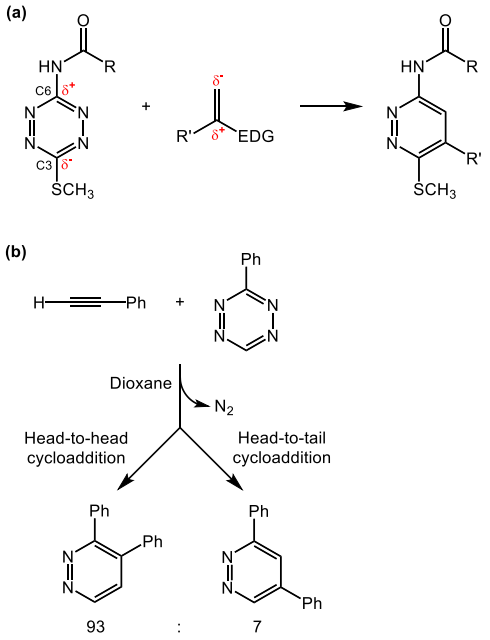

Figure 14. a) Regioselectivity in the reaction between 6-amide-substituted 3-methylthiotetrazines and electron-rich dienophiles controlled by the methylthio group. b) Head-to-head vs. head-to-tail cycloaddition in the reaction between phenylacetylene and phenyltetrazine.

FMO helps predicting the regioselectivity of an IEDDA reaction by assuming that the atom with the largest LUMO coefficient reacts with the atom with the largest HOMO coefficient. This was demonstrated in a study by Boger *et al.* where asymmetric 6-amide-substituted 3-methylthiotetrazines underwent regioselective cycloaddition with electron-rich dienophiles (**Fig. 14a**).[109] The methylthio group controlled the orientation through its ability to stabilize a partial negative charge in the transition state at C-3 of the tetrazine as was shown in AM1 computational models.[109] However, there are cases for which the experimentally observed outcome of IEDDA reactions is contrary to the regioselectivity predicted by FMO. One such example is the reaction between 3-methylsulfinyl-6-methylthiotetrazine and electron-rich ethylenes.[110] The unexpected selectivity was explained using the polar cycloaddition model which showed that the attack of the ethylene on the tetrazine according to the FMO predictions is energetically unfavorable as it diminishes the electron density of the tetrazine ring.[111] Regioselectivity was also studied with asymmetrically substituted phenylacetylene and phenyltetrazine IEDDA partners.[106] In this reaction, dispersion forces play a key role in determining the regioselectivity with the head-to-head cycloaddition (*syn* addition) being preferred over the head-to-tail attack (*anti* addition) (**Fig. 14b**). Although electronic interactions and steric repulsions exist between the phenyl rings in the head-to-head cycloaddition, these destabilizing forces are sufficiently compensated for by the attractive dispersion forces between the substituents.

3.2 Factors Affecting IEDDA Reactivity

IEDDA cycloadditions have emerged as one of the most important reactions in bioorthogonal chemistry.[12, 56, 57] Understanding the factors that affect the relative cycloaddition rates are key to tuning their efficacy in biological systems. Using a multivariate model to describe the factors that control the second-order rate constants of IEDDA cycloadditions of tetrazines and dienophiles, Coelho and co-workers identified ring strain, HOMO/LUMO levels, and steric repulsions as principal factors that determine the rates of IEDDA reactions.[112] The following sections discuss how these individual parameters affect the reaction rates.

3.2.1. Influence of Strain and Distortion on the Reactivity of Alkene/Alkyne Dienophiles

The energy gap between $LUMO_{diene}$ and $HOMO_{dienophile}$ levels critically controls the IEDDA reaction rates.[54, 109] Therefore, structural changes elevating the HOMO of the dienophile or lowering the LUMO of the diene generally accelerate the reaction. One approach to raise the $HOMO_{dienophile}$ is to apply strain. As outlined in section 2.3, inserting alkene and alkyne groups into a ring system can lead to deviations of the bond angles from those ideal for sp^2/sp-hybridized carbons and increase the $HOMO_{dienophile}$, which augments their propensity to undergo cycloaddition reactions.

3.2.1.1 Effect of Ring Size

Strained alkenes can react orders of magnitude faster with tetrazines than simple alkenes. Sauer *et al.* systematically investigated the effect of ring strain on the reaction of alkenes with tetrazines.[62] In the cycloalkene series the rates of reaction with tetrazines decreased in the order cyclopropene > cyclobutene > cyclopentene > cyclohexene (**Fig. 15**). Cyclobutene reacted 136-fold slower than cyclopropene with bis(methoxycarbonyl)tetrazine, but 3,800-fold faster than cyclohexene. This trend follows the ring strain for cycloalkenes (**Fig. 6**) and illustrates the effectiveness of using ring strain to make the IEDDA reaction faster.

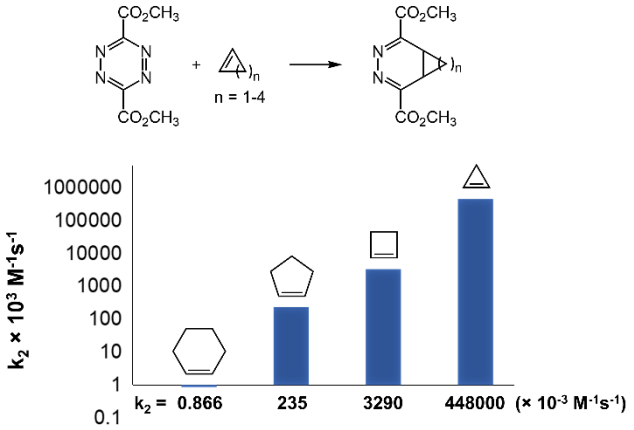

Figure 15. Dependence of IEDDA kinetics on ring strain. Relative rates of reactions between 3-6-membered cycloalkenes and 3,6-bis(methoxycarbonyl)tetrazine.

Considering the distinct accelerating effect of strain on IEDDA reactivity, it is unsurprising that small ring cycloalkenes such as cyclopropenes and cyclobutenes are used in bioorthogonal ligation reactions.[57] 1,3-distubstituted cyclopropenes have been shown to react with rates of up to 13 M^{-1} s^{-1} with monosubstituted tetrazines under aqueous conditions.[89] Prescher *et al.* introduced the cyclopropene-tetrazine chemistry to protein modification and live cell surface glycan labeling.[88] The scope of application was later expanded to DNA templated tetrazine ligations,[113] protein labeling[114] and live cell labeling in combination with fluorogenic tetrazines.[89] Similarly, 3-substituted cyclobutene derivatives have been used in conjugation with tetrazines to label both purified proteins and intact proteins in live cells,[115] and *N*-acylazetines have been used in activity-based protein profiling.[116]

The use of strain to accelerate IEDDA reaction is also used in the context of cycloalkynes.[82, 117] The deformation of the *sp* carbons from linear geometry translates into readily occurring reactions at room temperature. In particular, cyclooctyne as the smallest isolatable carbocycle with an alkyne group is frequently used in bioorthogonal chemistry.[82, 83, 118, 119]

Intriguingly, the reactivity of cycloalkenediones with tetrazine increases with larger rings, which is opposite to the trend observed for cycloalkenes and predicted by ring strain.[120] Computational calculations revealed that electrostatic interactions are responsible for this atypical reactivity trend. These electronic interactions are dependent on the ring size, and specifically on the presence or absence of methylene groups between the two carbonyls. The electropositive region around the methylene groups between the carbonyls in cyclopentenedione and cyclohexenedione interact with the electronegative region surrounding the nitrogen atoms of the tetrazine, giving rise to a stabilizing CH/π interaction in the transition state (**Fig. 16**). This stabilization is not present in the case of cyclobutenedione, leading to a lower reactivity.

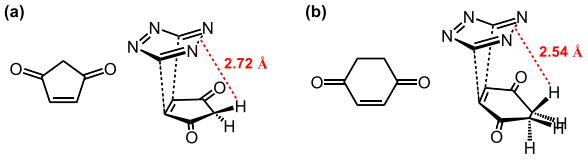

Figure 16. Stabilizing CH/π interactions (red dashed line) in the transition states of the reactions between tetrazine and (a) cyclopentenedione and (b) cyclohexenedione. Because of the absence of the methylene group, this stabilization is not present in cyclobutenone.

3.2.1.2 *Trans*-cycloalkenes

Cyclic alkenes typically adopt the *cis* conformation because incorporating a *trans*-alkene into a ring system is associated with significantly higher strain.[45, 52] *Trans*-cycloalkenes of small rings are unstable, and *trans*-cyclooctene (TCO) is the smallest stable carbocyclic alkene with a *trans* olefin (**Fig. 17**). The strain energy of *trans*-cyclooctene (17.9 kcal mol^{-1}) is substantially higher than that for *cis*-cyclooctene (6.8 kcal mol^{-1}).[52] Consequently, TCO reacts >10^5-fold faster with tetrazine relative to *cis*-cyclooctene.[62] The reaction of TCO derivatives and tetrazines is one of the fastest bioorthogonal reactions. Bimolecular reaction rates of up to 3.3×10^6 M^{-1} s^{-1} have been reported,[55] and the exceptional rate of this reaction has opened many opportunities in chemical biology, bioconjugation, and drug delivery.[55, 78, 80, 121-124] Even faster rates could be achieved by using *trans*-cycloheptene as the dienophile.[125] The parent *trans*-cycloheptene is unstable at room temperature,[126] but incorporation of a silicon atom into the cyclic structure can help relieve strain and impart stability due to the longer C-Si bonds.[127-132] *trans*-1-Sila-4-cycloheptene derivatives were shown to react with dipyridyltetrazine derivatives with rates of up to 1.14×10^7 M^{-1} s^{-1} (9:1 H_2O:MeOH, 25 °C),[125] which is the fastest known bioorthogonal reaction to date.

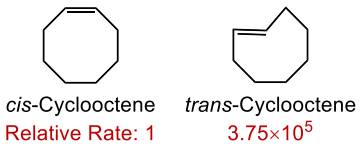

Figure 17. Relative rates of *cis*- and *trans*-cyclooctene reacting with 3,6-bis(methoxycarbonyl)tetrazine.

3.2.1.3 Cycloalkenes in Fused Ring Systems

Fusing a cycloalkene with a second, strained ring system is an effective strategy to increase its reactivity in cycloaddition reactions (**Fig. 18**). In their pioneering studies, Huisgen *et al.* reported that norbornene and similar bridged cyclic systems such as bicyclo[2.1.1]hex-2-ene and tricyclo[3.3.0.0^{2,6}]oct-3-ene are more reactive towards dienes than unstrained alkenes.[133] The reaction rate of norbornene with dipyridyltetrazine is an order of magnitude higher than that of cyclopentene, reflecting the increased ring strain in the tricyclic system.[87] Norbornenes combine good reactivity with high synthetic accessibility and stability under physiological conditions, which makes them popular reactants in bioorthogonal chemistry.[86, 87] Fusing small rings to cyclooctynes, as in Bicyclo[6.1.0]non-4-yne (BCN), also enhances their IEDDA reaction rates. BCN reacted 47-fold faster with diphenyltetrazine than cyclooctyne.[82]

The rate-accelerating effect of a bicyclic system with two strained rings was also evident for cyclopropyl derivatives. Spiro[2.3]hexene (Sph), which contains a fused cyclobutyl and 3,3-disubstituted cyclopropane ring (**Fig. 18**), was an order of magnitude more reactive than 3,3-disubstituted cyclopropene derivatives.[134, 135] The enhanced reactivity was attributed to the exocyclic cyclobutene increasing the cyclopropene ring strain, along with the alleviation of steric repulsion between the substituents at C3 of the cyclopropene and the incoming diene in the transition state because of the spirocyclic structure.[135]

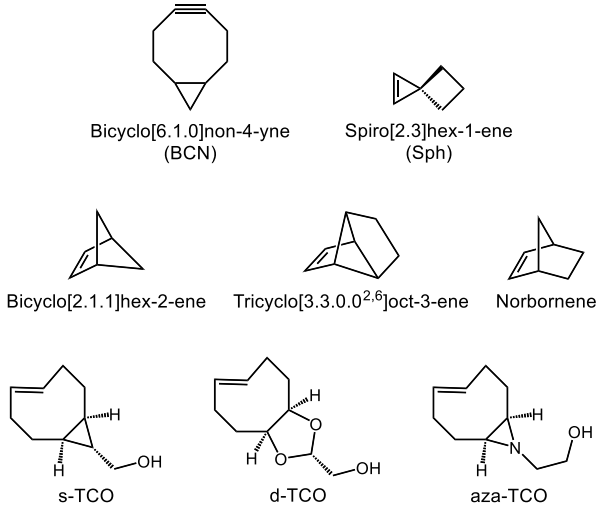

Figure 18. Strained fused ring systems used in IEDDA reactions.

In case of TCO, the fusion to a secondary ring enhance reactivity by locking the cyclooctene into a defined conformer associated with increased strain. *Ab initio* calculations predicted that the crown conformation of TCO is 5.6 kcal mol^{-1} more stable than its half-chair conformation (**Fig. 19a**).[55] Therefore, imposing structural constraints upon TCO which force it to adopt a half-chair conformation increase the rate of the reaction with dienes. Fox and co-workers reduced this concept to practice by incorporating a *cis*-fused cyclopropane ring into the TCO structure (**Fig. 19b**).[55] The resulting s-TCO reacts with diphenyltetrazine in MeOH at a rate constant of 3,100 M^{-1} s^{-1}, which is 160-fold faster than unsubstituted TCO. The rate further increased to 3.3×10^6 M^{-1} s^{-1} with dipyridyl tetrazine under aqueous conditions because polar solvents favor the IEDDA reaction (see sections 3.2.3.1 for tetrazine reactivity and 3.2.5 for solvent effects), which is one of the fastest reported examples of a bioorthogonal conjugation reaction. However, the high reactivity of s-TCO compromises its stability. s-TCO is prone to isomerization to the *cis*-cyclooctene isomer in the presence of thiols.[55] The authors proposed a free radical pathway for this isomerization.[81, 136] s-TCO derivatives can also polymerize and isomerize during storage. To circumvent these stability-related issues, the same authors designed a *cis*-dioxolane-fused TCO (d-TCO; **Figs. 18** and **19b**), which simultaneously imparted high reactivity and stability.[55] It was reasoned that the electronegative oxygen atoms would make the ring less electron-rich, therefore enhancing the stability of the ring at the expense of a modest decrease in reactivity. The *cis*-dioxolane moiety forced the ring into a half-chair conformation, which led to rate constants of >10^5 M^{-1} s^{-1} with a water-soluble dipyridyltetrazine derivative under aqueous conditions. Likewise, a conformationally strained aziridine-fused TCO (aza-TCO) was designed by Vrabel *et al* (**Fig. 18**).[137] Computational and experimental studies showed aza-TCO to be forced into a half-chair conformation similar to s-TCO and d-TCO (**Fig. 19a**). This TCO derivative reacted with dipyridyltetrazine with rates exceeding 6000 M^{-1} s^{-1}.

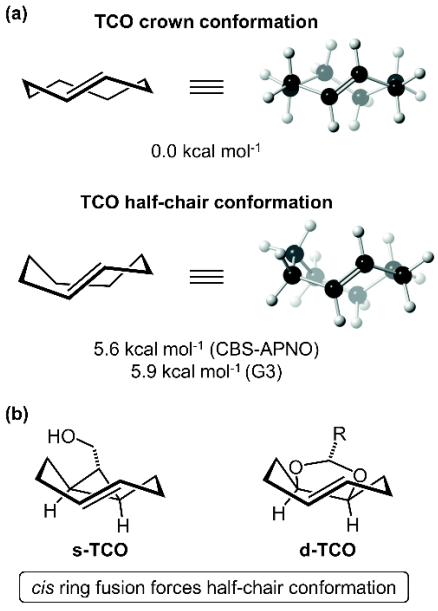

Figure 19. Conformational restriction can increase the reactivity of alkenes towards tetrazine. a) *Ab initio* calculations predict that the ground state of the half-chair conformation of TCO is 5.6-5.9 kcal mol^{-1} higher than the crown conformation; b) *cis* ring fusion in s-TCO and d-TCO confines the ring to a half-chair conformation, thereby decreasing the activation barrier. (3D structures adapted with permission from Ref. 55. Copyright 2014 Royal Society of Chemistry).

3.2.1.4 Use of Distortion/interaction Model to Explain Cycloalkene Reactivity

Although ring strain is a major driving force in IEDDA reactions, computational studies revealed that the activation energy of IEDDA reactions deviate from a linear correlation with ring strain.[63] Houk *et al.* hypothesized that instead of the strain in the alkene reactant, it is the energy needed to distort the molecules in the transition state that determines the energy of activation.[63] The distortion/interaction model (see section 2.3) made it possible to rationalize the reactivity of cycloalkenes in IEDDA reactions. The computed distortion energies of the IEDDA transition states decreased from cyclopropene to cyclohexene, which also correlates with a trend of early-to-late transition state. An early transition state indicates that the transition state geometry is closer to that of the ground state (i.e. the ground state is predistorted towards the transition-state), which results in a lower distortion energy.

The distortion/interaction model further allowed comparing the reactivities of alkenes and alkynes in Diels-Alder reactions, and to study the effect of strain. The IEDDA reactions of alkenes are typically faster than those of the corresponding alkynes.[53, 62, 138] There are substantial differences in the activation energies of the two dienophiles, 4-10 kcal mol^{-1} between *trans*-2-butene and 2-butyne, and 3-6 kcal mol^{-1} between TCO and cyclooctyne.[53] Ethylene reacted 1429-fold faster with bis(methoxycarbonyl)tetrazine than acetylene, and styrene reacted 89-fold faster than phenylacetylene.[62] Analogously, the rate of reaction of tetrazine with enamines is about 10 times higher than with ynamines.[139] The contrasting reactivity was clearly demonstrated in a theoretical study by Houk and co-workers of the reactions between a panel of symmetrically substituted tetrazines with varying electronic properties, and 2-butyne or *trans*-2-butene dienophiles.[53] The computed activation barriers for the alkyne were consistently higher than those for the alkene (**Fig. 20a**). This reactivity difference was rationalized by a combination of distortion and interaction energies.[53] Alkenes have a higher HOMO energy than alkynes which leads to a smaller HOMO-LUMO+1 (LUMO+1 is the π^* orbital interacting with the dienophile HOMO[53, 140]) gap and therefore a stronger interaction energy. The change in the distortion energies arises from a difference in the extent to which alkenes and alkynes are bent in the IEDDA transition state. For *trans*-2-butene, the distortion angle φ (the dihedral angle between the original and bent CH_3–C=C planes) changes from 180° in the ground state to 160° in the transition state, whereas for 2-butyne, the distortion angle θ (the angle between the bent bond and triple bond) changes from 180° to 140° (**Fig. 20b**). The greater bending of the alkyne results in a higher distortion energy in the transition state.

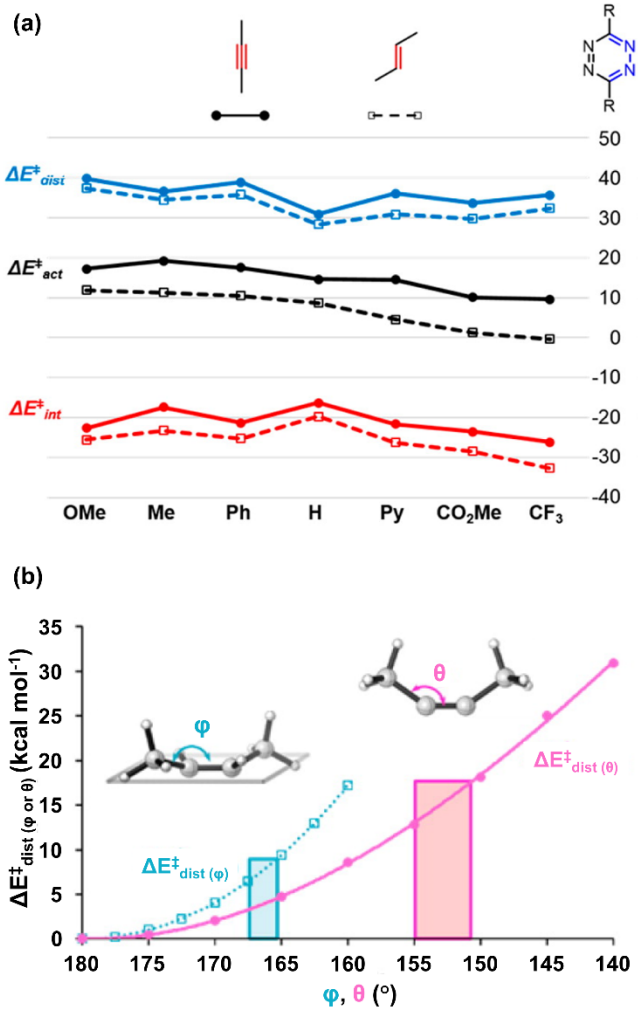

Figure 20. a) Plot of $\Delta E^{\ddagger}_{dist}$ (blue), $\Delta E^{\ddagger}_{act}$ (black) and $\Delta E^{\ddagger}_{int}$ (red) for disubstituted tetrazines in the reactions with 2-butyne (solid lines) and *trans*-2-butene (dashed lines). b) Plot of angular distortion energy ($\Delta E^{\ddagger}_{dist\,(\varphi\ or\ \theta)}$) vs. distortion angle (φ or θ) for *trans*-2-butene (blue) and 2-butyne (pink). The boxes show the angles in the transition state). (Adapted with permission from Ref. 53. Copyright 2014 American Chemical Society).

Structural strain in the dienophile therefore plays a central role in controlling the reactivity of IEDDA cycloadditions and is a leading strategy in enhancing kinetics of bioorthogonal reactions. Distortion towards the transition state is a major contributing factor to increase the reactivity of the dienophiles.

3.2.2. Effect of Stereochemistry

Stereochemistry of the dienophile is an important factor in the reactivity of IEDDA reactions. Several groups have reported that the axial isomers of functionalized TCOs are substantially more reactive than the equatorial isomers.[55,

[77-79, 141, 142] The observed rate difference has been attributed to transannular interactions in the axial isomer which results in a higher ground state energy (**Fig. 21**).[78, 143] Additionally, in the d-TCO derivatives, the *syn*-isomer is more reactive than the *anti*-isomer (not shown).[55] Similarly, the exo-isomer of norbornene-2-methanol reacts faster with tetrazine than the *endo*-isomer.[144] This difference was explained by a stronger hydrogen-bonding interaction in the transition state of the reaction with the *exo*-isomer.[144] However, *exo*-norbornene derivatives generally react faster with tetrazines than *endo*-substituted norbornenes independent of hydrogen-bond acceptors.[87] Furthermore, in cyclooctyne-tetrazine cycloadditions, *endo*-BCN is slightly faster than *exo*-BCN.[145]

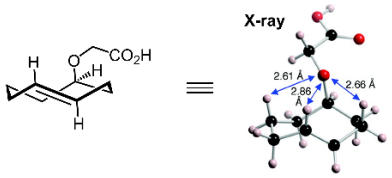

Figure 21. 1,3-diaxial interactions (blue arrows) in TCO with axial substituent. (Adapted with permission from Ref. 143. Copyright 2008 American Chemical Society).

3.2.3. Electronic Effects on the IEDDA Reaction

As discussed in sections 2.2 and 2.3, the difference in the HOMO-LUMO gap between the dienophile and diene critically affects the IEDDA reaction. In an attempt to elucidate these trends, Fukui functions ($f_{(r)}^+$), which describe electron density in frontier orbitals, have been computed for the IEDDA reactants.[146] The results revealed that the tetrazine diene is electron-deficient and strongly electrophilic, which established tetrazine as the 4π component in IEDDA reactions. By indicating the electron density on individual atoms of the diene, the $f_{(r)}^+$ function can also predict the regioselectivity of the IEDDA reactions.

By tuning the substituents on the reacting partners, it is possible to minimize the HOMO-LUMO gap to accelerate the reaction. Electron-donating groups elevate both the $HOMO_{dienophile}$ and $LUMO_{diene}$ levels, and electron-withdrawing groups lower them. As dictated by the nature of the inverse electron demand cycloaddition mechanism, electron-donating groups on the dienophile and electron-withdrawing groups on the diene are therefore expected to accelerate such reactions. These trends were verified both empirically and in theoretical analyses of the HOMO-LUMO gap.[109, 110, 138] The electronic effects of substituents on the diene and dienophiles are discussed individually in the following sections.

3.2.3.1. Diene Substituents

Electron-withdrawing substituents on the tetrazine increase the rate of IEDDA reactions by lowering the LUMO of the diene. IEDDA reactions have a positive reaction constant ρ with regard to tetrazine substituents (i.e. the rate constant increases with the substituent constant σ_{para}). Therefore, electron-withdrawing tetrazine substituents that lower its LUMO increase the IEDDA reaction.[147, 148]

In their seminal publication first reporting the reaction of tetrazines with dienophiles, Carboni and Lindsey noted the crucial role that electronics play in IEDDA reaction kinetics.[149] Electron-withdrawing substituents can greatly enhance the reactivity of tetrazines. While the reaction between 3,6-bis(difluoromethyl)tetrazine and styrene was rapid at room temperature, the reactions with dimethyltetrazine and diphenyltetrazine required heat to proceed. In early efforts to systematically study the effects of tetrazine substituents on IEDDA cycloadditions, Boger *et al.* compared the reactivity of a series of 3,6-disubstituted tetrazines towards *N*-vinyl pyrrolidinone.[109] The study confirmed the expected trend between the electronic nature of the tetrazine substituents and the reaction rate, which was corroborated by AM1 calculations (**Fig. 22**).[109, 110, 150] In a follow-up study, the authors showed that sulfoxide-substituted tetrazines are substantially more reactive than their sulfide counterparts and require less vigorous reaction conditions due to their enhanced electron-withdrawing nature.[110]

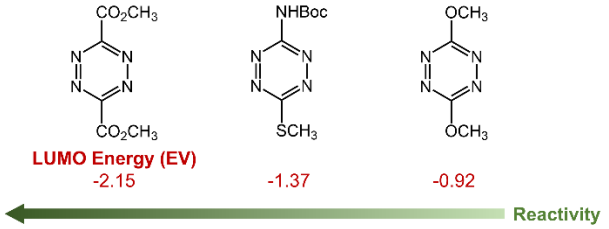

Figure 22. AM1 computational results for the LUMO energies of disubstituted tetrazines, which were shown to reflect their relative reactivities.

The rate-accelerating effect of electron-withdrawing groups on the reactivity of tetrazines is consistent among diverse dienophiles. Studies of the reaction of norbornene and TCO with tetrazines designed for bioconjugation revealed considerable differences in rate constants between tetrazines with electron-withdrawing and -donating groups.[151] A norbornene derivative reacted >40-fold faster with 3-aminopentyl-6-pyrimidyltetrazine than with 3-aminopentyl-6-methyltetrazine, as can be predicted from the electron-withdrawing nature of the pyrimidyl group. Similar variations were observed with TCO as the dienophile. The second order rate constant was 820 $M^{-1}\,s^{-1}$ with 3-methyl-6-phenyltetrazine and 2.2×10^4 $M^{-1}\,s^{-1}$ with 3-pyrimidyl-6-phenyltetrazine, which corresponds to a 27-fold difference. Likewise, a study on the effect of substituents on the reaction of cyclooctynes and tetrazines revealed a 203-fold rate difference between bis-hydroxyphenyltetrazine (k_2 = 0.58 $M^{-1}s^{-1}$) and dipyridyltetrazine (k_2 = 118 $M^{-1}s^{-1}$) when

reacted with hydroxy-BCN.[152] An excellent correlation was observed for the reaction rates of different tetrazines with an isonitrile and norbornene, indicating that the electronic effects are largely conserved for different dienophiles.[93]

A study by Mikula's group also highlighted the crucial role of electronics in IEDDA reaction kinetics exploring the effect of N-acylation of aminotetrazines, which have low reactivity because of the electron-donating nature of the amino group, was investigated.[153] Computational calculations showed that the $\Delta G^{\ddagger}$ for the reaction between TCO and *N*-acetylated tetrazines was around 4 kcal mol^{-1} lower than those with their non-acetylated counterparts (**Fig. 23**), which resulted in around a 600-fold predicted increase in reactivity. This discrepancy was also confirmed experimentally with multiple tetrazines.

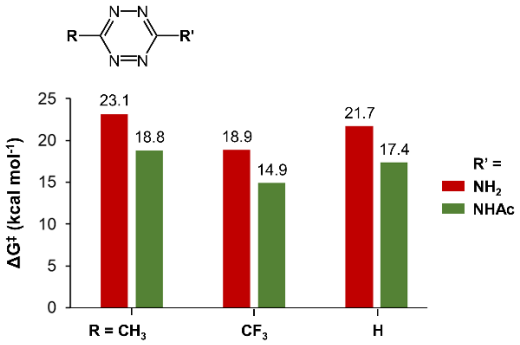

Figure 23. Kinetic measurements showing increased reactivity of *N*-acetylated aminotetrazines compared to aminotetrazines, reacting with TCO.

While EWGs offer a rate advantage, such substituents also render tetrazines less stable.[151] Highly reactive tetrazines are prone to hydrolysis and reaction with endogenous thiols,[154] which is unfavorable for bioorthogonal chemistry. In light of this, the development of stable tetrazines retaining the reactivity of using EWGs are currently being pursued.

3.2.3.2. Dienophile Substituents

Varying the electronics of dienophiles profoundly affects the kinetics of IEDDA reactions.[9] Electron-donating substituents increase the HOMO of dienophiles and consequently decrease the gap between $HOMO_{dienophile}$ and $LUMO_{diene}$, and several reports have confirmed this trend (**Fig. 24**). Carboni and Lindsey had shown that dienophiles with EDGs facilitate the reaction, while EWGs decelerate it.[149] Sauer *et al.* later showed that the electronics of the substituents on alkynes and alkenes can affect the rate constants to a remarkable extent.[62, 138, 155] The rate constants for the reaction of a series of alkynes with unsubstituted tetrazine spanned a range of several orders of magnitude.[138] For instance, the reaction of tetrazine with (dimethylamino)acetylene was 7.3×10^4-fold faster than that with methoxyacetylene. Similarly, the electropositive character of metal-substituents enhances the reactivity of alkynes towards tetrazines.[156] Organotin alkynes offered the highest rate constants, with bis(trimethyltin)acetylene being 7350-fold faster than tert-butylacetylene.

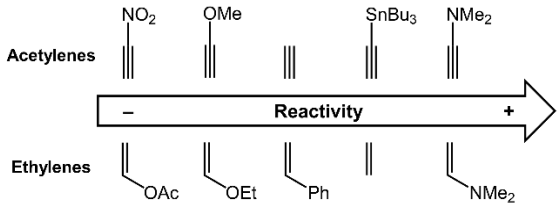

Figure 24. Reactivity trend for alkene and alkyne dienophiles in IEDDA reactions; EDGs increase reactivity.

Similar rate-enhancing effects of electron-donating dialkylamino groups were observed for alkene dienophiles; bis(dimethylamino)ethylene reacted 2.3×10^5-fold faster than bis(methylthio)ethylene.[138] Conversely, electron-deficient cyanoethylene reacted 3.9×10^4-fold slower than ethylene.[62] Additionally, cyclic enamines and enol ethers are highly reactive dienophiles. Rate constants for alkene dienophiles covered a range with a factor >10^6, with enamines giving the fastest rates.[138] Unfortunately, enamines are unstable in aqueous media and are therefore of limited use for bioorthogonal reactions. However, enamines formed *in situ* have been utilized in a bioorthogonal context for protein labeling. The enamine formed from aldehydes under proline-catalysis conditions reacted as a dienophile partner with tetrazines at second order rate constants of up to 13.8 M^{-1} s^{-1} (**Fig. 25**).[157, 158]

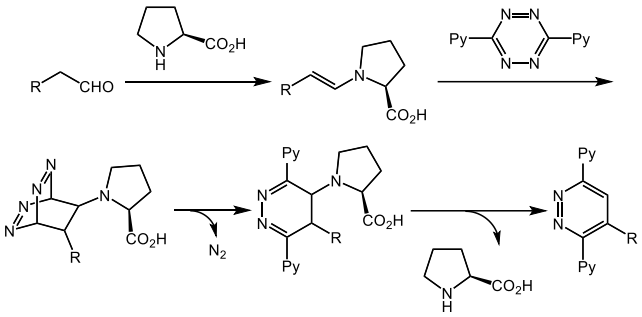

Figure 25. Mechanism of IEDDA reaction mediated by proline.

Reactions with substituted styrene dienophiles allowed studying the effect of electronics without interference by steric repulsions, and confirmed the enhanced reactivity afforded by electron-donating groups. *p*-Methoxystyrene and *p*-nitrostyrene reacted 3.8-fold faster and 7.5-fold slower than unsubstituted styrene, respectively.[62, 159] The effects were even more dramatic when the dienophilic olefin side-chain was directly substituted. *N*-α-morpholinostyrene reacted 72-fold and β-dimethylaminostyrene 3.6×10^4-fold faster than styrene.[62, 155, 159] When substituted with an EWG, the rate decreased, as in β-methoxystyrene, which was found to be 211-fold slower reacting than the unsubstituted counterpart.[155]

From the preceding discussion, it is evident that IEDDA reaction rates vary predictably with changes in the electronics of the substituents on the diene and dienophile. The reaction partners follow the FMO considerations, where EWGs on the diene and EDGs on the dienophile improve reaction kinetics by narrowing the $HOMO_{dienophile}$-$LUMO_{diene}$ gap. This understanding is crucial to the development of bioorthogonal reactions, which generally require fast kinetics under stringent physiological conditions.

3.2.3.3. Effect of Diene-Dienophile Coordination on Kinetics

Boronic acids possess unique electronic properties because of their vacant *p* orbital.[160, 161] As a result of electron donation by the oxygen atoms attached to boron, boronic acids are weak electron donors, and because of their Lewis acid character form boronates in aqueous media, which are strong electron donors.[160, 161] Inspired by these considerations, Bonger *et al.* studied the reaction of vinylboronic acids with tetrazines and observed significantly enhanced reactivity with some tetrazines compared to corresponding alkene derivatives lacking the boronic acid moiety.[162] For example, phenylvinylboronic acid reacted over two orders of magnitude faster with dipyridyltetrazine than styrene. These vinylboronic acids were shown to be outliers to the general rule of electronics in IEDDA reactions,[112] as the reaction is much faster than what the electronic nature of the dienophile would suggest.[163, 164] Furthermore, the rate-accelerating effect was observed only in the reaction with dipyridyltetrazine, and not phenyltetrazine and 3-methyl-6-phenyltetrazine. Similarly, a boronate-substituted norbornene showed reduced reactivity towards tetrazine relative to the unsubstituted norbornene.[165]

The discrepancies in the reactivity of vinylboronic acids towards different tetrazines were attributed to Lewis acid-Lewis base coordination between the boronic acid and the pyridyl substituent,[163, 164] rather than changes to the HOMO levels (**Fig. 26**). The nitrogen of the pyridyl ring coordinates to the vacant p orbital of the boron atom, which both makes the dienophile more electron-rich and induces proximity, thus enhancing the rate of the reaction. To further increase the coordination, the authors also designed tetrazines with ortho-hydroxy groups and showed that these had enhanced reactivity towards vinylboronic acids despite the substituent being electron-donating.[163] The requirement for the hydroxy substituent to be at the ortho-position unambiguously confirmed that the rapid reaction rates were a result of coordinative interactions. Coordination-assisted IEDDA reactions are among the fastest bioorthogonal reactions known.

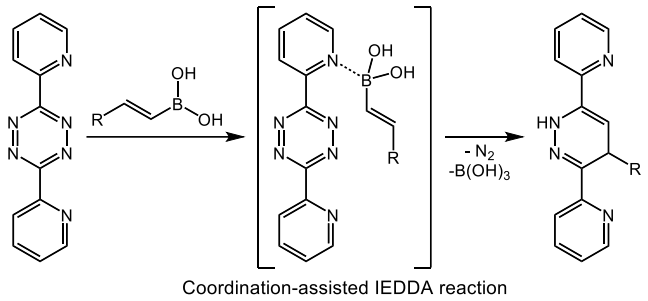

Figure 26. Coordination of the pyridine nitrogen of dipyridyltetrazine to the boron of vinyl boronic acid, enhancing the rate of reaction.

3.2.4. Steric Effects

Diels-Alder reactions are sensitive to exchange of hydrogen for a larger substituent, and steric repulsions in the crowded transition state impede the reaction. In general, steric bulk hinders the mutual approach of the diene and dienophile, and decreases the rate of IEDDA reactions. Whether an electronically-favorable substituent will enhance the reactivity or not depends on the extent to which the electronic properties of the substituents are capable of compensating for this steric hindrance.

3.2.4.1. Diene Substituents

Sterics play a crucial role in the kinetics of IEDDA cycloadditions. Several groups have shown that unsubstituted and monosubstituted tetrazines participate in IEDDA reactions faster than disubstituted derivatives.[113, 151] A systematic study of tetrazine substituent effects by Hilderbrand *et al*. clearly illustrated the role of sterics (**Fig. 27**).[151] Using norbornene carboxylic acid as the dienophile, the reaction with the monosubstituted 3-(4-aminomethylphenyl)tetrazine was around 20-fold faster than the disubstituted 3-(4-aminomethyl)phenyl-6-methyltetrazine. Similarly, the rate constant of 3-(5-aminopentyl)tetrazine with the same dienophile was found to be 35-fold greater than 3-(5-aminopentyl)-6-methyltetrazine. Likewise, with TCO as the dienophile, monosubstituted tetrazines showed faster reaction kinetics relative to disubstituted ones (**Fig. 27**).[151]

The effect of steric repulsion imparted by tetrazine substituents varies depending on the dienophile. Bulky TCO derivatives are especially sensitive to tetrazine substituents and decreases in reaction rates are more pronounced compared to those of, for example, norbornene.[151] Smaller cyclopropenes are comparably insensitive to bulky tetrazine substituents,[113] and slender isonitriles tolerate even highly encumbered tetrazines.[93] This difference in sensitivity of dienes to tetrazine substituents allows controlling the relative rates of IEDDA reactions, with implications for developing orthogonal pairs of bioorthogonal reactions. For example, introduction of an electron-withdrawing pyrimidyl ring to 3-

(4-aminomethylphenyl)tetrazine increased the rate of the reaction with norbornene while slowing the reaction with TCO.[151]

The effect of steric repulsions is especially pronounced when introducing bulky *tert*-butyl groups. Introducing a *tert*-butyl substituent onto a 3-phenyltetrazine ring decreases the rate of reaction with TCO by more than four orders of magnitude relative to the corresponding mono-substituted tetrazine.[113] Computational studies showed that the *tert*-butyl group leads to a decrease in the dihedral angle of the tetrazine plane in the transition state of the reaction with TCO.[113] This interaction results in a higher distortion energy requirement for the tetrazine in the transition state and consequently, a higher activation barrier. For structurally compact 1-methylcyclopropenes, the decrease in rate for introducing a *tert*-butyl group was a comparably modest 4-fold. This difference led to a reversal in the reactivity order of the dienophiles upon introduction of a *tert*-butyl group, with methylcyclopropene reacting faster than TCO with the *tert*-butyl-modified tetrazine, although it reacts 2-3 orders of magnitude slower with monosubstituted tetrazines (**Fig. 28**).[113]

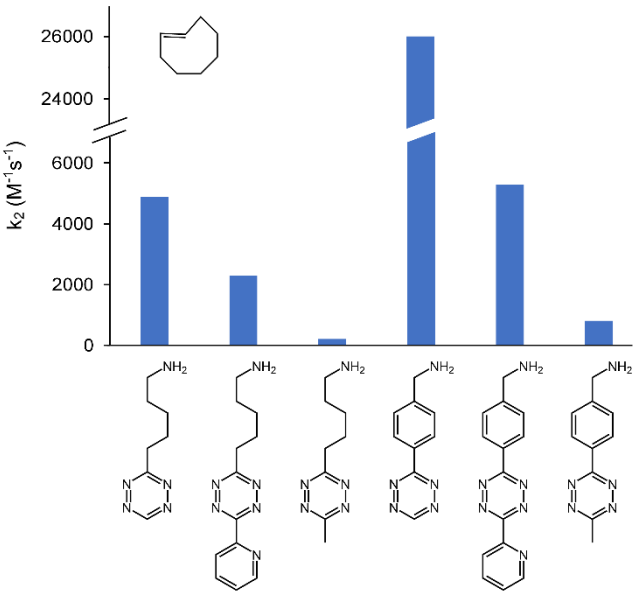

Figure 27. Reaction rates of tetrazines with TCO showing the effect of sterics on IEDDA reactivity. Monosubstituted tetrazines are more reactive than disubstituted ones due to steric hindrance.

A particular case with regards to steric interactions in IEDDA reactions are those with isonitriles.[16] The linear structure of isonitriles makes them nearly insensitive to steric repulsions.[93] Primary isonitriles react at an appreciable rate even with 3,6-bis-*tert*-butyltetrazine (k_2 = 0.083 M^{-1} s^{-1}, DMSO:H_2O 4:1, 37 °C), whereas other dienophiles including the small-size cyclopropenes are much less reactive (k_2 = <10^{-3} M^{-1} s^{-1}) towards this diene. In fact, isonitriles exhibit a highly unusual structure-reactivity trend with regard to the substituents on the tetrazine ring: the rate of the reaction increases with the bulkiness of the tetrazine substituents (**Fig. 29a**).[93] Phenylethyl isocyanide reacted 10.8 times faster with 3,6-bis-*tert*-butyltetrazine than with 3,6-dimethyltetrazine. Hydrophobic interactions were excluded as the cause for this effect. DFT calculations allowed rationalizing this unexpected reactivity trend and showed that steric attractions play a crucial role in the stabilization of the transition state. Using dispersion correction in the DFT calculations, the transition state energy for the bis-*tert*-butyltetrazine reaction was found to be lowered by 6 kcal mol^{-1} relative to the transition state without dispersion correction, while the dimethyltetrazine reaction was stabilized by only 3.1 kcal mol^{-1} (**Fig. 29b**). In case of bulky isonitriles however, steric repulsions with bulky tetrazine substituents become dominant.[93]

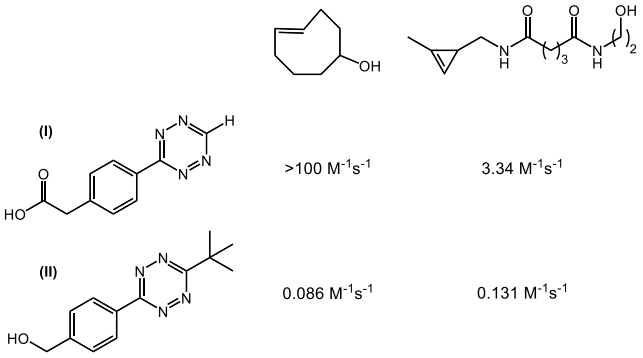

Figure 28. Second order rates of reactions of substituted TCO and methylcyclopropene with tetrazines **I** and **II**. The *tert*-butyl substituent on tetrazine **II** causes a steric clash with TCO, reversing the reactivity trend.

These results are especially significant in the field of bioorthogonal chemistry because tetrazines with fast kinetics are also typically unstable under physiological conditions. While EWGs increase reaction rates, they also render the tetrazines susceptible to nucleophilic attack.[151] On the other hand, sterically bulky groups make them stable but also hinder the approach of dienophiles.[113, 151, 166] In case of isonitriles as the dienophile, bulky tetrazine substituents are at the same time rate-accelerating and stability-enhancing. Based on this principle, it was possible to design 3-*tert*-butyl-6-pyrimidyl tetrazines that exhibited high stability in buffer and reacted with isonitriles at rates of up to 57 M^{-1} s^{-1}. This observation was specific for isonitriles and this chemistry allowed for developing triple-orthogonal protein labeling schemes.[93]

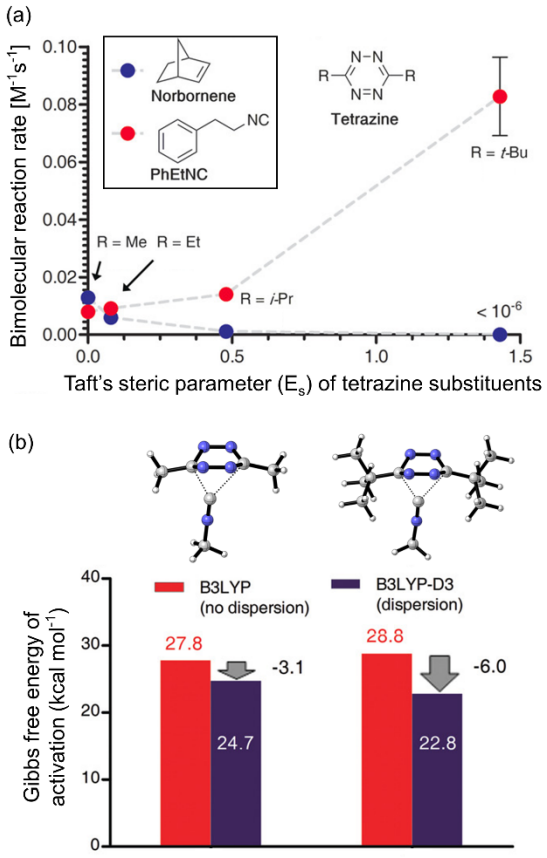

Figure 29. Steric attractions accelerate the reaction between tetrazines and isonitriles. a) Bimolecular reaction rates of norbornene and PhEtNC with tetrazines, as a function of the Taft's steric parameter of tetrazine substituents. b) DFT calculations for transition state geometries and Gibbs free energy of activation for the reactions between methylisocyanide and dimethyltetrazine or bis-*tert*-butyltetrazine. (Adapted with permission from Ref. 93. Copyright 2019 John Wiley and Sons).

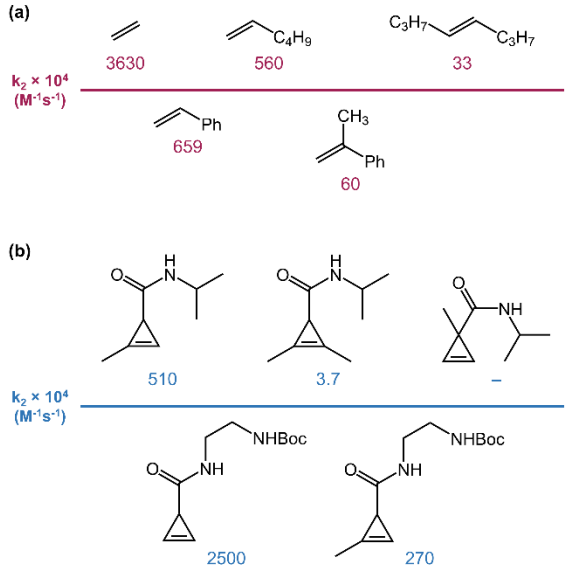

Figure 30. Reactivity trends of a) ethylenes and b) cyclopropenes in IEDDA reactions showing the effect of sterics.

3.2.4.2. Dienophile Substituents

Extensive studies were performed to elucidate the effects of substituents on the reactivity of alkene dienophiles. Most substitutions on the olefin result in a decrease in reaction rate that is often substantial (**Fig. 30**). For instance, 1-butylethylene reacted 6.5-fold slower than unsubstituted ethylene with bis(methoxycarbonyl)tetrazine, despite the electron-donating nature of the alkyl group.[62] The rate deceleration is even more pronounced in case of disubstituted alkenes. 1,2-dipropylethylene reacted 17 times slower than butylethylene (**Fig. 30a**).[62] Olefins with two substituents on the same carbon also exhibited significantly decreased reactivity.[155] These results led to the conclusion that dienophile steric effects on IEDDA kinetics usually eclipse electronic effects except for strongly electron-donating groups.[62] The same trend was extended to alkynes; for instance, *tert*-butylacetylene reacted 17-fold slower with tetrazine than unsubstituted acetylene.[138]

The ability to modulate the rate of IEDDA reactions, along with the biocompatibility of the reactants, is crucial in bioorthogonal chemistry. Several studies have looked at the steric effects of substituents on the reactivity of biocompatible dienophiles such as cyclopropene and norbornene. In case of C-3 monosubstituted cyclopropene, introduction of a methyl group at the C-1 position decreased the reactivity towards tetrazine about 10-fold (**Fig. 30b**).[91] Analogously, 1,3-disubstituted cyclopropenes reacted 1-2 orders of magnitude faster than 1,2,3-trisubstituted cyclopropenes.[167] Sauer and co-workers were the first to show that 3,3-disubstituted cyclopropenes dramatically slowed down the reaction rates with tetrazines.[62] Two substituents at C3 prevented access from either face of the dienophile;[167] quantitatively, 3,3-dimethylcyclopropene reacted 5.8×10^3-fold slower than unsubstituted cyclopropene.[62] Prescher's group corroborated these findings and showed that 3,3-disubstituted cyclopropenes give slow, and in some cases undetectable, reactions.[90] This reactivity has been utilized in developing orthogonal bioorthogonal chemistry. The IEDDA reaction between 1,3-disubstituted cyclopropenes and tetrazines is orthogonal to the 1,3-dipolar cycloaddition between 3,3-disubstituted cyclopropenes and nitrile imines.[90] This reactivity pattern provides opportunities for multicomponent imaging using isomeric cyclopropenes which are considered as a minimal sized bioorthogonal functionalities.[90]

Steric effects also influence the reactivity of norbornenes, and substituents generally decrease their reactivity compared to the unsubstituted dienophile.[87] For example, norbornene-2,3-dicarboxylate reacted 31 times slower than the unsubstituted dienophile.[87] Although the electron-withdrawing nature of the ester groups is expected to decelerate the reaction, the large reactivity difference was attributed partially to sterics. This effect was also evident in the case of benzonorbornadienes (BNBDs) with a heteroatom at the bridging position (**Fig. 31**).[168] Oxa-BNBD reacted 3.4 times

faster than the bulky *N*-Boc substituted aza-BNBD. Sterics at the bridgehead position also affected rates. A carbamoyl methyl moiety at the bridgehead position decreased the rate by 12-fold compared to the unsubstituted counterpart.[168]

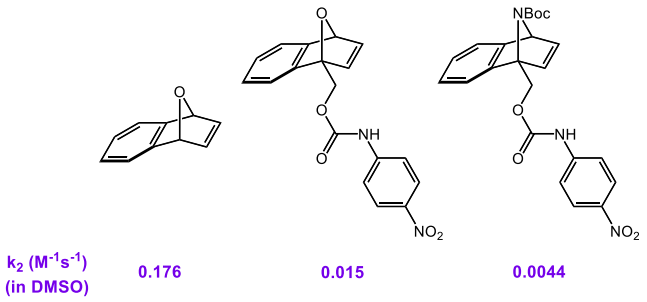

Figure 31. Second-order rate constants for the reactions between benzonorbornadienes and dipyridyltetrazine.

Similar steric effects were observed in the case of TCO. A doxorubicin carbamate moiety at the allylic position decreased the rate of the reaction with dipyridyltetrazine by over 3000-fold compared to the unmodified TCO.[169] Gräter *et al.* used computational studies to gain an understanding of the structural details of the reactants and activation barriers of the reactions of a set of tetrazines and cyclooctenes/ynes.[170] A significant rate difference between *trans*-cyclooctene methylcarbamate (TCO*) and cyclooctyne methylcarbamate (SCO) was observed and rationalized by sterics. SCO reacted around 3 orders of magnitude slower with 3-benzyl-6-methyltetrazine than with 3-benzyltetrazine, whereas the rate difference in case of TCO* was within an order of magnitude (**Fig. 32**). This reactivity was utilized in the dual labeling of cell surface proteins.[170] Computations showed that the cycloaddition of SCO with the disubstituted tetrazine gives rise to a 6 kcal mol^{-1} greater distortion energy than with the monosubstituted analog. This finding suggests that the sterically demanding methyl group, along with the carbamate next to the triple bond of SCO, creates a steric hindrance to the formation of the transition state.

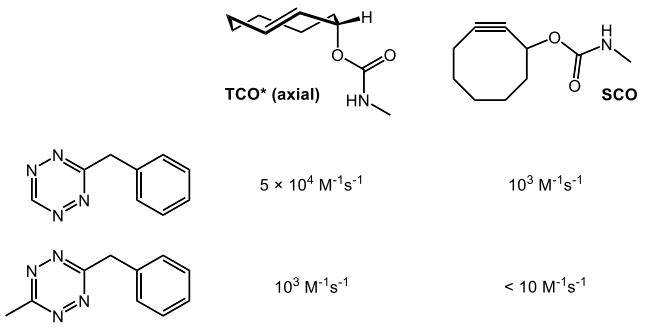

Figure 32. Approximate second order rate constants for the reactions of TCO* and SCO with 3-benzyltetrazine and 3-benzyl-6-methyltetrazine. (Values were estimated based on **Fig. 1** in Ref. 170).

In conclusion, bulky substituents on both the diene and dienophile partners in IEDDA reactions give rise to a steric hindrance to the transition state formation, which leads to decreased reaction rates. On the other hand, sterically bulky substituents improve the stability of tetrazines in biological media.[93, 113] It is an attractive possibility to harness this balance between sterics and electronics in dictating the reactivity and stability in IEDDA cycloadditions for the purpose of developing rapid and biocompatible reactions.

3.2.5. Solvent Effects

Polar protic solvents typically accelerate IEDDA reactions, which was attributed to a solvophobic binding of the reactants to each other.[171, 172] However, this acceleration is particularly evident in protic solvents, and especially in water.[147, 173] The proposed rationalization for this effect was that there is a stabilizing hydrogen bonding interaction between water and the transition state which lowers the activation barrier.[147, 174] This process resembles Lewis acid catalysis. The reaction between dipyridyltetrazine and styrene was found to be 13 times faster in ethylene glycol than in 1,4-dioxane, and 130 times faster in water/*tert*-butanol (95:5 mole fractions). Small Hammett ρ values for IEDDA reactions in aprotic solvents indicate only a modest charge buildup in the transition state under these conditions.[147] However, protic solvents influence the transition state and make it more dipolar, as indicated by an increase in ρ values. Stabilization is then brought about by hydrogen bonding, which increases the rate.

The rates of IEDDA reactions dramatically increases in aqueous media, beyond what can be predicted by transition state stabilization.[147] This observation was explained by enforced hydrophobic interactions.[147, 173] In aqueous solvents, the hydrophobic surface area of the reactants is reduced, which provides a driving force for the reaction. Computational studies have confirmed that the acceleration in aqueous solvents is due to both hydrogen bonding and hydrophobic interactions.[175, 176] These studies clearly demonstrate a strong solvent effect on the kinetics of IEDDA reactions. It is therefore critical to take differences in solvents into account when comparing rates of different IEDDA reactions.

3.3. Non-tetrazine Dienes

While most bioorthogonal IEDDA reactions involve tetrazines, other dienes can act as biocompatible reaction partners.[177-181] Triazines have for example been used in bioorthogonal chemistry;[177, 178] however, their reactivity is considerably reduced relative to that of tetrazines.[177] Several explanations have been brought forth for the exceptional propensity of tetrazines to undergo IEDDA reactions, and a series of recent studies suggest that differences in the aromaticity critically determine the reactivity of many dienes. Understanding these theoretical principles allowed

designing five-membered cyclopentadiene[181-186] and pyrazole dienes[179, 180] with the required reactivity for use in bioorthogonal chemistry. In addition to the representative set of widely used non-tetrazine dienes discussed below, other dienes such as thiophene *S*,*S*-dioxides,[187-189] oxadiazinones[190] and 1,2-quinones[191] have been successfully used in IEDDA cycloadditions.

3.3.1. Nitrogen-containing Benzene Derivatives

The rates of IEDDA reactions with 6-membered aromatic dienes increases dramatically with the number of nitrogen atoms in the ring.[192] Tetrazine reacts 5×10^4-fold faster with cyclooctyne than 1,2,4-triazine, which in turn reacts 2×10^6-fold faster than 1,2-diazine.[192] 1,2,4-triazines are sufficiently reactive to readily undergo IEDDA reactions under physiological conditions.[177, 178] The Prescher group first proposed using the reaction of 1,2,4-triazines with dienophiles in bioorthogonal chemistry.[177] 1,2,4-triazines react with dienophiles analogously to tetrazines and form new bonds across C3 and C6 followed by loss of nitrogen yielding pyridine molecules.[177, 193] The reaction of 1,2,4-triazines with TCO occurred with second-order rate constants of 1.2-7.5×10^{-2} $M^{-1}s^{-1}$. Substituent effects for triazines are comparable to those of tetrazines with electron-withdrawing groups increasing their reactivity and bulky substituents hindering the approach of the dienophile.[177, 194]

The lower reactivity of 1,2,4-triazines relative to tetrazines can be advantageous. 1,2,4-triazines tend to be highly stable in biological conditions[177] whereas 1,2,4,5-tetrazines, and especially those with hydrogen substituents and electron-withdrawing groups, tend to decompose in serum.[151, 154] Additionally, 1,2,4-triazines are amenable for the development of orthogonal reaction-pairs. Dienophiles that are less reactive than TCO such as norbornenes and cyclopropenes tend to be unreactive towards 1,2,4-triazines.[177] Rationalizing that substituents at the C3 and C6 could deter the reaction with bulky substituents, Prescher *et al.* explored this possibility for accessing mutually orthogonal reactions. As predicted computationally, 3- and 6-phenyl-1,2,4-triazines failed to react with the bulky alkyne 3,3,6,6-tetramethylthiacycloheptyne (TMTH; **Fig. 33**).[178] The same dienophile on the other hand readily reacted with 5-phenyl-1,2,4-triazine. Using methylcyclopropene as a dienophile that is less sensitive to steric repulsions, the reactivity of 1,2,4-triazines was determined by the electronic properties of the 1,2,4-triazines and the reactivity increased in the order 5-phenyltriazine < 6-phenyltriazine < 3,6-diphenyltetrazine (**Fig. 33**). This order is reversed relative to that observed for TMTH and allows for designing chemoselectivity.

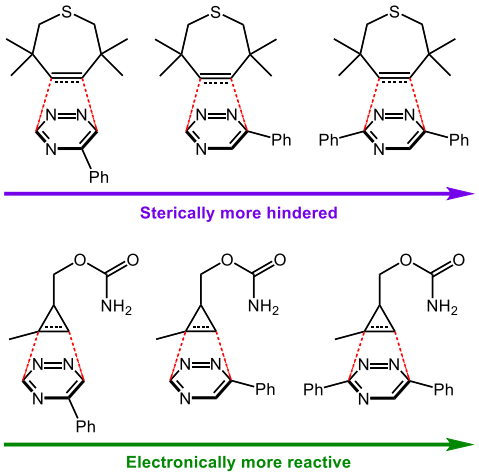

Figure 33. Reactivity trends of 5-phenyltriazine, 6-phenyltriazine and 3,6-diphenyltetrazine when reacting with 3,3,6,6-tetramethylthiacycloheptyne (TMTH; above) and methylcyclopropene (below).

Boger *et al.* carried out a systematic study of 1,2,3-triazine as the diene in IEDDA reactions and showed that substituents at C5 can predictably modulate their reactivity (**Fig. 34a**).[194] Several tested dienophiles showed progressively enhanced reactivity with electron-poor triazines. Ynamines and enamines showed limited reactivity with 1,2,3-triazines, but reacted cleanly with 5-phenyltriazine and 5-methoxycarbonyltriazine, and less reactive acetylenic and olefinic dienophiles only reacted with the electron-poor 5-methoxycarbonyltriazine. From this data, it is evident that 1,2,3-triazines follow the same basic electronic principles discussed above for tetrazines in IEDDA reactions. The authors recently developed the first monocyclic aromatic 1,2,3,5-tetrazine, 4,6-diphenyl-1,2,3,5-tetrazine.[195] The molecule was shown to be a robust diene for IEDDA reactions, and reacted efficiently with a range of dienophiles such as amidines, imidates, enamines, ynamines and styrenes including under aqueous conditions. The reaction proceeded through an IEDDA cycloaddition, followed by elimination of N_2 and NH_3 (**Fig. 34b**). A regiospecific C4/N1 over N2/N5 mode of cycloaddition was observed. These 4,6-diphenyl-1,2,3,5-triazines were shown to possess orthogonal reactivity to the commonly used bioorthogonal diene, 3,6-diphenyl-1,2,4,5-tetrazine.[195] While the former showed excellent reactivity with amidines, the latter reacted with high efficiency with strained alkynes, with minimal cross-reactivity.

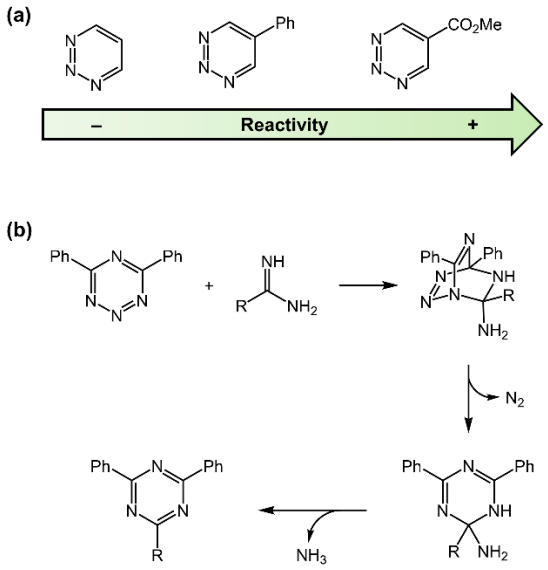

Figure 34. IEDDA reactions of 1,2,3-triazines and 1,2,3,5-tetrazines. a) Substituent effects on the reactivity 1,2,3-triazines. b) Mechanism of the reaction between 4,6-diphenyl-1,2,3,5-tetrazine and amidines.

It is apparent from this discussion that alternative nitrogen-containing aromatic rings can be used as robust dienes for bioorthogonal reactions. Their contrasting reactivities with tetrazines and with other isomeric triazines makes possible that they can be utilized in orthogonal bioorthogonal chemistry.

3.3.2 Nitrogen Atoms Increase the Reactivity of Benzene-derived Dienes by Decreasing Their Aromaticity

Multiple studies have aimed at elucidating the fundamental principles that underlie the increase of reactivity of dienes upon incorporation of nitrogen atoms. Molecular orbital considerations have been involved in explaining the different reactivity of such dienes.[177] Indeed, the calculated LUMO+1 energy level is higher for 1,2,4-triazines relative to tetrazines.[177] Bickelhaupt *et al.* argued that the polarizing effect of the nitrogen atoms would facilitate reactions with dienophiles by reducing closed-shell Pauli repulsions.[196] As an alternative explanation, Houk *et al.* hypothesized that the differences in IEDDA reactivity stem from reduced aromaticity in nitrogen-containing benzene rings.[197] Indeed, extensive computational studies revealed that nitrogen atoms reduced the aromaticity of six-membered rings as quantified by nucleus-independent chemical shift (NICS) analysis and isodesmic aromatic stabilization energies, and that these variations correlate with the observed differences in reactivity.[192, 197]

The distortion/interaction model helps explain the reactivity trend in azabenzenes. It was shown that each additional nitrogen in a 6-membered aromatic ring decreases its barrier for IEDDA cycloaddition. This was attributed to a combination of distortion and interaction energies.[197] Azabenzenes have lower distortion energies than benzene because of smaller out-of-plane bending dihedral angle distortion, which decreases with added nitrogen atoms. NICS(0) calculations showed that nitrogen substitution causes electron localization and reduces σ aromaticity. This reduced aromaticity makes the ring easier to distort, leading to lower distortion energies. In addition, adding nitrogen atoms to the ring lowers the LUMO energy, which leads to more favorable orbital interactions and higher interaction energies.[197] In this model, the strength of aromaticity is a primary determinant of the transition-state energy.

A recent study by Raines *et al.* provided valuable insight into the physical principles that determine IEDDA reactivity of aromatic dienes and confirmed aromaticity as a predominant factor.[192] The authors analyzed and compared the effect of addition of nitrogen atoms into six- and five-membered aromatic rings on physicochemical properties and reaction rates. This study was based on the premise that while introduction of nitrogen atoms into six-membered rings is associated by rate accelerations by many orders of magnitude, the effect on the reactivity of five-membered rings is comparably modest.[192] For example, cyclooctyne reacts with similar rates with 2,5-bis(trifluoromethyl)furan (k_2 = 1.0×10^{-5} M^{-1} s^{-1}) as with 2,5-bis(trifluoromethyl)-1,3,4-oxadiazole (k_2 = 1.3×10^{-4} M^{-1} s^{-1}).[192] Calculations revealed that differences in unoccupied orbital levels could not explain the different effects of nitrogen atoms on IEDDA reaction rates for five- and six-membered cyclic dienes. Furthermore, the polarizing effect of nitrogen was comparable in the two ring systems, indicating that reduced Pauli repulsions are not the main factor affecting reactivity. In contrast, while the calculated aromaticity of six-membered rings decreases substantially with addition of nitrogen atoms, such a trend is absent for five-membered rings.[192] This data led to the conclusion that differences in aromaticity can largely explain the rate variations of IEDDA reactions with different heterocyclic dienes.

3.3.3. Cyclopentadienes and Cyclopentadienones

The recognition that aromaticity of the diene system critically affects their reactivity in IEDDA reactions also translates into the design of five-membered ring systems suitable for bioorthogonal chemistry. Cyclopentadienes have long been studied as diene partners in Diels-Alder reactions. Studies by Schleyer *et al.* showed that substituents on the C-5 position affect the electronic properties of the cyclopentadiene π-system via hyperconjugation.[198-200] σ-acceptors, and in particular fluorine atoms, induce negative hyperconjugation resulting in a pseudo 4π-electron antiaromatic system (**Fig. 35a**). [179, 198-201] Some of this antiaromatic destabilization is offset by distortion of the C-X bond away from the plane of the diene (**Fig. 35b**).[201, 202] In contrast, electron-donating groups (i.e. silyl-substituents) favor an aromatic character of the diene. The degree of (anti)aromaticity of cyclopentadienes directly affects the distortion energy in the cycloaddition transition state and therefore the rate of the reaction.[201]

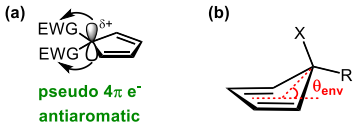

Figure 35. Effect of substituents on the reactivity of cyclopentadienes towards dienophiles. a) Schematic illustration of hyperconjugative antiaromaticity in cyclopentadiene with EWGs. b) Geometry of C5-X cyclopentadienes showing θ_{env}, the angle measuring the out-of-plane distortion of the C5 atom.

Sauer *et al.* studied tetrachlorocyclopentadienes as reactants in Diels-Alder reactions,[70, 203] and Houk *et al.* after extensive computational and experimental studies[185, 204-206] introduced them to bioorthogonal chemistry.[181] Such highly substituted cyclopentadienes are stable in solution in contrast to most cyclopentadienes that undergo dimerization.[70, 181, 203, 207] Furthermore, the geminal halogen substituents at the C-5 carbon increase reactivity by hyperconjugation. In early studies, Houk *et al.* used 7-substituted norbornadienes as the dienophiles to examine the reaction kinetics of hexachlorocyclopentadiene.[184, 185] Based on the obtained insights, they developed a new bioorthogonal moiety from the cyclopentadiene scaffold: 6,7,8,9-tetrachloro-1,4-dioxospiro[4,4]nona-6,8-diene (a substituted tetrachlorocyclopentadiene ketal, TCK; **Fig. 36a**).[181] TCK undergoes cycloaddition reactions with BCN and 5-hydroxy-TCO with rate constants of 0.26 and 0.25 $M^{-1}s^{-1}$, respectively. The dioxoalkyl group provides a straightforward attachment linker, and the biocompatibility of the TCK scaffold was demonstrated using peptide labeling. However, as was computationally predicted, no reaction was observed with dibenzocyclooctyne (DIBO) derivatives, which provides an opportunity for mutually exclusive bioorthogonal reactions (**Fig. 36b**).

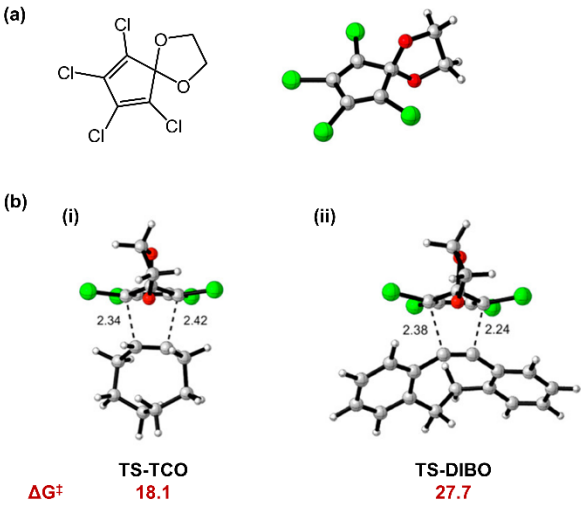

Figure 36. Tetrachlorocyclopentadiene ketals as bioorthogonal reactants. a) Structure of TCK. b) Transition state structures and activation free energies (in kcal mol^{-1}) for the Diels-Alder reactions between TCK and (i) TCO and (ii) DIBO. (Adapted with permission from Ref. 181. Copyright 2018 American Chemical Society).

In addition to substituted cyclopentadienes, cyclopentadienenones can act as diene in bioorthogonal reactions. Cyclopentadienenones have a significant antiaromatic resonance structure[208] that allows them to participate in IEDDA reactions. In a series of studies, Wang *et al.* explored the use of such molecules in a biologically relevant context and especially for the release of CO.[183, 209, 210] Cyclopentadienone reacts with alkynes that are either activated by strain or positioned nearby to form a norbornadiene-like intermediate that reverses to a benzene with concomitant release of CO (**Fig. 37**). This chemistry is of great interest for developing prodrugs that generate CO in vivo.[211, 212]

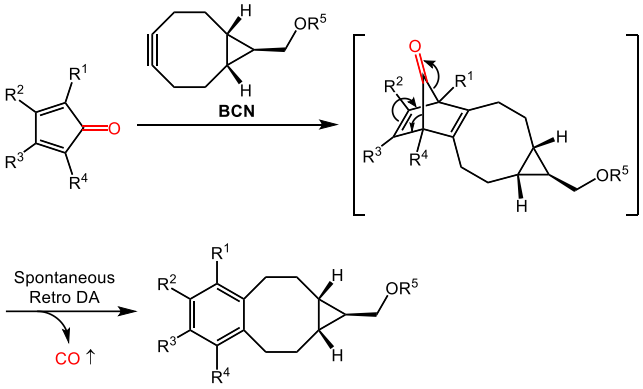

Figure 37. Mechanism of release of CO from the reaction between cyclopentadienone and BCN.

3.3.4. *4H*-pyrazoles

Most *4H*-pyrazoles require heating or acid catalysis to react with strained alkenes or alkynes.[213-216] However, strategically positioning σ-accepting groups (e.g. -F) at the C-4 position allow such reactions to proceed at room temperature by inducing hyperconjugative antiaromaticity (**Fig. 35a**).[179, 198-202] Recently, 4,4-difluoropyrazoles (DFP) were proposed as dienes suitable for use in bioorthogonal IEDDA reactions.[179, 202] The electrophilic geminal fluorine groups invoke hyperconjugative antiaromaticity which destabilizes the ground state and reduces the energy required to distort the diene in the transition state of the reaction with dienophiles. BCN reacted faster with diphenyl-DFP (k_2 = 5.2 M^{-1} s^{-1}) than with 3,6-diphenyltetrazine (k_2 = 3.2 M^{-1} s^{-1}).[179] However, 4,4-difluoro-*4H*-pyrazoles are sensitive towards biological nucleophiles and decompose in thiol-containing buffer. To address this issue, they developed the 4-fluoro-4-methylpyrazole (MFP) scaffold that has lower hyperconjugative aromaticity but is pre-distorted towards the transition-state geometry.[180] The rationale behind this design was that to lower the unfavorable σ*-π overlap leading to the hyperconjugative antiaromaticity, the C–F bond distorts away from the plane of the diene, as observed in the case of cyclopentadienes (**Fig. 35b**).[180, 201, 202] This predisposition of MFP towards an envelope geometry lowers the distortion energy in the cycloaddition transition state, and therefore favors the reaction. As designed, the rate of the reaction of MFP with BCN was only modestly reduced compared to that of

DFP despite the significantly lower hyperconjugative antiaromaticity (5.8 and 1.4 kcal mol^{-1} destabilization for DFP and MFP, respectively). Importantly, the replacement of one fluoro with a methyl group led to a 52% greater stability in serum.

Although the use of cyclopentadienes and 4*H*-pyrazoles is in its early stages, the above discussion suggests that they offer great potential as bioorthogonal reactants. They can be especially useful in advancing the orthogonal bioorthogonal field due to their contrasting reactivities with tetrazines.

3.4. Dissociative Chemistry Based on IEDDA Reactions

Although bioorthogonal reactions have been historically used for ligation reactions, recent interest has emerged in dissociative reactions.[12, 56] Such reactions, coined click-to-release reactions, have been used for unmasking molecules and releasing payloads and have been used in developing prodrug strategies.[77, 83, 92, 94, 123, 211] The IEDDA cycloadditions, being the most widely used reaction in bioorthogonal chemistry, have undergone detailed studies in this context. Such dissociative bioorthogonal reactions in the first step form unstable cycloadducts, which liberate leaving groups spontaneously. [12, 56] Tetrazine-reactive dienophiles, such as *trans*-cyclooctenes,[77, 79, 123] isonitriles,[92, 94] norbornadienes,[165, 168] and vinyl ethers,[217-219] have been linked to release steps. Recently, tetrazine-based caging groups that release molecules upon reaction with dienophiles have been reported.[94, 220]

3.4.1. Tetrazine-triggered Release Reactions

3.4.1.1 *trans*-Cyclooctenes

The reaction between TCOs and tetrazines is the fastest known bioorthogonal reaction, (see sections 3.2.1.2 and 3.2.1.3),[55] and it therefore comes as no surprise that it has received much attention for the development of dissociative chemistry. Leaving groups attached to both the TCO and the tetrazine partners have been developed,[77, 123, 220] and their mechanisms studied extensively.[220, 221]

Robillard *et al.* were the first to report the modification of the TCO-tetrazine IEDDA cycloaddition into a bioorthogonal release reaction.[77] They achieved tetrazine-mediated release by linking a leaving group via a carbamate at the allylic position of the TCO (**Fig. 38**). Mechanistically, the cycloaddition, upon expulsion of N_2, results in a 4,5-dihydropyridazine, which tautomerizes to a 1,4-dihydropyridazine.[77, 221] The lone pair on the NH of the 1,4-tautomer then initiates an electron cascade to liberate the carbamate, the formation of a conjugated pyridazine, and the subsequent aromatization.

Both the bimolecular rates and release yields were found to be highly dependent on the structure of the tetrazine with an inverse relationship between the two.[77] Tetrazines with electron-withdrawing substituents rapidly reacted with the TCO derivative, but release yields were low; in contrast, comparably electron-rich dialkyltetrazines afforded good release yields while their reactivity towards the tetrazine was sluggish. For example, while dipyridyltetrazine reacted at a rate of $k_2 = 58\ M^{-1}\ s^{-1}$ almost no release occurred. In contrast, the reaction with dimethyltetrazine had a second order rate constant of $0.54\ M^{-1}\ s^{-1}$ and a release yield of 60%. However, in PBS at 37°C, a dialkyl-substituted tetrazine developed for the purpose of triggering drug release from antibody-drug conjugates showed rates of up to $54.7\ M^{-1}\ s^{-1}$ and released 80-90% of the payload.[123] Stereochemistry also affected the reactivity of the TCOs. The axial isomer reacts >150-fold faster than the equatorial isomer.[77, 79] This difference was attributed to a steric hindrance to the approach of the tetrazine with the carbamate moiety in the equatorial position, along with the previously reported higher ground state energy of the axial isomer (see section 3.2.2).

Several studies have pursued the optimization of tetrazine structures to achieve high bimolecular rates and release yields simultaneously.[166, 221, 222] A study by Chen and coworkers systematically examined the effects of the electronics and sterics of tetrazine substituents on the release of carbamates from TCOs.[166] The study revealed that asymmetric tetrazines combining an electron-withdrawing aromatic substituent with a small alkyl group provided both favorable reaction rates and high release yields. Following these findings, they developed 3-hydroxyethyl-6-pyrimidyltetrazine, which allowed over 80% uncaging in 30 minutes.

Weissleder's group performed extensive mechanistic studies to understand the factors that affect the release step and to develop tetrazines that react rapidly with TCO and release the leaving groups in high yields.[221] They confirmed the previous hypothesis by Robillard *et al.*[77] that the 1,4-dihydropyridazine formed from the initial click reaction is the releasing tautomer, and any 2,5-tautomer formed must first convert to the desired isomer before release can take place (**Fig. 38**). Studies on the reaction environment revealed that acidic conditions substantially enhanced the rate and yield of the release step.[221] General acid-catalysis of the post-click tautomerization was proposed to explain this observation. Based on this hypothesis, they synthesized tetrazines functionalized with COOH-bearing substituents. Indeed, a propionic acid functionalized tetrazine showed a marked enhancement in release compared to dimethyltetrazine because of a carboxylic acid-mediated protonation of the dihydropyridazine nitrogen (**Fig. 39**). A symmetric bis-propionic acid substituted tetrazine, yielded quantitative payload release over a pH range of 4.2-8.0.[221] Similarly, aminoethyl substituents on tetrazines can catalyze the tautomerization step.[226] DFT calculations supported these results and revealed that the acidic substituents favor the regioselective initial formation of the releasing 1,4-tautomer.[226] In addition, the release from the mono-functionalized diene was

found to be biphasic. This was explained to be because of the orientation of the IEDDA cycloaddition wherein a head-to-head reaction preferentially forms the releasing 1,4-tautomer. On the other hand, a head-to-tail reaction leads to the formation of the non-releasing 2,5-tautomer, which first has to convert to the desired tautomer and, therefore slows down the release (**Fig. 39**). The formation of a non-releasing dead end product was also uncovered under certain conditions.[221] An intramolecular nucleophilic attack of the carbamate –NH on the 4,5-tautomer, which is an intermediate in the cycloaddition, forms a stable tricyclic product which lowered release yields (**Fig. 38**). *N*-methyl substitution of the carbamate precludes cyclization and consequently increases release yields significantly. Oxidation of the dihydropyridazine intermediate before the elimination step can occur also prevents release.[221]

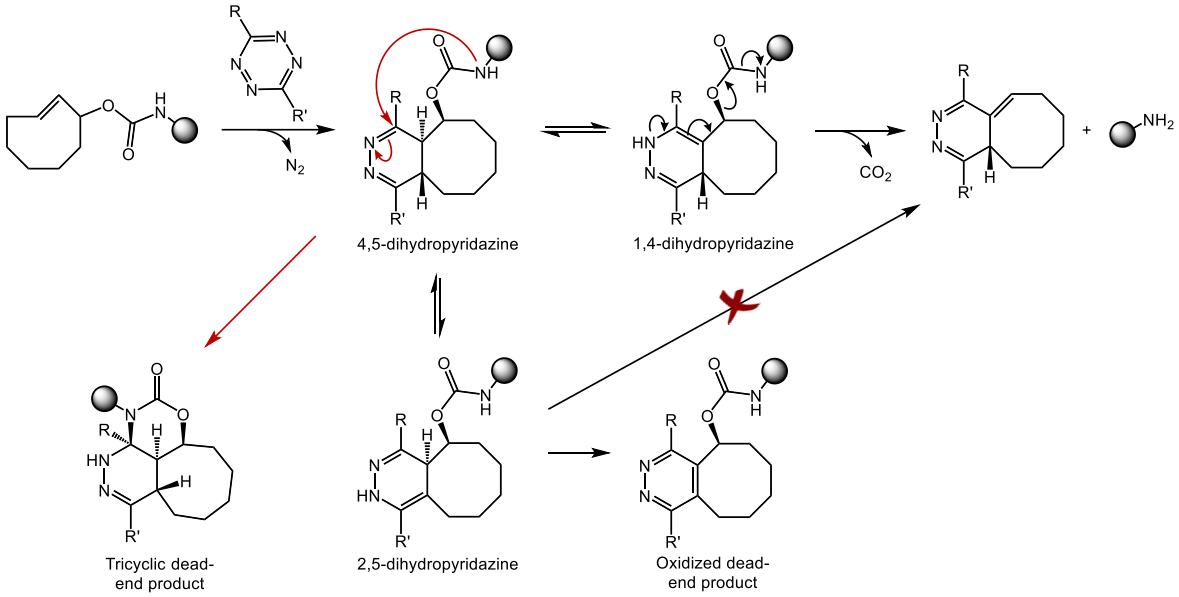

Figure 38. Mechanism of reaction between TCO-carbamate and tetrazines. Following cycloaddition, the 4,5-dihydropyridazine intermediate can give two tautomers; the 1,4-tautomer, from which release takes place and the 2,5-tautomer, which first has to isomerize to the 1,4-tautomer before release can occur. The tricyclic and aromatized (oxidized) products are dead ends.

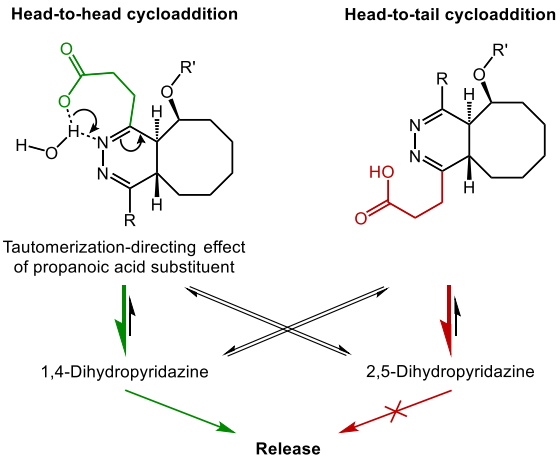

Figure 39. Tautomerization-directing effect of propanoic acid substituent upon head-to-head cycloaddition, leading to fast release. The absence of this effect in head-to-tail cycloaddition leads to slow release.

Further investigations have expanded the scope of releasable groups to carboxylic acids, alcohols, and phenols through ester, carbonate and ether linkages, respectively.[169, 223] These advancements will be central to the utility of this reaction in chemical biology and drug delivery.

A variation of the TCO-tetrazine release reaction was recently reported by Royzen's group.[224] In this reaction, the payload is released via an intramolecular cyclization upon cycloaddition, forming a δ- or ε-lactam (**Fig. 40**). Efficient and fast uncaging of phenols (over 80% release within 6 h) were shown using TCO-esters at physiological pH.[224]

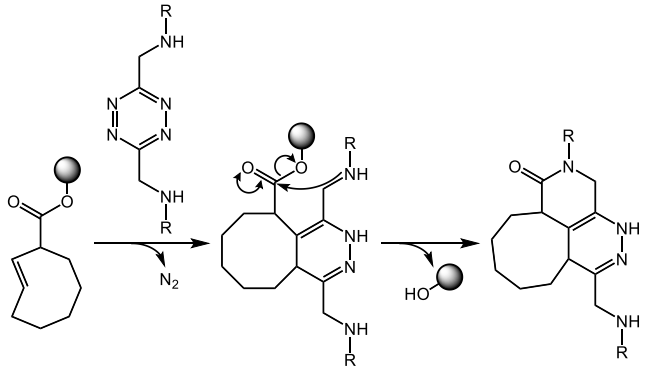

Figure 40. Mechanism of payload release from TCO by intramolecular cyclization.

3.4.1.2. Isocyanopropyl (ICPr) Chemistry

The isocyano group is the most structurally compact bioorthogonal functional group available, which is beneficial for modifying biomolecules. [93, 94, 225-228] Recently, we expanded the utility of the isonitrile to the chemically-triggered release of payload molecules and developed the 3-isocyanopropyl (ICPr) group, which can be deprotected upon exposure to tetrazines. [16, 92, 94, 229]

The reaction of tetrazines and isonitriles involves an inverse electron demand (4+1) cycloaddition which, on N_2 expulsion, forms a 4*H*-pyrazole with an exocyclic C=N bond that in most cases rapidly tautomerizes to the corresponding imine (**Fig. 41**).[92, 230] Hydrolysis of this imine gives the 4-aminopyrazole and an aldehyde. When using ICPr as the isonitrile fragment, a 3-oxopropyl group is afforded upon hydrolysis, which was hypothesized to release payloads by β-elimination.[92, 231, 232] To validate this hypothesis, ICPr groups were reacted with 3,6-dipyridyltetrazine, and were found to release phenols and amines with near-quantitative yields. Second order rate constants of up to 4 M^{-1} s^{-1} with dipyridyltetrazine and release rates of up to 4.2×10^{-3} s^{-1} for phenol payloads were observed. Various factors affect the release step. First, serum albumins catalyze the β-elimination.[92, 233] The catalysis is thought to be caused by a general-base effect from lysine residues in subdomain IIA of serum albumin.[234] Second, EWGs at the β-position of ICPr accelerate the elimination.[95] This acceleration is the result of a decrease in the proton affinity of the β-carbon, and 2-phenyl-ICPr showed significantly higher rates; for instance, a 13.4-fold rate enhancement was observed for phenol leaving groups using dipyridyltetrazine.[95]

Substituents on both the tetrazine and isonitrile directly affect the hydrolysis of the imine intermediate. Leeper *et al.* showed that tertiary isonitriles form stable adducts with tetrazines because the tautomerization is blocked.[227] Similarly, propionate-derivatives of isonitriles form stable adducts with tetrazines by tautomerizing to a vinylogous urethane product.[227] Our group investigated the dependence of the hydrolysis on the structure of the tetrazine.[95] It was revealed that sterically bulky tetrazines prevented the hydrolysis of the imine even with primary isonitriles, and the imine intermediate from the reaction of *n*-BuNC and 3,6-bis-*tert*-butyltetrazine was remarkably stable (18% hydrolysis over 72 h). These results prompted us to revisit the mechanism of release in the ICPr chemistry, which was initially hypothesized to release from the aldehyde after hydrolysis. Indeed, a near-quantitative release can occur from the bis-*tert*-butylpyrazole imine intermediate, which is resistant to hydrolysis.[95] This result led to the conclusion that release can occur directly from the imine intermediate without going through hydrolysis (**Fig. 41**). Depending on the hydrolytic stability of the imine, the elimination can therefore occur directly from the imine or from the aldehyde.

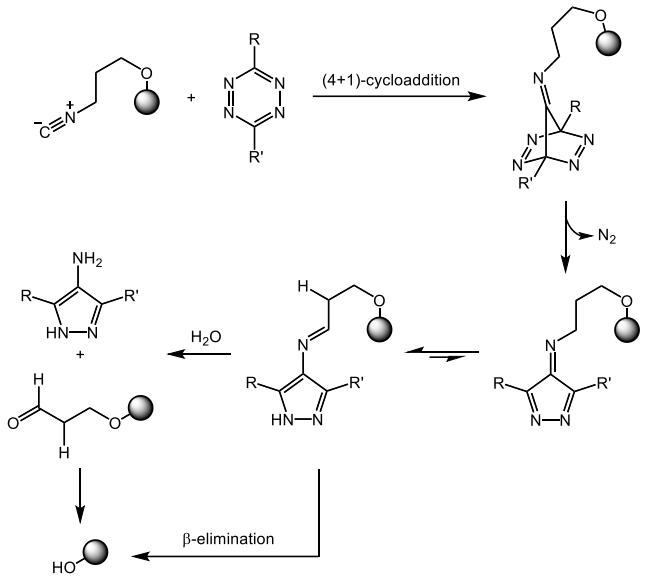

Figure 41. Proposed mechanism of tetrazine-triggered payload release from isocyanopropyl derivatives. Following cycloaddition and isomerization, release can take place before hydrolysis from the imine or after hydrolysis from the aldehyde.

3.4.1.3. Benzonorbornadienes

Norbornenes have long been used as dienophiles in IEDDA reactions and form stable adducts with tetrazines.[84, 86, 87, 144, 151] However, benzonorbornadienes (BNBD) with a heteroatom at the bridging position react with tetrazines to yield labile products.[168] The initial cycloaddition forms an intermediate which undergoes rapid N_2 elimination to give isoindoles and isobenzofurans,[235] which are known to be high energy molecules due to their lack of aromaticity.[236, 237] We utilized the intrinsic instability of these heterocycles to design a bioorthogonal BNBD-tetrazine dissociative reaction to release payloads.[168] In this design, the leaving groups are attached via a methylene linker to the bridgehead carbon. The isoindole/isobenzofuran decomposes upon formation to release the molecule of interest, and form a stable aromatic side-product in the process (**Fig. 42**). Mechanistic studies suggested that the 1-methylene-isoindole/isobenzofuran cation formed upon elimination reacts with water to form 3-methylene-isoindolin-1-ol/isobenzofuran-1-ol, which is capable of reacting with another molecule of tetrazine to form further adducts (**Fig. 42**).[165]

A panel of BNBDs were synthesized which reacted with dipyridyltetrazine with a maximum k_2 of 0.2 M^{-1} s^{-1}.[168] Although the bimolecular rate constant is lower than that with TCO or isonitrile, the release was rapid with yields of 80-90% within 6 hours. Initially, only carbamates were used as leaving groups which gave amines upon CO_2 elimination. Later, the scope was expanded to esters, carbonates and trialkylphosphates.[165] Along with the stability and biocompatibility of the reactants, the range of possible payloads and

release rates make BNBDs attractive bioorthogonal functionalities for controlled release of molecules.

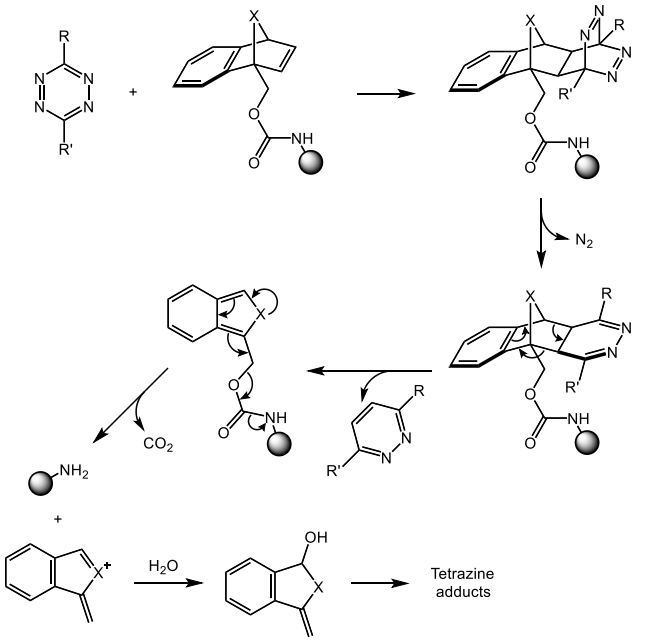

Figure 42. Mechanism of payload release from benzonorbornadienes. Cycloaddition with tetrazines forms the unstable isoindole/isobenzofuran, which releases the payload.

3.4.1.4. Vinyl Ethers

Sauer *et al.* explored the reaction of vinyl ethers with tetrazines and noted that it was accompanied by elimination of the alcohol to achieve aromatization.[62] Several groups have independently harnessed this reaction for the tetrazine-mediated release of payloads from vinyl ethers.[217-219] Advantages of this chemistry include the compactness of the caging group, as well as the prompt release of alcohols which is difficult to achieve with other click-to-release reactions.

Quantum mechanical studies of the reaction of phenyl vinyl ether and tetrazine revealed that the first and rate-limiting step in the reaction sequence is an IEDDA cycloaddition, which is followed by expulsion of N_2.[219] The resulting 4,5-dihydropyridazine tautomerizes to 1,4-dihydropyridazine, which undergoes phenoxy group cleavage to decage the leaving group (**Fig. 43**). The driving force for the elimination is the formation of aromatic pyridazine end-product. Amines (from carbamates), phenols and aliphatic alcohols have been decaged using this reaction. [217-219]

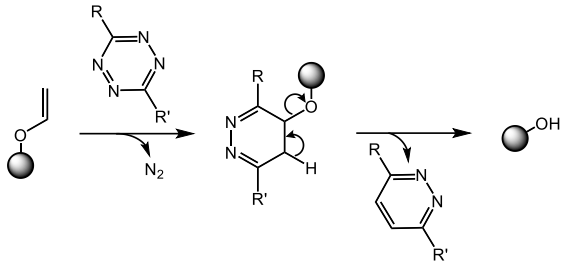

Figure 43. Mechanism of reaction between vinyl ethers and tetrazines. Cycloaddition and expulsion of N_2 gives a pyridazine, which efficiently eliminates the leaving group to aromatize the ring.

A limitation of vinyl ethers as caging groups is the slow rate of the bimolecular reaction (e.g. $k_2 = 5.4\times10^{-4}$ $M^{-1}s^{-1}$ for the reaction between phenyl vinyl ether and 6-pyridyl-tetrazine-3-carboxylic acid[219]) that is orders of magnitude slower than some of the other click-to-release reactions.[92, 123] Bonger *et al.* addressed this limitation by using vinyl boronic acid caging groups inspired by their discovery that these groups react rapidly with dipyridyltetrazines and other tetrazines that can coordinate to the boronic acid (see section 3.2.3.3).[162] As designed, the vinylboronic acid reacted 4-fold faster than unsubstituted vinyl ether with dipyridyltetrazine.[238] However, the rates were lower than that of vinylboronic acids without the ether substituent, which was attributed to the electron-donating nature of the ether on the vinylic position that lowers the Lewis acidity of the boronic acid. Vinylboronic acid derivatives reacted with dipyridyltetrazine to release alcohols (from ethers) and amines (from carbamates) with high yields. Vinylboronic ethers reacting with dipyridyltetrazines are therefore a useful addition to the click-to-release toolbox.

3.4.2. Dienophile-triggered Release Reactions

The release groups described in 3.4.1 are all based on modified dienophiles that eliminate the product by reaction with tetrazines. The inverse design consisting of tetrazines that release a payload by reaction of a dienophile may offer advantages for example to release two groups simultaneously and to overcome some of the rate-limiting effects of dienophile modifications.

3.4.2.1. Isonitrile as Dienophile

Tetrazylmethyl (TzMe) chemistry was independently developed by us and Robillard *et al.* to release groups by reacting with different dienophiles.[94, 220] Isonitriles could effectively release phenol and amine groups from TzMe and tetrazylmethylcarbamate (Tzmoc) groups.[94] The design is based on the idea that the 4-aminopyrazole formed by the reaction of isonitriles with tetrazine would spontaneously eliminate leaving groups at the benzylic positions as has

been described for other 5-membered heterocycles (**Fig. 44a**).[239, 240] Indeed, *n*-BuNC readily release amine and phenol leaving groups from TzMe and Tzmoc moieties, respectively. For example, the release of *p*-nitroaniline from the intermediate formed by the reaction of *n*-BuNC and the 6-*tert*-butyltetrazylmethlyoxycarbonyl derivative occurred at a rate of $k_1 = 1.1\times10^{-5}$ s^{-1}. Mechanistic studies showed that release can occur directly from the imine intermediate without hydrolyzing to 4-aminopyrazole.

An intriguing observation was that (trimethylsilyl)methyl isocyanide was especially effective in mediating the liberation of cargo molecules. The trimethylsilyl group in addition to accelerating the bimolecular step ~3-fold as would be expected from the nature of IEDDA reactions also greatly accelerated the elimination step (30-fold compared to *n*-BuNC). To investigate this unexpected result, NMR studies were carried out, which indicated the cleavage of the C–Si bond to form trimethylsilanol. DFT calculations showed that upon formation of the 4*H*-pyrazol-4-imine (**A1**), water acted as a nucleophile to form the imine **A3** in an S_N2 reaction (**Fig. 44b**). The reaction went through a highly stabilized anion **A2**, making it an excellent leaving group. The calculated barrier for the reaction was 16.4 kcal mol^{-1}, which is in accordance with the fast reaction rates. The TzMe chemistry was combined with ICPr chemistry to achieve dual release of molecules.[94]

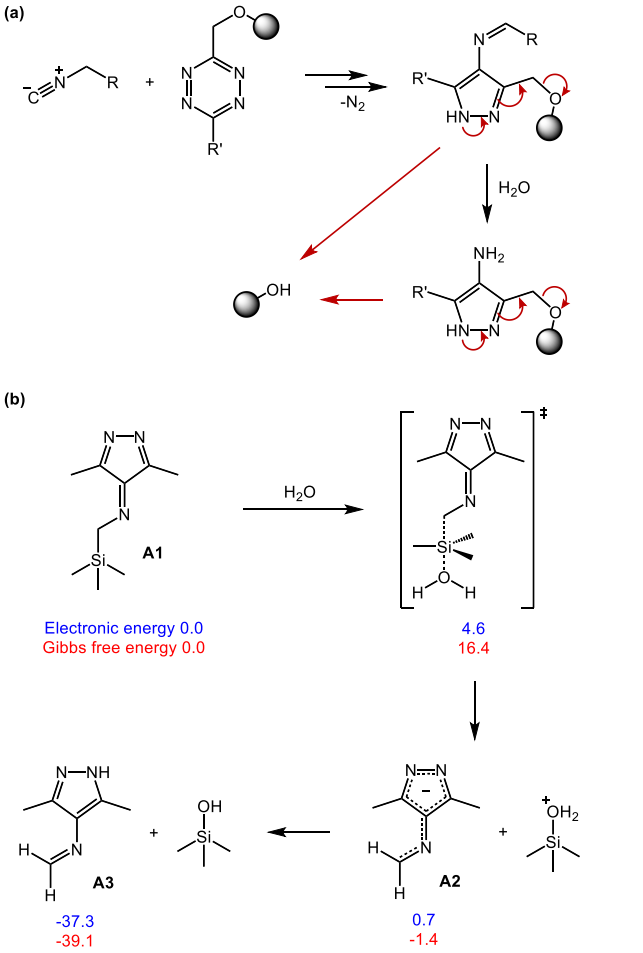

Figure 44. Mechanism of reaction between tetrazylmethyl derivatives and isonitriles. a) Following cycloaddition, cycloreversion and isomerization, release can take place from either imine or aldehyde. b) Lowest energy pathway calculated for the reaction between (trimethylsilyl)methyl isocyanide and tetrazines. C–Si cleavage is induced by water with subsequent protonation.

Therefore, the TzMe chemistry with isonitriles show rapid and tunable bimolecular and elimination rates, which is crucial for the development of bioorthogonal dissociative reactions. It has also shown biocompatibility *in vivo* and can be used for dual release.

3.4.2.2. *trans*-Cyclooctene as Dienophile

Robillard and co-workers used TCO as the triggering dienophile to uncage TzMe-protecting groups.[220] Mechanistically, upon cycloaddition of TCO and tetrazine, the 4,5-dihydropyridazine tautomerizes to the 2,5-tautomer (major) and 1,4-tautomer (minor). When the tetrazine is substituted with a methylene-linked carbamate, a 1,4-elimination of the carbamate leads to the liberation of leaving groups from the 2,5-tautomer, which was shown through spectroscopic studies to be the releasing tautomer (**Fig. 45**). Acidic

conditions accelerated the tautomerization step and promoted uncaging of the payload.[221] Release half-lives ranged from 1.5 to 10 h. Structure-activity relationships revealed that release is facilitated by a methyl substituent on the methylene bridge to the tetrazine due to the stabilization of the increasing positive charge during the release step. An *N*-methyl substituent on the carbamate -NH was also found to be crucial for high-yielding release. Payload release correlated with the water content in the reaction medium. This dependence was proposed to be caused by the aqueous stabilization of charges formed upon elimination, or as a result of water acting as a proton carrier in a proton-assisted cleavage mechanism.[220]

The TCO-TzMe chemistry offers a reactivity advantage over the traditional release chemistry with the leaving group on the TCO: the use of more reactive TCOs, which are too unstable for a cleavage reaction from TCO, is permissible.[55, 220] For instance, sTCO, which reacts with tetrazines in the fastest known bioorthogonal reaction, reacted with methylene-linked tetrazines with rates of up to 23,800 M^{-1} s^{-1} (25% MeCN/PBS), which is significantly faster than the reaction with unsubstituted TCO.[220] The TCO-triggered elimination from TzMe was demonstrated in a biological environment by releasing MMAE, a chemotherapeutic drug, from an antibody-drug conjugate. Norbornene and cyclopropane also can induce the release of groups from the benzylic position of tetrazines.[94]

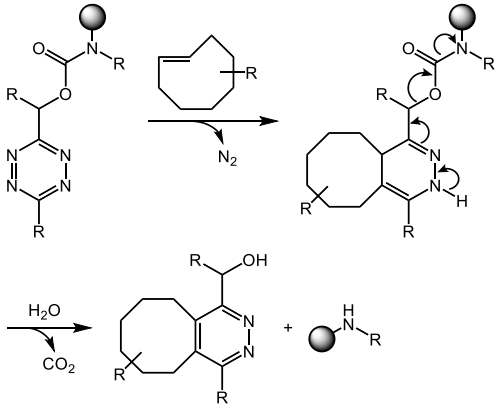

Figure 45. Mechanism of payload release from tetrazylmethyl derivatives triggered by TCO.

3.4.2.3. Cyclooctyne as Dienophile

Highly strained cyclooctynes are known to be robust dienophiles for IEDDA reactions.[82] Wang *et al.* linked the reaction between cyclooctynes and tetrazines to a release step and showed release of the drug doxorubicin as a proof of concept.[83] By using a propargylic alcohol substituent on the dienophile and linking the drug to the tetrazine through an amide linkage, they developed the 'click, cyclization and release system'. Cycloaddition of the two reactants yielded a cyclooctene-fused pyridazine, which then underwent lactonization between the alcohol and amide to release the active drug (**Fig. 46**). Two regio-isomers were possible in the reaction, of which only one would lead to lactonization and drug release. Fortunately, the reaction was found to favor the desired isomer, which was also confirmed by theoretical calculations to have a lower activation barrier. This regioselectivity resulted in release yields of over 80%. The bimolecular rate was found to be highly dependent on the substituent at the propargylic position, and a methyl substituent decreased the rate by >30-fold compared to the unsubstituted reactant.

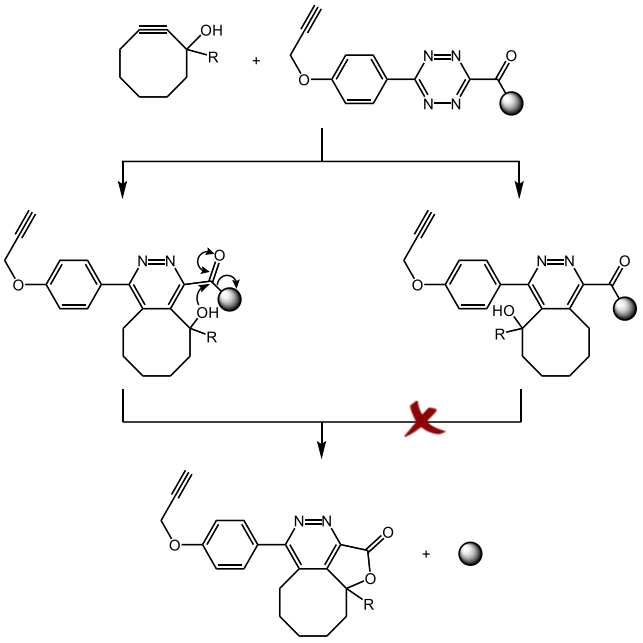

Figure 46. Mechanism of payload release from cyclooctynes triggered by tetrazines. Two regioisomers are possible. The releasing isomer undergoes lactonization and liberates the payload.

The authors also used a cyclooctyne-cyclopentadienone reaction pair, which released the neurotransmitter carbon monoxide upon cycloaddition.[209, 210] In a later study, the two prodrugs were combined for the dual release of doxorubicin and CO.[241] The novel 'click, cyclization and release' approach to dissociative bioorthogonal chemistry, as opposed to the traditional 'click and release' chemistry can open up new opportunities for drug design.

3.5 Summary of IEDDA Reactions in Bioorthogonal Chemistry

The IEDDA reaction and in particular the reaction of tetrazines and a series of dienophiles have greatly impacted bioorthogonal chemistry.[12, 56] A distinct feature of these reactions are that they can be extremely fast. Combined with the synthetic accessibility and the physiological stability of the reactants, this has made IEDDA reactions the fastest

growing area in bioorthogonal chemistry. The chemistry has found widespread applications and even opened new opportunities in drug delivery.[83, 123, 124]

4. 1,3-DIPOLAR CYCLOADDITIONS

A class of pericyclic reactions that has been widely used in bioorthogonal chemistry is the 1,3-dipolar cycloaddition. This cycloaddition occurs between a polarized 1,3-dipole molecule comprising of three atoms and a dipolarophile of two atoms (**Fig. 47**). 1,3-dipolar cycloaddition transformations have been known and studied since the discovery of diazoacetic ester by Curtius in 1883,[242] which Buchner in 1888 used in the first disclosed 1,3-dipolar cycloaddition with α,β-unsaturated esters.[243] The synthetic utility of such reactions for the construction of 5-membered ring systems became apparent in the 1960s when Huisgen established systematic studies on its mechanism based on kinetics, stereochemistry, solvent, and substituent effects.[244-246] The development of the theory of conservation of orbital symmetry by Woodward and Hoffmann greatly aided the theoretical understanding of this concerted pericyclic reaction (see section 2.2).

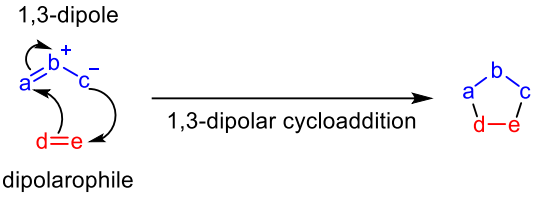

Figure 47. General concerted pericyclic mechanism of 1,3-dipolar cycloaddition reactions between 1,3-dipoles and dipolarophiles.

Useful bioorthogonal reactions involve reactants that exhibit high chemoselectivity and react rapidly with one another while minimally interacting with surrounding biomolecules. The principles of orbital symmetry conservation provide a theoretical basis for the 1,3-dipolar cycloaddition reaction. Mechanistically, the reaction involves the π-systems of the 1,3-dipole and dipolarophile, with HOMO and LUMO interactions dictating reactivity. The 1,3-dipole and dipolarophile are minimally reactive towards nucleophiles and electrophiles providing high orthogonality to biological molecules. An additional factor to consider for the use of the 1,3-dipolar cycloadditions in bioorthogonal chemistry is the bimolecular reaction rate. While typically not a major concern for synthetic chemists, bioorthogonal reactions need to proceed rapidly to be used on biomolecules of low abundance or to monitor biological processes occurring on the timescale of minutes. Through understanding the reaction mechanism, chemists have been able to employ structural changes to tune the reaction partners to achieve fast second-order kinetics. [8, 135, 247] These properties provide the basis for the use of 1,3-dipolar cycloadditions in bioorthogonal chemistry.

All 1,3-dipolar cycloadditions involve a three-atom 1,3-dipole and a two-atom dipolarophile (alkene or alkyne) to form a five-membered ring (**Fig. 47**). The azide group, because of its absence from living organisms and inert reactivity towards biological functional groups, is the most used 1,3-dipole in bioorthogonal chemistry.[8] The dipolarophile partners used are typically electron-deficient and/or highly strained molecules. Understanding the chemical advancements to the 1,3-dipolar cycloaddition in bioorthogonal chemistry requires a deeper appreciation of the general reactivities of its individual components as discussed in the following sections.

4.1. Structure of Dipolarophiles and 1,3-Dipoles

In 1,3-dipolar cycloadditions, the 2π reactant is the dipolarophile, which can be virtually any alkene or alkyne. The chemical properties that affect the reactivity of dipolarophiles used in bioorthogonal chemistry are discussed in section 4.5. The 4π-component is referred to as the 1,3-dipole, a three-atom molecule commonly defined as an a—b—c structure with four π-electrons delocalized over the three atoms (**Fig. 48**).[245] 1,3-Dipoles can be divided into two categories: those that have an allyl anion or a propargyl/allenyl anion type system. These molecules can be drawn as two resonance structures either with the central atom b having an electron octet or as either atom a or c having an electron sextet (**Fig. 48**). Representative 1,3-dipoles are depicted in **Table 1** (single resonance structure shown). Those of the allyl anion type are characterized by four electrons in three parallel p_z-orbitals perpendicular to the plane of the dipole affording a bent structure. Alternatively, an additional double bond (π orbital) orthogonal to the allenyl anion type molecular orbital causes the propargyl/allenyl anion type molecules to be nearly linear.[248] The additional double bond in the propargly/allenyl anion type has little effect on the cycloaddition reactions because the 4π allyl system governs the reactivity.[245]

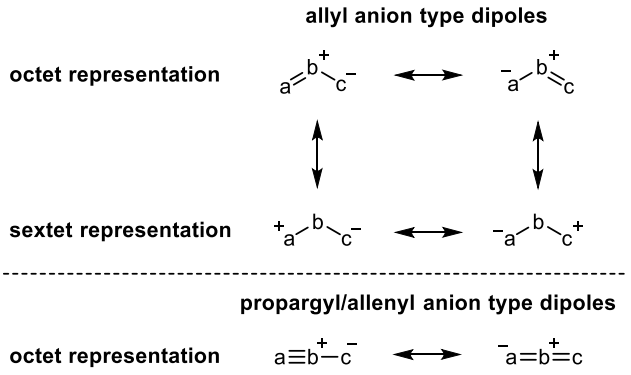

Figure 48. Basic resonance structures of allyl anion and propargyl/allenyl anion type 1,3-dipoles.

1,3-Dipoles consist principally of elements from main groups IV, V, and VI. In allyl-type dipoles, the central atom b is commonly from group V or VI (N or O) while in the propargyl/allenyl type, the central atom b is limited to nitrogen, as only a group V element can harbor a positive charge in the tetravalent state. Higher row elements such as phosphorus or sulfur rarely occur in 1,3-dipoles.[249]

Table 1. Examples of 1,3-dipoles

Allyl anion type dipoles

Nitrogen-centered		Oxygen-centered	
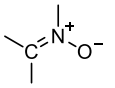	Nitrones	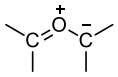	Carbonyl ylides
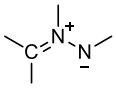	Azomethine imines	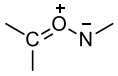	Carbonyl imines
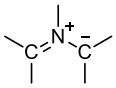	Azomethine ylides	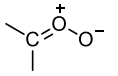	Carbonyl oxides
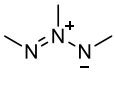	Azimines	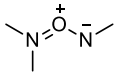	Nitrosimines
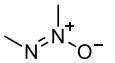	Azoxy compounds	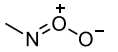	Nitrosoxides
	Nitro compounds		Ozone

Propargyl/allenyl anion type dipoles

Nitrilium betaines		Diazonium betaines	
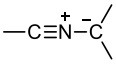	Nitrile ylides	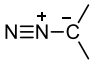	Diazoalkanes
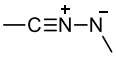	Nitrile imines	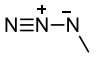	Azides
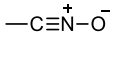	Nitrile oxides	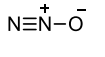	Nitrous oxides

4.2. General Mechanism of 1,3-Dipolar Cycloaddition Reactions

Several reaction mechanisms were initially proposed for 1,3-dipolar cycloadditions and the mechanism was subject to extensive debates in the 1960s. Three types of reaction pathways were initially proposed that proceed through either a concerted mechanism,[245, 250, 251] involved singlet diradical intermediates,[252-255] or zwitterionic intermediates[256] (**Fig. 49**).

Huisgen *et al.* presented extensive experimental data supporting a concerted mechanism.[244-246, 250, 251] Concerted 1,3-dipolar cycloadditions are thermally allowed [$\pi^4s + \pi^2s$] reactions according to the Woodward-Hoffmann rules between a 1,3-dipole and a dipolarophile (**Fig. 3**). In the concerted mechanism, the three p_z orbitals from the 1,3-dipole and the two p_z orbitals from the dipolarophile arrange in two parallel planes to combine stereospecifically in a suprafacial manner (**Fig. 49**).[249] As an alternative to the concerted mechanism, Firestone proposed a two-step mechanism for the 1,3-dipolar cycloaddition.[252-255] This stepwise mechanism involved a spin-paired diradical intermediate (**Fig. 49**). A mechanism involving a zwitterionic intermediate has also been proposed.[256]

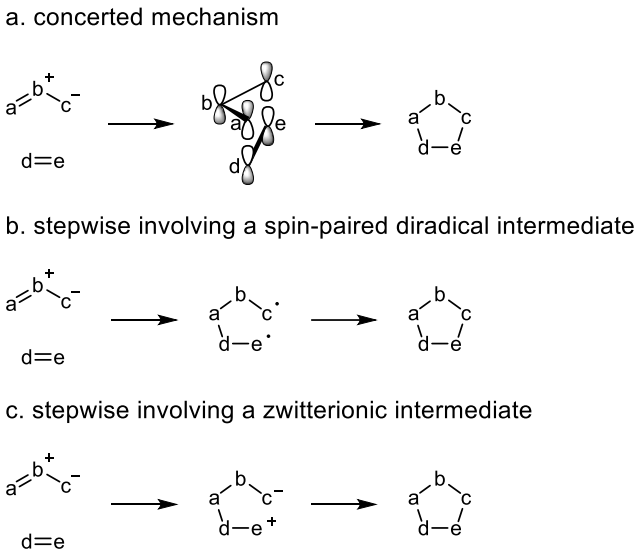

Figure 49. Postulated mechanisms for 1,3-dipolar cycloaddition reactions: concerted mechanism, stepwise mechanism involving a spin-paired diradical intermediate, and stepwise mechanism involving a zwitterionic intermediate.

Rigorous studies to identify the nature of the 1,3-dipolar cycloadditions yielded convincing evidence that the majority of such reactions proceed through a concerted mechanism (**Fig. 49**). Analysis of the effect of solvent polarity on the reaction provided important mechanistic evidence.[257, 258] The influence of solvent polarity on the reaction rate is typically modest for 1,3-dipolar cycloadditions. For example, the rate of the reaction between N-benzylidenemethylamine N-oxide and ethyl acrylate increased less than 6-fold when changing solvents from toluene to DMSO, despite a 20-fold increase in the dielectric constants between the two solvents.[257, 258] Such an outcome is difficult to reconcile with a mechanism involving a zwitterionic species (**Fig. 49**), because the rate enhancement from solvent polarity is typically considerably more pronounced for cycloadditions going through a zwitterionic intermediate. For example, the rate constants for the cycloaddition of tetracyanoethylene to anethole, 2,3-dihydro-4H-pyrane, or butyl vinyl ether,

reactions known to involve a zwitterionic intermediate, increased by factors of 29,000, 17,000, and 2,600, respectively, in going from the non-polar cyclohexane to the polar acetonitrile solvent.[259] However, the lack of solvent effect is also consistent with 1,3-dipolar cycloadditions that proceed via spin-paired diradical species (**Fig. 49**). The formation of minimal byproducts when considering regioselectivity in the nitrone-olefin reaction provided further support for a radical mechanism. For example, the reaction between benzonitrile oxide and styrene or methyl acrylate gave the 5-substituted isooxazoline as the predominant product, which is readily rationalized by a mechanism involving a diradical intermediate because of the higher stability afforded to secondary radicals (**Fig. 50**).[255]

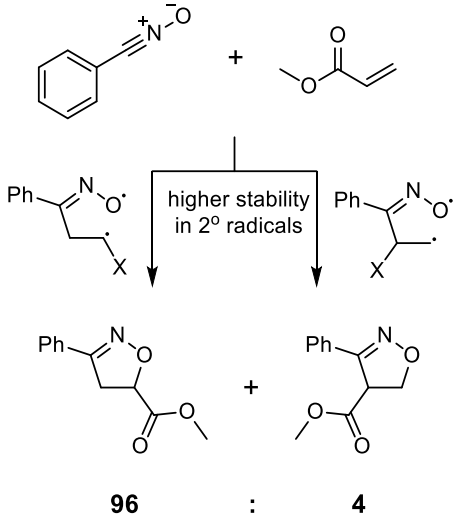

Figure 50. Regioselectivity observed in the reactions between benzonitrile oxide and styrene or methyl acrylate can be rationalized by considering the stability of possible diradical intermediates.

A collaboration between Houk and Firestone eventually demonstrated a concerted cycloaddition mechanism through computational means and stereochemical results.[260] It is possible to distinguish between a concerted and a stepwise mechanism by analyzing the stereochemistry of the products. If the reaction proceeded via a diradical intermediate, a 180° rotation at the terminal bond would be allowed, forming a mixture of the *cis* and *trans* products. Instead, in support of a concerted mechanism, only a single suprafacially produced stereoisomer was observed experimentally as the product from a cycloaddition reaction. The reaction between benzonitrile oxide and *trans*-dideuterated ethylene yielded *trans*-isoxazoline as the only product (>98%, **Fig. 51**).[260] A diradical intermediate is conceivable assuming that the rotation of the intermediate is slower than the rate of ring closure to the product. However, through computational calculations, it was determined that if a diradical intermediate were formed, the barrier to rotation about the terminal bond would have to be at least 2.3 kcal mol^{-1} higher than the barrier to cyclization for it to form only one isomer. Because the computed rotational barrier of the bond in question is <0.4 kcal mol^{-1} (value excepted for a normal primary radical), it makes a concerted mechanism the most plausible reaction path.[260] Although rare cases of stepwise 1,3-dipolar cycloadditions that involved an intermediate that destroys stereospecificity have been observed,[261, 262] the 1,3-dipolar reactions used in bioorthogonal chemistry follow a concerted mechanism.

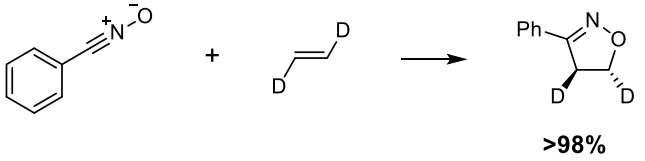

Figure 51. Stereoselectivity in the reaction between benzonitrile oxide and *trans*-dideuterated ethylene gave virtually exclusively the *trans*-isoxazoline product, supporting a concerted mechanism.

4.3. Orbital Interactions in 1,3-Dipolar Cycloadditions

Considerations of the interactions of the frontier orbitals of the reactants provide effective rationales for understanding 1,3-dipolar cycloaddition reactions (**Fig. 52**). Sustmann first applied FMO theory to 1,3-dipolar cycloaddition reactions and classified them into three types based on the relative FMO energies between the dipole and dipolarophile as discussed in section 2.2 (**Fig. 4**).

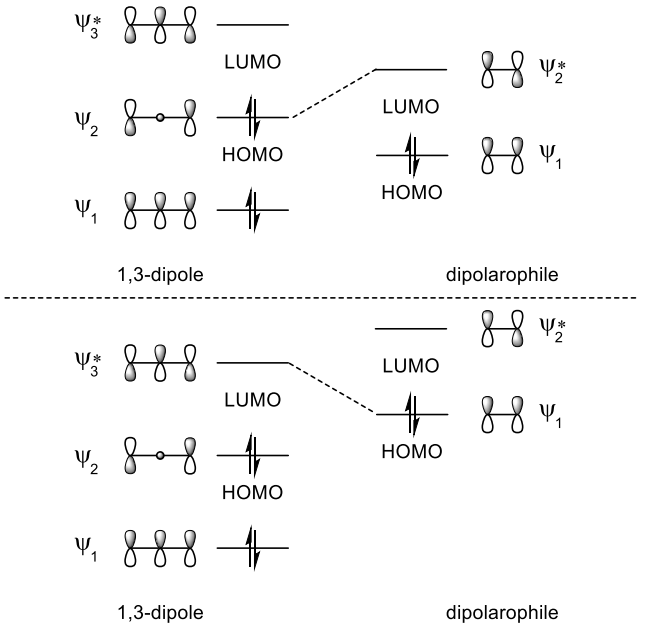

Figure 52. Molecular orbital interactions of a 1,3-dipole and a dipolarophile.

Type I reactions include 1,3-dipoles such as the carbonyl ylide, nitrile ylide, azomethine ylide, and carbonyl imine (**Table 1**). These reactions are HOMO-controlled dipole or nucleophilic dipole reactions in which the 1,3-dipole readily reacts with electrophilic dipolarophiles. Electron-withdrawing groups (EWG) on the dipolarophile increase the rate of the reaction by lowering the LUMO whereas electron donating groups (EDG) decrease the rate of the reaction. Type II reactions encompass ambiphilic dipoles, which are dipoles that exhibit both electrophilic and nucleophilic character, such as nitrones, nitrile oxides, and azides. Type II reactions are the ones primarily employed in bioorthogonal applications. Because these reactions are dominated by either the $HOMO_{dipole}$—$LUMO_{dipolarophile}$ interaction or the $HOMO_{dipolarophile}$—$LUMO_{dipole}$ interaction, substituents on either the dipole or dipolarophile can accelerate the reaction by decreasing the energy gap. For example, adding EDG or EWG to an alkene dipolarophile markedly enhanced the rate of cycloaddition to both phenyl azide and benzonitrile oxide (**Fig. 53**).[244, 263] A more in-depth discussion of the type II azide reaction is provided in sections 4.4 and 4.5 because it is the most prominent type in a bioorthogonal context. Lastly, type III reactions are the rarest and include dipoles such as nitrous oxide, sydnones, and ozone. In contrast to type I reactions, these reactions are LUMO-controlled dipole or electrophilic dipole reactions. EWG on the dipolarophile decreases the rate of type III reactions while EDG accelerate the reaction by raising the energy of the HOMO.

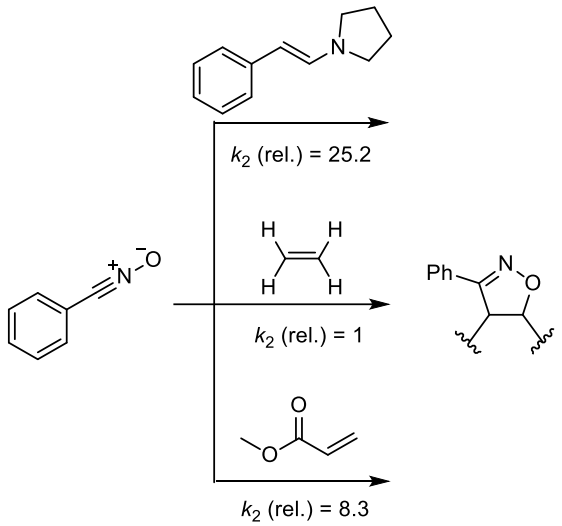

Figure 53. Adding either EDG or EWG to an alkene dipolarophile enhanced the rate of 1,3-dipolar cycloaddition to benzonitrile as demonstrated by the relative rate constants shown

4.4. 1,3-Dipoles in Bioorthogonal Chemistry

1,3-dipolar cycloaddition reactions involving various dipoles (**Table 1**) are employed extensively in synthetic chemistry to construct 5-membered heterocycles. However, only a select few 1,3-dipoles have been implemented in bioorthogonal chemistry, which will be highlighted herein, while stability concerns make others unsuitable for use in biologically relevant environments. Azides are by far the most widely employed 1,3-dipoles in a bioorthogonal context. Other such 1,3-dipoles include nitrile oxides, nitrones, nitrile imines, diazoalkanes, and sydnones. The various dipoles have their individual benefits and complications that are discussed in the subsequent sections.

4.4.1. Azides

The most prevalent 1,3-dipole in bioorthogonal chemistry is the azide group. Early kinetic experiments demonstrated that in reactions with phenyl azide, both electron-donating and electron-withdrawing substituents on the alkene dipolarophile increase the reaction rate, exhibiting typical type II dipole behavior (see section 4.3).[244] Hammett relationships were also determined for the reaction between 4-substituted phenyl azides and olefins (**Fig. 54**).[244] Reactions with maleic anhydride and N-phenyl maleimide afforded negative ρ values (-0.8 and -1.1, respectively). In contrast, the reaction with pyrrolidino-cyclohexene provided a positive ρ value of 2.5. Therefore, electron-poor olefins prefer electron-rich phenyl azides, whereas electron-rich and neutral alkenes react faster with phenyl azides that have electron-withdrawing substituents. The sign of the ρ-values allows for the recognition of the dominant HOMO-LUMO interaction. A negative ρ-value indicates that the $HOMO_{dipole}$-$LUMO_{dipolarophile}$ is the reactivity-determining interaction whereas a positive ρ-value indicates $LUMO_{dipole}$-$HOMO_{dipolarophile}$ as the leading interaction. In conclusion, for aryl azides, the dominant FMO interaction is between $LUMO_{dipole}$-$HOMO_{dipolarophile}$, where electron-donating groups on the dipolarophile increase reactivity (see section 4.6).

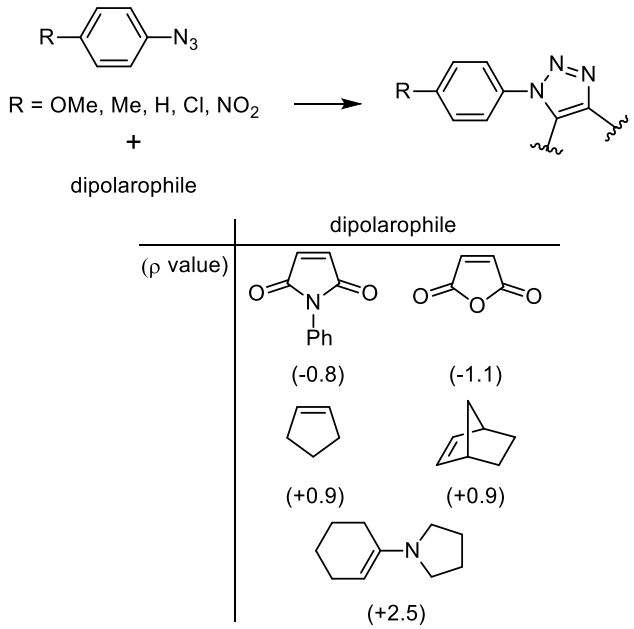

Figure 54. Hammett correlations in 1,3-dipolar cycloadditions of alkenes of different electron density with 4-subsituted phenyl azides

In contrast to aryl azides, Houk, Henri-Rousseau and coworkers used computational models to explain that aliphatic azides (and other type II dipoles) are electron-rich ylide species, characterized by having both high-lying HOMOs and LUMOs.[37] Therefore, the reaction between a type II dipole and a dipolarophile is dominated by the $HOMO_{dipole}$—$LUMO_{dipolarophile}$ interaction and such dipoles preferentially react with electron-deficient olefins. More recent studies have elucidated substituent effects of azides on the strain-promoted azide-alkyne cycloaddition (SPAAC) reaction (discussed in more detail in section 4.5), which is arguably the most widely implemented 1,3-dipolar cycloaddition transformation in bioorthogonal chemistry.[8] Indeed, a recent study investigated the reactivity of aryl azides to aliphatic cyclooctynes in the SPAAC reaction. Further corroborating the Hammett relationship observed by Huisgen *et al.* (**Fig. 54**), it was demonstrated that aliphatic and aromatic azides display a striking difference in reactivity, as they prefer either benzoannulated or aliphatic cyclooctynes, respectively.[264] The dominant FMO interaction involved in the reaction between aliphatic cyclooctyne bicyclo[6.1.0]nonyne (BCN) and an aromatic azide is between the $LUMO_{dipole}$-$HOMO_{dipolarophile}$ as expected from previous studies.[244, 264]

However, unexpectedly, the sterically-congested azido group of 2,6-disubstituted phenyl azides, despite the steric hindrance, reacts significantly faster than unsubstituted phenyl azide in the 1,3-dipolar cycloaddition with an alkyne.[265] Experimental and computational work indicated that the steric hindrance inhibited the resonance between the azido group and the aromatic ring,[265] effectively enhancing the reactivity by assumably shifting the major FMO interaction to between the $HOMO_{dipole}$—$LUMO_{dipolarophile}$. Indeed, in a follow-up study, it was shown that the introduction of an amino group at the *para* position of the doubly sterically-hindered aryl azides significantly enhanced their reactivity towards strained alkynes;[266] the electron-donating *para*-amino group increases the HOMO energy level of the azide, effectively decreasing the gap between the $HOMO_{dipole}$—$LUMO_{dipolarophile}$. Furthermore, using the distortion/interaction model (see section 2.3), it was found that the two bulky *ortho* substituents enhance the distortability of the azido group.[266] The same group recently investigated the effect of resonance and its inhibition by steric hindrance on the reactivity of various alkyl and alkenyl azides towards aliphatic cycloalkynes.[267] It was observed that the resonance that exists between the azido and alkenyl groups slow the cycloaddition rate. However, the introduction of a phenyl group to the alkenyl azide significantly accelerated its cycloaddition reaction rate to that comparable to the cycloaddition rates aliphatic azides exhibit as the phenyl group effectively inhibits the resonance between the two groups.[267] Continued work towards understanding the reactivity of azides towards strained cycloalkynes will further expand the usefulness of the SPAAC reaction in various schemes in chemical biology.

4.4.2. Nitrile Oxides

Nitrile oxides boast faster reaction rates compared to azides in 1,3-dipolar cycloaddition reactions. A computational study predicted an activation barrier of 20.2 kcal mol^{-1} for the uncatalyzed cycloaddition between acetonitrile oxide and propyne, which is 6 kcal mol^{-1} lower than that for a reaction between methyl azide and propyne.[268] Experimentally, 4-dibenzocyclooctynol (DIBO) reacted 57-fold faster with a nitrile oxide derived from imidoyl chloride than with benzyl azide (**Fig. 55**).[269]

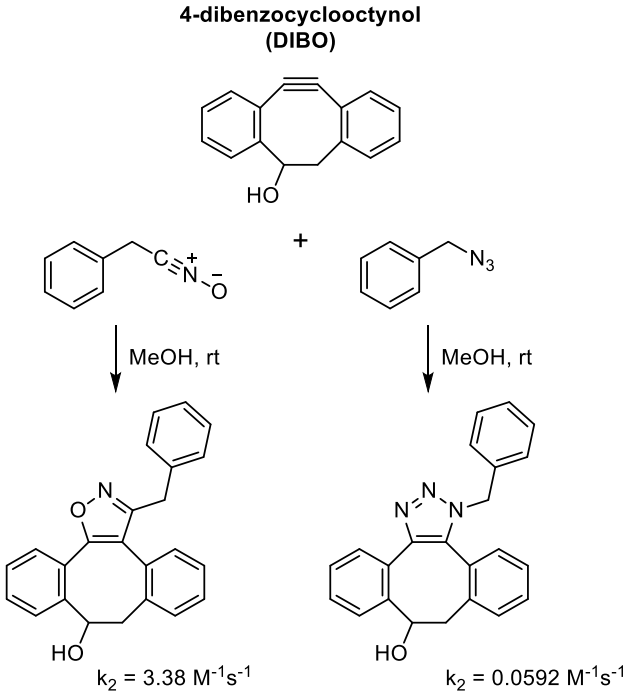

Figure 55. Rate constants of cycloadditions of DIBO with either a nitrile oxide or azide demonstrating the more rapid bimolecular kinetics achieved with nitrile oxide dipoles. The nitrile oxide was generated in the presence of triethylamine from the corresponding imidoyl chloride precursor.

However, nitrile oxides decompose under physiological conditions and must be generated *in situ*. Nitrile oxides can be generated either through the exposure of an imidoyl chloride precursor to a base or by oxidation of an oxime precursor by [bis(acetoxy)iodo]benzene (BAIB; **Fig. 56**).[269] In one-pot oxidation/conjugation reaction schemes, it was established that the oxidation step by BAIB is fast and the cycloaddition is rate-limiting.[269] However, employing an oxidant is problematic in living systems. Furthermore, nitrile oxides readily undergo dimerization reactions to form the corresponding furoxans (**Fig. 56a**).[270] Under physiological conditions, the high electrophilicity of the nitrile oxide make it also susceptible to nucleophilic attack by endogenous functional groups (**Fig. 56a**).[271] The reactivity towards

nucleophiles has been exploited in a bioorthogonal reaction of chlorooximes with isonitriles forming stable adducts (**Fig. 56b**).[272]

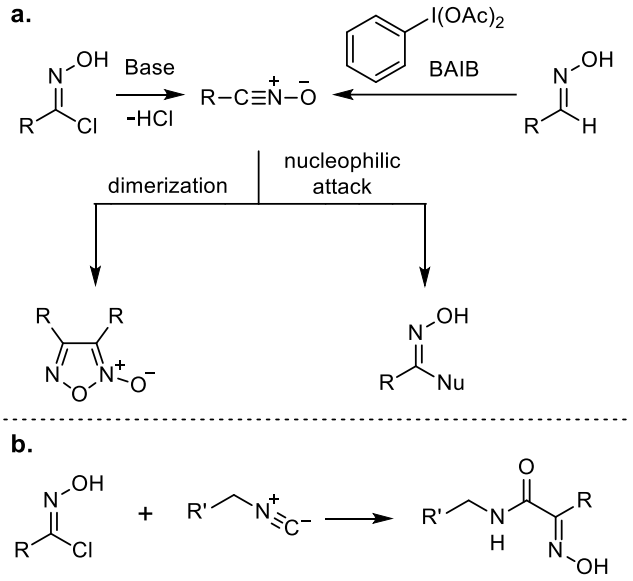

Figure 56. Reactivity of nitrile oxides. a) *In situ* generation of nitrile oxides through use of base or by oxidation with [bis(acetoxy)iodo]benzene and subsequent degradation pathways through dimerization or nucleophilic attack. b) Nucleophilic addition of isonitriles across chlorooximes to achieve stable adducts for bioorthogonal labeling applications

4.4.3. Nitrones

An alternative 1,3-dipole used in bioorthogonal chemistry is the nitrone.[273,274] Nitrones are more stable than nitrile oxides and still provide a 59-fold rate enhancement relative to a reaction between benzyl azide and DIBO (**Fig. 57**).[274] Nitrones are hydrolytically unstable, reverting to the hydroxylamine and carbonyl precursors (**Fig. 58**). Nitrones can also dimerize, which leads to loss of reactivity. However, cyclic nitrones exhibit prolonged stability in aqueous environments compared to their acyclic counterparts[274] because the equilibrium is shifted towards the nitrone in the intramolecular reaction (**Fig. 58**). In either acidic or basic conditions, more than 50% of acyclic nitrones are hydrolyzed back to their corresponding hydroxylamine and carbonyl precursors, while cyclic nitrones were demonstrated to be stable under the same conditions for at least 2 hours.[274]

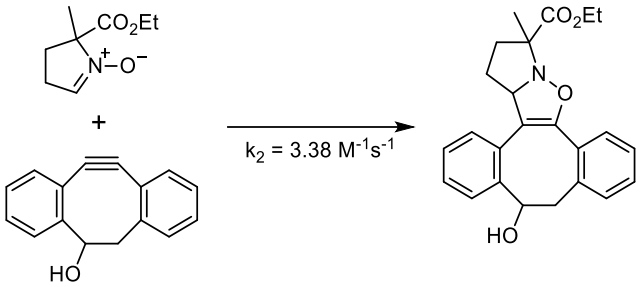

Figure 57. Reaction between DIBO and a cyclic nitrone to form the corresponding isooxazoline product.

Cyclic nitrones were employed in labeling proteins both *in vitro* and on cell surfaces.[274] However, the resulting isoxazole heterocycle from a reaction with nitrile oxides or nitrones contains an N—O bond. It is speculated that such a bond could be sensitive to reductive scission under physiological conditions leading to opening of the heterocyclic ring.[275] Nonetheless, nitrones and nitrile oxides have been employed for the labeling of biomolecules and efforts to employ dipoles other than azides in a bioorthogonal context continue to be pursued.[276]

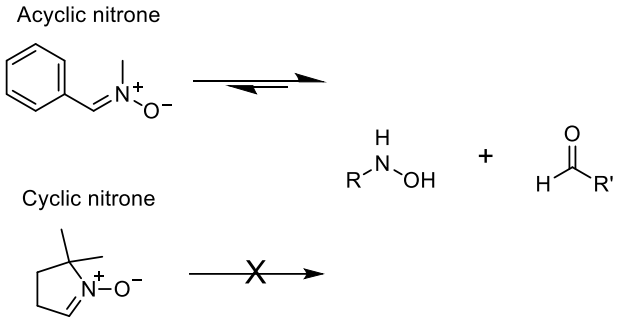

Figure 58. Comparison of equilibrium formation of acyclic and cyclic nitrones.

4.4.4. Nitrile Imines

Another 1,3-dipole requiring *in situ* production is the nitrile imine. Nitrile imines can be generated by elimination of HCl from hydrazonoyl chloride derivatives. Conversion of hydrazonoyl chlorides to nitrile imines occurs spontaneously under ambient temperatures in PBS buffer pH 7.4 and was used to label proteins in a controlled *in vitro* environment.[277] However, the lack of specificity in generating nitrile imines is a limitation of this approach.

Alternatively, nitrile imines can be accessed photochemically, conferring high spatial accuracy to where cycloaddition occurs. Huisgen *et al.* first reported the *in situ* formation of a nitrile imine by photoirradiation of a 2,5-diphenyltetrazole precursor in tandem with a 1,3-dipolar cycloaddition with methyl crotonate.[278] Photoirradiation induces the

expulsion of nitrogen gas from the precursor generating the nitrile imine that readily reacts with methyl crotonate to afford methyl 5-methyl-1,3-diphenyl-4,5-dihydro-1H-pyrazole-4-carboxylate (**Fig. 59**).

Lin *et al.* recognized the potential for photoactivatable dipoles to enhance spatiotemporal resolution in the study of biomolecules.[279] They demonstrated that the photolysis of tetrazoles to generate nitrile imines is highly efficient and the subsequent bimolecular reaction rate between an acrylamide dipolarophile in PBS occurs with a second-order rate constant of k_2 = 11.0 M^{-1} s^{-1},[279] and the use of strained alkenes further enhances the reaction rate.[280]

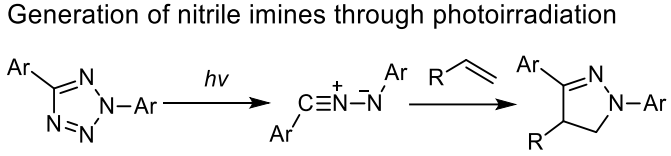

Figure 59. Photoirradiation of tetrazoles generates nitrile imines that can under cycloaddition reactions with dipolarophiles.

A limitation of nitrile imine dipoles is that they are subject to deactivation by water and endogenous nucleophiles.[280] Photoirradiated unencumbered tetrazoles gave a nitrile imine with a half-life of less than 7.5 seconds in PBS:MeCN (1:1). Furthermore, in competition assays, glutathione or water adducts were the predominant products formed over the adduct with various dipolarophiles (example shown with styrene in **Fig. 60**).[280] Lin *et al.* explored whether steric shielding could enhance the biostability of nitrile imines. They attached bulky substituents at the ortho position of the N-aryl ring and measured the rate of the reaction of the corresponding nitrile imines with dipolarophiles and performed competition experiments between 1,3-dipolar cycloadditions and side reactions with water or glutathione (**Fig. 60**).[280] The nitrile imine generated from the sterically shielded tetrazole exhibited a half-life of 102 seconds in PBS:MeCN (1:1), which is about an order of magnitude longer than for unobstructed nitrile imines. In the competition assay, this nitrile imine demonstrated a propensity towards cycloaddition, and the reaction yields with various dipolarophiles were above 85% even in aqueous solutions containing an equal amount of glutathione. For example, in the presence of styrene the sterically shielded nitrile imine resulted in 96% of cycloaddition product, whereas for the simple diphenyltetrazole only 5% cycloaddition product was formed with the GSH-adduct being the predominant product (**Fig. 60**). Bulky substituents can therefore enhance chemoselectivity without interfering with the reaction.

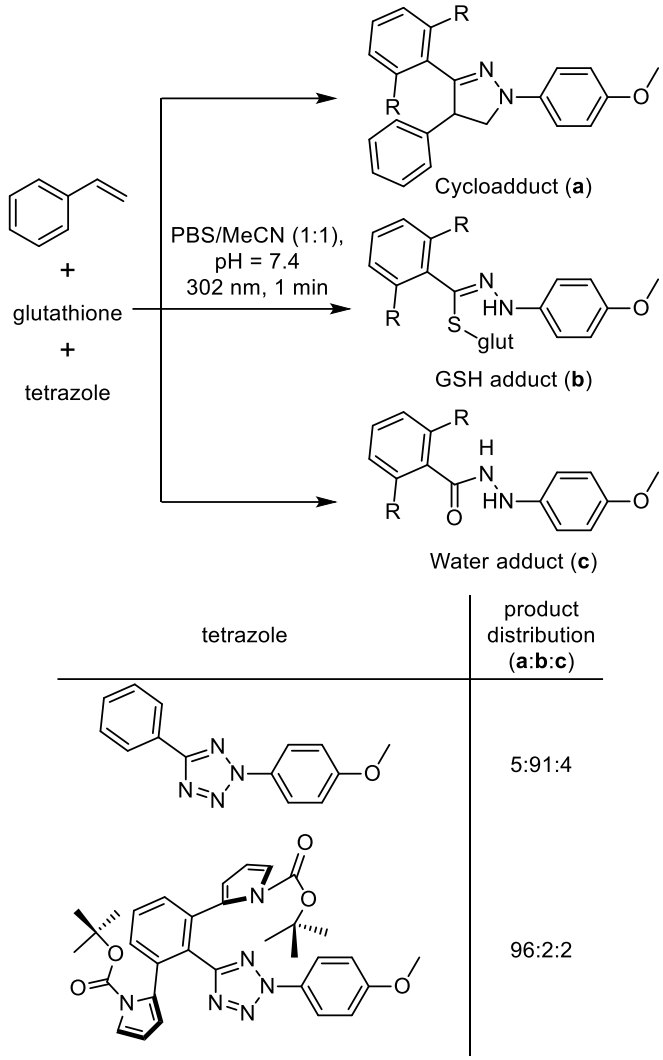

Figure 60. Product distribution of non-sterically hindered and sterically hindered tetrazoles with styrene demonstrating that sterically shielded tetrazole precursors form nitrile imines that prefer to perform the desired cycloaddition over being quenched by glutathione or water

Furthermore, extensive effort has been dedicated to acquiring tetrazoles that generate nitrile imines upon visible light-induced.[281] Initial tetrazoles relied on UV light centered at 302 or 365 nm for ring opening (**12**, **Fig. 61**).[278] UV light in those regions can cause phototoxicity. A 405 nm light activatable terthiophene-tetrazole was designed to alleviate such concerns (**13**, **Fig. 61**).[282] The thiophene moiety was chosen as it accommodates the isosteric tetrazole ring without disrupting the extended π-conjugation system. This tetrazole could be activated by a 405 nm laser and allowed for the spatiotemporal labeling of microtubules in live cells. A near-infrared (NIR) compatible tetrazole was further designed (**14**, **Fig. 61**).[283] These naphthalene tetrazoles showed strong two-photon absorption when excited at 700 nm and led to efficient formation of the nitrile imine. The NIR-responsive tetrazole provided higher signal-to-noise ratios relative to the terthiophene-tetrazole probe.[282] Red-

shifted, photo-controlled probes demonstrating high reactivity and improved spatial control, further increases the utility of nitrile imines in bioorthogonal chemistry.

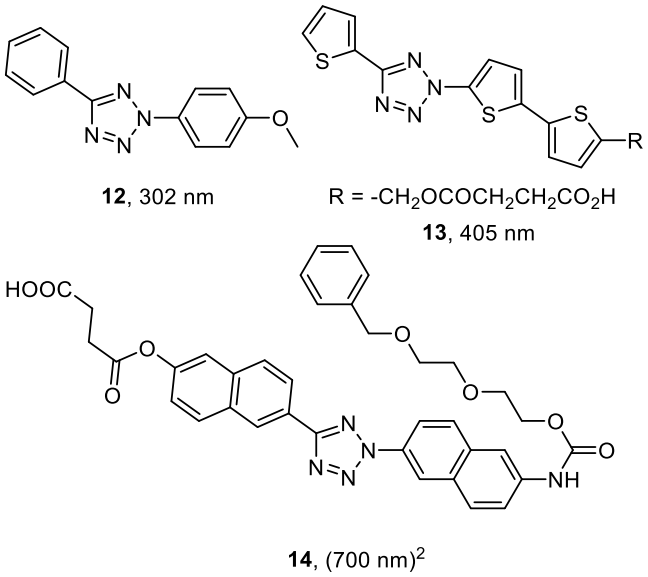

Figure 61. Design of tetrazoles with variable photoactivation wavelengths to generate the nitrile imine 1,3-dipole. Wavelength necessary for photolysis given ((700 nm)^2 indicates two-photon absorption).

4.4.5. Diazoalkanes

Type I and III dipoles are used occasionally in biological settings (**Table 1**). Type I reactants are formally derived from the carbon allyl system by introduction of nitrogen. Reactions involving diazoalkanes have been used in bioorthogonal chemistry and fall under the type I classification.[284] The diazo group has been of immense utility to organic chemists for example in alkylation, carbene generation, and nucleophilic addition reactions.[285]

While diazo compounds are generally highly reactive, diazoacetamides are sufficiently stable under biological conditions to be used in bioorthogonal chemistry.[286, 287] Furthermore, they are synthetically accessible from azidoacetamide precursors (see section 5.8.2).[288] The reactions of diazo compounds with alkenes and alkynes have been known for decades;[243] however, it was Raines *et al.* that first introduced the reaction to bioorthogonal chemistry.[289] The Raines group used diazoacetamides in reactions with peptides[286] and for labeling studies on cell surfaces by metabolically incorporating sugars containing the diazoacetate functionality.[287] Leeper *et al.* also used the reaction of diazoacetamides with strained alkynes for protein labeling.[290] Being a type I reaction, the diazo group reacts rapidly with electron-deficient olefins to form pyrazolines (**Fig. 62**). Kinetics experiments with diphenyldiazomethane show an increase in reactivity with the number and strength of electron-withdrawing groups in the olefin.[284] For example, a 1750-fold rate enhancement was demonstrated in reactions between diphenyldiazomethane and dimethyl fumarate relative to that with styrene (**Fig. 62**).[284]

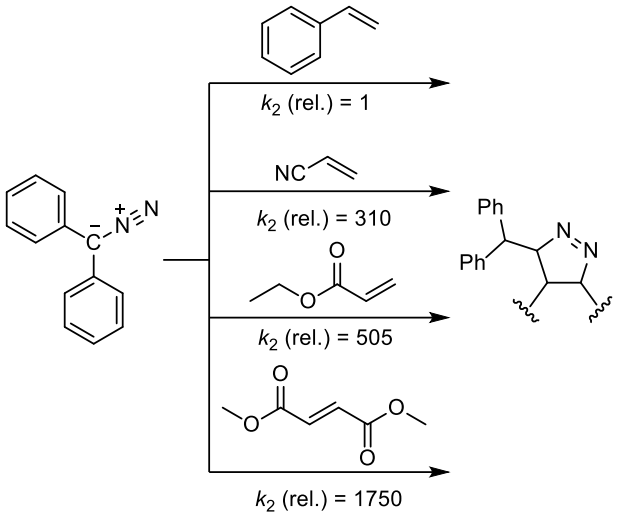

Figure 62. Increasing the number and strength of electron-withdrawing groups on the dipolarophile leads to an increased rate of 1,3-dipolar cycloaddition to a diazoalkane type 1,3-dipole as demonstrated by the relative rate constants shown with diphenyldiazomethane. Pyrazolines are formed as products.

4.4.6. Sydnones

A type III cycloaddition involving a reaction between sydnones and strained alkynes has been gaining traction as a bioorthogonal reaction.[291] Sydnones are part of a class of molecules known as mesoionic compounds.[292] Mesoionic compounds are 5-membered aromatic heterocycles encompassing two opposite charges.[293] While Huisgen identified several mesoionic compounds that react with alkene and alkyne dipolarophiles,[294, 295] sydnones have attracted the most attention in bioorthogonal chemistry because of their stability and ease of synthesis. Simple sydnones such as phenyl sydnone can be prepared in two steps from N-phenyl glycine via N-nitrosylation followed by intramolecular cyclization using acetic anhydride.[296] Sydnones have been used in various schemes involving protein labeling in aqueous buffer environments at 37°C.[297]

In 1968, Huisgen and Gotthardt initially investigated the reaction of 4-methyl-3-phenylsydnone with various acetylenes and found that electron-poor alkynes reacted faster than electron-rich alkynes (acetylene(di)carboxylate reacted 430-fold faster than tetradic-1-yne), although several outliers were observed.[298] Such a result is indicative of a type II or even a type I 1,3-dipolar cycloaddition. However, using semi-empirical quantum calculations, in 1973 Houk *et*

al. calculated the average HOMO and LUMO energies for azomethine-imines (HOMO = -8.6 eV and LUMO = 0.3 eV) as the dipole underlying the structure of sydnones. They predicted that an electron-withdrawing carboxylate group would decrease the LUMO energy of the sydnone. This result implies that sydnones are involved in a LUMO-controlled type III reaction.[299] For the reaction between 4-substitued phenyl sydnones with dimethyl acetylenedicarboxylate (DMAD), positive Hammett ρ-values were observed, confirming that these reactions are LUMO-controlled.[300]

Interest in using sydnones in bioorthogonal chemistry has recently prompted studies on their cycloaddition with strained cycloalkynes. Hammett correlations were plotted for a kinetics study involving 3-phenylsydnones with substituents at the 4-position of the phenyl ring reacting with bicyclo[6.1.0]nonyne (BCN).[301] The study revealed a ρ-value of 1.35, which is in agreement with a type III mechanism. However, although it is likely that sydnones participate in reactions with dipolarophiles in a LUMO-controlled fashion, factors other than HOMO-LUMO interactions may principally influence sydnone reactivity. The effect of sterics on the rates of sydnone reacting with strained alkynes appear to be modest. For example, large substituents at the 4-position of the sydnone have little effect on the reaction and 4-phenylsydnone reacts with comparable rates with BCN as unsubstituted sydnones.[302]

A study conducted on the reactivity of 4-substituted sydnones with BCN shed light into a major causative factor that governs the reactivity of sydnones towards strained cycloalkynes.[303] According to FMO theory and following a type III reaction, the primary orbital interactions between the sydnone and BCN involves the LUMO of the sydnone and the HOMO of BCN. However, it was found empirically that 4-halogen substituents increased the reactivity of sydnones more than traditional electron-withdrawing groups such as the cyano group.[303] This trend was confirmed in theoretical studies, and calculated activation energies for 4-halogen substituted sydnones (4-fluoro-sydnone ΔG = 16.7 kcal mol^{-1}) were lower than those of 4-nitrile containing sydnones (4-nitrile-sydnone ΔG = 22.6 kcal mol^{-1}). Interestingly, calculated LUMO levels revealed that the 4-cyanosydnone has a lower-lying LUMO compared to 4-fluorosydnone (0.40 versus 0.81 eV). Moreover, comparing 4-fluorosydnone to 4*H*-sydnone, the decrease in LUMO energy levels is small (0.81 versus 0.99 eV). Therefore, the LUMO-lowering ability of the 4-fluoro substituent only partially explains its reactivity-enhancing effect.

Employing the distortion/interaction model (see section 2.3), it was found that the primary mechanism by which fluoro substituents at the C4 position increase the reaction with dipolarophiles is that it facilitates the distortion of the sydnone.[303] This effect accounts for a decrease in the activation energy of 5 kcal mol^{-1}. A comparison between the reactivity of 4-cyano versus 4-unsubstituted sydnone further exemplifies the importance of distortion/interaction energies. Although the LUMO level of the 4-cyanosydnone is lower than that of unsubstituted sydnone (0.40 versus 0.99 eV), the measured reaction rate is 10-fold slower (0.003 M^{-1}s^{-1} versus 0.03 M^{-1}s^{-1}). According to the distortion/interaction model, while the 4-cyano increases the stabilizing interaction energy between the reactants, it also increases the energy needed to distort the reactant in the transition state (16.6 kcal mol^{-1} for 4-cyanosydnone versus 13.6 kcal mol^{-1} for 4*H*-sydnone), leading to an overall higher reaction barrier compared to 4-unsubstituted sydnone (22.6 versus 21.7 kcal mol-1). Therefore, the sydnone distortion and interaction energies are the major influencing factors that control their reactivity towards strained alkynes (**Fig. 63**).[303]

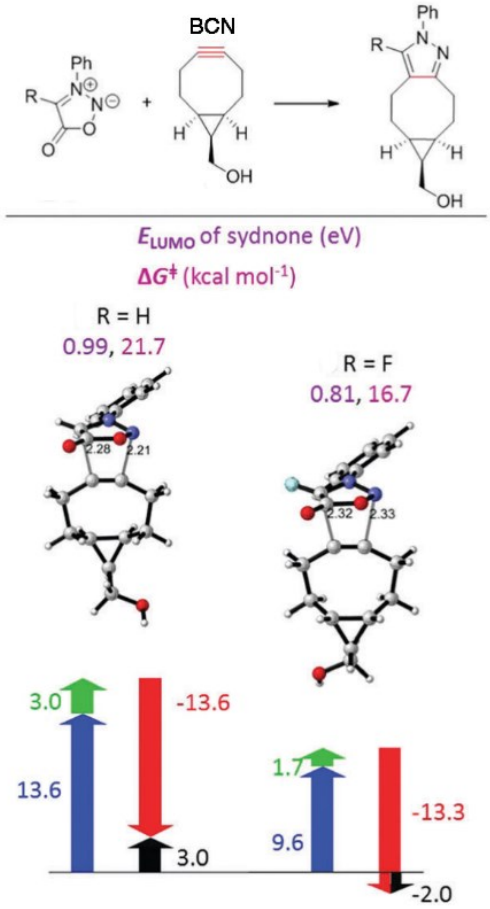

Figure 63. Transition-state structures and distortion/interaction analyses of the cycloadditions of a 4-H sydnone versus a 4-F sydnone with bicyclo[6.1.0]nonyne (BCN). Computed LUMO energies of sydnones and activation free energies are shown. Distortion/interaction analyses are shown below either transition state structure where black arrows represent activation energies, blue and green arrows represent the distortion energies for sydnones and BCN, respectively, and the red arrows represent the interaction energies. Activation energy is the sum of distortion and interaction energy. (Aadapted with permission from Ref. 303. Copyright 2018 Royal Society of Chemistry).

These examples show the value and diversity of 1,3-dipolar cycloadditions as reactions for bioorthogonal chemistry. Only a fraction of known 1,3-dipoles (**Table 1**) have been demonstrated to be useful in a biologically relevant environment. While the disclosed dipoles have their individual benefits, expanding the number of 1,3-dipoles compatible with physiological conditions will surely increase the applicable uses such a transformation can be implemented in.

4.5. Dipolarophiles in Bioorthogonal Chemistry

Azides and other dipoles employed in bioorthogonal chemistry discussed in section 4.4 react with strained alkenes or alkynes. The reaction of unstrained acyclic dipolarophiles typically requires the addition of a metal catalyst or high temperatures. For example, the widely used copper(I)-catalyzed azide-alkyne cycloaddition[304] has a calculated activation barrier of 14.9 kcal mol^{-1}, which is significantly lower than the barrier for the uncatalyzed reaction (25.7 kcal mol^{-1} for the 1,4-substituted 1,2,3-triazole and 26.0 kcal mol^{-1} for the 1,5-substituted 1,2,3-triazole), explaining the considerable rate acceleration of the copper-catalyzed process compared to a purely thermal reaction.[268] While the copper-catalyzed azide-alkyne cycloaddition is widely used in synthesis[305, 306] and chemical biology,[30] this review focuses on metal-free bioorthogonal reactions.

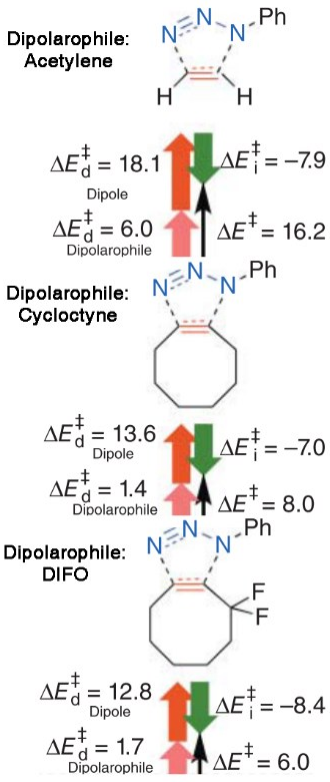

Figure 64. B3LYP/6-31G(d) calculated distortion/interaction energies for the concerted transition states of phenyl azide cycloaddition with acetylene, cyclooctyne, and DIFO in kcal/mol. (Adapted with permission from Ref. 52. Copyright 2009 American Chemical Society).

The strain-promoted azide-alkyne cycloaddition (SPAAC) reaction is among the most widely used bioorthogonal reactions, [2, 8, 307] and how structural features of dipolarophiles affect the reaction with azides has been studied in detail. Strained cyclooctynes react with azides at room temperature whereas the rate of reaction with acyclic alkynes is slow. Studies using the distortion/interaction model confirmed the rate-accelerating effect of strain by showing that the activation energy decreased from 16.2 kcal mol^{-1} for acetylene to 6.0 kcal mol^{-1} for the fluorinated cyclooctyne derivative difluorocyclooctyne (DIFO; **Fig. 64**).[308] The same study further established that a reduction in the distortion energy of the alkyne is primarily responsible for the decreased activation barrier, and that interaction energies are relatively constant for different dipolarophiles. In fact, another study found that increasing ring strain correlates with decreasing activation energies for the 1,3-dipolar cycloaddition reaction between azides and alkynes.[52] Intriguingly, ring strain lowers the distortion energy of both the dipolarophile and the dipole because the reaction proceeds through an earlier transition state with the azide distorted to 143° rather than 138° as required for the reaction with the linear alkyne.[308]

4.5.1. Strained Cycloalkynes as Bioorthogonal Dipolarophiles

Strained dipolarophiles allow 1,3-dipolar cycloadditions to proceed at physiological temperatures without a metal catalyst. **Figure 65** shows representative strained dipolarophiles employed in bioorthogonal chemistry. Blomquist and Liu documented in 1953 that phenyl azide reacts explosively with cyclooctyne at room temperature.[58] Wittig and Krebs subsequently reported that indeed a rapid reaction occurs between phenyl azide and cyclooctyne at room temperature resulting in the triazole.[309] The reaction between phenyl azide and cyclononyne required slight heating in accordance with the decrease in ring strain.[309] From this precedence, Bertozzi introduced the concept of strain-promoted cycloadditions to bioorthogonal chemistry. By using a cyclooctyne derivative (OCT, **Fig. 65**) as the dipolarophile, they achieved azide-alkyne cycloaddition reactions independent of metal catalysis.[119]

For use of strained triple bonds as a bioorthogonal reagent, a balance between stability and reactivity had to be achieved. As ring size decreases, the ring strain energy increases.[52] Efforts to synthesize smaller fully carbon-based strained rings led to the conclusion that the eight-membered ring alkyne is the smallest size that can tolerate the two sp-hybydrized carbons of the alkyne and can be isolated as a stable molecule.[310] Compared to cyclooctynes,

cyclononyes are less reactive and have been employed in the design and development of dual-click diyne reagents.[311]

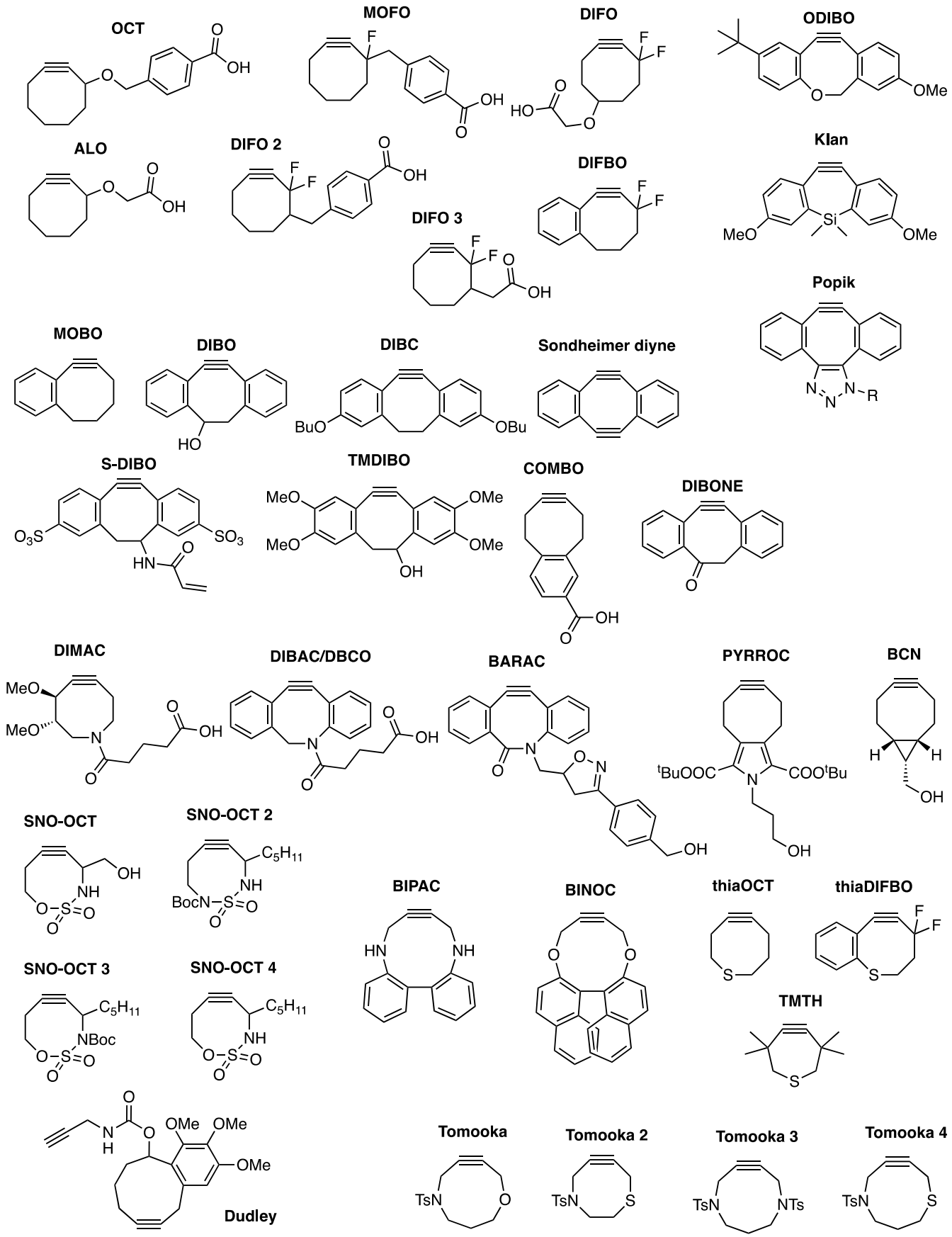

Figure 65. Representative strained dipolarophiles used in bioorthogonal chemistry.

4.5.2. Reactant Destabilization through Higher Ring Strain

A limitation of the reaction between azides and first-generation strained alkynes was the comparably slow kinetics (aliphatic azide and OCT $k_2 = 2.4 \times 10^{-3}$ M^{-1} s^{-1}).[119] Extensive efforts have been made to synthesize a diverse range of cyclooctynes (**Fig. 65**) in the pursuit for faster kinetics. One such method to increase reactivity of such reactants was to incur more strain energy on the triple-bond by incorporating additional sp^2 centers into the ring (**Fig. 66**). Early efforts yielded 4-dibenzocyclooctynol (DIBO, **Fig. 65** and **66**).[312] DIBO contains two benzene rings fused to the cyclooctyne backbone, which impose additional ring strain and conjugate with the alkyne. As a result, DIBO exhibited a 24-fold increase in reactivity compared to OCT (**Fig. 66**). Alternatively, fusion of a cyclopropane ring was pursued to add more sp^2-like hybrid orbitals to cyclooctyne.[313] The banana orbitals from the exocyclic cyclopropyl C-C bonds that expand into the cyclooctyne ring have a distinct sp^2 character.[314] Such an approach led to the construction of bicyclo[6.1.0]nonyne (BCN), which proved to be 60-fold more reactive than OCT (**Fig. 66**).[313] Alternatively, inspired by the increased reactivity observed for DIBO and the increased hydrophilicity of DIMAC (**Fig. 65**),[315] van Delft *et al.* set out to synthesize a dipolarophile with both fast kinetics and high solubility in an aqueous environment. Thus, van Delft *et al.* arrived at dibenzoazacyclooctyne (DIBAC, **Fig. 65** and **66**), which proved to have 129-fold higher reactivity compared to OCT and surprisingly, 5-fold higher reactivity compared to DIBO.[316] Bertozzi *et al.* noticed that in DIBAC, the addition of one more sp^2-like center to the dibenzocyclooctyne ring can have a further rate-enhancing effect; however, a dibenzocyclooctyne with one extra degree of unsaturation across the ring to form an ene-yne is highly reactive but also unstable.[317] Thus to further reactivity but avoid instability, Bertozzi *et al.* explored the incorporation of an endocyclic amide bond to impart double bond character into the ring through electron delocalization. The incorporated amide bond in the ring, which has a resonance structure, yielded an internal double bond. Biarylazacyclooctynone (BARAC, **Fig. 65**), which contains such an internal amide group along with two benzene rings fused to the core structure, exhibited 400-fold higher reactivity compared to OCT, 17-fold higher reactivity compared to DIBO, and 3-fold higher reactivity compared to DIBAC (**Fig. 66**).[318] Interestingly, the early assumption was that the higher incorporation of sp^2-character imparts higher reactivity—such a phenomenon can be seen to account for the reactivity order of BARAC>DIBAC>DIBO given that the number of sp^2-hybridized atoms in the ring decreases from 6 to 4, respectively. However, more recent studies have shown that despite the difference in reactivity, the alkyne angle compression for such molecules varies very little. Such an observation suggests that alkyne bending has little to do with the observed differences in reactivity. According to distortion/interaction analysis (see section 2.3), the higher reactivity for the various dibenzocyclooctynes is not due to the additional strain of the sp^2-hybridized atoms. Instead, it originates from the greater interaction energy.[319] These energies are much larger than the analogous cyclooctyne interaction energy (–12.5 to –11.2 vs. –8 kcal mol^{-1}).[310] In addition to the widely-encountered examples discussed, a wide range of cyclooctynes suitable for bioorthogonal chemistry have been disclosed since the inception of OCT (**Fig. 65**).

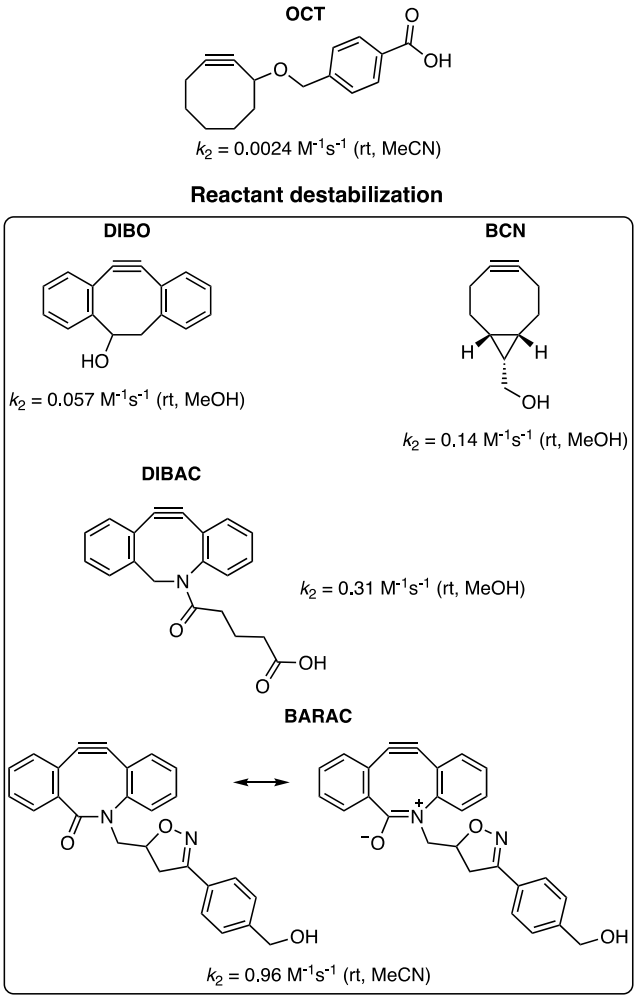

Figure 66. Adding positions with sp^2-character to cyclooctyne increases reactivity by reactant destabilization. Reported rates are with benzyl azide or a similar aliphatic azide at room temperature in the indicated solvents.

4.5.3. Stereoelectronic Effects

An alternative proven route to increasing reactivity of cycloalkynes is to exploit stereoelectronic effects. Bertozzi introduced DIFO (**Fig. 65**), which reacts 32-fold faster than OCT.[118] Computational studies concluded that charge-transfer interactions were the primary reason for the rate-accelerating effects of the fluorine groups and that differences in distortion/interaction were secondary.[308] The reaction between an azide and an alkyne is dominated by the $HOMO_{dipole}$-$LUMO_{dipolarophile}$ interaction. The 3,3-difluoro moiety

exerts an electron-withdrawing effect, lowering the LUMO of the dipolarophile. Indeed, Houk *et al.* calculated that the difluoro substitution lowers the LUMO from 1.1 eV in cyclooctyne to 0.9 eV in DIFO.[308] The lowered LUMO reduces the energy gap of the $HOMO_{dipole}$-$LUMO_{dipolarophile}$ interaction, effectively accelerating the rate of reaction.

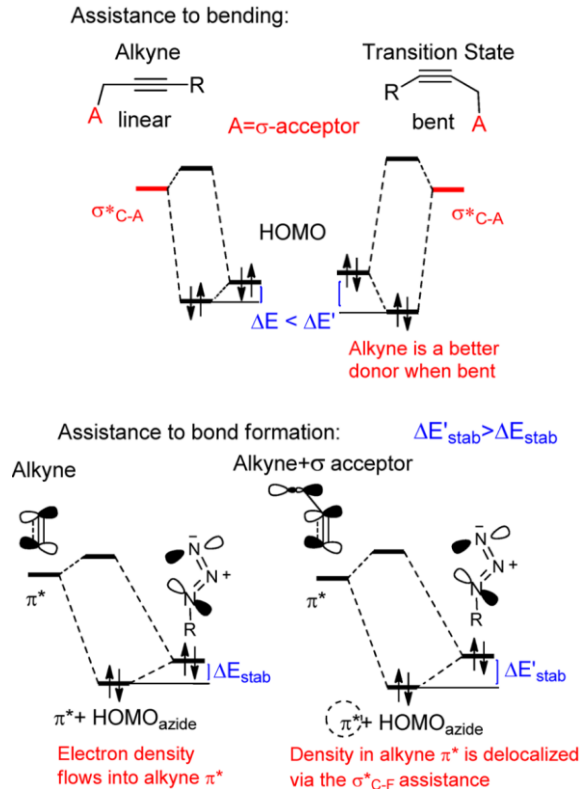

Figure 67. Components of sterelectronic assistance demonstrated between the azide-alkyne cycloaddition. (Adapted with permission from Ref. 319. Copyright 2013 American Chemical Society).

In addition to the LUMO-lowering effect of the propargylic difluoro moiety, the fluorines also facilitate the reaction by hyperconjugation. The donor-acceptor interaction between the distorted alkyne π-system donor and the $\sigma^*_{C\text{-}F}$ orbital acceptor from the vicinal fluorine can aid alkyne bending and stabilization of the transition state (**Fig. 67**).[320]

However, the exocyclic placement of the fluorine groups in DIFO is suboptimal for hyperconjugation. Endocyclic σ-acceptors would have a more pronounced effect by being able to adopt an antiperiplanar arrangement (**Fig. 68**).[320] This concept led groups to explore structural designs to fully exploit hyperconjugative interactions through incorporation of endocyclic heteroatoms (**Fig. 68**). Computational analyses predicted that cyclooctynes with endocyclic heteroatoms with participating orbitals in the desired antiperiplanar orientation could further decrease the activation energy relative to DIFO.[320] Empirical studies with several cyclooctynes based on this design concept have confirmed this prediction.

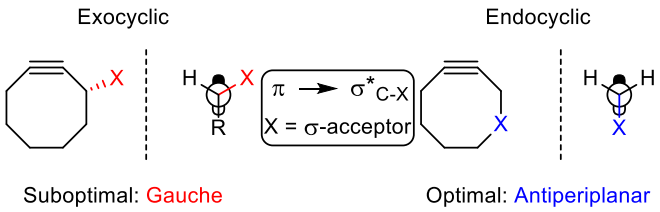

Figure 68. Suboptimal (gauche) and optimal (antiperiplanar) placement of σ-acceptors for hyperconjugation. Maximal hyperconjugation is achieved with endocyclic propargylic σ-acceptors X.

The group of Tomooka synthesized cycloalkynes with endocyclic heteroatoms and demonstrated increased rates over OCT (compounds referred to as Tomooka 1-3; **Fig. 65**).[321] However, synthetic difficulties prevented the access of smaller ring sizes, which partially reversed the electronic benefit of these chemical changes. Although Tomooka 2 (**Fig. 65**) is an 8-membered ring, the inclusion of two C-S bonds lowers the strain energy because of its longer length than C-C bonds, reducing its reactivity. The loss of strain energy ultimately prevents the reaction rates of Tomooka 1-3 to surpass that of DIFO. Nonetheless, the incorporation of heteroatoms still endowed the them with higher reactivity compared to OCT. Tomooka 1-3 reacted 2 to 8-fold faster, when compared to OCT.[321] Thus, larger cycloalkynes with properly aligned endocyclic σ-acceptors still outcompete the smaller ring size compounds with improperly placed σ-acceptors.

Stereoelectronic assistance by heteroatoms also contributed to rapid reactions of cyclooctynes with endocyclic sulfamates (SNO-OCTs, **Fig. 65** and **69**).[322] SNO-OCT 1 (**Fig. 65**) demonstrated 36-fold higher reactivity than OCT and was slightly faster than DIFO. In this design, the heteroatoms at the propargylic (R^1 in **Fig. 69**) and the homopropargylic (X in **Fig. 69**) positions had a positive impact on stability and reactivity demonstrating that stereoelectronic effects could be utilized to relieve ring strain. SNO-OCT 1-4 were used for postpolymerization modifications[323] and recently were shown to be rapidly internalized by mammalian cells and remain functional in the cytosol for live-cell labeling experiments.[324] For a more in-depth look into stereoelectronic assistance in the context of cyclooctynes, readers are directed to a review focused on such a concept.[310]

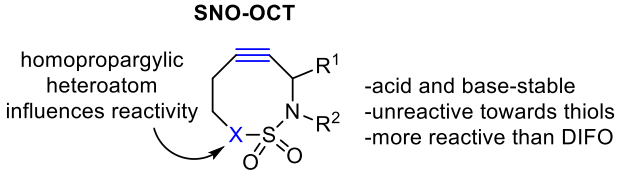

Figure 69. Strained cyclooctynes containing a sulfamate backbone show that inclusion of heteroatoms has a positive impact on and allows for tuning both stability and reactivity, where electronic effects could relieve ring strain.

4.5.4. Combining Stereoelectronic Effects with Ring Strain

The effect of the position of phenyl rings in the cyclooctyne ring on the reaction with methyl azide was investigated. Monobenzocyclooctynes (MOBOs, **Fig. 65**) that differ in the position of the fused benzene ring result in MOBOs with different alkyne angle strains.[310] However, the rates of the 1,3-dipolar cycloaddition reaction with azides did not correlate with ring strain within the MOBO series.[310] Given the established effects of both ring strain (see section 4.5.2) and stereoelectronic effects (see section 4.5.3) on alkyne reactivity, it is plausible that cycloalkyne reactivity is controllable by combining effects of both ring strain and electronics.

Indeed, evidence of success can be seen with the introduction of TMTH (**Fig. 65**).[325] While long believed that eight-membered rings are the smallest cycloalkynes that could be isolated, TMTH is a stable seven-membered ring. Sulfur atoms have been introduced into cyclooctynes (thiaOCT and thiaDIFBO, **Fig. 65** and **4.18**) previously but led to lower reactivities than OCT and DIFO, respectively,[325] because of the longer C-S bond, which decreases ring strain.[321] However, because of the longer C-S bond, TMTH was synthetically accessible, which regains the lost strain energy. Furthermore, while sulfur is a weak σ-acceptor, the endocyclic placement of a sulfur atom allows TMTH to still benefit from hyperconjugative assistance (**Fig. 68**). TMTH is ~1,700-fold more reactive than OCT (k_2 = 4.0 $M^{-1}s^{-1}$, rt, MeCN; **Fig. 70**).[325] TMTH is an example of the cooperative use of strain and electronic activation to allow for impressive rate enhancements and is a route worth exploring further. TMTH has been used for labeling purposes in cell lysates and on azide-functionalized proteins *in vitro*.[325]

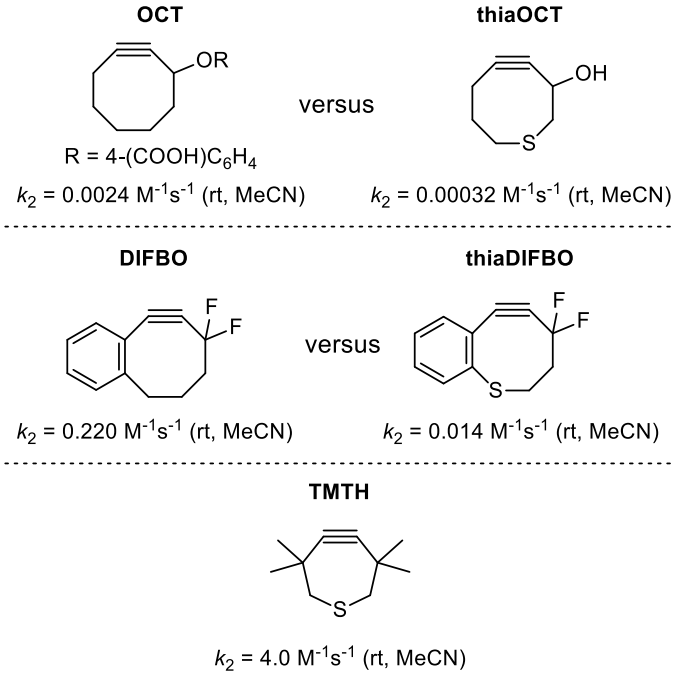

Figure 70. Introducing an endocyclic sulfur atom, while a weak σ-acceptor, allows for stereoelectronic assistance and due to the longer bond length for C-S bond compared to that of a C-C bond, TMTH was able to be synthesized contributing high strain energy.

4.5.5. Steric Effects

1,3-dipolar cycloadditions are sensitive to steric repulsions in the transition state. While increasing strain by fusing aryl rings to the cycloalkyne clearly increased reactivity (see 4.5.2), the "flagpole" hydrogen atoms ortho to the aryl/cyclooctyne ring junction were predicted by Goddard *et al.* to cause steric interference with the azide in the transition state.[326] The increase in reactivity of DIBO and BARAC reflects a shifted balance towards the rate-enhancing effect of aryl ring fusion over that of the rate-diminishing effect from steric hindrance.

A study conducted on various BARAC structures gave insight into the effects of sterics on cyclooctyne reactivity (**15**-**24**, **Fig. 71**).[327] Compared to the parent compound 1 (k_2 = 0.9 $M^{-1}s^{-1}$; kinetics were measured in MeCN at room temperature), compounds with two hydrogens as "flagpole" substituents (structures **16**-**21** in **Fig. 71**) exhibited rate constants that varied within experimental error. However, compounds with a fluoro or methyl "flagpole" substituent ortho to the alkyne displayed one to two orders of magnitude decreases in their rates relative to

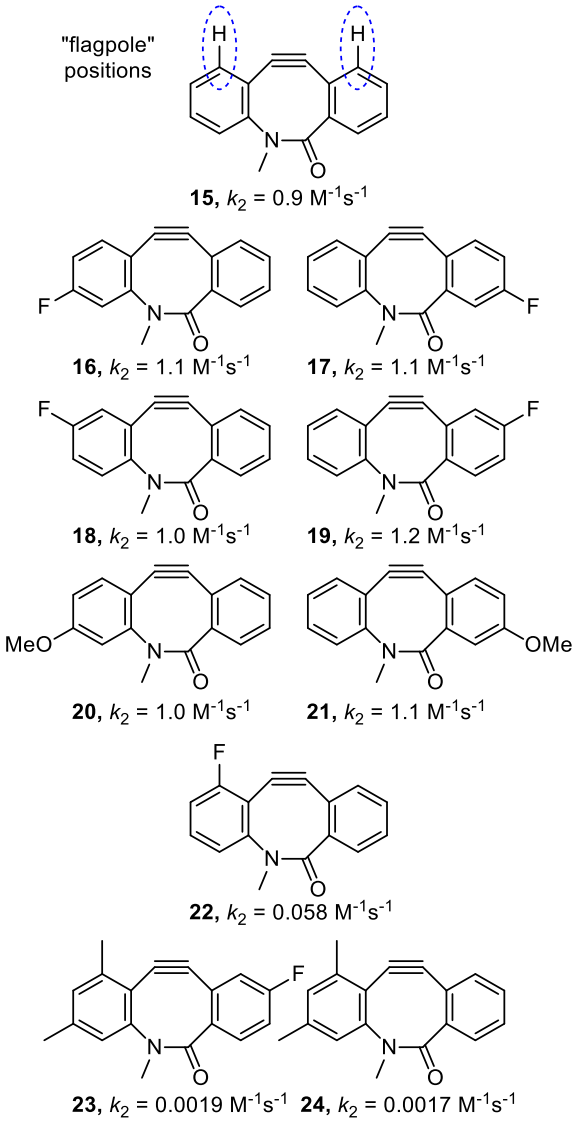

Figure 71. BARAC analogues tested to determine effects of strain on cycloaddition rates with benzyl azide

compound **15** (k_2(**22**) = 5.8 × 10^{-2} M^{-1} s^{-1} (CD_3CN), k_2(**23**) = 1.9 × 10^{-3} M^{-1} s^{-1} ($CDCl_3$), k_2(**24**) = 9.0 × 10^{-4} M^{-1} s^{-1} ($CDCl_3$)). Computational calculations using the distortion/interaction model (see section 2.3) show that the flagpole substituents require additional distortion in the transition states for the reaction to occur, explaining the reduced reaction rates of compounds **22**-**24** relative to **15**-**21**. The proximity of the substituent to the alkyne and its geometry relative to the incoming azide requires a higher degree of distortion of the cyclooctyne in the transition state (**Fig. 72**). Calculated transition states for reactions between methyl azide and compound **15** or **23** show how the methyl group in compound **23** causes unfavorable steric interactions with the incoming azide (**Fig. 72**).[327]

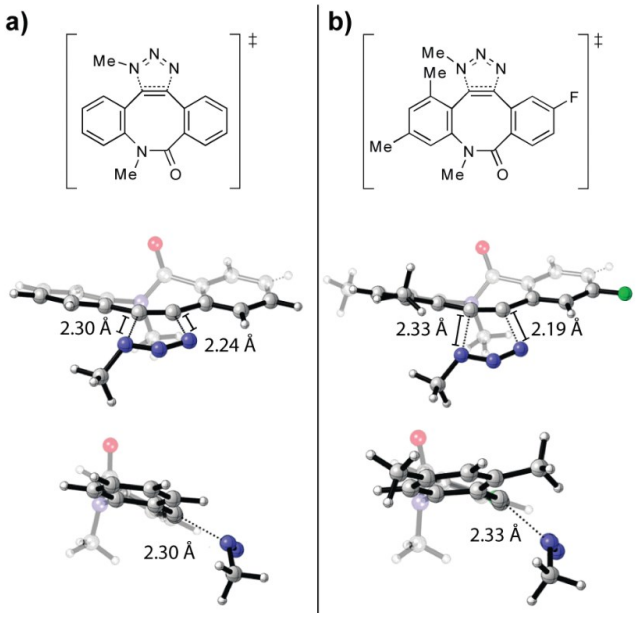

Figure 72. Flagpole methyl substituents sterically hinder the transition state. a) Front and side views of the transition state of the reaction of BARAC **15** (**Fig. 71**) with methyl azide; b) Front and side views of the transition state of the reaction of BARAC **23** (**Fig. 71**) with methyl azide. Transition states were modeled using B3LYP/6-31G(d). (Adapted with permission from Ref. 328. Copyright 2012 American Chemical Society).

4.5.6. Dipolarophile Stability

Increasing the reactivity of dipolarophiles either by (stereo)electronic effects or augmented ring strain comes at the detriment of making the cycloalkynes susceptible to side reactions. Rigidified cyclooctynes (DIBO, BCN, BARAC) form covalent bonds with biological functionalities and especially thiols, which limits their potential use in biological systems (**Fig. 73**).[328] Compounds that include both higher ring strain and electronic effects like DIFBO (**Fig. 65**) are unstable and undergo spontaneous trimerization in solution (**Fig. 73**).[329] Moreover, highly reactive strained cycloalkynes such as TMTH can undergo hydrogen transfer reactions with alcohols, amines, and thiols (**Fig. 73**).[330] Attempts to increase the ring strain of cycloalkynes beyond that of TMTH may lead to incompatibility in biological settings. However, the SNO-OCTs offer the benefits of fast reaction kinetics and high stability in the presence of glutathione (see section 4.5.3).[322] The inclusion of the heteroatoms in the ring of SNO-OCTs attribute to the higher stability by lessening the strain imposed in the ring while also enforcing electronic activation to allow for considerable rate acceleration. It is pertinent to continue the development of dipolarophiles that balance reactivity, stability, and specificity for use in bioorthogonal contexts.

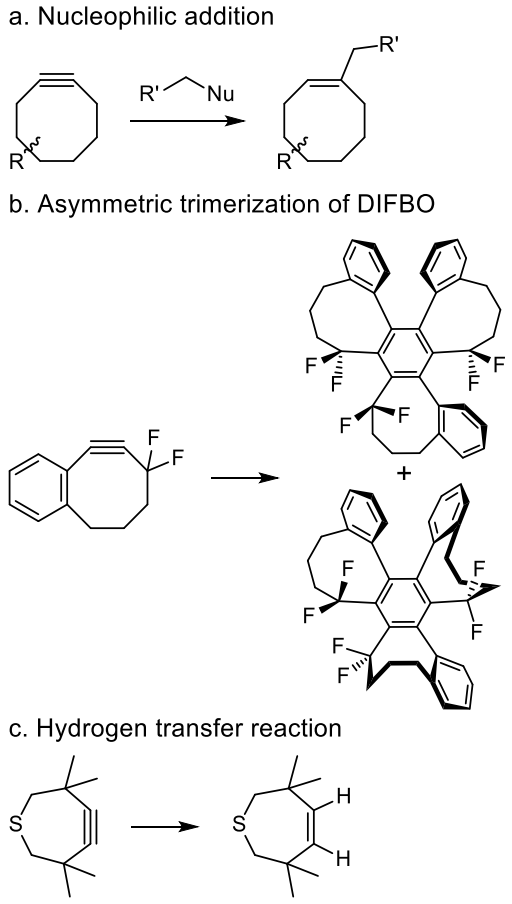

Figure 73. Routes of dipolarophile deactivation. a) nucleophilic addition by endogenous biological nucleophiles, especially from thiols (thiol-yne reaction); b) Reported spontaneous trimerization of DIFBO in solution; c) Reported hydrogen transfer reaction on TMTH from alcohols, amines, and thiols

4.5.7. Photoactived Azide-Alkyne Cycloadditions

As with photoactivatable 1,3-dipoles (nitrile imines, see section 4.4.4), photoactivatable dipolarophiles are being developed for bioorthogonal chemistry to access higher spatial and temporal control of the labeling of the target substrates. It has been long known that single[331, 332] or two-photon excitation[333] of cyclopropenones results in the formation of the corresponding acetylenes. From that precedence, the groups of Boons and Popik introduced cycloalkynes caged with cyclopropenone groups that dissociate upon irradiation with UV light to the bioorthogonal community (**Fig. 74**).[334] Such an approach has been altered to cage otherwise unstable dipolarophiles so that they can be released by photoirradiation for the rapid reaction with available 1,3-dipoles. For example, the two fastest 1,3-dipolar cycloaddition reactions reported to date involve photoactivatable dipolarophiles (Klan and Popik, **Fig. 65**).[335, 336] Klan *et al.* reported a dibenzosilacyclohept-4-yne photochemically generated in situ from its corresponding cyclopropenone derivative. The Klan dipolarophile upon photogeneration was shown to react with benzyl azide with a rate constant of 22.5 M^{-1} s^{-1} (**Fig. 74**).[335] The cyclopropenone precursor was stable in water for 72 h and the 1,3-dipolar cycloaddition reaction was shown to proceed in aqueous media. While the authors suggest possible use in a bioorthogonal context for labeling purposes, this capability remains untested. Additionally, Popik *et al.* presented a triazole fused dibenzocyclooctyne that reacted with butyl azide with a rate constant of 34 M^{-1} s^{-1} (**Fig. 74**).[336] The triazole fused dibenzocyclooctyne was accessed with sequential photoactivation and SPAAC. Such a strain-promoted "double-click" reaction was first introduced by Hosoya *et al.* using the Sondheimer diyne (**Fig. 65**), which enabled them to chemically modify an azido-biomolecule with a reporter azido-molecule in studies *in vitro* and in living cells.[337] In the study involving the double click reaction introduced by Popik *et al.*, they were able to demonstrate the use of their system for in vitro protein labeling.[336] However, to induce decarbonylation of the cyclopropenone to afford the strained alkyne, UV light ranging from 300 – 350 nm is used, which may pose phototoxicity issues to biological samples.

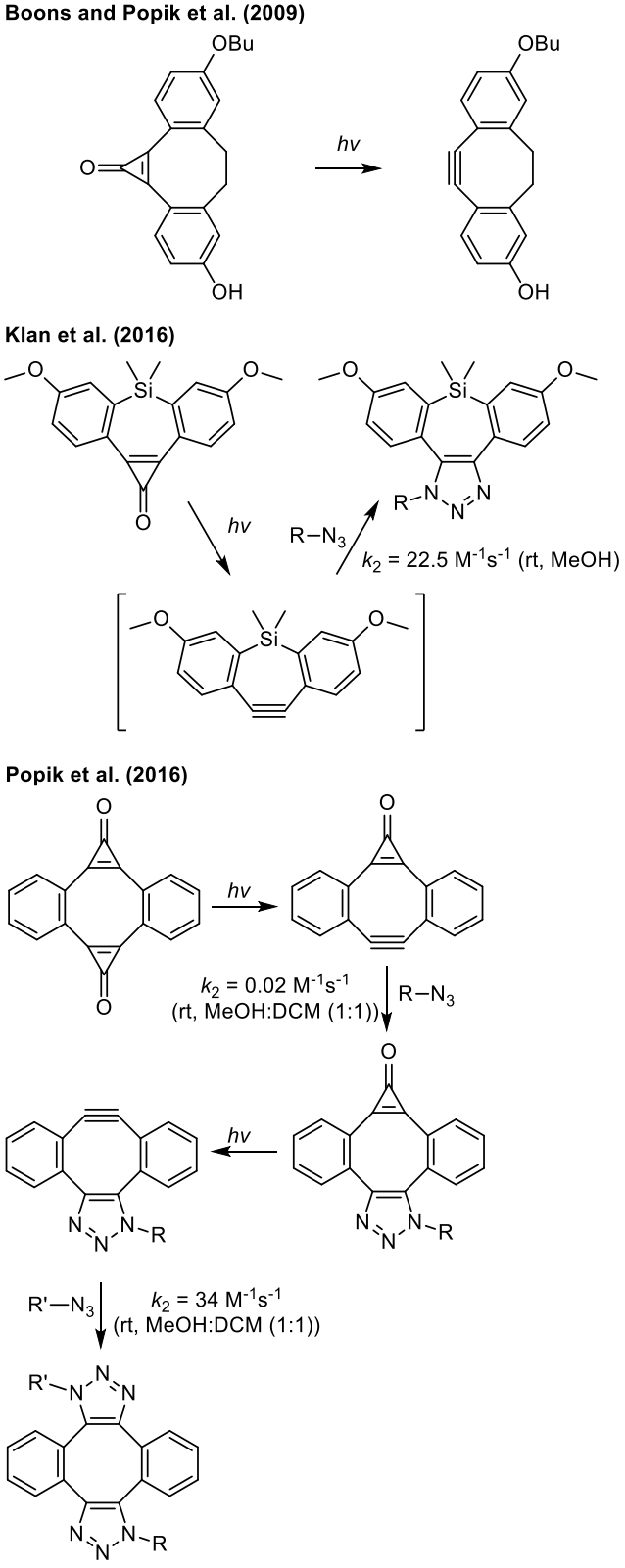

Figure 74. Cyclopropenones and the corresponding strained cycloalkynes upon photoactivation

4.5.8. Reactions with Strained Alkenes

While the previous sections mainly discussed the 1,3-dipolar cycloaddition of alkynes, 1,3-dipoles also react with alkenes. Huisgen compared the rate constants for 1,3-dipolar cycloadditions of various 1,3-dipoles onto double and triple C-C bonds by reacting them with styrene and phenylacetylene, respectively.[245] For the most part, the reaction rates were comparable. For example, phenyl azide reacted 1.4 times faster with styrene than with phenylacetylene.[245] However, the reaction between azides and alkenes forms 1,2,3-triazoline heterocycle adducts that are unstable in aqueous conditions.[338, 339]

The triazoline heterocycle could not be isolated. Instead, a rearrangement rapidly occurs to release diatomic nitrogen and leads to imine intermediates (**Fig. 75**).[339] In the presence of water, the imine products are labile to hydrolysis, and the reaction of alkenes with azides is therefore of limited use for labeling and bioconjugation applications. However, the instability of the 1,2,3-triazoline intermediate towards the formation of the imine compounds makes it attractive for click-to-release applications (see section 4.6). Suitable for bioconjugation purposes, route c leads to an aziridine compound (**Fig. 75**). In one account, aziridination of norbornenes in reactions with electron-deficient sulfonyl azides has been employed for bioconjugation purposes.[340]

In reactions with other 1,3-dipoles, the lability of the 1,2,3-triazoline is not an issue. For example, the reaction between cyclic nitrones and cyclooctenes to form isoxazolidine products have been used in metabolic labeling of bacteria with unnatural amino acids[341] and the reaction between nitrile oxides and norbornene to form isooxazoline products has been used for the functionalization of oligodeoxyribonucleotides.[342, 343] However, reaction rates with strained alkenes are typical in the same range as for reactions with strained alkynes, and therefore there is no strong rationale for using alkenes over alkynes. For example, the highly reactive *trans*-cyclooctene molecule reacts with nitrones at a rate of 0.08 M^{-1} s^{-1} in MeOH at room temperature.[341] For comparison, cyclic nitrones have been reported to react with DIBO at a rate of 3.38 M^{-1} s^{-1} in MeCN at room temperature.[274] There are however 1,3-dipoles that prefer to react with strained alkenes. Diazoacetamide was demonstrated to react faster with ethyl acrylate ($k_2 = 1.6 \times 10^{-3}$ M^{-1} s^{-1}) than with ethyl propiolate ($k_2 = 5.8 \times 10^{-4}$ M^{-1} s^{-1}).[286] While studied to a lesser extent in the ligation context of bioorthogonal chemistry, the reaction of 1,3-dipoles with alkenes has therefore gathered more attention in bioorthogonal dissociative studies.

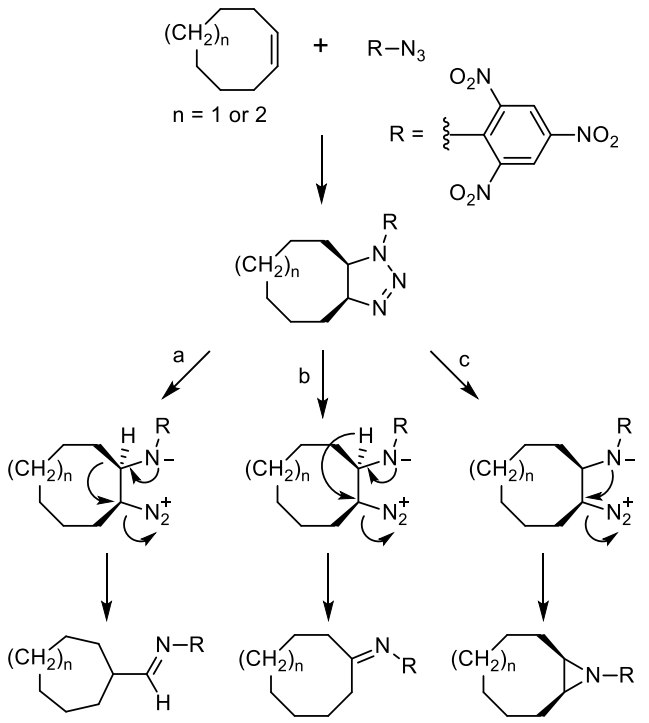

Figure 75. 1,3-dipolar cycloaddition between an azide and cyclooctene resulting in imine products that are labile under aqueous conditions.

4.6. Linking 1,3-Dipolar Cycloadditions to a Release Step

The reaction between an azide and oxanorbornadiene was the first demonstration of a 1,3-dipolar cycloaddition reaction to feature a release of a molecule.[344, 345] Trifluoromethyl-substituted oxanorbornadienes reacts with azides and undergoes a tandem 1,3-dipolar cycloaddition to form a labile triazoline intermediate, followed by a retro-Diels-Alder, expelling furan, leading to the final formation of a stable 1,2,3-triazole linkage.

The first dissociative bioorthogonal reaction based on a 1,3-dipolar cycloaddition step to release structurally diverse payloads was based on the reaction between aryl azides and *trans*-cyclooctene (TCO).[346] Gamble *et al.* designed a para-azidobenzyloxycarbonyl molecule (**25**, **Fig. 76a** and **76b**) that upon reacting with TCO (**28**, **Fig. 76a** and **76c**) formed a 1,2,3-triazoline intermediate. As mentioned in section 4.5.8, such intermediates are labile in the presence of water and undergo rapid rearrangements to form an imine. The imine further hydrolyzes to afford p-aminobenzyloxycarbonyl (PABC), which is a well-established self-immolative linker that releases leaving groups by 1,6-elimination (**Fig. 76a**).[347, 348]

In dissociative bioorthogonal reactions, both the rate of cycloaddition and the rate of hydrolysis of the ensuing labile intermediate affect the release of caged molecules.[12] Tuning of the reactants allowed making both the bimolecular reaction and the release step rapid. First, addition of fluorine atoms on the aryl azide improves reactivity towards alkenes (**Fig. 76b**).[349] The reaction of aryl azides and alkenes falls under a type II 1,3-dipolar cycloaddition and therefore changes to reduce the energy gap between the LUMO of the dipole and the HOMO of the dipolarophile are expected to accelerate the cycloaddition. It was established previously in various studies that aromatic azides react faster with electron-rich dipolarophile partners (see section 4.4.1).[244] Indeed, the LUMO-lowering effect of fluorines on the phenylazide group decreased the energy gap to TCO's HOMO, which translated into a faster reaction.[349] In a PBS:MeCN (18:1) solution, **26** (**Fig. 76b**) reacted with a highly strained cis-dioxolane-fused *trans*-cyclooctene (**29**, **Fig. 76c**) at a bimolecular rate of 4.9 M^{-1} s^{-1}.[350] However, the fluorines deterred the rate of elimination by stabilizing the intermediates.[350] PABC-type linkers have shown to benefit from a faster release when containing a benzylic methyl substituent because of the stabilization of the buildup of positive charge in the transition state.[348, 351, 352] With the combination of aryl azide **27** (**Fig. 76b**), Gamble *et al.* achieved rapid bimolecular kinetics and release from tetrafluorobenzyloxy type linkers within an hour ($t_{1/2}$ = 54 min) and maximum release (94%) after 146 min.[350]

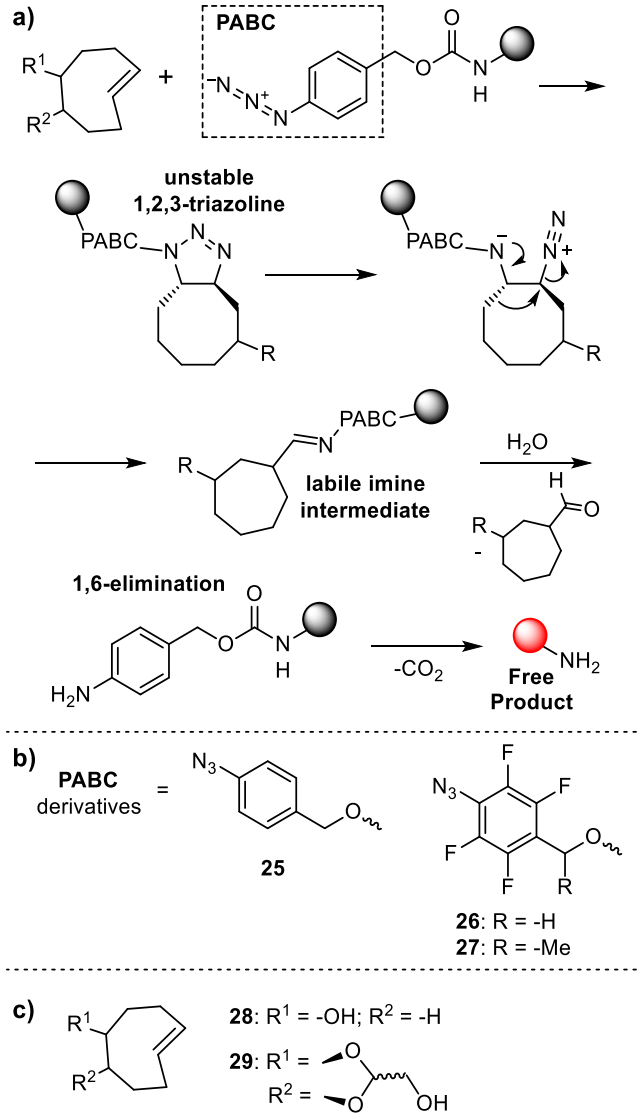

Figure 76. Release reaction based on the 1,3-dipolar cycloaddition between an aryl azide and cyclooctene. a) Proposed mechanism for the decaging of molecules following the bioorthogonal 1,3-dipolar cycloaddition reaction; b) representative structures of aryl azide self-immolative linkers used in these studies; c) representative structures of TCO derivatives used in these studies.

Another 1,3-dipolar cycloaddition reaction that has been adapted for release purposes is the cycloaddition between sydnones and alkynes (see section 4.4.6). The original reaction contains an innate release step as after the initial cycloaddition to form a bicyclic intermediate, a retro [4+2] cycloreversion occurs to expel carbon dioxide (**Fig. 77a**).[353] Taran *et al.* modified the sydnone structure to an iminosydnone to instead expel acyl isocyanates.[354] Water spontaneously hydrolyzes the acyl isocyanate, which is followed by decarboxylation to form a urea molecule (**Fig. 77b**).

As mentioned in section 4.4.6, 4-halogen substituents on the sydnone accelerate the cycloaddition reaction with strained alkynes.[302, 303] For example, a sydnone with a bromine atom at the 4-position reacted 16-fold faster with BCN (k_2 = 3.73 M^{-1} s^{-1}; PBS at room temperature) than the original sydnone (**Fig. 77c**).[355] It will be interesting to explore iminosydnones that have a fluorine atom at the 4-position to determine whether such a substituent will lead to dramatic rate accelerations as demonstrated with sydnones (see section 4.4.6). An alternative design involving sulfonyl-modified iminosydnones allowed for the release of sulfonamides.[356] Instead of expelling acyl isocyanate as in Taran's design, such sulfonyl-modified iminosydnones expel sulfonyl isocyanate, which is also highly unstable in aqueous media and quantitatively undergoes decarboxylation to form the desired sulfonamide.

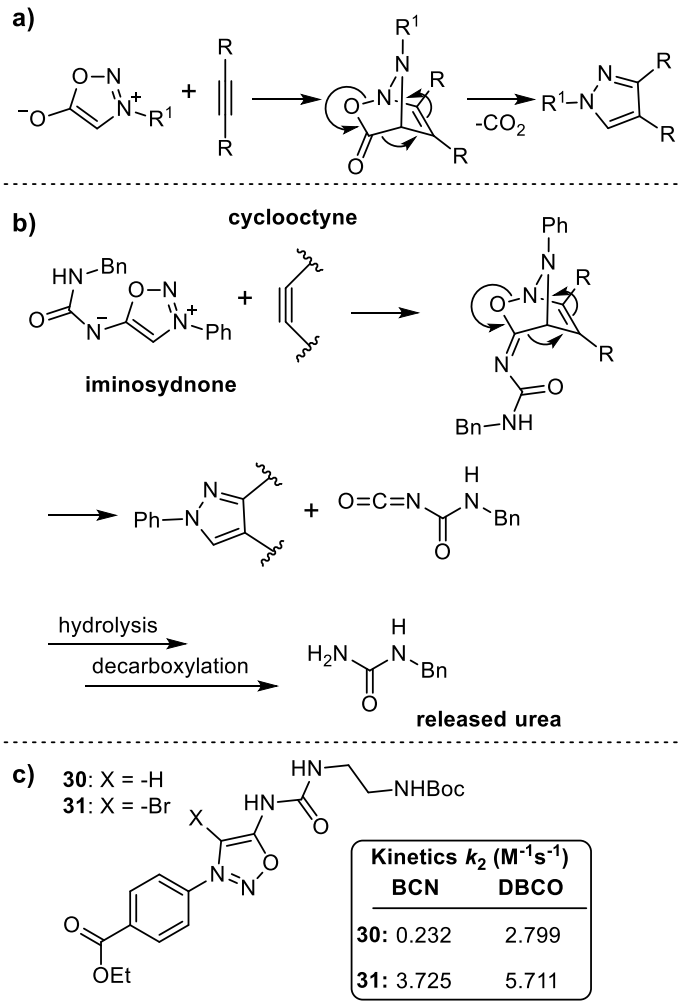

Figure 77. Release reaction based on the 1,3-dipolar cycloaddition between a sydnone and cyclooctyne. a) Mechanism for the sequential 1,3-dipolar cycloaddition of sydnones to alkynes followed by the spontaneous retro [4+2] reversion to release CO_2; b) mechanism for the release of urea structures from iminosydnones; following cycloreversion, the resulting acyl isocyanate spontaneously undergoes hydrolysis and decarboxylation to form the urea; c) representative halogen substituted

(4-Br) iminosydnone, **30**, demonstrating faster kinetics (in PBS with 1% DMSO, room temperature) over its non-halogen substituted (4-H) counterpart, **31**.

4.7 Summary of Bioorthogonal 1,3-Dipolar Cycloadditions

Reactions of dipoles and alkenes/alkynes are widely used in bioorthogonal chemistry. The availability of several biocompatible dipoles has led to a diverse range of chemistry. Similarly, mechanistic knowledge has led the design of numerous strained cycloalkyne rings with greatly enhanced reactivity over the first-generation cycloalkyne reagents. Despite these extensive efforts 1,3-dipolar cycloadditions are orders of magnitude slower than the fastest IEDDA reactions. The compactness of some of the dipoles and in particular the azide group is an advantage for applications in which the bulky substituents are problematic.

5. STAUDINGER REACTION

The conversion of organic azides and phosphines into iminophosphoranes is a classic reaction in synthetic organic chemistry that was first reported by Meyer and Staudinger in 1919.[357] Iminophosphoranes are important synthetic intermediates that for example, can be hydrolyzed to primary amines or react with carbonyl compounds in the aza-Wittig reaction.[358] The absence of azides and phosphines from living organisms and their high chemoselectivity against most biomolecules have made the Staudinger reaction one of the most widely pursued bioorthogonal transformations.[1, 19] The Staudinger reaction proceeds through a series of intermediates in steps that are each sensitive to structural modifications. The resulting possibility to diverge the reaction in different directions has yielded several modified versions of the Staudinger reaction that are relevant to use with biomolecules. A detailed account on the scope of the Staudinger reaction can be found in a recent review.[25]

5.1 Mechanism of the Staudinger Reaction

Several rigorous studies have provided detailed insights into the mechanism of the Staudinger reaction. The initial bimolecular reaction of organic azides and phosphines generates a phosphazide intermediate, which in a second step proceeds to the iminophosphorane (also known as phosphane imide, phosphine imide, and phosphorus aza-ylide) with concomitant release of nitrogen gas (**Fig. 78**).[248, 359] Hydrolysis of the iminophosphorane provides the primary amine and phosphine oxide.[360] The transition state energies of the three steps are of comparable magnitude and depend on the structures of the reagents. Chemical modifications of both the azide and phosphine allow fine tuning of the reaction. Understanding the mechanistic principles and the effect of substituents on the kinetics of the individual steps is therefore critical to design modified versions of the Staudinger reaction for applications with biomolecules. Key principles for each step are provided below.

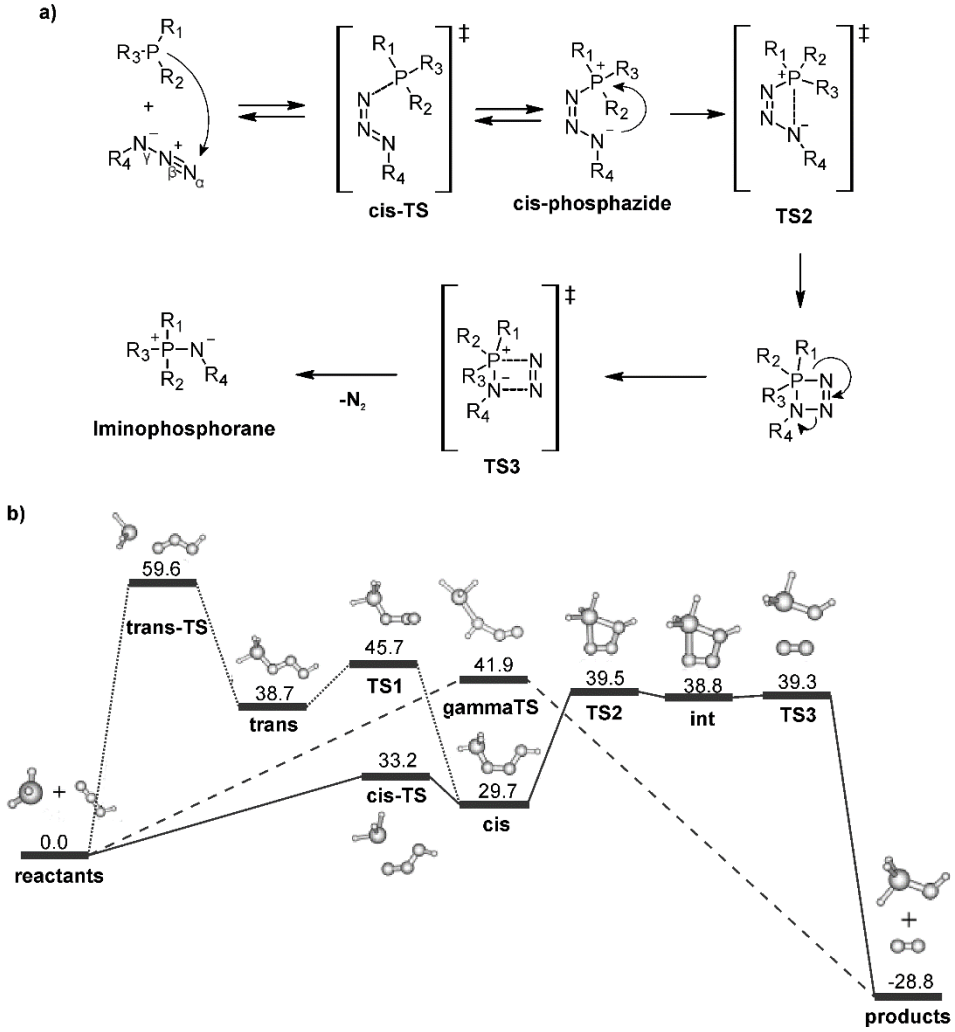

Figure 78. Mechanism of the Staudinger reaction. a) Intermediates and transitions states for the conversion of azides and phosphines to iminophosphoranes. b) Energy profile of the reaction of PH_3 and N_3H calculated using density functional theory. (Adapted with permission from Ref. 248. Copyright 2004 American Chemical Society).

5.2 Bimolecular Step of the Reaction of Phosphines and Azides

5.2.1 Phosphazide Intermediate

The initial step of the Staudinger reaction is the attack of the phosphine lone pair onto the terminal Nα nitrogen of the azide group (**Fig. 78a**). Computational studies revealed that the *cis*-phosphazide forms preferentially (**Fig. 78b**).[248, 361, 362] DFT calculations predicted the transition-state free energy for the *cis*-isomer to be 25 kcal mol^{-1} lower than for the *trans*-isomer.[248] Interactions between the juxtaposed phosphorus and Nγ nitrogen atoms stabilize the cis-intermediate.[248] A further disadvantage with the *trans*-isomer is that it requires a bond-rotation step to arrange the atoms for the subsequent cyclization step (**Fig. 78b**). The bimolecular step is reversible, and the phosphazide is in equilibrium with the phosphine and the azide.[363] To give an idea of the stability of the phosphazide, the thermodynamic parameters for the formation of the *cis*-phosphazide from tricyclohexylphosphine and 1-adamantylazide have been reported as ΔH = -18.7 kcal mol^{-1} and ΔS = -52.5 kcal mol^{-1} K^{-1}.[364]

5.2.2 Electronic Substituent Effects

The substituent effects of the bimolecular step are intuitive when considering it as a polar reaction of the phosphine lone pair and the terminal azide nitrogen. Substituents that increase the electron-density on the phosphine or reduce the electron-density of the azide are anticipated to accelerate the reaction. Consequently, electron-donating phosphine substituents and electron-withdrawing azide modifications favor the Staudinger reaction.

Experimental results confirmed the predicted electronic effects of phosphine substituents on the reaction. The

logarithm of the second order rate constant of the reaction of phenyl azide with variable trivalent phosphorus compounds correlated with Taft's polar parameter σ^* (see section 2.1),[365] which is in agreement with a buildup of positive charge on the phosphorus atom in the transition state.[248, 361, 362] For the reaction of phenyl azide with triarylphosphines, the slope of the rate constants to σ^* was -2.43, which corresponds to a Hammett reaction parameter of ρ = -0.73 (benzene, 25 °C).[365] The same reactivity trend was observed for compounds with one or more oxygens linked to the phosphorus (instead of three carbon-based substituents);[365, 366] however, the slope was offset by an increase in free energy of activation of 1.93 kcal mol^{-1}. Trialkylphosphines react several-fold faster than triphenylphosphine (PPh_3), possibly because of the lack of conjugation of the phosphorus atom.[365]

Studies confirmed that the reactivity towards phosphines increases with decreasing electron density on the azide. The reaction of PPh_3 with aryl azides yielded a Hammett reaction parameter of ρ = 1.25 with regard to aryl azides, which corresponds to a ~10-fold rate enhancement from phenyl azide to 4-nitrophenyl azide (benzene, 25 °C).[359] Likewise, azidodifluoroacetamides react about 1000-fold faster than an unfluorinated alkyl azide (**Fig. 79**).[367] This trend reflects the ability of electron-withdrawing substituents to stabilize the increased negative charge on the Nγ position in the cisTS transition state.[248, 361, 362] The observation that acyl azides and sulfonyl azides react several orders of magnitude faster than aryl azides further supports the effect of electron-withdrawing groups on the kinetics.[368] Remarkably, aryl azides form phosphazides more readily than alkyl azides.[367] In fact, phosphines can chemoselectively reduce aryl azides in the presence of their aliphatic counterparts.[369] Increased conjugation in the phosphazide-like transition state[248] relative to the initial azide molecule may explain the kinetics difference between aryl and alkyl azides.

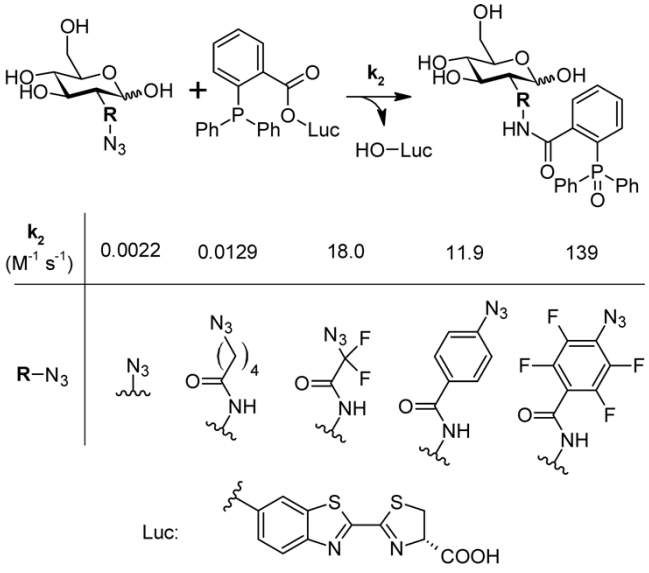

Fig. 79. Influence of azide structure on the rate of the reaction with phosphines.

5.2.3 Steric Substituent Effects

The bimolecular reaction of azides and phosphines is rather insensitive to sterics, in contrast to the pronounced electronic substituent effects. Trivalent phosphorus compounds with bulky substituents readily react with azides. For instance, replacing methyl in $P(OMe)_3$ by adamantyl groups leaves the rate of the reaction nearly unchanged.[366] The effect of steric crowding on the azide is more pronounced than for the phosphines. *Ortho*-substituted phenyl azides react slower with PPh_3 than those substituted at the *meta*- and *para*-position.[359] The reactivity towards phosphines also decreases from primary, to secondary and tertiary azides,[370] and certain sterically encumbered azides are unreactive to PPh_3.[371]

5.2.4 Solvent Effects

Polar solvents slightly accelerate the reaction of azides and phosphines indicating a modest buildup of charge in the transition state. Phenyl azide reacts with PPh_3 at 25 °C about 3.2-fold faster in DMSO than in benzene.[359] Protic solvents disproportionally accelerate the reaction relative to the dielectric constant[372] indicating that hydrogen bonds may stabilize the transition state.

5.2.5 Designing Fast Staudinger Reactions

Implementing the aforementioned substituent effects (see 5.2.2) makes it possible to design fast-reacting Staudinger reaction substrates. Such structural changes can overcome one of the most important drawbacks of the reaction of alkyl azides with PPh_3, which is that it is among the slowest bioorthogonal transformations.[9]

One approach to enhance reaction rates is to increase the electron-density on the phosphorus atom. The practical value of enhancing the reactivity of phosphines to accelerate Staudinger reactions, for example in the form of trialkylphosphines or triarylphosphines with electron-donating substituents, is mitigated by the increased air sensitivity of such phosphorus compounds.[23, 373, 374] Oxidative deactivation of phosphines is especially problematic in biological samples because thiols catalyze their oxidation. For example, PPh_3 derivatives are stable for hours in plain buffer,[375, 376] but are oxidized rapidly to the phosphine oxide in the presence of the disulfide of dithiothreitol,[376] which rapidly forms in the presence of air.

As an alternative, several groups have explored electron-deficient azides for fast bioconjugation based on the Staudinger reaction,[369, 377-380] and 2,3,5,6-tetrafluorophenyl azides have proven to be especially reactive.[379, 381] A tetrafluorophenyl azide with a *para*-carboxamide group reacted with a substituted triphenylphosphine derivative at a rate of k_2 = 139 M^{-1} s^{-1} under physiological conditions (PBS, pH 7.4, room temperature),[367] which compares favorably to other widely-used bioorthogonal reactions (**Fig. 79**).[9, 382] Within the tetrafluorophenyl azide series, electron-withdrawing substituents increased the reactivity (Hammett reaction parameter: ρ = 0.43),[381] although the effect is weaker than for the parental phenyl azides.[359] The high reaction rate of halogenated phenyl azides is especially significant because iminophosphoranes generated from electron-deficient azides are inert to hydrolysis (see section 5.4).[377-379, 381] Therefore, the reaction of tetrafluorophenyl azides with phosphines is attractive for bioconjugation applications. Aromatic azides with electron-withdrawing substituents are also unusually reactive towards thiols undergoing reduction to the amine.[380] This characteristic is important to consider when designing azide-based photoaffinity probes,[383] and it is advantageous for aryl azide-based sensors of hydrogen sulfides[384] because the signal response is rapid.[380, 385]

In summary, the bimolecular reaction of organic azides and phosphines generates phosphazide intermediates and this step is often rate-limiting. Electronic effects strongly modify the rate of this step and electron-deficient aromatic azides react especially rapidly with phosphines and generate stable adducts.

5.3 Conversion of Phosphazides to Iminophosphoranes

The second step on the trajectory of the phosphine-mediated transformation of organic azides to amines is the conversion of the initial phosphazide intermediate to the iminophosphorane (**Fig. 78**).[248, 386] Although this step is generally rapid relative to the initial bimolecular reaction, it can become rate-limiting depending on the structure of the reactants.[359, 386] There are many examples of phosphazides that are stable enough for structural analysis.[363] These intermediates can be chemically trapped, and stalled phosphazides can participate in diverse reactions.

5.3.1 Overall Mechanism

The conversion of the phosphazide to the iminophosphorane is a two-step process according to theoretical studies (**Fig. 78**).[248] First, the geometry of the *cis*-phosphazide promotes the formation of a bond between the phosphorus and the Nγ azide atom to generate a four-membered ring intermediate. This non-planar cyclic structure rapidly extrudes nitrogen in a second step. The energy levels of the transition states of the bond-forming/breaking processes and the cyclic intermediate are very close. The cyclic intermediate is therefore experimentally undetectable, and the formation of the P-Nγ bond controls the rate of the reaction step.[248]

5.3.2 Electronic Substituent Effects

The cyclization involves interaction of the phosphorus-centered LUMO with the Nγ-localized HOMO and is associated with a decrease of polarity in the transition state. This mechanism implies that substituents that increase the electron density on the Nγ atom and those that decrease the electron density on the phosphorus favor the cyclization step. Leffler and Temple reported a modestly negative Hammett reaction parameter of ρ = -0.19 for substituted phenyl azides and a Hammett parameter of ρ = 0.43 with regard to triarylphosphine substituents.[359] The electronic effects on the intramolecular steps are therefore less pronounced than those for the bimolecular reaction (see section 5.2.2).[359, 365] However, the sensitivity of the cyclization step on the electronic properties of the phosphines become more pronounced for electron-deficient azides. For example, in case of 2,3,5,6-tetrafluoro-4-methylcarboxyphenyl azide the cyclization of the phosphazide formed with PPh_3 occurred 8-fold faster compared to $P(4\text{-}MeOC_6H_4)_3$.[378] Azides with bulky and/or strongly electron-withdrawing substituents are privileged to form stable phosphazides because cyclization is disfavored. For instance, the phosphazide of diphenylcyanomethyl azide and PPh_3 could be isolated even though it adopted the cis-conformation that favors conversion to the iminophosphorane (**Fig 80a**).[387]

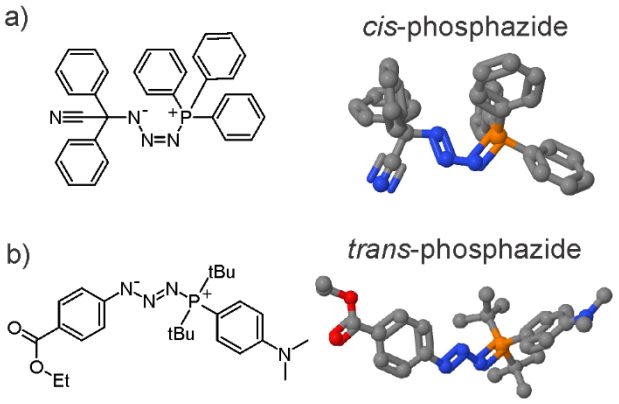

Figure 80. Examples of X-ray crystal structures of isolatable phosphazides. a) The phosphazide formed from diphenylcyanomethyl azide and triphenylphosphine adopted the *cis*-conformation. b) The phosphazide formed from ethyl 4-azidobenzoate and APhos adopted the *trans*-conformation.

5.3.3 Steric Substituent Effects

The size of phosphine substituents strongly affects the cyclization step, contrasting the relative insensitivity of the bimolecular reaction of azides and phosphines to sterics.[366] The dependency of the cyclization rate on the bulkiness of the substituents is intuitive in light of the crowded transition state.[248] For instance, the reaction of 4-methylcarboxyphenyl azide with tributylphosphine (THF/H_2O, 10/1; rt, 12 h) quantitatively yielded the aniline, whereas the yield for tricyclohexylphosphine dropped to 26%, and tri-tert-butylphosphine formed no product.[369] There are numerous examples of stable phosphazides generated from phosphines with bulky substituents.[363] In particular, two tert-butyl groups such as in bis-(tert-butyl)phenyl phosphine completely block iminophosphorane formation by generating stable *trans*-phosphazides (**Fig. 80b**), whereas substantial product formation occurs with phosphines with a single tert-butyl group.[388]

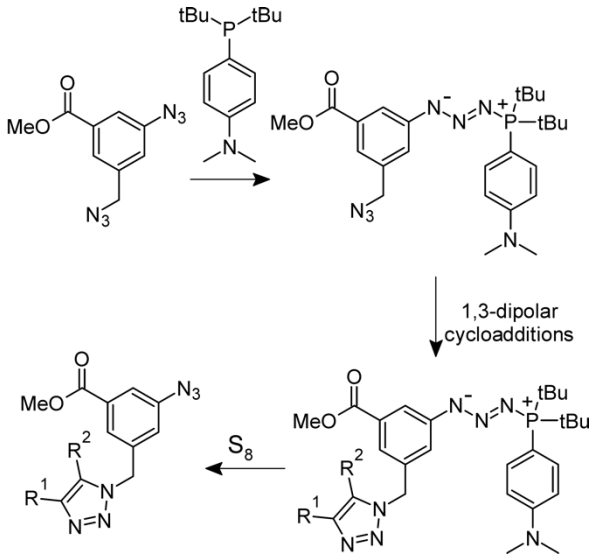

Figure 81. Protecting azides as phosphazides.

5.3.4 Phosphazides as Protecting Groups for Azides

Hosoya *et al.* exploited the aforementioned substituent effects (see sections 5.3.2 and 5.3.3) to design azide protecting groups.[388] Aryl azides could be trapped as phosphazides by exposure to bis-(*tert*-butyl)phenyl phosphine and block the 1,3-dipolar cycloaddition with strained alkynes. Because phosphazides are in equilibrium with the free azide, it was necessary to stabilize the complex by incorporating electron-donating phenyl substituents to prevent residual reaction. [4-(Dimethylamino)phenyl]bis(tert-butyl)phosphine (APhos) completely protected azides from 1,3-dipolar cycloaddition with strained alkynes, and it was possible to chemoselectively protect aryl azides in the presence of alkyl azides (**Fig. 81**). Treatment with S_8 conveniently removed the phosphazide protecting group. Such an azide protecting group will be of great value in bioorganic chemistry, for example in multi-labeling applications. While the use of sulfur is incompatible with living organism, such an approach may be used for selective modification of biomolecules. The reversibility of phosphazide formation opens additional opportunities for future developments in bioorganic chemistry.

In conclusion, bulky substituents hinder the cyclization step required to convert phosphazides into iminophosphoranes. This effect can be used to form chemically reversible azide adducts, for example as protecting groups.

5.4 Iminophosphorane Hydrolysis

5.4.1 Controlling the Hydrolysis of the Iminophosphorane Intermediate: Rapid Formation of Amines or Generating Stable Adducts

Bioorthogonal reactions are typically performed in water, which in the case of the Staudinger reaction can lead to the hydrolysis of the iminophosphorane to amines and phosphine oxides.[386] The inertness of iminophosphoranes to water varies widely. Depending on the application of interest, rapid generation of the amine or the formation of stable iminophosphorane linkages is desired. For example, phosphine-responsive reporter probes based on azide-containing fluorophores have been reported and implemented in detection schemes.[374, 389, 390] The electronic changes associated with reduction of an azide (Hammett substituent parameters:[391] σ_m = 0.37, σ_p = 0.08) to the primary amine (Hammett substituent parameters:[391] σ_m = -0.16, σ_p = -0.66) can induce readily detectable fluorescence turn-on signals.[384] In such applications, rapid and quantitative release of the amine is advantageous. This need is particularly evident in the detection of nucleic acid markers with template-mediated probes,[392] because stable linkages prevent the dissociation of the strands and signal amplification.[393, 394] On the other hand, in cases where stable iminophosphorane linkages are preferred, such as for bioconjugation applications, it is necessary to suppress its hydrolysis (see section 5.4.4). Understanding the mechanism and kinetics of iminophosphorane hydrolysis is therefore important for

designing modified Staudinger reactions for uses in biology and bioorganic chemistry.

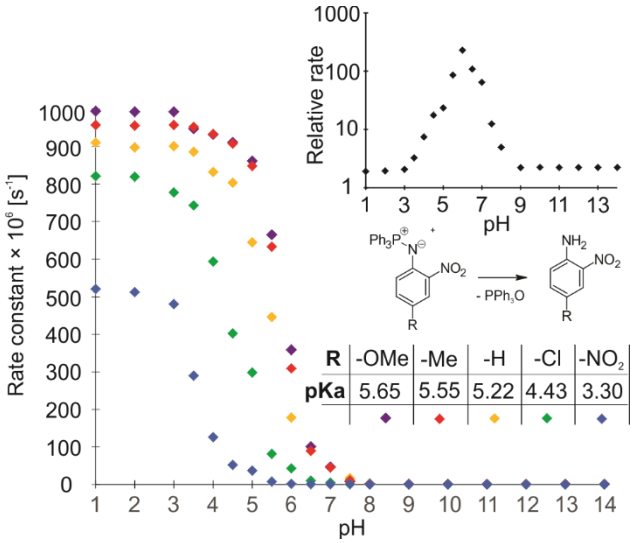

Figure 82. Dependence of the rate of aniline formation on the degree of iminophosphorane protonation. Inset: relative rate of hydrolysis for iminophosphorane with R: -OMe and -NO_2 (relative rate = k(OMe)/k(NO_2)) .

5.4.2 Mechanism of Iminophosphorane Hydrolysis

Kim *et al.* performed a detailed kinetics analysis of the hydrolysis of N-aryliminotriphenylphosphoranes.[360] The pH-dependence of the iminophosphorane hydrolysis was determined for five phenyl azides reacting with PPh_3 (**Fig. 82**). In all experiments, the reaction followed a unimolecular rate law. The hydrolysis rate was constant above pH 8 and increased with hydronium concentration before leveling off at pH 3-5 depending on the pK_a of the iminophosphorane (**Fig. 82**). This kinetics profile implicates a mechanism that involves the protonation of the iminophosphorane followed by attack of water or hydroxide and elimination of phosphorus oxide and the free amine (**Fig. 83**).

At high pH, protonation of the iminophosphorane by water is the limiting step resulting in a constant rate. Hydroxide attacks the phosphonium ion and the pentavalent intermediate disintegrates rapidly. At lower pH, the rate of the reaction becomes proportional to the fraction of protonated iminophosphorane. Water attacks the phosphonium and induces its decomposition. In case of the hydrolysis from the protonated iminophosphorane, attack of water is rate limiting if the general base concentration is high, whereas in the absence of general base the deprotonation step becomes rate limiting.

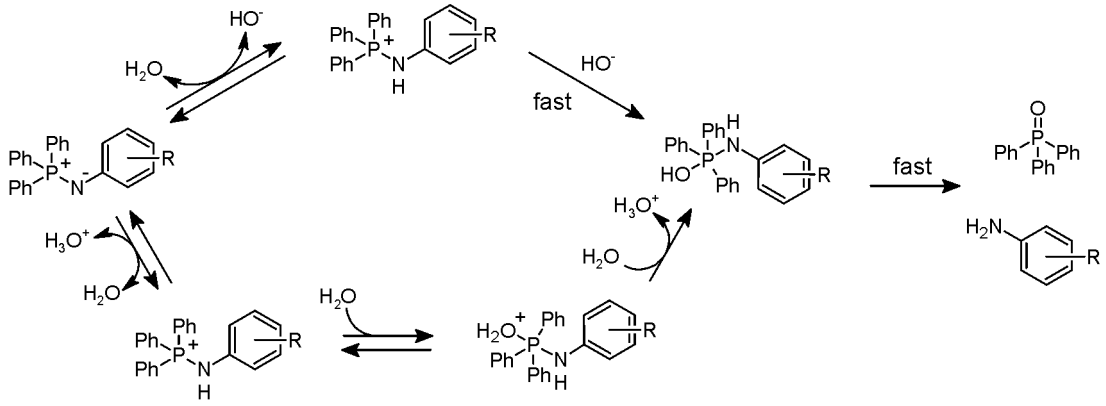

Figure 83. Mechanism of iminophosphorane hydrolysis.

5.4.3 Effects of Phosphine and Azide Structure on Hydrolysis

The phosphine structure markedly influences the kinetics of iminophosphorane hydrolysis. Phenyl azides reacting with triphenylphosphines typically persist for hours in aqueous solution.[390] This result agrees with the outlined mechanism (**Fig. 83**), because many of these iminophosphoranes are predominantly deprotonated at physiological pH (**Fig. 82**).[360] Phosphines with electron-withdrawing substituents (tris[3,5-bis(trifluoromethyl)phenyl]phosphine and tri(2-furyl)phosphine[395]) favored the hydrolysis of the iminophosphoranes to the amine relative to PPh_3.[377] This observation conflicts with the proposed mechanism, which predicts that iminophosphorane hydrolysis decreases with the basicity of the iminophosphorane.[360, 369] However, the mechanistic study by Kim *et al.* was limited to iminophosphoranes of PPh_3,[360] and it is conceivable that alternative reaction mechanisms emerge as the electron density on the phosphorus decreases, and this possibility remains to be

studied. Iminophosphoranes formed from tri(n-alkyl)phosphines with aromatic azides readily hydrolyze in minutes in water.[374] Steric shielding on aliphatic phosphines can stabilize their iminiphosphoranes either by preventing protonation or blocking attack by water.[369, 377]

5.4.4 Neighboring Group Participation

Persistence of iminophosphoranes from phosphines with aromatic groups is problematic for applications that require prompt amine release. Although aliphatic phosphines readily liberate the amines, their use under physiological conditions is limited by their ease of oxidation.[374] Dithiols are also effective in reducing azides to amines;[390, 396] however, air rapidly oxidizes dithiols to disulfides.[397] Abe *et al.* exploited neighboring group participation to develop phosphines that readily reduced aromatic azides to amines (**Fig. 84**).[398] Triphenylphosphine *ortho*-carboxamide generated 4-(methylcarboxy)aniline from the corresponding azide in less than 10 minutes and in near-quantitative yield.[398] The proposed mechanism involved the intramolecular attack of the nearby carboxamide oxygen onto the phosphorus ylide followed by breakdown of the pentavalent intermediate to release the amine and generate phosphine oxide by attack of water (**Fig. 84**).

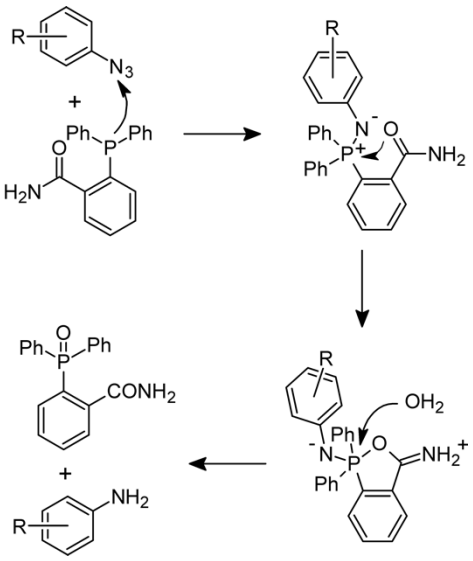

Figure 84. Neighboring groups accelerate the hydrolysis of iminophosphoranes.

5.4.5 Inert Iminophosphoranes

Research groups aimed to identify azide/phosphine combinations that form biostable iminophosphorane linkages.[399] Such easily accessible reactant pairs would have favorable properties for applications in bioconjugation and materials chemistry. Based on the mechanism of iminophosphorane hydrolysis that involves attack of water or hydroxide on the protonated aza-ylide (**Fig. 83**),[360] electron-withdrawing azide substituents are predicted to slow the dissociation step. Indeed, electron deficient phenyl azides (e.g. tetrafluorophenyl azides) formed the iminophosphoranes quantitatively upon reaction with PPh_3, whereas methoxy-substituted phenyl azides partially hydrolyzed to the amine.[377] At pH 8, the Hammett reaction parameter with regard to the phenyl azide substituents is negative (ρ = -0.63) in agreement with a reduced polarity in the transition state.[360] However, at pH 6 the triphenyliminophosphorane of 4-methoxyphenyl azide hydrolyzed 230-fold faster than the aza-ylide of 4-nitrophenyl azide, whereas at pH 9 the relative ratio of the rates is only 2.2-fold (Inset in **Fig. 82**).[360] This result establishes that the difference in iminophosphoranes protonation is the primary mechanism by which azide substituents affect amine formation at neutral pH. Furthermore, steric shielding of the iminophosphorane by bulky ortho-substituents (e.g. isopropyl) hindered the hydrolysis to the amine.[377]

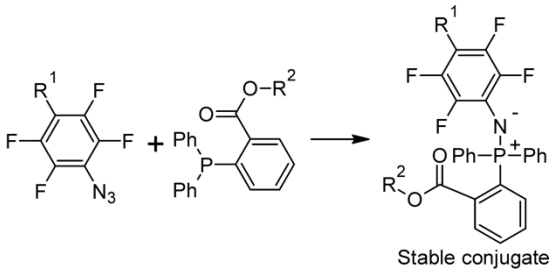

Figure 85. Fast-reacting Staudinger reaction forming inert iminophosphoranes.

Electron-deficient phenyl azides were applied to bioconjugation. 2,6-dichloro,[377] 2,6-difluoro,[380] and 2,3,5,6-tetrafluorophenylazides[378, 379] formed iminophosphoranes that were inert to hydrolytic dissociation (**Fig. 85**). An iminophosphorane of 2,3,5,6-tetrafluoro-4-methylcarboxyphenyl azide and a triphenylphosphine was stable for at least 35 days in CD_3CN/D_2O (9:1).[378] The stability of the linkage combined with the fast kinetics of the bimolecular step (see 5.2.4) make the nonhydrolytic Staudinger reaction attractive for applications in chemical biology and related disciplines as illustrated by several recent reports.[367, 378, 400-402]

5.5 Summary of Substituent Effects

Taken together, the mechanism of the Staudinger reaction allows tuning the individual steps by simple structural changes. These structure-reactivity trends are summarized in **Fig. 86**. The initial bimolecular step is highly sensitive to the electron density on the phosphine and azide, and electron-deficient aromatic azides react ~10^4-fold faster than simple alkyl azides (**Fig. 79**). The conversion of phosphazides to iminophosphoranes is highly sensitive to steric

repulsions in the transition states, and phosphines with bulky substituents form phosphazides that are stable in solution and can even be isolated (**Fig. 80**). Hydrolysis of the iminophosphorane is controlled by the protonation of the aza-ylide and is therefore responsive to electronic effects on the azide (**Figs. 82** and **83**). In this way, it is possible to generate stable iminophosphorane linkages for bioconjugation chemistry (**Fig. 85**).

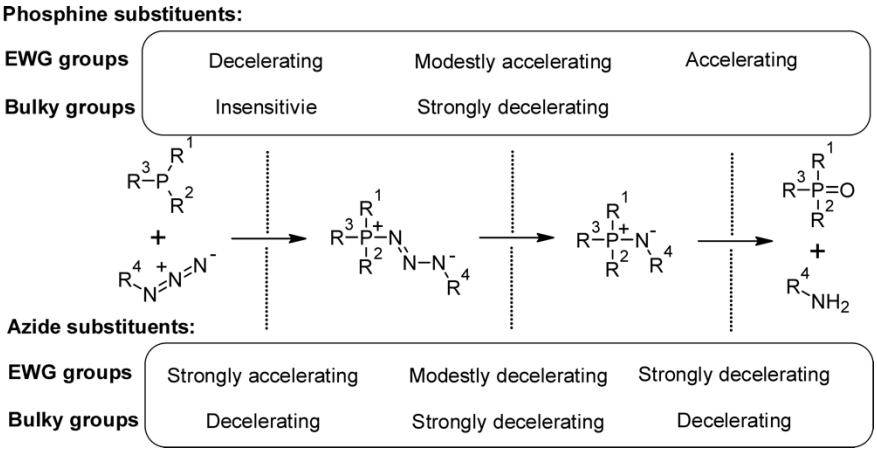

Fig. 86. Summary of electronic and steric effects on the individual steps of the Staudinger reaction.

5.6 Intramolecular Trapping of the Iminophosphorane Intermediate

The iminophosphorane is a good nucleophile and reacts with diverse groups.[386] For example, acylating reagents readily react with iminophosphoranes generating amides and other products.[403] Vilarrasa and his group pioneered the formation of amide bonds from azides and carboxylic acids mediated by phosphines in synthesis.[404-406] It should therefore be possible to form stable conjugates by strategically placing electrophiles to trap the iminophosphorane. In seminal studies, Bertozzi and coworkers harnessed this concept to covalently label azide-containing carbohydrates on cells.[407-409] They designed methyl 2-(diphenylphosphino)benzoate derivatives that undergo a Staudinger reaction with azides and form stable amide linkages by intramolecular reaction of the iminophosphorane with the ester at the ortho position (**Figs. 87** and **88**).[407] The phosphine could be modified with fluorophores for imaging purposes and linked to molecules of interest for bioconjugation.[19, 25] This reaction, often called the Staudinger-Bertozzi ligation, is broadly used in biological chemistry,[19, 25] and it was one of the first reactions to be applied to the labeling of molecules in living vertebrates.[409] Analogous to the original 2-(diphenylphosphino)benzoate esters, a proline-derived diphenylphosphine derivative[410] and phosphines with electrophilic fluorosulfate traps[411] can also undergo Staudinger ligation reactions with azides (**Fig. 87**).

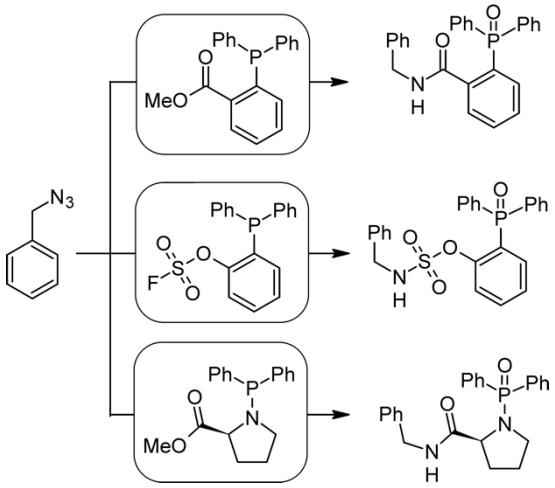

Figure 87. Ligation reactions of reacting azides with phosphines containing electrophilic traps.

5.6.1 Mechanism of the Staudinger-Bertozzi Ligation

The mechanism and substituent effects of the Staudinger-Bertozzi ligation have been investigated. The effects of substituents on the reaction kinetics mirror the trends observed for the general Staudinger reaction (see sections 5.2.1 and 5.2.2). Electron-withdrawing phosphine substituents slow the transformation and polar solvents have a modestly accelerating effect.[372] The structure of the ester group has little effect on the overall kinetics.

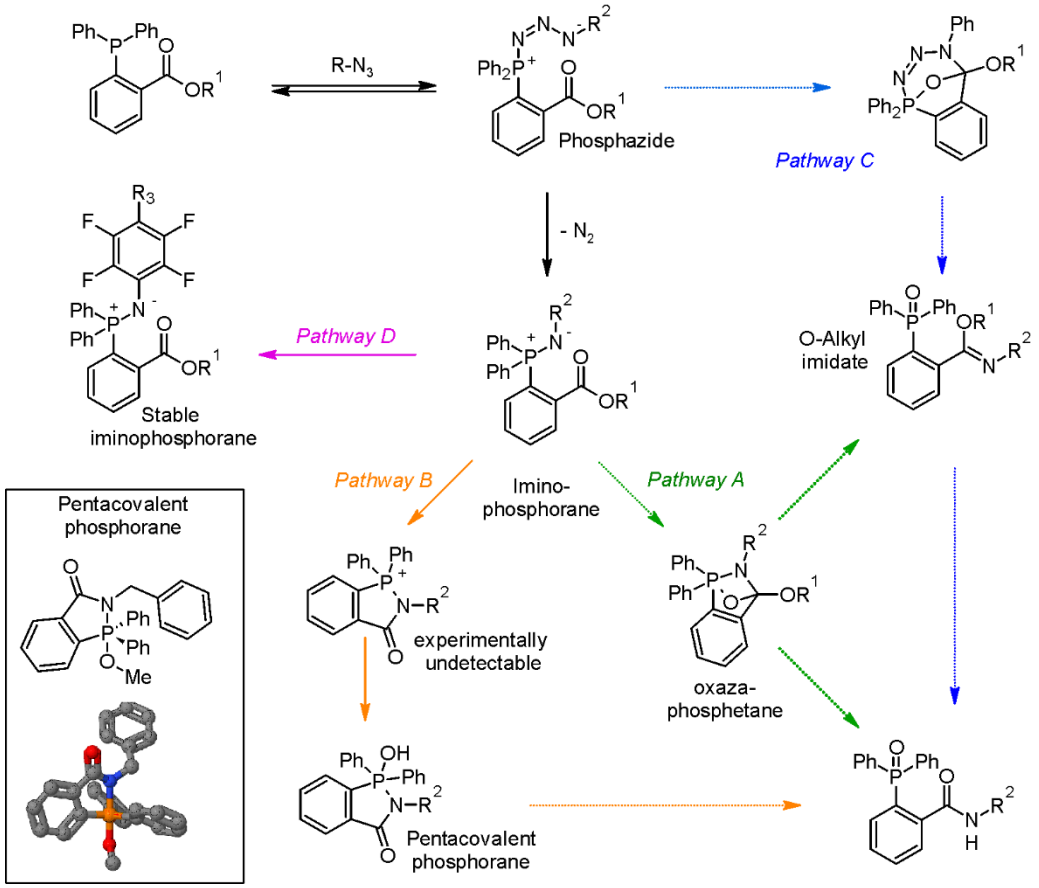

Figure 88. Mechanism of Bertozzi-Staudinger ligation. Pathway A (green): initially proposed mechanism for the conversion of the iminophosphorane to the amide through a oxazaphosphetane intermediate; Pathway B (orange): Revised mechanism for conversion of iminophosphorane to the amide through a pentacovalent phosphorane supported by X-ray structure analysis (see inset); Pathway C (blue): Proposed mechanism of accessing O-alkyl imidates from aromatic azides by intramolecular attack of the phosphazide on the ester; Pathway D: formation of stable iminophosphoranes for electron-deficient aromatic azides.

The initial steps of the proposed mechanism follow that of the general Staudinger reaction, generating the iminophosphorane via formation of the phosphazide, cyclization, and loss of nitrogen (**Figs. 81** and **88**). An intramolecular attack of the nucleophilic aza-ylide onto the nearby ester generates the C-N bond of the amide. In case of bulky *tert*-butyl esters, the amine and triphenylphosphine oxide ester formed as side products. This observation suggests that amide-bond formation and iminophosphorane hydrolysis are in kinetic competition. Relatedly, a proline-derived trivalent phosphorus compound (**Fig. 87**) required more reactive phenolic esters and thioesters for amide bond formation to occur.[410] Therefore, the electrophilicity of the ester group and the nucleophilicity of the iminophosphoranes appear to influence the rate of amide bond formation.

In water, the Staudinger-Bertozzi ligation proceeded directly to the amide. However, an intermediate with a ^{31}P NMR signal at -54.47 ppm was observed in MeCN containing substoichiometric amounts of water.[408] Initially, this intermediate was interpreted as a bridged bicyclic oxazaphosphetane species according to an aza-Witting mechanism (Pathway A in **Fig. 88**).[408] Subsequent X-ray crystallography analysis revealed that the intermediate instead was a pentacovalent phosphorane with an axial methoxy group bound to the phosphorus (inset in **Fig. 88**).[372] Accordingly, the nucleophilic attack is likely followed by decomposition of the tetrahedral intermediate, attack by water in aqueous solution, and ring opening to generate the final product containing an amide linkage and a phosphine oxide moiety (Pathway B in **Fig. 88**).

5.6.2 Staudinger Ligation with Aromatic Azides

Studies revealed that there are differences between the Staudinger ligation reaction mechanisms for alkyl and aryl azides. Rajski *et al.* reported that certain aryl azides reacting with 2-(diphenylphosphino)benzoate esters form *O*-alkyl imidates instead of amides and that such imidates could be inert to hydrolysis (**Fig. 88**).[412] In contrast, Bertozzi *et al.* observed the rapid formation of iminophosphoranes from

the reaction of *ortho*-substituted triphenylphosphine esters and aryl azides.[372] The generation of the reported *O*-alkyl imidates was proposed to involve a cyclic intermediate formed from an intramolecular reaction of the phosphazide and the ester group (Pathway C in **Fig. 88**). An analogous intermediate was implicated in the conversion of an alkyl azide reacting with PPh_3 in the presence of acetyl chloride to the corresponding chlorimine (not shown).[403] However, experimental evidence for the existence of an oxaphosphatriazine intermediate during the formation of *O*-alkyl imidates was lacking.[403] The nucleophilicity of the phosphazide is significantly lower than that of the iminophosphorane, and replacing acetyl chloride in the aforementioned study by acetic anhydride suppressed chlorimine formation.[403] A reaction sequence going through the oxazaphosphetane intermediate (pathway A in **Fig. 88**) appears as a plausible alternative; such a mechanism has been proposed for the generation of chlorimines from iminophosphoranes and acetyl chloride[403] and in the formation of side products in the traceless Staudinger-ligation.[413] Additional studies are needed to fully elucidate these processes.

Cyclization of the iminophosphorane is the critical step towards amide bond formation from aryl azides. Electron-withdrawing substituents on phenyl azides impede the intramolecular nucleophilic attack onto the ester group and instead generate stable iminophosphoranes (pathway D in **Fig. 88**)[379] as confirmed by X-ray crystallography.[378] In case of phenol esters, attack of the ester group has been reported to occur even with electron-deficient azides.[367]

5.6.3 Phosphine-induced Peptide Cleavage

Trapping of Staudinger reaction intermediates was reported to lead to cleavage of amide bonds C-terminal to an azidohomoalanine residue in peptides and proteins (**Fig. 89**).[414] The reaction generated a C-terminal homoserine-lactone ring that could be further functionalized by treatment with amines.[414] In the proposed mechanism, the phosphorus-nitrogen moiety (i.e. protonated iminophosphorane or phosphazide) acts as a leaving group and the peptide amide bond as the nucleophile. The imidate subsequently hydrolyzes to the lactone ring. Direct evidence for the proposed steps and intermediates is lacking, and additional experiments are needed to fully elucidate how this intriguing reaction occurs.

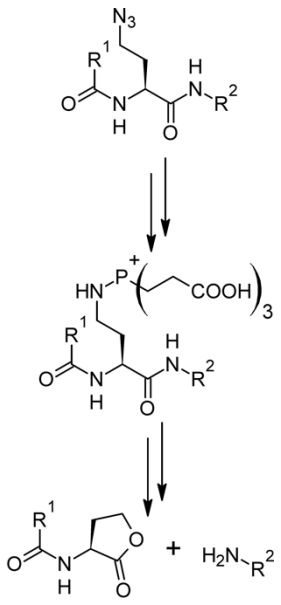

Figure 89. Phosphine-induced peptide-cleavage next to azidohomoalanine residues.

5.7 O/S→N Acyl Transfer – the Traceless Staudinger Ligation and Related Reactions

The Staudinger-Bertozzi ligation is not traceless because it forms a diphenylphosphine oxide group as an integral part of the linker (**Fig. 88**).[407] While such a moiety is acceptable for many bioconjugation applications and labeling of azidosugars, other implementations (i.e. chemical protein synthesis[415]) require the sole formation of the amide bond. Traceless versions of the Staudinger ligation were developed to overcome this limitation.[416-418]

Traceless Staudinger ligations rely on an auxiliary that consists of an activated ester and a nearby phosphine group. An incoming azide reacts with the phosphine, which is followed by an intramolecular attack of the ester group, formation of the peptide bond, and hydrolytic dissociation of the auxiliary group.[20] Several designs of such auxiliaries for traceless Staudinger ligations have been explored based on esters, phenol esters, thioesters, and thiophenyl esters (**Fig 90a**).[416-420] The diphenylphosphine methyl thioester is the most widely used group for traceless Staudinger ligations. Comprehensive summaries of traceless versions of the Staudinger ligation are available in dedicated review articles.[20, 25]

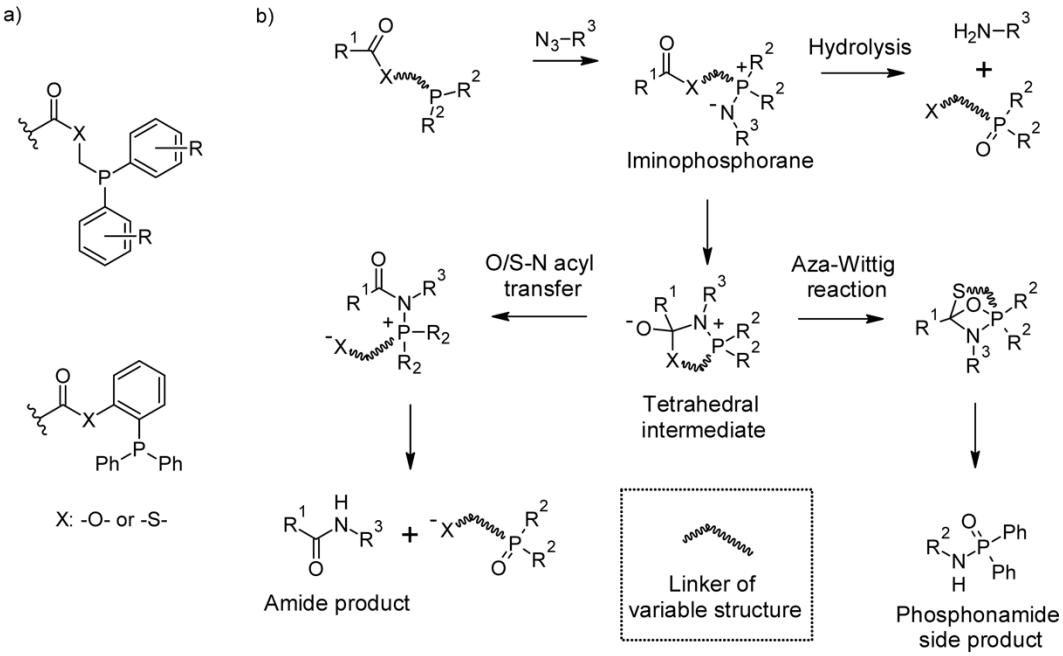

Figure 90. Mechanism of traceless Staudinger ligation.

5.7.1 Mechanism of the Traceless Staudinger Ligation

Rigorous studies provided detailed insights into the mechanism of the traceless Staudinger ligation (**Fig. 90**).[413] The bimolecular reaction of azides and ester/phosphine hybrid groups generates the iminophosphorane, which intramolecularly attacks the ester and forms a cyclic tetrahedral intermediate. Breakdown of the tetrahedral intermediate and hydrolysis of the P-N bond yield the amide. The observation that the presence of $H_2{}^{18}O$ during the reaction led to incorporation of ^{18}O to the phosphine oxide instead of the amide supports the outlined mechanism over an aza-Wittig like reaction.[413] NMR studies with ^{13}C-labeled molecules confirmed the presence of the ring-opened intermediate formed by O/S→N acyl transfer with the phosphorus-nitrogen bond.[413]

5.7.2 Enhancing the Yield of the Traceless Staudinger Ligation

Both the iminophosphorane and the cyclic intermediate can convert into different molecules, and the degree to which this happens affects the yield of the Staudinger ligation reaction (**Fig. 90**). Iminophosphorane hydrolysis competes with O/S→N acyl transfer.[420] Protonation of the iminophosphorane in aqueous buffer critically shifts the reaction away from amide-bond formation because it impedes with the cyclization step[420] and at same time promotes the hydrolysis to the amine and phosphine oxide (see section 5.4.1). Along this rationale, structural modifications that lower the pKa of the iminophosphorane enhance the yields of the traceless Staudinger ligation.[417, 419] Strategically placed positive charges (i.e. protonated dimethylaminomethyl groups)[419] reduce iminophosphorane deprotonation without decreasing the nucleophilicity of the nitrogen. In this way, positively charged phosphine auxiliaries enhance the yields of amide-bond formation in water.[419, 421]

The O/S→N acyl transfer step is further sensitive to steric repulsions in the transition state. Initial studies used glycine-derived azides and activated esters.[416-418] Replacing either of the glycine residues by alanine hindered the cyclization step and reaction yields were typically low.[413] NMR studies provided experimental evidence for the differences in the reaction path; the iminophosphorane intermediate was barely noticeable for the glycine-glycine coupling but accumulated for the alanine-alanine reaction.[413]

On the level of the cyclic intermediate, there is competition between the fragmentation step to the ring-opened intermediate and an aza-Witting side-reaction leading to a phosphonamide product (**Fig. 90**).[413] This effect can be rationalized by steric clash of substituents in the tetrahedral intermediate that can be released by formation of the oxazaphosphetane intermediate by formation of a P-O bond.[419] Electron-donating substituents that lower the oxophilicity of the phosphorus atom decrease the aza-Witting side reaction. For instance, p-methoxyphenyl phosphine substituents increased amide synthesis yields whereas electron-withdrawing p-chlorophenyl groups decreased them.[419]

5.7.3 Phosphine-mediated Peptide Switch

Coupling the Staudinger reaction to an O→N acyl transfer step further allowed controlling the structure of a peptide (**Fig. 91**).[422] It is known that nucleophiles in the proximity of an ester group can lead to acyl-transfer and the Staudinger reaction allows for the controlled generation of a nucleophile within a biomolecule. In the present example, the initial peptide contained an O-acyl isopeptide linkage that disrupted its α-helical structure and an azide group adjacent to the subsequent amide bond. Treatment of the azide with tris(2-carboxyethyl)phosphine (TCEP) under physiological conditions reduced it to the amine, which then attacked the ester and formed the amide bond to reach the peptide's desired conformation. Hydrolysis of TCEP-derived iminophosphoranes was rapid and preceded the cyclization step that involved the amine group.

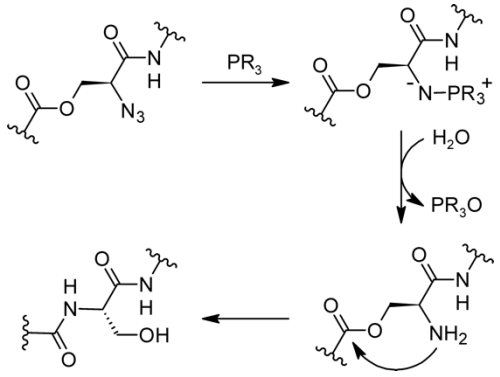

Figure 91. Phosphine-controlled peptide rearrangement.

In summary, auxiliary phosphines allow coupling azides and activated esters to form amide bonds in a traceless manner. Forming amide bonds between non-glycine residues and under aqueous conditions constitute challenges that however can be overcome by structural design. The exemplary use in the peptide-switch application illustrates the potential utility of coupling the Staudinger reaction to an O→N acyl transfer beyond peptide synthesis.

5.8 Trapping of the Phosphazide Intermediate – A Convenient Route to Diazo-compounds

5.8.1 Intramolecular Reaction of Phosphazides with Esters

In a conventional Staudinger reaction, the phosphazide intermediate rapidly transforms to the iminophosphorane by a cyclization step associated with loss of nitrogen (**Fig. 81**). Depending on the reactants, this step can become rate limiting,[359] and there are numerous phosphazides that are stable enough to be isolated and characterized (**Fig. 79**).[363] The phosphazide intermediate can be trapped chemically, although more reactive electrophiles are required than for the iminophosphorane.[386, 403] Therefore, phosphazides react intramolecularly with appropriately positioned electrophiles in analogy to the trapping of the iminophosphoranes in the Staudinger-Bertozzi ligation.[372] An informative example of an intramolecular reaction of a phosphazide is the recently described treatment of α-azidoesters with trialkyl phosphines that generates 2H-1,2,3-triazol-4-ol (**Fig. 92**).[423, 424] The phosphazide's Nα atom acts as a nucleophile attacking the ester and releasing the alcohol in an addition-elimination mechanism. Hydrolysis of the P-N bond and tautomerization generates the hydroxytriazole (**Fig. 92**). Increasing the leaving group ability (i.e. phenolic esters instead of alkyl esters) improved reaction yields and hydroxytriazoles were formed selectively over six-membered rings.[424] These outcomes reflect the lower nucleophilicity of the phosphazide compared to the iminophosphorane[403] and the resulting need for strategically positioning the electrophile trap and tuning the electrophilicity to access downstream reactions.

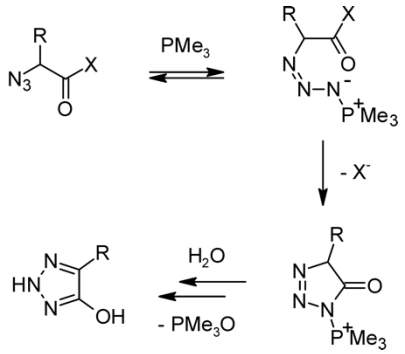

Figure 92. Intramolecular trapping of phosphazide – synthesis of hydroxytriazoles.

5.8.2 Phosphine-induced Conversion of Azides into Diazo Compounds

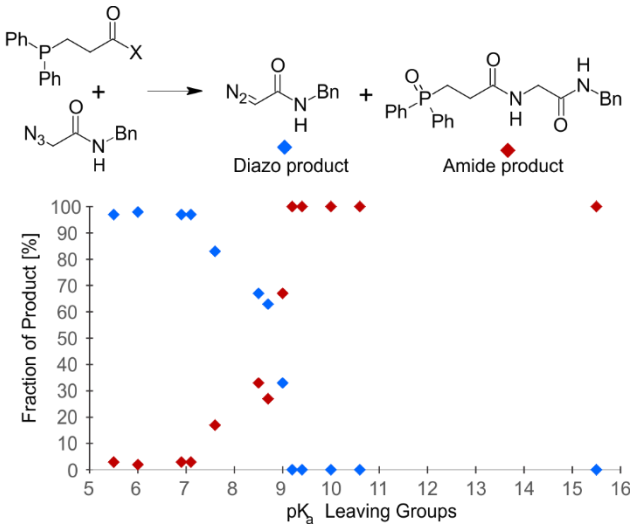

Figure 93. Influence of the ester leaving group in determining the relative ratio of diazo and amide products. 2-(diphenylphosphino)benzoic acid esters with leaving groups having a pK_a of >9.2 quantitatively generate the amide, and those with leaving groups having a pK_a of <7.1 yielded the diazo product. (Figure was drawn based on data in Ref. 425).

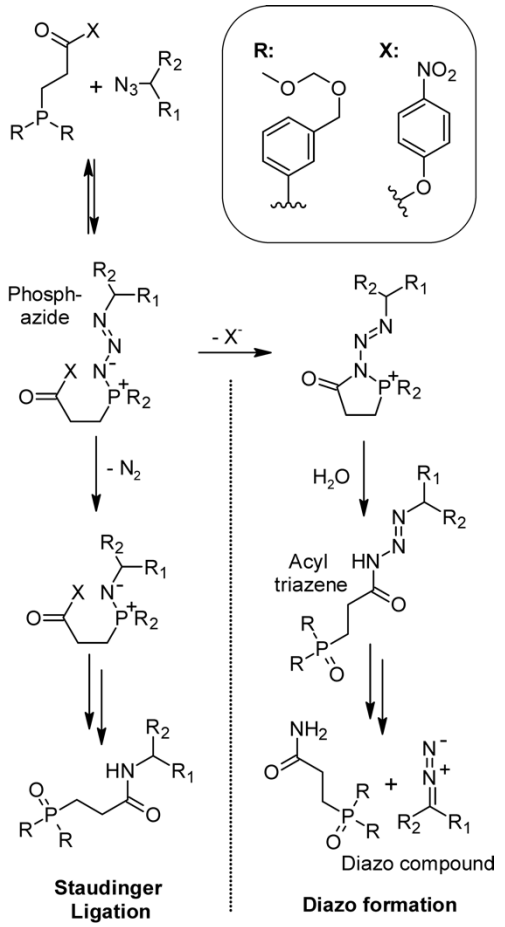

Figure 94. Phosphine-mediated conversion of azides into diazo-compounds.

Raines and his research group explored the intramolecular acylation of phosphazides to access diazo compounds.[288] The underlying hypothesis was that replacing the methyl ester group of 2-(diphenylphosphino)benzoic acid by better leaving groups would trap the phosphazides as acyltriazenes that then would dissociate into the diazo-compound and a carboxamide (**Fig. 94**).[288] Experiments confirmed that thioester and N-hydroxysuccinimide esters of 2-(diphenylphosphino)benzoic acid yielded the diazo compounds, and X-ray crystallography confirmed the structure of the acyltriazene intermediate that originated from a phenylazide.[288] A 3-diphenylphosphino propionyl ester was subsequently developed to favor the intramolecular attack by reducing delocalization of the phosphazide charge.[288] Using this scaffold, the effect of the ester group was assessed and revealed a correlation between the leaving group ability and the formation of the diazo-compound (**Fig. 93**).[425] Esters whose leaving groups had a pK_a of 9.2 or higher yielded the amide as the exclusive product; in contrast, for leaving groups with pK_a below 7.1 the diazo-compound formed selectively. The 4-nitrophenol leaving group was identified as a good compromise between high-yielding diazo formation and hydrolytic stability for applications in water.[425] This synthetic strategy provides straightforward access to diazo compounds, which are valuable functional groups in biological systems readily undergoing cycloaddition (see section 4.4.5) and esterification reactions.[426]

5.9 The Staudinger-phosphite Reaction

Azides react with various trivalent phosphorus compounds including phosphites that contain alkoxy substituents.[386] The reaction of phosphites with azides proceeds analogously to that with phosphines. However, the formed P-N bond is stable for phosphites, and hydrolysis leads to replacement of alkoxy groups.[427]

5.9.1 Mechanism of Phosphite Iminophosphorane Hydrolysis

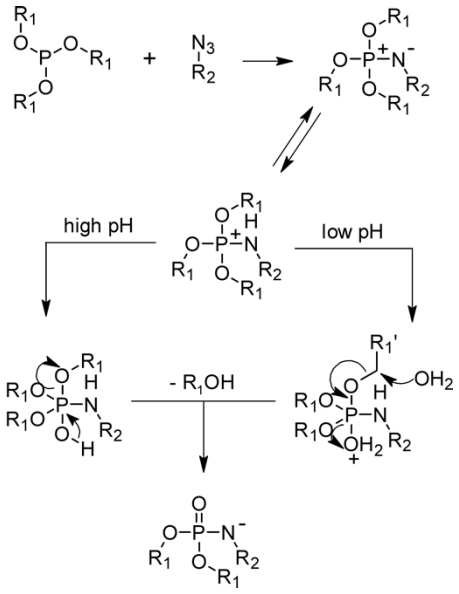

Figure 95. Reaction of phosphites with azides and subsequent hydrolysis to phosphamides.

Chaturvedi *et al.* studied the mechanism of the hydrolysis of phosphite iminophosphoranes.[427] The reaction rate's pH dependence was similar to that of iminophosphoranes of PPh_3 (**Fig. 82**).[360] Hydrolysis was fast at low pH and dropped as the pH of the solution exceeded the pK_a of the iminophosphorane (pK_a = 6.3 for N-phenyl triethoxyiminophosphorane), and protonation of the iminophosphorane is therefore required for hydrolysis. Furthermore, incorporation of ^{18}O from isotopically labeled water was dependent on the pH of the solution. These observations agreed with a tentative mechanism in which the iminophosphorane formed from the reaction of azides with phosphites is protonated and attacked by either water or hydroxide to form a pentavalent intermediate. Depending on pH, the intermediate proceeds to the products either via dealkylation by solvent attack with consecutive expulsion of the water molecule or alternatively by expulsion of ethoxide with concomitant deprotonation (**Fig. 95**).[427]

The Staudinger-phosphite reaction has been applied to generate phosphotyrosine mimetics, using photodeprotection to remove the phosphite alkyl group.[428] Furthermore, the stable P-N bond can also be used in bioconjugation applications[429-431] although the bimolecular reaction of azides with phosphites tends to be slower than for the corresponding aryl/alkyl phosphines (see section **5.2.2**).[365] Phosphonites[431, 432] and phosphoramidates[433] also undergo bioorthogonal reactions with azide-labeled molecules.

5.10 Linking the Staudinger Reaction to a Dissociative Step

Conversion of azide groups to an iminophosphorane or amine is associated with an increased electron-donating ability (Hammett substituent constants:[391] $\sigma_p(-N_3)$ = 0.08, $\sigma_p(-NH_2)$ = -0.66, $\sigma_p(-N{=}PPh_3)$ = -0.77). Leaving groups at the α-carbon are therefore prone to elimination upon reduction of the azide. Several examples of biocompatible phosphine-responsive protecting groups have been reported based on this mechanistic principle (**Fig. 96**). For example, many α-azidoethers are stable in water for hours to days,[434] whereas the corresponding hemiaminal ethers dissociate rapidly. Examples of such structures include the azidomethyl[435] and azidomethyloxycarbonyl[436] protecting groups. The α-azidoether group can also be part of phosphine-cleavable linkers.[375, 437, 438] Similarly, 4-azidobenzyloxycarbonyl[439] and 4-(azidomethoxy)benzyloxycarbonyl[440] protecting groups release amines by a 1,6-elimination upon reduction.

The studies reporting such phosphine-responsive release chemistry left it unanswered whether the elimination step occurs from the amine or from the iminophosphorane intermediate for these protecting groups. At least in case of 4-azidobenzyloxycarbonyls, release from the iminophosphorane is likely[439] given the hydrolytic stability of iminophosphoranes of aryl azides (see section **5.4**).[390]

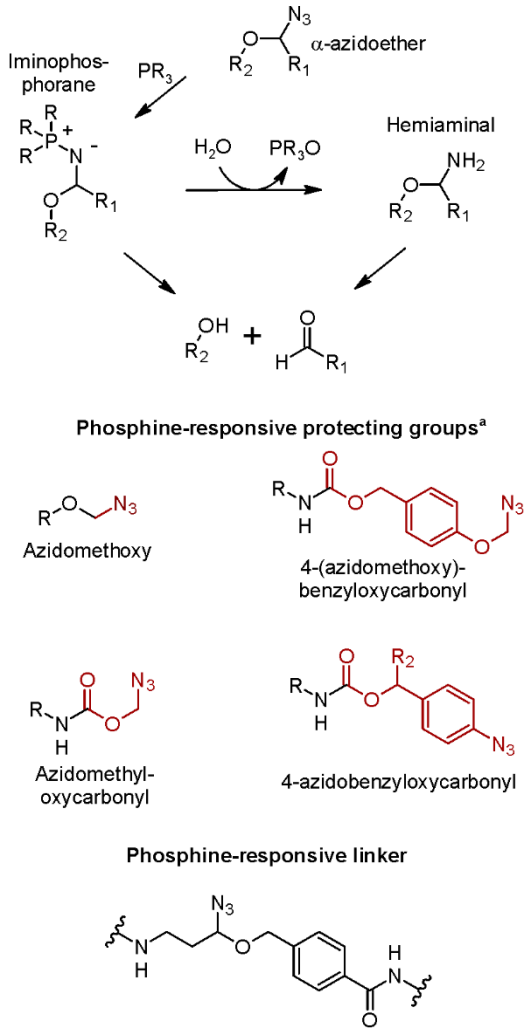

Figure 96. Coupling the Staudinger reaction to an elimination step. The structures in red indicate protecting groups.

A related case for which the dissociative step was demonstrated to occur from the iminophosphorane was the phosphine-induced opening of an azido-substituted benzocyclobutene ring (**Fig. 97**).[371] Electron-donating groups favor the opening of benzocyclobutene.[441] The corresponding aminobenzocyclobutene was stable at room temperature whereas phosphine-reduction of the azide-modified benzocyclobutene ring led to formation of *ortho*-quinodimethane and this intermediate could be trapped intramolecularly by a nearby vinyl group (not shown).[371] This result indicates that elimination from the iminophosphoranes is likely the major mechanism of these dissociative reactions and that such chemistry may possibly be applied to releasing groups that are normally difficult to deprotect.

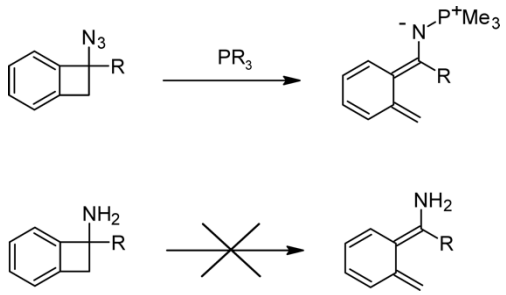

Figure 97. Iminophosphorane-promoted opening of benzocyclobutene ring.

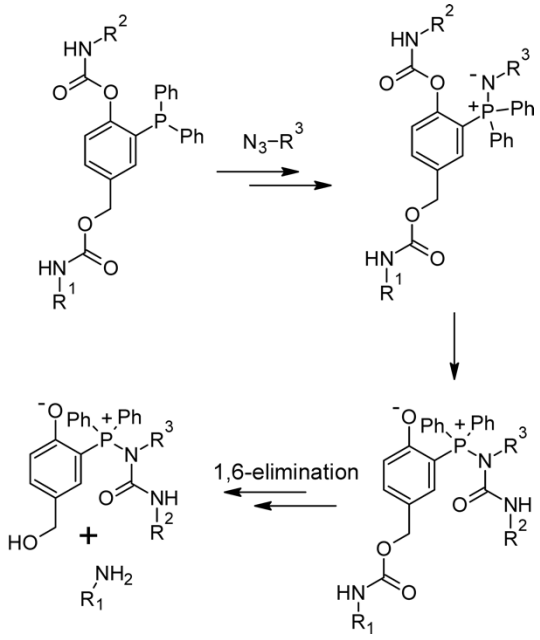

Figure 98. Azide-responsive release linker.

The Staudinger ligation intrinsically includes a dissociative step (i.e. elimination of alcohol) that may be exploited for release applications. Azoulay *et al.* developed a phosphine with a phenolic carbamate as an electrophile trap (**Fig. 98**).[442] Reaction with azides generates the iminophosphoranes that attack the carbamate and release the phenol; this step is coupled to a 1,6-elimination to release amines. A potential problem with such designs is the propensity of phosphines to oxidation, and azides are considerably more stable under physiological conditions.

In conclusion, the intrinsic dissociative character of the Staudinger reaction and the change in electronic properties from the azide to amine/iminophosphorane groups make possible the design of protecting groups and chemically cleavable linker structures. To illustrate the importance of such chemistry, azidomethoxy and α-azidoether groups are at the heart of the chemistry used in Illumina DNA-sequencers.[443]

5.11 Summary of Staudinger Reactions in Bioorthogonal Chemistry

In summary, the Staudinger reaction is a valuable transformation for biology-related research because the azide and phosphine starting products are xenobiotic and react with each other at room temperature. The stepwise mechanism allows directing the reaction towards different outcomes such as formation of stable conjugates, reduction of the azide to the amine, formation of diazo compounds, and release of payloads. Furthermore, understanding structure-reactivity relationships made it possible to accelerate the reaction by more than 10^4-fold. The diverse chemistry resulting from a single reaction illustrates how mechanistic understanding can help advance bioorthogonal chemistry.

6. CONCLUSIONS

Recent years have brought about tremendous progress in developing innovative bioorthogonal chemistry. The restricted scope of bioorthogonal functional groups made necessary the detailed mechanistic understanding of relevant transformations to access reactions with new capabilities. Combining computer-based theoretical studies and structure-reactivity analyses with chemical ingenuity allowed accessing reactions that can be extremely fast, predictably provide stable conjugates or release of a molecule, and open new capabilities in the life sciences. The extensive mechanistic knowledge available will constitute a solid foundation for developing future chemistry for use in biological systems.

AUTHOR INFORMATION

Corresponding Author

* Raphael.franzini@utah.edu.

Author Contributions

‡ These authors contributed equally.

ACKNOWLEDGMENT

We thank for support from the National Science Foundation (2004010). J.T. gratefully acknowledges financial support from a University of Utah Skaggs Graduate Fellowship and from an American Foundation for Pharmaceutical Education Pre-Doctoral Fellowship.

BIOGRAPHIES

Titas Deb received her undergraduate degree in Pharmacy from the West Bengal University of Technology, India. She obtained her M.S. degree in Medicinal Chemistry from NIPER, India, working in the group of Prof. Sankar K. Guchhait. She then moved to the University of Utah to pursue Ph.D., and is currently a graduate student in the group of Prof. Raphael Franzini.

Julian Tu received his Bachelor of Science degree in Biochemistry from the University of California, Santa Barbara where he worked in the group of Prof. L. Zhang. He then moved to the University of Utah to pursue his Ph.D. where he is currently a graduate student in the group of Prof. Raphael M. Franzini, working on the development of bioorthogonal chemistry towards implementation in drug delivery applications.

Raphael Franzini received his Ph.D. in organic chemistry from Stanford University working in the group of Prof. Eric T. Kool. He then went on to perform postdoctoral research in the group of Prof. Dario Neri at ETH Zürich, Switzerland. In 2015, he was appointed as an assistant professor in the Department of Medicinal Chemistry at the University of Utah. Research interests include the development of bioorthogonal chemistry for applications in drug delivery and chemical biology and DNA-encoded libraries for drug discovery.

REFERENCES

1. Sletten, E. M.; Bertozzi, C. R., Bioorthogonal Chemistry: Fishing for Selectivity in a Sea of Functionality. *Angew. Chem., Int. Ed.* **2009,** *48*, 6974-6998.
2. McKay, C. S.; Finn, M. G., Click Chemistry in Complex Mixtures: Bioorthogonal Bioconjugation. *Chem. Biol.* **2014,** *21*, 1075-1101.
3. Zheng, M.; Zheng, L.; Zhang, P.; Li, J.; Zhang, Y., Development of Bioorthogonal Reactions and Their Applications in Bioconjugation. *Molecules* **2015,** *20*, 3190-3205.
4. King, M.; Wagner, A., Developments in the Field of Bioorthogonal Bond Forming Reactions - Past and Present Trends. *Bioconjugate Chem.* **2014,** *25*, 825-839.
5. Jang, S. Y.; Murale, D. P.; Kim, A. D.; Lee, J. S., Recent Developments in Metal-Catalyzed Bio-orthogonal Reactions for Biomolecule Tagging. *ChemBioChem* **2019,** *20*, 1498-1507.
6. Soldevila-Barreda, J. J.; Metzler-Nolte, N., Intracellular Catalysis with Selected Metal Complexes and Metallic Nanoparticles: Advances toward the Development of Catalytic Metallodrugs. *Chem. Rev.* **2019,** *119*, 829-869.
7. Yang, M.; Yang, Y.; Chen, P. R., Transition-Metal-Catalyzed Bioorthogonal Cycloaddition Reactions. *Top. Curr. Chem.* **2016,** *374*, 2.
8. Dommerholt, J.; Rutjes, F.; van Delft, F. L., Strain-Promoted 1,3-Dipolar Cycloaddition of Cycloalkynes and Organic Azides. *Top. Curr. Chem.* **2016,** *374*, 16.
9. Oliveira, B. L.; Guo, Z.; Bernardes, G. J. L., Inverse Electron Demand Diels–Alder Reactions in Chemical Biology. *Chem. Soc. Rev.* **2017,** *46*, 4895-4950.
10. Wu, H.; Devaraj, N. K., Advances in Tetrazine Bioorthogonal Chemistry Driven by the Synthesis of Novel Tetrazines and Dienophiles. *Acc. Chem. Res.* **2018,** *51*, 1249-1259.
11. Patterson, D. M.; Nazarova, L. A.; Prescher, J. A., Finding the Right (Bioorthogonal) Chemistry. *ACS Chem. Biol.* **2014,** *9*, 592-605.

12. Tu, J.; Xu, M.; Franzini, R. M., Dissociative Bioorthogonal Reactions. *ChemBioChem* **2019,** *20*, 1615-1627.
13. Debets, M. F.; van Berkel, S. S.; Dommerholt, J.; Dirks, A. T.; Rutjes, F. P.; van Delft, F. L., Bioconjugation with Strained Alkenes and Alkynes. *Acc. Chem. Res.* **2011,** *44*, 805-815.
14. Bucci, R.; Sloan, N. L.; Topping, L.; Zanda, M., Highly Strained Unsaturated Carbocycles. *Eur. J. Org. Chem.* **2020,** *33*, 5278-5291.
15. Mayer, S.; Lang, K., Tetrazines in Inverse-Electron-Demand Diels–Alder Cycloadditions and Their Use in Biology. *Synlett* **2017,** *49*, 830-848.
16. Deb, T.; Franzini, R. M., The Unique Bioorthogonal Chemistry of Isonitriles. *Synlett* **2020**, *31*, 938-944.
17. Debets, M. F.; van der Doelen, C. W.; Rutjes, F. P.; van Delft, F. L., Azide: a Unique Dipole for Metal-free Bioorthogonal Ligations. *ChemBioChem* **2010,** *11*, 1168-1184.
18. Kohn, M.; Breinbauer, R., The Staudinger Ligation - A Gift to Chemical Biology. *Angew. Chem., Int. Ed. Engl.* **2004,** *43*, 3106-3116.
19. van Berkel, S. S.; van Eldijk, M. B.; van Hest, J. C., Staudinger Ligation as a Method for Bioconjugation. *Angew. Chem., Int. Ed.* **2011,** *50*, 8806-8827.
20. Wang, Z. P. A.; Tian, C. L.; Zheng, J. S., The Recent Developments and Applications of the Traceless-Staudinger Reaction in Chemical Biology Study. *RSC Adv.* **2015,** *5*, 107192-107199.
21. Kolmel, D. K.; Kool, E. T., Oximes and Hydrazones in Bioconjugation: Mechanism and Catalysis. *Chem. Rev.* **2017,** *117*, 10358-10376.
22. Agten, S. M.; Dawson, P. E.; Hackeng, T. M., Oxime Conjugation in Protein Chemistry: From Carbonyl Incorporation to Nucleophilic Catalysis. *J. Pept. Sci.* **2016,** *22*, 271-279.
23. Sletten, E. M.; Bertozzi, C. R., From Mechanism to Mouse: A Tale of Two Bioorthogonal Reactions. *Acc. Chem. Res.* **2011,** *44*, 666-676.
24. Pickens, C. J.; Johnson, S. N.; Pressnall, M. M.; Leon, M. A.; Berkland, C. J., Practical Considerations, Challenges, and Limitations of Bioconjugation via Azide-Alkyne Cycloaddition. *Bioconjugate Chem.* **2018,** *29*, 686-701.
25. Bednarek, C.; Wehl, I.; Jung, N.; Scheperds, U.; Brase, S., The Staudinger Ligation. *Chem. Rev.* **2020,** *120*, 10, 4301-4354.
26. Agarwal, P.; van der Weijden, J.; Sletten, E. M.; Rabuka, D.; Bertozzi, C. R., A Pictet-Spengler Ligation for Protein Chemical Modification. *Proc. Natl. Acad. Sci. U. S. A.* **2013,** *110*, 46-51.
27. Cui, L.; Rao, J., 2-Cyanobenzothiazole (CBT) Condensation for Site-specific Labeling of Proteins at the Terminal Cysteine Residues. *Methods Mol. Biol.* **2015,** *1266*, 81-92.
28. Neumann, S.; Biewend, M.; Rana, S.; Binder, W. H., The CuAAC: Principles, Homogeneous and Heterogeneous Catalysts, and Novel Developments and Applications. *Macromol. Rapid Commun.* **2020,** *41*, e1900359.
29. Li, L.; Zhang, Z., Development and Applications of the Copper-Catalyzed Azide-Alkyne Cycloaddition (CuAAC) as a Bioorthogonal Reaction. *Molecules* **2016,** *21*, 1393-1415.
30. Presolski, S. I.; Hong, V. P.; Finn, M. G., Copper-Catalyzed Azide-Alkyne Click Chemistry for Bioconjugation. *Curr. Protoc. Chem. Biol.* **2011,** *3*, 153-162.
31. Shieh, P.; Bertozzi, C. R., Design Strategies for Bioorthogonal Smart Probes. *Org. Biomol. Chem.* **2014,** *12*, 9307-9320.
32. Herner, A.; Lin, Q., Photo-Triggered Click Chemistry for Biological Applications. *Top. Curr. Chem.* **2016,** *374*, 1.
33. Li, Y.; Fu, H. Bioorthogonal Ligations and Cleavages in Chemical Biology. *Chem. Open* **2020**, *9*, 835-853.
34. Li, J.; Chen, P. R., Development and Application of Bond Cleavage Reactions in Bioorthogonal Chemistry. *Nat. Chem. Biol.* **2016,** *12*, 129-137.
35. Shorter, J., The Separation of Polar, Steric, and Resonance Effects in Organic Reactions by the Use of Linear Free Energy Relationships. *Q. Rev. Chem. Soc.* **1970,** *24*, 433-453.
36. Fukui, K.; Yonezawa, T.; Shingu, H., A Molecular Orbital Theory of Reactivity in Aromatic Hydrocarbons. *J. Chem. Phys.* **1952,** *20*, 722-725.
37. Houk, K. N., The Frontier Molecular Orbital Theory of Cycloaddition Reactions. *Acc. Chem. Res.* **1975,** *8*, 361-369.
38. Woodward, R. B.; Hoffmann, R., The Conservation of Orbital Symmetry. *Angew. Chem., Int. Ed. Engl.* **1969,** *8*, 781-853.
39. Hoffmann, R.; Woodward, R. B., Selection Rules for Concerted Cycloaddition Reactions. *J. Am. Chem. Soc.* **1965,** *87*, 2046-2048.
40. Hoffmann, R.; Woodward, R. B., Conservation of Orbital Symmetry. *Acc. Chem. Res.* **1967,** *1*, 17-22.
41. Sustmann, R., Orbital Energy Control of Cycloaddition Reactivity. *Pure Appl. Chem.* **1974,** *40*, 569-593.
42. Sustmann, R.; Trill, H., Substituent Effects in 1,3-Dipolar Cycloadditions of Phenyl Azide. *Angew. Chem., Int. Ed.* **1972,** *11*, 838-840.
43. Sustmann, R., A Simple Model for Substituent Effects in Cycloaddition Reactions. I. 1,3-Dipolar Cycloadditions. *Tetrahedron Lett.* **1971,** *12*, 2717-2720.
44. Anslyn, E. V.; Dougherty, D. A. *Modern Physical Organic Chemistry*; University Science Books: Mill Valley, 2006.
45. Liebman, J. F.; Greenberg, A., A Survey of Strained Organic Molecules. *Chem. Rev.* **1976,** *76*, 311-365.
46. Smith, M. B.; March, J. *March's Advanced Organic Chemistry: Reactions, Mechanisms, and Structure*; John Wiley & Sons: New Jersey, 2007.
47. Wiberg, K. B., Bent Bonds in Organic Compounds. *Acc. Chem. Res.* **1996,** *29*, 229-234.
48. Dunitz, J. D.; Venkatesan, K., Die Strukturen der mittleren Ringverbindungen VI. 1,6-cis-Diaminocyclodecan-dihydrochlorid. *Helv. Chim. Acta* **1961,** *44*, 2033-2041.
49. Randić, M.; Maksić, Z., Maximum Overlap Hybridization in Cyclopropane and some Related Molecules. *Theor. Chim. Acta* **1965,** *3*, 59-68.
50. Foote, C. S., The Effect of Bond Angle on Hybridization. *Tetrahedron Lett.* **1963,** *4*, 579-583.
51. Weigert, F. J.; Roberts, J. D., Nuclear Magnetic Resonance Spectroscopy. Carbon-carbon Coupling in Cyclopropane Derivatives. *J. Am. Chem. Soc.* **1967,** *89*, 5962-5963.
52. Bach, R. D., Ring Strain Energy in the Cyclooctyl System. The Effect of Strain Energy on [3 + 2] Cycloaddition Reactions with Azides. *J. Am. Chem. Soc.* **2009,** *131*, 5233-5243.
53. Liu, F.; Liang, Y.; Houk, K. N., Theoretical Elucidation of the Origins of Substituent and Strain Effects on the Rates of Diels–Alder Reactions of 1,2,4,5-Tetrazines. *J. Am. Chem. Soc.* **2014,** *136*, 11483-11493.
54. Png, Z. M.; Zeng, H.; Ye, Q.; Xu, J., Inverse-Electron-Demand Diels–Alder Reactions: Principles and Applications. *Chem. Asian J.* **2017,** *12*, 2142-2159.
55. Darko, A.; Wallace, S.; Dmitrenko, O.; Machovina, M. M.; Mehl, R. A.; Chin, J. W.; Fox, J. M., Conformationally Strained trans-Cyclooctene with Improved Stability and Excellent Reactivity in Tetrazine Ligation. *Chem. Sci.* **2014,** *5*, 3770-3776.
56. Yu, B.; Wang, B.; Pan, Z.; De La Cruz, L. K.; Ke, B.; Zheng, Y.; Ji, X., Click and release: bioorthogonal approaches to "on-demand" activation of prodrugs. *Chem. Soc. Rev.* **2019,** *48*, 1077-1094.
57. Devaraj, N. K., The Future of Bioorthogonal Chemistry. *ACS Cent. Sci.* **2018**, *4*, 952-959.
58. Blomquist, A. T.; Liu, L. H., Many-membered Carbon Rings. VII. Cycloöctyne. *J. Am. Chem. Soc.* **1953,** *75*, 2153-2154.

59. Cope, A. C.; Martin, M. M.; McKervey, M. A., Transannular reactions in medium-sized rings. *Quart. Rev. Chem. Soc.* **1966,** *20*, 119-152.

60. Chickos, J. S.; Hesse, D. G.; Panshin, S. Y.; Rogers, D. W.; Saunders, M.; Uffer, P. M.; Liebman, J. F., The Strain Energy of Cyclotetradecane is Small. *J. Org. Chem.* **1992,** *57*, 1897-1899.

61. Huber-Buser, E.; Dunitz, J. D., Strukturen der mittleren Ringverbindungen. IV. 1, 6-trans-Diaminocyclodecan-dihydrochlorid, trikline Modifikation. *Helv. Chim. Acta* **1960,** *43*, 760-768.

62. Thalhammer, F.; Wallfahrer, U.; Sauer, J., Reaktivität einfacher offenkettiger und cyclischer dienophile bei Diels-Alder-reaktionen mit inversem elektronenbedarf. *Tetrahedron Lett.* **1990,** *31*, 6851-6854.

63. Liu, F.; Paton, R. S.; Kim, S.; Liang, Y.; Houk, K. N., Diels–Alder Reactivities of Strained and Unstrained Cycloalkenes with Normal and Inverse-Electron-Demand Dienes: Activation Barriers and Distortion/Interaction Analysis. *J. Am. Chem. Soc.* **2013,** *135*, 15642-15649.

64. Paton, R. S.; Kim, S.; Ross, A. G.; Danishefsky, S. J.; Houk, K. N., Experimental Diels–Alder Reactivities of Cycloalkenones and Cyclic Dienes Explained through Transition-State Distortion Energies. *Angew. Chem., Int. Ed.* **2011,** *50*, 10366-10368.

65. van Zeist, W.-J.; Bickelhaupt, F. M., The Activation Strain Model of Chemical Reactivity. *Org. Biomol. Chem.* **2010,** *8*, 3118-3127.

66. Ess, D. H.; Houk, K. N., Theory of 1,3-Dipolar Cycloadditions: Distortion/Interaction and Frontier Molecular Orbital Models. *J. Am. Chem. Soc.* **2008,** *130*, 10187-10198.

67. Ess, D. H.; Houk, K. N., Distortion/Interaction Energy Control of 1,3-Dipolar Cycloaddition Reactivity. *J. Am. Chem. Soc.* **2007,** *129*, 10646-10647.

68. Palomo, J. M., Diels–Alder Cycloaddition in Protein Chemistry. *Eur. J. Org. Chem.* **2010,** *2010*, 6303-6314.

69. Fringuelli, F.; Taticchi, A., *The Diels-Alder Reaction : Selected Practical Methods*. Wiley: Chichester, 2002.

70. Eibler, E.; Höcht, P.; Prantl, B.; Roßmaier, H.; Schuhbauer, H. M.; Wiest, H.; Sauer, J., Transitions of Electron Demand in Pericyclic Reactions: Normal, Neutral, and Inverse Diels–Alder Reactions of Polyhalogenated Cyclopentadienes. *Liebigs Annalen* **1997,** *1997*, 2471-2484.

71. Sustmann, R., A Simple Model for Substituent Effects in Cycloaddition Reactions. II. The Diels-Alder Reaction. *Tetrahedron Lett.* **1971,** *12*, 2721-2724.

72. Sauer, J.; Sustmann, R., Mechanistic Aspects of Diels-Alder Reactions: A Critical Survey. *Angew. Chem., Int. Ed.* **1980,** *19*, 779-807.

73. Hill, K. W.; Taunton-Rigby, J.; Carter, J. D.; Kropp, E.; Vagle, K.; Pieken, W.; McGee, D. P. C.; Husar, G. M.; Leuck, M.; Anziano, D. J.; Sebesta, D. P., Diels–Alder Bioconjugation of Diene-Modified Oligonucleotides. *J. Org. Chem.* **2001,** *66*, 5352-5358.

74. Pozsgay, V.; Vieira, N. E.; Yergey, A., A Method for Bioconjugation of Carbohydrates Using Diels–Alder Cycloaddition. *Org. Lett.* **2002,** *4*, 3191-3194.

75. St. Amant, A. H.; Lemen, D.; Florinas, S.; Mao, S.; Fazenbaker, C.; Zhong, H.; Wu, H.; Gao, C.; Christie, R. J.; Read de Alaniz, J., Tuning the Diels–Alder Reaction for Bioconjugation to Maleimide Drug-Linkers. *Bioconjugation Chem.* **2018**, *29*, 2406-2414.

76. Bachmann, W. E.; Deno, N. C., The Diels-Alder Reaction of 1-Vinylnaphthalene with α,β- and α,β,γ,δ-Unsaturated Acids and Derivatives. *J. Am. Chem. Soc.* **1949,** *71*, 3062-3072.

77. Versteegen, R. M.; Rossin, R.; Ten Hoeve, W.; Janssen, H. M.; Robillard, M. S., Click to Release: Instantaneous Doxorubicin Elimination upon Tetrazine Ligation. *Angew. Chem., Int. Ed.* **2013,** *52*, 14112-14116.

78. Rossin, R.; van den Bosch, S. M.; ten Hoeve, W.; Carvelli, M.; Versteegen, R. M.; Lub, J.; Robillard, M. S., Highly Reactive trans-Cyclooctene Tags with Improved Stability for Diels–Alder Chemistry in Living Systems. *Bioconjugate Chem.* **2013,** *24*, 1210-1217.

79. Rossin, R.; Van Duijnhoven, S. M. J.; Ten Hoeve, W.; Janssen, H. M.; Kleijn, L. H. J.; Hoeben, F. J. M.; Versteegen, R. M.; Robillard, M. S., Triggered Drug Release from an Antibody-Drug Conjugate Using Fast "Click-to-Release" Chemistry in Mice. *Bioconjugate Chem.* **2016,** *27*, 1697-1706.

80. Blackman, M. L.; Royzen, M.; Fox, J. M., Tetrazine Ligation: Fast Bioconjugation Based on Inverse-Electron-Demand Diels-Alder Reactivity. *J. Am. Chem. Soc.* **2008,** *130*, 13518-13519.

81. Taylor, M. T.; Blackman, M. L.; Dmitrenko, O.; Fox, J. M., Design and Synthesis of Highly Reactive Dienophiles for the Tetrazine–trans-Cyclooctene Ligation. *J. Am. Chem. Soc.* **2011,** *133*, 9646-9649.

82. Chen, W.; Wang, D.; Dai, C.; Hamelberg, D.; Wang, B., Clicking 1,2,4,5-Tetrazine and Cyclooctynes with Tunable Reaction Rates. *Chem. Commun.* **2012,** *48*, 1736-1738.

83. Zheng, Y.; Ji, X.; Yu, B.; Ji, K.; Gallo, D.; Csizmadia, E.; Zhu, M.; Choudhury, M. R.; De La Cruz, L. K. C.; Chittavong, V.; *et al.,* Enrichment-triggered Prodrug Activation Demonstrated through Mitochondria-targeted Delivery of Doxorubicin and Carbon Monoxide. *Nat. Chem.* **2018**, *10*, 787-794.

84. Devaraj, N. K.; Weissleder, R.; Hilderbrand, S. A., Tetrazine-based Cycloadditions: Application to Pretargeted Live Cell Imaging. *Bioconjugate Chem.* **2008,** *19*, 2297-2299.

85. Plass, T.; Milles, S.; Koehler, C.; Szymański, J.; Mueller, R.; Wießler, M.; Schultz, C.; Lemke, E. A., Amino Acids for Diels-Alder Reactions in Living Cells. *Angew. Chem., Int. Ed.* **2012,** *51*, 4166-4170.

86. Lang, K.; Davis, L.; Torres-Kolbus, J.; Chou, C.; Deiters, A.; Chin, J. W., Genetically Encoded Norbornene Directs Site-Specific Cellular Protein Labelling via a Rapid Bioorthogonal Reaction. *Nat. Chem.* **2012,** *4*, 298-304.

87. Knall, A. C.; Hollauf, M.; Slugovc, C., Kinetic Studies of Inverse Electron Demand Diels-Alder Reactions (iEDDA) of Norbornenes and 3,6-Dipyridin-2-yl-1,2,4,5-tetrazine. *Tetrahedron Lett.* **2014,** *55*, 4763-4766.

88. Patterson, D. M.; Nazarova, L. A.; Xie, B.; Kamber, D. N.; Prescher, J. A., Functionalized Cyclopropenes As Bioorthogonal Chemical Reporters. *J. Am. Chem. Soc.* **2012,** *134*, 18638-18643.

89. Yang, J.; Šečkutė, J.; Cole, C. M.; Devaraj, N. K., Live-Cell Imaging of Cyclopropene Tags with Fluorogenic Tetrazine Cycloadditions. *Angew. Chem., Int. Ed.* **2012,** *51*, 7476-7479.

90. Kamber, D. N.; Nazarova, L. A.; Liang, Y.; Lopez, S. A.; Patterson, D. M.; Shih, H.-W.; Houk, K. N.; Prescher, J. A., Isomeric Cyclopropenes Exhibit Unique Bioorthogonal Reactivities. *J. Am. Chem. Soc.* **2013,** *135*, 13680-13683.

91. Xiong, D.-C.; Zhu, J.; Han, M.-J.; Luo, H.-X.; Wang, C.; Yu, Y.; Ye, Y.; Tai, G.; Ye, X.-S., Rapid Probing of Sialylated Glycoproteins in vitro and in vivo via Metabolic Oligosaccharide Engineering of a Minimal Cyclopropene Reporter. *Org. Biomol. Chem.* **2015,** *13*, 3911-3917.

92. Tu, J.; Xu, M.; Parvez, S.; Peterson, R. T.; Franzini, R. M., Bioorthogonal Removal of 3-Isocyanopropyl Groups Enables the Controlled Release of Fluorophores and Drugs in Vivo. *J. Am. Chem. Soc.* **2018,** *140*, 8410-8414.

93. Tu, J.; Svatunek, D.; Parvez, S.; Liu, A. C.; Levandowski, B. J.; Eckvahl, H. J.; Peterson, R. T.; Houk, K. N.; Franzini, R. M., Stable, Reactive, and Orthogonal Tetrazines: Dispersion Forces Promote the Cycloaddition with Isonitriles. *Angew. Chem., Int. Ed.* **2019,** *58*, 9043-9048.

94. Tu, J.; Svatunek, D.; Parvez, S.; Eckvahl, H. J.; Xu, M.; Peterson, R. T.; Houk, K. N.; Franzini, R. M., Isonitrile-Responsive

and Bioorthogonally Removable Tetrazine Protecting Groups. *Chem. Sci.* **2020,** *11*, 169-179.

95. Xu, M.; Deb, T.; Tu, J.; Franzini, R. M., Tuning Isonitrile/Tetrazine Chemistry for Accelerated Deprotection and Formation of Stable Conjugates. *J. Org. Chem.* **2019,** *84*, 15520-15529.

96. Yang, Y. F.; Yu, P.; Houk, K. N., Computational Exploration of Concerted and Zwitterionic Mechanisms of Diels-Alder Reactions between 1,2,3-Triazines and Enamines and Acceleration by Hydrogen-Bonding Solvents. *J. Am. Chem. Soc.* **2017,** *139*, 18213-18221.

97. Sustmann, R.; Tappanchai, S.; Bandmann, H., a(E)-1-Methoxy-1,3-butadiene and 1,1-Dimethoxy-1,3-butadiene in (4 + 2) Cycloadditions. A Mechanistic Comparison. *J. Am. Chem. Soc.* **1996,** *118*, 12555-12561.

98. Sustmann, R.; Sicking, W., Influence of Reactant Polarity on the Course of (4 + 2) Cycloadditions. *J. Am. Chem. Soc.* **1996,** *118*, 12562-12571.

99. Hartmann, K.-P.; Heuschmann, M., Steric Effects on the Regioselectivity in Two-Step Diels–Alder Reactions of 1,2,4,5-Tetrazines with 2-Cyclopropylidene-4,5-dihydro-1,3-dimethyl-imidazolidine. *Tetrahedron* **2000,** *56*, 4213-4218.

100. Yu, Z.-X.; Dang, Q.; Wu, Y.-D., Aromatic Dienophiles. 1. A Theoretical Study of an Inverse-Electron Demand Diels–Alder Reaction between 2-Aminopyrrole and 1,3,5-Triazine. *J. Org. Chem.* **2001,** *66*, 6029-6036.

101. De Rosa, M.; Arnold, D., Electronic and Steric Effects on the Mechanism of the Inverse Electron Demand Diels–Alder Reaction of 2-Aminopyrroles with 1,3,5-Triazines: Identification of Five Intermediates by ^{1}H, ^{13}C, ^{15}N, and ^{19}F NMR Spectroscopy. *J. Org. Chem.* **2009,** *74*, 319-328.

102. Yu, Z.-X.; Dang, Q.; Wu, Y.-D., Clarification of the Mechanism of the Cascade Reactions between Amino-Substituted Heterocycles and 1,3,5-Triazines. *J. Org. Chem.* **2005,** *70*, 998-1005.

103. Kranjc, K.; Kočevar, M., Diels–Alder Reaction of Highly Substituted 2H-Pyran-2-ones with Alkynes: Reactivity and Regioselectivity. *New J. Chem.* **2005,** *29*, 1027-1034.

104. Gomez-Bengoa, E.; Helm, M. D.; Plant, A.; Harrity, J. P. A., The Participation of Alkynylboronates in Inverse Electron Demand [4 + 2] Cycloadditions: A Mechanistic Study. *J. Am. Chem. Soc.* **2007,** *129*, 2691-2699.

105. Vogel, P.; Houk, K. N.; Organic Chemistry : Theory, Reactivity and Mechanisms in Modern Synthesis; Wiley-VCH: Weinheim, 2019.

106. Cioslowski, J.; Sauer, J.; Hetzenegger, J.; Karcher, T.; Hierstetter, T., Ab initio Quantum-mechanical and Experimental Mechanistic Studies of Diels-Alder Reactions between Unsubstituted and Phenyl-substituted Acetylenes and 1,2,4,5-Tetrazines. *J. Am. Chem. Soc.* **1993,** *115*, 1353-1359.

107. Shihab, M. S., Theoretical Study of the Mechanism of an Inverse-Demand Diels–Alder Reaction. *Arab. J. Sci. Eng.* **2012,** *37*, 75-90.

108. Sadasivam, D. V.; Prasad, E.; Flowers, R. A.; Birney, D. M., Stopped-Flow Kinetics of Tetrazine Cycloadditions; Experimental and Computational Studies toward Sequential Transition States. *J. Phys. Chem. A* **2006,** *110*, 1288-1294.

109. Boger, D. L.; Schaum, R. P.; Garbaccio, R. M., Regioselective Inverse Electron Demand Diels–Alder Reactions of N-Acyl 6-Amino-3-(methylthio)-1,2,4,5-tetrazines. *J. Org. Chem.* **1998,** *63*, 6329-6337.

110. Hamasaki, A.; Ducray, R.; Boger, D. L., Two Novel 1,2,4,5-Tetrazines that Participate in Inverse Electron Demand Diels–Alder Reactions with an Unexpected Regioselectivity. *J. Org. Chem.* **2006,** *71*, 185-193.

111. Domingo, L. R.; Picher, M. T.; Sáez, J. A., Toward an Understanding of the Unexpected Regioselective Hetero-Diels–Alder Reactions of Asymmetric Tetrazines with Electron-Rich Ethylenes: A DFT Study. *J. Org. Chem.* **2009,** *74*, 2726-2735.

112. Ravasco, J. M. J. M.; Coelho, J. A. S., Predictive Multivariate Models for Bioorthogonal Inverse-Electron Demand Diels–Alder Reactions. *J. Am. Chem. Soc.* **2020,** *142*, 4235-4241.

113. Yang, J.; Liang, Y.; Šečkute, J.; Houk, K. N.; Devaraj, N. K., Synthesis and Reactivity Comparisons of 1-Methyl-3-substituted Cyclopropene Mini-tags for Tetrazine Bioorthogonal Reactions. *Chem. Eur. J.* **2014,** *20*, 3365-3375.

114. Yu, Z.; Pan, Y.; Wang, Z.; Wang, J.; Lin, Q., Genetically Encoded Cyclopropene Directs Rapid, Photoclick-Chemistry-Mediated Protein Labeling in Mammalian Cells. *Angew. Chem., Int. Ed.* **2012,** *51*, 10600-10604.

115. Liu, K.; Enns, B.; Evans, B.; Wang, N.; Shang, X.; Sittiwong, W.; Dussault, P. H.; Guo, J., A Genetically Encoded Cyclobutene Probe for Labelling of Live Cells. *Chem. Commun.* **2017,** *53*, 10604-10607.

116. Engelsma, S. B.; Willems, L. I.; van Paaschen, C. E.; van Kasteren, S. I.; van der Marel, G. A.; Overkleeft, H. S.; Filippov, D. V., Acylazetine as a Dienophile in Bioorthogonal Inverse Electron-Demand Diels–Alder Ligation. *Org. Lett.* **2014,** *16*, 2744-2747.

117. Lang, K.; Davis, L.; Wallace, S.; Mahesh, M.; Cox, D. J.; Blackman, M. L.; Fox, J. M.; Chin, J. W., Genetic Encoding of Bicyclononynes and trans-Cyclooctenes for Site-specific Protein Labeling in vitro and in Live Mammalian Cells via Rapid Fluorogenic Diels-Alder Reactions. *J. Am. Chem. Soc.* **2012,** *134*, 10317-10320.

118. Baskin, J. M.; Prescher, J. A.; Laughlin, S. T.; Agard, N. J.; Chang, P. V.; Miller, I. A.; Lo, A.; Codelli, J. A.; Bertozzi, C. R., Copper-free Click Chemistry for Dynamic in vivo Imaging. *Proc. Natl. Acad. Sci. U. S. A.* **2007,** *104*, 16793-16797.

119. Agard, N. J.; Prescher, J. A.; Bertozzi, C. R., A Strain-promoted [3 + 2] Azide-Alkyne Cycloaddition for Covalent Modification of Biomolecules in Living Systems. *J. Am. Chem. Soc.* **2004,** *126*, 15046-15047.

120. Levandowski, B. J.; Hamlin, T. A.; Eckvahl, H. J.; Bickelhaupt, F. M.; Houk, K. N., Diels-Alder Reactivities of Cycloalkenediones with Tetrazine. *J. Mol. Modell.* **2019,** *25*, 2-6.

121. Devaraj, N. K.; Upadhyay, R.; Haun, J. B.; Hilderbrand, S. A.; Weissleder, R., Fast and Sensitive Pretargeted Labeling of Cancer Cells through a Tetrazine/trans-Cyclooctene Cycloaddition. *Angew. Chem., Int. Ed.* **2009,** *48*, 7013-7016.

122. Seitchik, J. L.; Peeler, J. C.; Taylor, M. T.; Blackman, M. L.; Rhoads, T. W.; Cooley, R. B.; Refakis, C.; Fox, J. M.; Mehl, R. a., Genetically Encoded Tetrazine Amino Acid Directs Rapid Site-Specificin Vivo Bioorthogonal Ligation with trans-Cyclooctenes. *J. Am. Chem. Soc.* **2012,** *134*, 2898-2901.

123. Rossin, R.; Versteegen, R. M.; Wu, J.; Khasanov, A.; Wessels, H. J.; Steenbergen, E. J.; ten Hoeve, W.; Janssen, H. M.; van Onzen, A. H. A. M.; Hudson, P. J.; Robillard, M. S., Chemically Triggered Drug Release from an Antibody-Drug Conjugate Leads to Potent Antitumour Activity in Mice. *Nat. Commun.* **2018,** *9*, 1484-1484.

124. Mejia Oneto, J. M.; Khan, I.; Seebald, L.; Royzen, M., In Vivo Bioorthogonal Chemistry Enables Local Hydrogel and Systemic Pro-Drug To Treat Soft Tissue Sarcoma. *ACS Cent. Sci.* **2016,** *2*, 476-482.

125. Fang, Y.; Zhang, H.; Huang, Z.; Scinto, S. L.; Yang, J. C.; am Ende, Christopher W.; Dmitrenko, O.; Johnson, D. S.; Fox, J. M., Photochemical Syntheses, Transformations, and Bioorthogonal Chemistry of trans-Cycloheptene and sila trans-Cycloheptene Ag(I) Complexes. *Chem. Sci.* **2018,** *9*, 1953-1963.

126. Squillacote, M. E.; DeFellipis, J.; Shu, Q., How Stable Is trans-Cycloheptene? *J. Am. Chem. Soc.* **2005,** *127*, 15983-15988.

127. Shimizu, T.; Shimizu, K.; Ando, W., Synthesis, Structure, and Stabilities of trans-1,2-Diphenyl-4,4,5,5,6,6-hexamethyl-4,5,6-trisilacycloheptene. *J. Am. Chem. Soc.* **1991,** *113*, 354-355.

128. Krebs, A.; Pforr, K.-I.; Raffay, W.; Thölke, B.; König, W. A.; Hardt, I.; Boese, R., A Stable Hetero-trans-cyclopentene. *Angew. Chem., Int. Ed.* **1997,** *36*, 159-160.

129. Krebs, A. W.; Thölke, B.; Pforr, K.-I.; König, W. A.; Scharwächter, K.; Grimme, S.; Vögtle, F.; Sobanski, A.; Schramm, J.; Hormes, J., Synthesis of Enantiomerically Pure (E)-1,1,3,3,6,6-Hexamethyl-1-sila-4-cycloheptene and its Absolute Configuration. *Tetrahedron Asymm.* **1999,** *10*, 3483-3492.

130. Santucci, J.; Sanzone, J. R.; Woerpel, K. A., [4+2] Cycloadditions of Seven-Membered-Ring trans-Alkenes: Decreasing Reactivity with Increasing Substitution of the Seven-Membered Ring. *Eur. J. Org. Chem.* **2016,** *2016*, 2933-2943.

131. Hurlocker, B.; Hu, C.; Woerpel, K. A., Structure and Reactivity of an Isolable Seven-Membered-Ring trans-Alkene. *Angew. Chem., Int. Ed.* **2015,** *54*, 4295-4298.

132. Sanzone, J. R.; Woerpel, K. A., Reactivity of Seven-Membered-Ring trans-Alkenes with Electrophiles. *Synlett* **2017,** *28*, 2478-2482.

133. Huisgen, R.; Ooms, P. H. J.; Mingin, M.; Allinger, N. L., Exceptional Reactivity of the Bicyclo[2.2.1]heptene Double Bond. *J. Am. Chem. Soc.* **1980,** *102*, 3951-3953.

134. Yu, Z.; Lin, Q., Design of Spiro[2.3]hex-1-ene, a Genetically Encodable Double-Strained Alkene for Superfast Photoclick Chemistry. *J. Am. Chem. Soc.* **2014,** *136*, 4153-4156.

135. Ramil, C. P.; Dong, M.; An, P.; Lewandowski, T. M.; Yu, Z.; Miller, L. J.; Lin, Q., Spirohexene-Tetrazine Ligation Enables Bioorthogonal Labeling of Class B G Protein-Coupled Receptors in Live Cells. *J. Am. Chem. Soc.* **2017**, *139*, 13376-13386.

136. Winterbourn, C. C.; Metodiewa, D., Reactivity of Biologically Important Thiol Compounds with Superoxide and Hydrogen Peroxide. *Free Radical Biol. Med.* **1999,** *27*, 322-328.

137. Siegl, S. J.; Vázquez, A.; Dzijak, R.; Dračínský, M.; Galeta, J.; Rampmaier, R.; Klepetářová, B.; Vrabel, M., Design and Synthesis of Aza-Bicyclononene Dienophiles for Rapid Fluorogenic Ligations. *Chem. Eur. J.* **2018**, 2426-2432.

138. Sauer, J.; Heldmann, D. K.; Hetzenegger, J.; Krauthan, J.; Sichert, H.; Schuster, J., 1,2,4,5-Tetrazine : Synthesis and Reactivity in [4+2] Cycloadditions. *Eur. J. Org. Chem.* **1998**, 2885-2896.

139. Prokhorov, A. M.; Kozhevnikov, D. N., Reactions of Triazines and Tetrazines with Dienophiles. *Chem. Heterocycl. Compd.* **2012,** *48*, 1153-1176.

140. Plugge, M.; Alain-Rizzo, V.; Audebert, P.; Brouwer, A. M., Excited State Dynamics of 3,6-Diaryl-1,2,4,5-tetrazines. Experimental and Theoretical Studies. *J. Photochem. Photobiol. A* **2012,** *234*, 12-20.

141. Hoffmann, J.-E.; Plass, T.; Nikić, I.; Aramburu, I. V.; Koehler, C.; Gillandt, H.; Lemke, E. A.; Schultz, C., Highly Stable trans-Cyclooctene Amino Acids for Live-Cell Labeling. *Chem. Eur. J.* **2015,** *21*, 12266-12270.

142. Li, J.; Jia, S.; Chen, P. R., Diels-Alder Reaction–triggered Bioorthogonal Protein Decaging in Living Cells. *Nat. Chem. Biol.* **2014,** *10*, 1003-1005.

143. Royzen, M.; Yap, G. P. A.; Fox, J. M., A Photochemical Synthesis of Functionalized trans-Cyclooctenes Driven by Metal Complexation. *J. Am. Chem. Soc.* **2008,** *130*, 3760-3761.

144. Vrabel, M.; Kölle, P.; Brunner, K. M.; Gattner, M. J.; López-Carrillo, V.; de Vivie-Riedle, R.; Carell, T., Norbornenes in Inverse Electron-Demand Diels–Alder Reactions. *Chem. Eur. J.* **2013,** *19*, 13309-13312.

145. Nikić, I.; Kang, J. H.; Girona, G. E.; Aramburu, I. V.; Lemke, E. A., Labeling Proteins on Live Mammalian Cells Using Click Chemistry. *Nat. Protocols* **2015,** *10*, 780-791.

146. Li, C.; Ge, H.; Yin, B.; She, M.; Liu, P.; Li, X.; Li, J., Novel 3,6-Unsymmetrically Disubstituted-1,2,4,5-Tetrazines: S-Induced One-pot Synthesis, Properties and Theoretical Study. *RSC Adv.* **2015,** *5*, 12277-12286.

147. Wijnen, J. W.; Zavarise, S.; Engberts, J. B. F. N.; Charton, M., Substituent Effects on an Inverse Electron Demand Hetero Diels–Alder Reaction in Aqueous Solution and Organic Solvents: Cycloaddition of Substituted Styrenes to Di(2-pyridyl)-1,2,4,5-tetrazine. *J. Org. Chem.* **1996,** *61*, 2001-2005.

148. Roberts, D. A.; Pilgrim, B. S.; Cooper, J. D.; Ronson, T. K.; Zarra, S.; Nitschke, J. R., Post-assembly Modification of Tetrazine-Edged FeII4L6 Tetrahedra. *J. Am. Chem. Soc.* **2015,** *137*, 10068-10071.

149. Carboni, R. A.; Lindsey, R. V., Reactions of Tetrazines with Unsaturated Compounds. A New Synthesis of Pyridazines. *J. Am. Chem. Soc.* **1959,** *81*, 4342-4346.

150. Sakya, S. M.; Groskopf, K. K.; Boger, D. L., Preparation and Inverse Electron Demand Diels-Alder Reactions of 3-Methoxy-6-methylthio-1,2,4,5-tetrazine. *Tetrahedron Lett.* **1997,** *38*, 3805-3808.

151. Karver, M. R.; Weissleder, R.; Hilderbrand, S. A., Synthesis and Evaluation of a Series of 1,2,4,5-Tetrazines for Bioorthogonal Conjugation. *Bioconjugate Chem.* **2011,** *22*, 2263-2270.

152. Wang, D.; Chen, W.; Zheng, Y.; Dai, C.; Wang, K.; Ke, B.; Wang, B., 3,6-Substituted-1,2,4,5-tetrazines: Tuning Reaction Rates for Staged Labeling Applications. *Org. Biomol. Chem.* **2014,** *12*, 3950-3955.

153. Kronister, S.; Svatunek, D.; Denk, C.; Mikula, H., Acylation-Mediated 'Kinetic Turn-On' of 3-Amino-1,2,4,5-tetrazines. *Synlett* **2018,** *29*, 1297-1302.

154. Jain, S. 1,2,4,5-Tetrazine Mediated Decaging of Biologically Relevant Molecules. Ph.D. Thesis, The University of Edinburgh, 2016.

155. Meier, A.; Sauer, J., Donor-Akzeptor substituierte Dienophile bei Diels-Alder-Reaktionen mit inversem Elektronenbedarf. *Tetrahedron Lett.* **1990,** *31*, 6855-6858.

156. Heldmann, D. K.; Sauer, J., Synthesis of Metallated (Metal = Si, Ge, Sn) Pyridazines by Cycloaddition of Metal Substituted Alkynes to 1,2,4,5-Tetrazine. *Tetrahedron Lett.* **1997,** *38*, 5791-5794.

157. Lai, S.; Mao, W.; Song, H.; Xia, L.; Xie, H., A Biocompatible Inverse Electron Demand Diels–Alder Reaction of Aldehyde and Tetrazine Promoted by Proline. *New J. Chem.* **2016,** *40*, 8194-8197.

158. Xie, H.; Zu, L.; Oueis, H. R.; Li, H.; Wang, J.; Wang, W., Proline-Catalyzed Direct Inverse Electron Demand Diels–Alder Reactions of Ketones with 1,2,4,5-Tetrazines. *Org. Lett.* **2008,** *10*, 1923-1926.

159. Sauer, J.; Heinrichs, G., Kinetik und Umsetzungen von 1.2.4.5-Tetrazinen mit winkelgespannten und elektronenreichen Doppelbindungen. *Tetrahedron Lett.* **1966,** *7*, 4979-4984.

160. Hall, D. G.; Boronic Acids: Preparation and Applications in Organic Synthesis, Medicine and Materials; Wiley-VCH: Weinheim, 2011.

161. Akgun, B.; Hall, D. G., Boronic Acids as Bioorthogonal Probes for Site-Selective Labeling of Proteins. *Angew. Chem., Int. Ed.* **2018,** *57*, 13028-13044.

162. Eising, S.; Lelivelt, F.; Bonger, K. M., Vinylboronic Acids as Fast Reacting, Synthetically Accessible, and Stable Bioorthogonal Reactants in the Carboni-Lindsey Reaction. *Angew. Chem., Int. Ed.* **2016,** *55*, 12243-12247.

163. Eising, S.; Engwerda, A. H. J.; Riedijk, X.; Bickelhaupt, F. M.; Bonger, K. M., Highly Stable and Selective Tetrazines for the Coordination-Assisted Bioorthogonal Ligation with Vinylboronic Acids. *Bioconjugate Chem.* **2018,** *29*, 3054-3059.

164. Eising, S.; Xin, B.-T.; Kleinpenning, F.; Heming, J. J. A.; Florea, B. I.; Overkleeft, H. S.; Bonger, K. M., Coordination-Assisted Bioorthogonal Chemistry: Orthogonal Tetrazine Ligation with Vinylboronic Acid and a Strained Alkene. *ChemBioChem* **2018,** *19*, 1648-1652.

165. Xu, M.; Galindo-Murillo, R.; Cheatham, T. E.; Franzini, R. M., Dissociative Reactions of Benzonorbornadienes with Tetrazines: Scope of Leaving Groups and Mechanistic Insights. *Org. Biomol. Chem.* **2017,** *15*, 9855-9865.

166. Fan, X.; Ge, Y.; Lin, F.; Yang, Y.; Zhang, G.; Ngai, W. S. C.; Lin, Z.; Zheng, S.; Wang, J.; Zhao, J.; *et al.*, Optimized Tetrazine Derivatives for Rapid Bioorthogonal Decaging in Living Cells. *Angew. Chem., Int. Ed.* **2016,** *55*, 14046-14050.

167. Ravasco, J. M. J. M.; Monteiro, C. M.; Trindade, A. F., Cyclopropenes: A New Tool for the Study of Biological Systems. *Org. Chem. Front.* **2017,** *4*, 1167-1198.

168. Xu, M.; Tu, J.; Franzini, R. M., Rapid and Efficient Tetrazine-induced Drug Release from Highly Stable Benzonorbornadiene Derivatives. *Chem. Commun.* **2017,** *53*, 6271-6274.

169. Versteegen, R. M.; Ten, W.; Rossin, R.; de Geus, M. A. R.; Janssen, H. M.; Robillard, M. S., Click-to-Release from trans-Cyclooctenes: Mechanistic Insights and Expansion of Scope from Established Carbamate to Remarkable Ether Cleavage. *Angew. Chem., Int. Ed.* **2018**, *57*, 10494-10499.

170. Wagner, J. A.; Mercadante, D.; Nikić, I.; Lemke, E. A.; Gräter, F., Origin of Orthogonality of Strain-Promoted Click Reactions. *Chem. Eur. J.* **2015,** *21*, 12431-12435.

171. Sedov, I. A.; Kornilov, D. A.; Kiselev, V. D., Solvophobic Acceleration of a Diels–Alder Reaction in True Solutions in Organic Solvents. *Int. J. Chem. Kin.* **2018,** *50*, 319-324.

172. Breslow, R.; Guo, T., Diels-Alder Reactions in Nonaqueous Polar Solvents. Kinetic Effects of Chaotropic and Antichaotropic Agents and of β-Cyclodextrin. *J. Am. Chem. Soc.* **1988,** *110*, 5613-5617.

173. Rideout, D. C.; Breslow, R., Hydrophobic Acceleration of Diels-Alder Reactions. *J. Am. Chem. Soc.* **1980,** *102*, 7816-7817.

174. Blokzijl, W.; Engberts, J. B. F. N., Initial-state and Transition-state effects on Diels-Alder Reactions in Water and Mixed Aqueous Solvents. *J. Am. Chem. Soc.* **1992,** *114*, 5440-5442.

175. Blake, J. F.; Jorgensen, W. L., Solvent Effects on a Diels-Alder Reaction from Computer Simulations. *J. Am. Chem. Soc.* **1991,** *113*, 7430-7432.

176. Blake, J. F.; Lim, D.; Jorgensen, W. L., Enhanced Hydrogen Bonding of Water to Diels-Alder Transition States. Ab Initio Evidence. *J. Org. Chem.* **1994,** *59*, 803-805.

177. Kamber, D. N.; Liang, Y.; Blizzard, R. J.; Liu, F.; Mehl, R. A.; Houk, K. N.; Prescher, J. A., 1,2,4-Triazines Are Versatile Bioorthogonal Reagents. *J. Am. Chem. Soc.* **2015,** *137*, 8388-8391.

178. Kamber, D. N.; Nguyen, S. S.; Liu, F.; Briggs, J. S.; Shih, H.-W.; Row, R. D.; Long, Z. G.; Houk, K. N.; Liang, Y.; Prescher, J. A., Isomeric Triazines Exhibit Unique Profiles of Bioorthogonal Reactivity. *Chem. Sci.* **2019,** *10*, 9109-9114.

179. Levandowski, B. J.; Abularrage, N. S.; Houk, K. N.; Raines, R. T., Hyperconjugative Antiaromaticity Activates 4H-Pyrazoles as Inverse-Electron-Demand Diels–Alder Dienes. *Org. Lett.* **2019,** *21*, 8492-8495.

180. Abularrage, N. S.; Levandowski, B. J.; Raines, R. T., Synthesis and Diels-Alder Reactivity of 4-Fluoro-4-Methyl-4H-Pyrazoles. *Int. J. Mol. Sci.* **2020,** *21*, 3964.

181. Levandowski, B. J.; Gamache, R. F.; Murphy, J. M.; Houk, K. N., Readily Accessible Ambiphilic Cyclopentadienes for Bioorthogonal Labeling. *J. Am. Chem. Soc.* **2018,** *140*, 6426-6431.

182. Gagnon, E.; Halperin, S. D.; Métivaud, V.; Maly, K. E.; Wuest, J. D., Tampering with Molecular Cohesion in Crystals of Hexaphenylbenzenes. *J. Org. Chem.* **2010,** *75*, 399-406.

183. Wang, D.; Viennois, E.; Ji, K.; Damera, K.; Draganov, A.; Zheng, Y.; Dai, C.; Merlin, D.; Wang, B., A Click-and-Release Approach to CO Prodrugs. *Chem. Commun.* **2014,** *50*, 15890-15893.

184. Mazzocchi, P. H.; Stahly, B.; Dodd, J.; Rondan, N. G.; Domelsmith, L. N.; Rozeboom, M. D.; Caramella, P.; Houk, K. N., π-Facial Stereoselectivity: Rates and Stereoselectivities of Cycloadditions of Hexachlorocyclopentadiene to 7-Substituted Norbornadienes and Photoelectron Spectral and Molecular Orbital Computation Investigations of Norbornadienes. *J. Am. Chem. Soc.* **1980,** *102*, 6482-6490.

185. Houk, K. N.; Mueller, P. H.; Wu, Y.-D.; Mazzocchi, P. H.; Shook, D.; Khachik, F., Cycloadditions of Hexachlorocyclopentadiene to 7-Substituted Norbornadienes: Remote Substituent Effects on Reacfivity and Stereoselectivity. *Tetrahedron Lett.* **1990,** *31*, 7285-7288.

186. Levandowski, B. J.; Houk, K. N., Theoretical Analysis of Reactivity Patterns in Diels–Alder Reactions of Cyclopentadiene, Cyclohexadiene, and Cycloheptadiene with Symmetrical and Unsymmetrical Dienophiles. *J. Org. Chem.* **2015,** *80*, 3530-3537.

187. Meguro, T.; Sakata, Y.; Morita, T.; Hosoya, T.; Yoshida, S., Facile Assembly of Three Cycloalkyne-modules onto a Platform Compound Bearing Thiophene S,S-Dioxide Moiety and Two Azido Groups. *Chem. Commun.* **2020**, *56*, 4720-4723.

188. Meguro, T.; Yoshida, S.; Hosoya, T., Sequential Molecular Conjugation Using Thiophene S,S-Dioxides Bearing a Clickable Functional Group. *Chem. Lett.* **2017**, *46*, 1137-1140.

189. Wang, W.; Ji, X.; Du, Z.; Wang, B., Sulfur Dioxide Prodrugs: Triggered Release of SO_2 via a Click Reaction. *Chem. Commun.* **2017,** *53*, 1370-1373.

190. Meguro, T.; Chen, S.; Kanemoto, K.; Yoshida, S.; Hosoya, T., Modular Synthesis of Unsymmetrical Doubly-ring-fused Benzene Derivatives Based on a Sequential Ring Construction Strategy Using Oxadiazinones as a Platform Molecule. *Chem. Lett.* **2019,** *48*, 582-585.

191. Borrmann, A.; Fatunsin, O.; Dommerholt, J.; Jonker, A. M.; Löwik, D. W. P. M.; van Hest, J. C. M.; van Delft, F. L., Strain-Promoted Oxidation-Controlled Cyclooctyne–1,2-Quinone Cycloaddition (SPOCQ) for Fast and Activatable Protein Conjugation. *Bioconjugate Chem.* **2015**, *26*, 257-261.

192. Levandowski, B. J.; Abularrage, N. S.; Raines, R. T., Differential Effects of Nitrogen Substitution in 5- and 6-Membered Aromatic Motifs. *Chem. Eur. J.* **2020,** *26*, 8862-8866.

193. Horner, K. A.; Valette, N. M.; Webb, M. E., Strain-Promoted Reaction of 1,2,4-Triazines with Bicyclononynes. *Chem. Eur. J.* **2015,** *21*, 14376-14381.

194. Anderson, E. D.; Boger, D. L., Inverse Electron Demand Diels–Alder Reactions of 1,2,3-Triazines: Pronounced Substituent Effects on Reactivity and Cycloaddition Scope. *J. Am. Chem. Soc.* **2011,** *133*, 12285-12292.

195. Wu, Z.-C.; Boger, D. L., Synthesis, Characterization, and Cycloaddition Reactivity of a Monocyclic Aromatic 1,2,3,5-Tetrazine. *J. Am. Chem. Soc.* **2019,** *141*, 16388-16397.

196. Talbot, A.; Devarajan, D.; Gustafson, S. J.; Fernández, I.; Bickelhaupt, F. M.; Ess, D. H., Activation-Strain Analysis Reveals Unexpected Origin of Fast Reactivity in Heteroaromatic Azadiene Inverse-Electron-Demand Diels–Alder Cycloadditions. *J. Org. Chem.* **2015,** *80*, 548-558.

197. Yang, Y.-F.; Liang, Y.; Liu, F.; Houk, K. N., Diels–Alder Reactivities of Benzene, Pyridine, and Di-, Tri-, and Tetrazines: The Roles of Geometrical Distortions and Orbital Interactions. *J. Am. Chem. Soc.* **2016,** *138*, 1660-1667.

198. Nyulászi, L.; Schleyer, P. v. R., Hyperconjugative π-Aromaticity: How To Make Cyclopentadiene Aromatic. *J. Am. Chem. Soc.* **1999,** *121*, 6872-6875.

199. von Ragué Schleyer, P.; Nyulászi, L.; Kárpáti, T., To What Extent Can Nine-Membered Monocycles Be Aromatic? *Eur. J. Org. Chem.* **2003,** *2003*, 1923-1930.

200. Fernández, I.; Wu, J. I.; von Ragué Schleyer, P., Substituent Effects on "Hyperconjugative" Aromaticity and Antiaromaticity in Planar Cyclopolyenes. *Org. Lett.* **2013,** *15*, 2990-2993.

201. Levandowski, B. J.; Zou, L.; Houk, K. N., Schleyer Hyperconjugative Aromaticity and Diels–Alder Reactivity of 5-Substituted Cyclopentadienes. *J. Comp. Chem.* **2016,** *37*, 117-123.

202. Levandowski, B. J.; Zou, L.; Houk, K. N., Hyperconjugative Aromaticity and Antiaromaticity Control the Reactivities and π-Facial Stereoselectivities of 5-Substituted Cyclopentadiene Diels–Alder Cycloadditions. *J. Org. Chem.* **2018,** *83*, 14658-14666.

203. Eibler, E.; Burgemeister, T.; Höcht, P.; Prantl, B.; Roßmaier, H.; Schuhbauer, H. M.; Wiest, H.; Sauer, J., Polyhalogenated Cyclopentadienes in [4+2] Cycloadditions: Preparative Aspects. *Liebigs Annalen* **1997,** *1997*, 2451-2469.

204. Pieniazek, S. N.; Houk, K. N., The Origin of the Halogen Effect on Reactivity and Reversibility of Diels–Alder Cycloadditions Involving Furan. *Angew. Chem., Int. Ed.* **2006,** *45*, 1442-1445.

205. Padwa, A.; Crawford, K. R.; Straub, C. S.; Pieniazek, S. N.; Houk, K. N., Halo Substituent Effects on Intramolecular Cycloadditions Involving Furanyl Amides. *J. Org. Chem.* **2006,** *71*, 5432-5439.

206. Gupta, Y. N.; Houk, K. N., Diels-Alder Cycloaddition of Tetrachlorothiophene-S,S-dioxide to Azulene. *Tetrahedron Lett.* **1985,** *26*, 2607-2608.

207. Khambata, B. S.; Wassermann, A., Kinetics of Formation and Decomposition of Dicyclo-Pentadiene. *Nature* **1936,** *137*, 496-497.

208. Pal, R.; Mukherjee, S.; Chandrasekhar, S.; Guru Row, T. N., Exploring Cyclopentadienone Antiaromaticity: Charge Density Studies of Various Tetracyclones. *J. Phys. Chem. A* **2014,** *118*, 3479-3489.

209. Ji, X.; Zhou, C.; Ji, K.; Aghoghovbia, R. E.; Pan, Z.; Chittavong, V.; Ke, B.; Wang, B., Click and Release: A Chemical Strategy toward Developing Gasotransmitter Prodrugs by Using an Intramolecular Diels–Alder Reaction. *Angew. Chem., Int. Ed.* **2016,** *55*, 15846-15851.

210. Pan, Z.; Chittavong, V.; Li, W.; Zhang, J.; Ji, K.; Zhu, M.; Ji, X.; Wang, B., Organic CO Prodrugs: Structure–CO-Release Rate Relationship Studies. *Chem. Eur. J.* **2017,** *23*, 9838-9845.

211. Ji, X.; Wang, B., Strategies toward Organic Carbon Monoxide Prodrugs. *Acc. Chem. Res.* **2018,** *51*, 1377-1385.

212. Ji, X.; Damera, K.; Zheng, Y.; Yu, B.; Otterbein, L. E.; Wang, B., Toward Carbon Monoxide-Based Therapeutics: Critical Drug Delivery and Developability Issues. *J. Pharm. Sci.* **2016,** *105*, 406-415.

213. Beck, K.; Höhn, A.; Hünig, S.; Prokschy, F., Azobrücken aus Azinen, I. Isopyrazole als elektronenarme Diene zur Synthese von 2,3-Diazabicyclo[2.2.1]heptenen. *Chem. Ber.* **1984,** *117*, 517-533.

214. Beck, K.; Hünig, S.; Klärner, F.-G.; Kraft, P.; Artschwager-Perl, U., Azobrücken aus Azinen, VII Diels-Alder-Reaktionen mit inversem Elektronenbedarf zwischen Isopyrazolen und Cycloalkenen sowie Cycloalkadienen. – Ein Vergleich von Säure-Katalyse und Beschleunigung durch Druck. *Chem. Ber.* **1987,** *120*, 2041-2051.

215. Adam, W.; Harrer, H. M.; Nau, W. M.; Peters, K., Electronic Substituent Effects on the Acid-Catalyzed [4+2] Cycloaddition of Isopyrazoles with Cyclopentadiene and the Photochemical and Thermal Denitrogenation of the Resulting 1,4-Diaryl-7,7-dimethyl-2,3-diazabicyclo[2.2.1]hept-2-ene Azoalkanes to Bicyclo[2.1.0]pentanes. *J. Org. Chem.* **1994,** *59*, 3786-3797.

216. Adam, W.; Ammon, H.; Nau, W. M.; Peters, K., 4-Halo-4H-pyrazoles: Cycloaddition with Cyclopentadiene to Azoalkanes of the 2,3-Diazabicyclo[2.2.1]hept-2-ene Type versus Electrophilic Addition with Cyclopentene. *J. Org. Chem.* **1994,** *59*, 7067-7071.

217. Wu, H.; Alexander, S. C.; Jin, S.; Devaraj, N. K., A Bioorthogonal Near-Infrared Fluorogenic Probe for mRNA Detection. *J. Am. Chem. Soc.* **2016,** *138*, 11429-11432.

218. Neumann, K.; Jain, S.; Gambardella, A.; Walker, S. E.; Valero, E.; Lilienkampf, A.; Bradley, M., Tetrazine-Responsive Self-immolative Linkers. *ChemBioChem* **2017,** *18*, 91-95.

219. Jiménez-Moreno, E.; Guo, Z.; Oliveira, B. L.; Albuquerque, I. S.; Kitowski, A.; Guerreiro, A.; Boutureira, O.; Rodrigues, T.; Jiménez-Osés, G.; Bernardes, G. J. L., Vinyl Ether/Tetrazine Pair for the Traceless Release of Alcohols in Cells. *Angew. Chem., Int. Ed.* **2017,** *56*, 243-247.

220. van Onzen, A. H. A. M.; Versteegen, R. M.; Hoeben, F. J. M.; Filot, I. A. W.; Rossin, R.; Zhu, T.; Wu, J.; Hudson, P. J.; Janssen, H. M.; ten Hoeve, W.; Robillard, M. S., Bioorthogonal Tetrazine Carbamate Cleavage by Highly Reactive trans-Cyclooctene. *J. Am. Chem. Soc.* **2020,** *142*, 10955-10963.

221. Carlson, J. C. T.; Mikula, H.; Weissleder, R., Unraveling Tetrazine-Triggered Bioorthogonal Elimination Enables Chemical Tools for Ultrafast Release and Universal Cleavage. *J. Am. Chem. Soc.* **2018,** *140*, 3603-3612.

222. Sarris, A. J. C.; Hansen, T.; de Geus, M. A. R.; Maurits, E.; Doelman, W.; Overkleeft, H. S.; Codée, J. D. C.; Filippov, D. V.; van Kasteren, S. I., Fast and pH-Independent Elimination of trans-Cyclooctene by Using Aminoethyl-Functionalized Tetrazines. *Chem. Eur. J.* **2018,** *24*, 18075-18081.

223. Davies, S.; Qiao, L.; Oliveira, B. L.; Navo, C. D.; Jiménez-Osés, G.; Bernardes, G. J. L., Tetrazine-Triggered Release of Carboxylic-Acid-Containing Molecules for Activation of an Anti-inflammatory Drug. *ChemBioChem* **2019,** *20*, 1541-1546.

224. Wu, X.; Wu, K.; Gaye, F.; Royzen, M., Bond-Breaking Bio-orthogonal Chemistry Efficiently Uncages Fluorescent and Therapeutic Compounds under Physiological Conditions. *Org. Lett.* **2020,** *22*, 6041-6044.

225. Wainman, Y. A.; Neves, A. A.; Stairs, S.; Stöckmann, H.; Ireland-Zecchini, H.; Brindle, K. M.; Leeper, F. J., Dual-sugar Imaging Using Isonitrile and Azido-based Click Chemistries. *Org. Biomol. Chem.* **2013,** *11*, 7297-7300.

226. Stairs, S.; Neves, A. A.; Stöckmann, H.; Wainman, Y. A.; Ireland-Zecchini, H.; Brindle, K. M.; Leeper, F. J., Metabolic Glycan Imaging by Isonitrile-Tetrazine Click Chemistry. *ChemBioChem* **2013,** *14*, 1063-1067.

227. Stöckmann, H.; Neves, A. A.; Stairs, S.; Brindle, K. M.; Leeper, F. J., Exploring Isonitrile-based Click Chemistry for Ligation with Biomolecules. *Org. Biomol. Chem.* **2011,** *9*, 7303-7305.

228. Chen, Y.; Wu, K.-L.; Tang, J.; Loredo, A.; Clements, J.; Pei, J.; Peng, Z.; Gupta, R.; Fang, X.; Xiao, H., Addition of Isocyanide-Containing Amino Acids to the Genetic Code for Protein Labeling and Activation. *ACS Chem. Biol.* **2019,** *14*, 2793-2799.

229. Tu, J.; Xu, M.; Franzini, R. M., A Stable Precursor for Bioorthogonally Removable 3-Isocyanopropyloxycarbonyl (ICPrc) Protecting Groups. *Synlett* **2020**, *31*, 1701-1706.

230. Imming, B. P.; Mohr, R.; Miiller, E.; Overheu, W.; Seitz, G., [4+1] Cycloaddition of Isocyanides to 1,2,4,5-Tetrazines: A Novel Synthesis of Pyrazole *Angew. Chem., Int. Ed.* **1982,** *21*, 20133-20133.

231. Fedor, L. R.; Glave, W. R., Base-catalyzed β-elimination Reactions in Aqueous Solution. V. Elimination from 4-(p-Substituted-phenoxy)-2-butanones. *J. Am. Chem. Soc.* **1971,** *93*, 985-989.

232. Sicart, R.; Collin, M.-P.; Reymond, J.-L., Fluorogenic Substrates for Lipases, Esterases, and Acylases using a TIM-mechanism for Signal Release. *Biotechnol. J.* **2007,** *2*, 221-231.

233. Klein, G.; Reymond, J.-L., An Enantioselective Fluorimetric Assay for Alcohol Dehydrogenases Using Albumin-catalyzed β-Elimination of Umbelliferone. *Bioorg. Med. Chem. Lett.* **1998,** *8*, 1113-1116.

234. Roller, S. G.; Dieckhaus, C. M.; Santos, W. L.; Sofia, R. D.; Macdonald, T. L., Interaction between Human Serum Albumin and the Felbamate Metabolites 4-Hydroxy-5-phenyl-[1,3]oxazinan-2-one and 2-Phenylpropenal. *Chem. Res. Toxicol.* **2002,** *15*, 815-824.

235. M. Priestley, G.; N. Warrener, R., A New Route to Isoindole (Benzo[c]indole) and its Derivatives. *Tetrahedron Lett.* **1972,** *13*, 4295-4298.

236. Dewar, J. S.; Harget, A. J.; Trinajstić, N.; Worley, S. D., Ground States of Conjugated Molecules–XXI: Benzofurans and Benzopyrroles. *Tetrahedron* **1970,** *26*, 4505-4516.

237. Warrener, R. N., Isolation of Isobenzofuran, a Stable but Highly Reactive Molecule. *J. Am. Chem. Soc.* **1971,** *93*, 2346-2348.

238. Lelieveldt, L. P. W. M.; Eising, S.; Wijen, A.; Bonger, K. M., Vinylboronic Acid-caged Prodrug Activation Using Click-to-release Tetrazine Ligation. *Org. Biomol. Chem.* **2019,** *17*, 8816-8821.

239. Ao, X.; Bright, S. A.; Taylor, N. C.; Elmes, R. B. P., 2-Nitroimidazole Based Fluorescent Probes for Nitroreductase; Monitoring Reductive Stress in cellulo. *Org. Biomol. Chem.* **2017,** *15*, 6104-6108.

240. Jin, C.; Zhang, Q.; Lu, W., Synthesis and biological evaluation of hypoxia-activated prodrugs of SN-38. *Eur. J. Med. Chem.* **2017,** *132*, 135-141.

241. Ji, X.; Aghoghovbia, R. E.; De La Cruz, L. K. C.; Pan, Z.; Yang, X.; Yu, B.; Wang, B., Click and Release: A High-Content Bioorthogonal Prodrug with Multiple Outputs. *Org. Lett.* **2019,** *21*, 3649-3652.

242. Curtius, T., Ueber die Einwirkung von salpetriger Säure auf salzsauren Glycocoläther. *Ber. Deutsch. Chem. Gesell.* **1883,** *16*, 2230-2231.

243. Buchner, E., Einwirkung von Diazoessigäther auf die Aether ungesättigter Säuren. *Ber. Deutsch. Chem. Gesell.* **1888,** *21*, 2637-2647.

244. Huisgen, R.; Szeimies, G.; Möbius, L., 1.3-Dipolare Cycloadditionen, XXXII. Kinetik der Additionen organischer Azide an CC-Mehrfachbindungen. *Chem. Ber.* **1967,** *100*, 2494-2507.

245. Huisgen, R., Kinetics and Mechanism of 1,3-Dipolar Cycloadditions. *Angew. Chem., Int. Ed.* **1963,** *2*, 633-645.

246. Huisgen, R., 1,3-Dipolar Cycloadditions. Past and Future. *Angew. Chem., Int. Ed.* **1963,** *2*, 565-598.

247. Qin, L.-H.; Hu, W.; Long, Y.-Q., Bioorthogonal Chemistry: Optimization and Application Updates During 2013–2017. *Tetrahedron Lett.* **2018,** *59*, 2214-2228.

248. Tian, W. Q.; Wang, Y. A., Mechanisms of Staudinger Reactions within Density Functional Theory. *J. Org. Chem.* **2004,** *69*, 4299-4308.

249. Gothelf, K. V.; Jorgensen, K. A., Asymmetric 1,3-Dipolar Cycloaddition Reactions. *Chem. Rev.* **1998,** *98*, 863-910.

250. Huisgen, R., Mechanism of 1,3-Dipolar Cycloadditions. *J. Org. Chem.* **2002,** *33*, 2291-2297.

251. Huisgen, R., 1,3-Dipolar cycloadditions. 76. Concerted Nature of 1,3-Dipolar Cycloadditions and the Question of Diradical Intermediates. *J. Org. Chem.* **1976,** *41*, 403-419.

252. Firestone, R. A., Application of the Linnett Electronic Theory to Organic Chemistry. V. Orientation in 1,3-Dipolar Cycloadditions According to the Diradical Mechanism. Partial Formal Charges in the Linnett Structures of the Diradical Intermediate. *J. Org. Chem.* **1972,** *37*, 2181-2191.

253. Firestone, R. A., Applications of the Linnett Electronic Theory to Organic Chemistry. Part III. Linnett Structures for 1,3-Dipoles and for the Diradical Intermediates in 1,3-Dipolar Cycloadditions. *J. Chem. Soc. A* **1970**, 1570-1575.

254. Firestone, R. A., The Diradical Mechanism for 1,3-Dipolar Cycloadditions and Related Thermal Pericyclic Reactions. *Tetrahedron* **1977,** *33*, 3009-3039.

255. Firestone, R. A., Mechanism of 1,3-Dipolar Cycloadditions. *J. Org. Chem.* **1968,** *33*, 2285-2290.

256. Confalone, P. N.; Huie, E. M., The [3 + 2] Nitrone-Olefin Cycloaddition Reaction. In *Organic Reactions*, John Wiley & Sons, Inc.: Hoboken, NJ, USA, 2004; pp 1-173.

257. Black, D. S. C.; Crozier, R. F.; Rae, I. D., Nitrones and Oxaziridines. XXI. Electronic Substituent Effects in Nitrone Cycloadditions to Highly Polarized Alkenes. *Aust. J. Chem.* **1978,** *31*, 2239-2246.

258. Chang, Y.-M.; Sims, J.; Houk, K. N., Mechanisms of 1.3-Dipolar Cycloadditions to Highly Electron-deficient Dipolarophiles. *Tetrahedron Lett.* **1975,** *16*, 4445-4448.

259. Steiner, G.; Huisgen, P., 2+2→4 Cycloadditions of Tetracyanoethylene to Enol Ethers; Activation Parameters as Mechanistic Criteria. *Tetrahedron Lett.* **1973,** *14*, 3769-3772.

260. Houk, K. N.; Firestone, R. A.; Munchausen, L. L.; Mueller, P. H.; Arison, B. H.; Garcia, L. A., Stereospecificity of 1,3-Dipolar Cycloadditions of p-Nitrobenzonitrile Oxide to cis- and trans-Dideuterioethylene. *J. Am. Chem. Soc.* **1985,** *107*, 7227-7228.

261. Huisgen, R.; Mloston, G.; Langhals, E., The First Two-step 1,3-Dipolar Cycloadditions: Interception of Intermediate. *J. Org. Chem.* **1986,** *51*, 4085-4087.

262. Huisgen, R.; Mloston, G.; Langhals, E., The First Two-step 1,3-Dipolar Cycloadditions: Non-stereospecificity. *J. Am. Chem. Soc.* **1986,** *108*, 6401-6402.

263. Bast, K.; Christl, M.; Huisgen, R.; Mack, W., 1,3-Dipolare Cycloadditionen, 73. Relative Dipolarophilen-Aktivitäten bei Cycloadditionen des Benzonitriloxids. *Chem. Ber.* **1973,** *106*, 3312-3344.

264. Dommerholt, J.; van Rooijen, O.; Borrmann, A.; Guerra, C. F.; Bickelhaupt, F. M.; van Delft, F. L., Highly Accelerated Inverse Electron-demand Cycloaddition of Electron-deficient Azides with Aliphatic Cyclooctynes. *Nat. Commun.* **2014**, *5*, 5378.

265. Yoshida, S.; Shiraishi, A.; Kanno, K.; Matsushita, T.; Johmoto, K.; Uekusa, H.; Hosoya, T., Enhanced Clickability of Doubly Sterically-hindered Aryl Azides. *Sci. Rep.* **2011,** *1*, 82.

266. Yoshida, S.; Tanaka, J.; Nishiyama, Y.; Hazama, Y.; Matsushita, T.; Hosoya, T., Further Enhancement of the Clickability of Doubly Sterically-hindered Aryl Azides by para-Amino Substitution. *Chem. Commun.* **2018**, *54*, 13499-13502.

267. Yoshida, S.; Goto, S.; Nishiyama, Y.; Hazama, Y.; Kondo, M.; Matsushita, T.; Hosoya, T., Effect of Resonance on the Clickability of Alkenyl Azides in the Strain-promoted Cycloaddition with Dibenzo-fused Cyclooctynes. *Chem. Lett.* **2019**, *48*, 1038-1041.

268. Himo, F.; Lovell, T.; Hilgraf, R.; Rostovtsev, V. V.; Noodleman, L.; Sharpless, K. B.; Fokin, V. V., Copper(I)-catalyzed Synthesis of Azoles. DFT Study Predicts Unprecedented Reactivity and Intermediates. *J. Am. Chem. Soc.* **2005,** *127*, 210-216.

269. Sanders, B. C.; Friscourt, F.; Ledin, P. A.; Mbua, N. E.; Arumugam, S.; Guo, J.; Boltje, T. J.; Popik, V. V.; Boons, G. J., Metal-free Sequential [3 + 2]-Dipolar Cycloadditions Using Cyclooctynes and 1,3-Dipoles of Different Reactivity. *J. Am. Chem. Soc.* **2011,** *133*, 949-957.

270. Roscales, S.; Plumet, J., Metal-catalyzed 1,3-Dipolar Cycloaddition Reactions of Nitrile Oxides. *Org. Biomol. Chem.* **2018,** *16*, 8446-8461.

271. Domingo, L. R.; Chamorro, E.; Pérez, P., An Analysis of the Regioselectivity of 1,3-Dipolar Cycloaddition Reactions of BenzonitrileN-Oxides Based on Global and Local Electrophilicity and Nucleophilicity Indices. *Eur. J. Org. Chem.* **2009,** *2009*, 3036-3044.

272. Schafer, R. J. B.; Monaco, M. R.; Li, M.; Tirla, A.; Rivera-Fuentes, P.; Wennemers, H., The Bioorthogonal Isonitrile-Chlorooxime Ligation. *J. Am. Chem. Soc.* **2019,** *141*, 18644-18648.

273. McKay, C. S.; Moran, J.; Pezacki, J. P., Nitrones as Dipoles for Rapid Strain-promoted 1,3-Dipolar Cycloadditions with Cyclooctynes. *Chem. Commun.* **2010,** *46*, 931-933.

274. McKay, C. S.; Blake, J. A.; Cheng, J.; Danielson, D. C.; Pezacki, J. P., Strain-promoted Cycloadditions of Cyclic Nitrones with Cyclooctynes for Labeling Human Cancer Cells. *Chem. Commun.* **2011,** *47*, 10040-10042.

275. Kouklovsky, C.; Vincent, G., 8.14 Reduction of NN, N–N, N–O, and O–O Bonds. In *Comprehensive Organic Synthesis II (Second Edition)*, Knochel, P., Ed. Elsevier: Amsterdam, 2014; pp 493-534.

276. Kumar, R. A.; Pattanayak, M. R.; Yen-Pon, E.; Eliyan, J.; Porte, K.; Bernard, S.; Riomet, M.; Thuery, P.; Audisio, D.; Taran, F., Strain-Promoted 1,3-Dithiolium-4-olates-Alkyne Cycloaddition. *Angew. Chem., Int. Ed. Engl.* **2019,** *58*, 14544-14548.

277. Kaya, E.; Vrabel, M.; Deiml, C.; Prill, S.; Fluxa, V. S.; Carell, T., A Genetically Encoded Norbornene Amino Acid for the Mild and Selective Modification of Proteins in a Copper-free Click Reaction. *Angew. Chem., Int. Ed.* **2012,** *51*, 4466-4469.

278. Clovis, J. S.; Eckell, A.; Huisgen, R.; Sustmann, R., 1.3-Dipolare Cycloadditionen, XXV. Der Nachweis des freien Diphenylnitrilimins als Zwischenstufe bei Cycloadditionen. *Chem. Ber.* **1967,** *100*, 60-70.

279. Song, W.; Wang, Y.; Qu, J.; Madden, M. M.; Lin, Q., A Photoinducible 1,3-Dipolar Cycloaddition Reaction for Rapid, Selective Modification of Tetrazole-containing Proteins. *Angew. Chem., Int. Ed.* **2008,** *47*, 2832-2835.

280. An, P.; Lewandowski, T. M.; Erbay, T. G.; Liu, P.; Lin, Q., Sterically Shielded, Stabilized Nitrile Imine for Rapid Bioorthogonal Protein Labeling in Live Cells. *J. Am. Chem. Soc.* **2018,** *140*, 4860-4868.

281. Ramil, C. P.; Lin, Q., Photoclick Chemistry: A Fluorogenic Light-triggered in vivo Ligation Reaction. *Curr. Opin. Chem. Biol.* **2014,** *21*, 89-95.

282. An, P.; Yu, Z.; Lin, Q., Design of Oligothiophene-based Tetrazoles for Laser-triggered Photoclick Chemistry in Living Cells. *Chem. Commun.* **2013,** *49*, 9920-9922.

283. Yu, Z.; Ohulchanskyy, T. Y.; An, P.; Prasad, P. N.; Lin, Q., Fluorogenic, Two-photon-triggered Photoclick Chemistry in Live Mammalian Cells. *J. Am. Chem. Soc.* **2013,** *135*, 16766-16769.

284. Huisgen, R.; Stangl, H.; Sturm, H. J.; Wagenhofer, H., 1.3-Dipolare Additionen mit Nitril-yliden. *Angew. Chem.* **1962,** *74*, 31.

285. Regitz, M.; Maas, G. Diazo compounds: properties and synthesis, Academic Press, 1986.

286. Aronoff, M. R.; Gold, B.; Raines, R. T., 1,3-Dipolar Cycloadditions of Diazo Compounds in the Presence of Azides. *Org. Lett.* **2016,** *18*, 1538-1541.

287. Andersen, K. A.; Aronoff, M. R.; McGrath, N. A.; Raines, R. T., Diazo Groups Endure Metabolism and Enable Chemoselectivity in cellulo. *J. Am. Chem. Soc.* **2015,** *137*, 2412-2415.

288. Myers, E. L.; Raines, R. T., A Phosphine-mediated Conversion of Azides into Diazo Compounds. *Angew. Chem., Int. Ed.* **2009,** *48*, 2359-2363.

289. McGrath, N. A.; Raines, R. T., Diazo Compounds as Highly Tunable Reactants in 1,3-Dipolar Cycloaddition Reactions with Cycloalkynes. *Chem Sci* **2012,** *3*, 3237-3240.

290. Josa-Culleré, L.; Wainman, Y. A.; Brindle, K. M.; Leeper, F. J., Diazo Group as a New Chemical Reporter for Bioorthogonal Labelling of Biomolecules. *RSC Adv.* **2014,** *4*, 52241-52244.

291. Decuypere, E.; Plougastel, L.; Audisio, D.; Taran, F., Sydnone-alkyne Cycloaddition: Applications in Synthesis and Bioconjugation. *Chem. Commun.* **2017,** *53*, 11515-11527.

292. Baker, W.; Ollis, W. D., Meso-ionic compounds. *Quart. Rev. Chem. Soc* **1957,** *11*, 15-29.

293. Lopchuk J.M. Mesoionics. In: Gribble G. (eds) Metalation of Azoles and Related Five-Membered Ring Heterocycles. Topics in Heterocyclic Chemistry, vol 29. Springer, Berlin, Heidelberg, 2012.

294. Huisgen, R.; Gotthardt, H.; Grashey, R., Reactions of Sydnones with Alkenes. *Angew. Chem., Int. Ed.* **1962,** *1*, 49.

295. Huisgen, R.; Gotthardt, H.; Grashey, R., 1.3-Dipolare Cycloadditionen, XXXIV. Pyrazole aus Sydnonen und acetylenischen Dipolarophilen. *Chem. Ber.* **1968,** *101*, 536-551.

296. Earl, J. C.; Mackney, A. W., 204. The Action of Acetic Anhydride on N-Nitrosophenylglycine and some of its Derivatives. *J. Chem. Soc.* **1935,** 899-900.

297. Wallace, S.; Chin, J. W., Strain-promoted Sydnone Bicyclo-[6.1.0]-nonyne Cycloaddition. *Chem. Sci.* **2014,** *5*, 1742-1744.

298. Huisgen, R.; Gotthardt, H., 1.3-Dipolare Cycloadditionen, XXXIX. Kinetik und Mechanismus der Cycloadditionen der Sydnone. *Chem. Ber.* **1968,** *101*, 1059-1071.

299. Houk, K. N.; Sims, J.; Duke, R. E.; Strozier, R. W.; George, J. K., Frontier Molecular Orbitals of 1,3-Dipoles and Dipolarophiles. *J. Am. Chem. Soc.* **1973,** *95*, 7287-7301.

300. Youn, B. H. L., H. S.; Han, J. H.; Kim, S. H., Kinetics of the 1,3-Dipolar Cycloaddition of p-Substituted 3-Phenylsydnones with DMAD. *Bull. Korean Chem. Soc.* **1987,** *8*, 233-235.

301. Plougastel, L.; Koniev, O.; Specklin, S.; Decuypere, E.; Creminon, C.; Buisson, D. A.; Wagner, A.; Kolodych, S.; Taran, F., 4-Halogeno-sydnones for Fast Strain Promoted Cycloaddition with Bicyclo-[6.1.0]-nonyne. *Chem. Commun.* **2014,** *50*, 9376-9378.

302. Liu, H.; Audisio, D.; Plougastel, L.; Decuypere, E.; Buisson, D. A.; Koniev, O.; Kolodych, S.; Wagner, A.; Elhabiri, M.; *et al.*, Ultrafast Click Chemistry with Fluorosydnones. *Angew. Chem., Int. Ed.* **2016,** *55*, 12073-12077.

303. Tao, H.; Liu, F.; Zeng, R.; Shao, Z.; Zou, L.; Cao, Y.; Murphy, J. M.; Houk, K. N.; Liang, Y., Origins of Halogen Effects in Bioorthogonal Sydnone Cycloadditions. *Chem. Commun.* **2018,** *54*, 5082-5085.

304. Hein, J. E.; Fokin, V. V., Copper-catalyzed Azide-Alkyne Cycloaddition (CuAAC) and Beyond: New Reactivity of Copper(I) Acetylides. *Chem. Soc. Rev.* **2010,** *39*, 1302-1315.

305. Meldal, M.; Tornoe, C. W., Cu-catalyzed Azide-Alkyne Cycloaddition. *Chem. Rev.* **2008,** *108*, 2952-3015.

306. Liang, L.; Astruc, D., The Copper(I)-catalyzed Alkyne-azide cycloaddition (CuAAC) "Click" Reaction and its Applications. An Overview. *Coord. Chem. Rev.* **2011,** *255*, 2933-2945.

307. Jewett, J. C.; Bertozzi, C. R., Cu-free Click Cycloaddition Reactions in Chemical Biology. *Chem. Soc. Rev.* **2010,** *39*, 1272-1279.

308. Ess, D. H.; Jones, G. O.; Houk, K. N., Transition States of Strain-promoted Metal-free Click Chemistry: 1,3-Dipolar Cycloadditions of Phenyl Azide and Cyclooctynes. *Org. Lett.* **2008,** *10*, 1633-1636.

309. Wittig, G.; Krebs, A., Zur Existenz niedergliedriger Cycloalkine, I. *Chem. Ber.* **1961,** *94*, 3260-3275.

310. Harris, T.; Alabugin, I. V., Strain and Stereoelectronics in Cycloalkyne Click Chemistry. *Mendeleev Commun.* **2019,** *29*, 237-248.

311. Ramsubhag, R. R.; Dudley, G. B., Orthogonal Dual-click diyne for CuAAC and/or SPAAC Couplings. *Org. Biomol. Chem.* **2016**, *14*, 5028-5031.

312. Ning, X.; Guo, J.; Wolfert, M. A.; Boons, G. J., Visualizing Metabolically Labeled Glycoconjugates of Living Cells by Copper-free and Fast Huisgen Cycloadditions. *Angew. Chem., Int. Ed.* **2008,** *47*, 2253-2255.

313. Dommerholt, J.; Schmidt, S.; Temming, R.; Hendriks, L. J.; Rutjes, F. P.; van Hest, J. C.; Lefeber, D. J.; Friedl, P.; van Delft, F. L., Readily Accessible Bicyclononynes for Bioorthogonal Labeling and Three-dimensional Imaging of Living Cells. *Angew. Chem., Int. Ed.* **2010,** *49*, 9422-9425.

314. Alabugin, I. V.; Bresch, S.; dos Passos Gomes, G., Orbital Hybridization: A Key Electronic Factor in Control of Structure and Reactivity. *J. Phys. Org. Chem.* **2015,** *28*, 147-162.

315. Sletten, E. M.; Bertozzi, C. R., A Hydrophilic Azacyclooctyne for Cu-free Click Chemistry. *Org. Lett.* **2008**, *10*, 3097-3099.

316. Debets, M. F.; van Berkel, S. S.; Schoffelen, S.; Rutjes, F. P.; van Hest, J. C.; van Delft, F. L., Aza-Dibenzocyclooctynes for Fast and Efficient Enzyme PEGylation via Copper-free (3+2) Cycloaddition. *Chem. Commun.* **2010**, *46*, 97-99.

317. Wong, H. N. C.; Garratt, P. J.; Sondheimer, F., Unsaturated Eight-membered Ring Compounds. XI. Synthesis of sym-Dibenzo-

1,5-cyclooctadiene-3,7-diyne and sym-Dibenzo-1,3,5-cyclooctatrien-7-yne, Presumably Planar Conjugated Eight-membered Ring Compounds. *J. Am. Chem. Soc.* **1974**, *96*, 5604-5605.

318. Jewett, J. C.; Sletten, E. M.; Bertozzi, C. R., Rapid Cu-free Click Chemistry with Readily Synthesized Biarylazacyclooctynones. *J. Am. Chem. Soc.* **2010,** *132*, 3688-3690.

319. Gold, B.; Dudley, G. B.; Alabugin, I. V., Moderating Strain without Sacrificing Reactivity: Design of Fast and Tunable Noncatalyzed Alkyne-Azide Cycloadditions via Stereoelectronically Controlled Transition State Stabilization. *J. Am. Chem. Soc.* **2013,** *135*, 1558-1569.

320. Ni, R.; Mitsuda, N.; Kashiwagi, T.; Igawa, K.; Tomooka, K., Heteroatom-embedded Medium-sized Cycloalkynes: Concise Synthesis, Structural Analysis, and Reactions. *Angew. Chem., Int. Ed.* **2015,** *54*, 1190-1194.

321. Burke, E. G.; Gold, B.; Hoang, T. T.; Raines, R. T.; Schomaker, J. M., Fine-Tuning Strain and Electronic Activation of Strain-Promoted 1,3-Dipolar Cycloadditions with Endocyclic Sulfamates in SNO-OCTs. *J. Am. Chem. Soc.* **2017,** *139*, 8029-8037.

322. Burke, E. G.; Schomaker, J. M., Synthetic Applications of Flexible SNO-OCT Strained Alkynes and Their Use in Postpolymerization Modifications. *J. Org. Chem.* **2017,** *82*, 9038-9046.

323. Yun, H.; Jessica M., R.; Henry R., K.; Amirah Mat, L.; Ronald, R.; Jennifer, S., Triple, Mutually Orthogonal Cycloadditions Through the Design of Electronically Activated SNO-OCTs. *J. Am. Chem. Soc.* **2020**, *142*, 18826-18835.

324. Hu, Y.; Roberts, J. M.; Kilgore, H.; Lani, A. M.; Raines, R.; Schomaker, J. Triple, Mutually Orthogonal Cycloadditions Through the Design of Electronically Activated SNO-OCTs. *J. Am. Chem. Soc. 142*, 18826-18835.

325. de Almeida, G.; Sletten, E. M.; Nakamura, H.; Palaniappan, K. K.; Bertozzi, C. R., Thiacycloalkynes for Copper-free Click Chemistry. *Angew. Chem., Int. Ed.* **2012,** *51*, 2443-2447.

326. Chenoweth, K.; Chenoweth, D.; Goddard, W. A., Cyclooctyne-based Reagents for Uncatalyzed Click Chemistry: A Computational Survey. *Org. Biomol. Chem.* **2009,** *7*, 5255-5258.

327. Gordon, C. G.; Mackey, J. L.; Jewett, J. C.; Sletten, E. M.; Houk, K. N.; Bertozzi, C. R., Reactivity of Biarylazacyclooctynones in Copper-free Click Chemistry. *J. Am. Chem. Soc.* **2012,** *134*, 9199-9208.

328. van Geel, R.; Pruijn, G. J.; van Delft, F. L.; Boelens, W. C., Preventing Thiol-yne Addition Improves the Specificity of Strain-promoted Azide-Alkyne Cycloaddition. *Bioconjugate Chem.* **2012,** *23*, 392-398.

329. Sletten, E. M.; Nakamura, H.; Jewett, J. C.; Bertozzi, C. R., Difluorobenzocyclooctyne: Synthesis, Reactivity, and Stabilization by β-cyclodextrin. *J. Am. Chem. Soc.* **2010,** *132*, 11799-11805.

330. Krebs, A.; Wilke, J. In *Angle strained cycloalkynes*, Berlin, Heidelberg, Springer Berlin Heidelberg: Berlin, Heidelberg, 1983; pp 189-233.

331. Chapman, O. L.; Gano, J.; West, P. R.; Regitz, M.; Maas, G., Acenaphthyne. *J. Am. Chem. Soc.* **1981,** *103*, 7033-7036.

332. Dehmlow, E. V.; Neuhaus, R.; Schell, H. G., Cyclopropenonchemie, X. 2-Alkoxy-3-alkylcyclopropenone. *Chem. Ber.* **1988,** *121*, 569-571.

333. Urdabayev, N. K.; Poloukhtine, A.; Popik, V. V., Two-photon Induced Photodecarbonylation Reaction of Cyclopropenones. *Chem. Commun.* **2006,** 454-456.

334. Poloukhtine, A. A.; Mbua, N. E.; Wolfert, M. A.; Boons, G. J.; Popik, V. V., Selective Labeling of Living Cells by a Photo-triggered Click Reaction. *J. Am. Chem. Soc.* **2009,** *131*, 15769-15776.

335. Martinek, M.; Filipova, L.; Galeta, J.; Ludvikova, L.; Klan, P., Photochemical Formation of Dibenzosilacyclohept-4-yne for Cu-Free Click Chemistry with Azides and 1,2,4,5-Tetrazines. *Org. Lett.* **2016,** *18*, 4892-4895.

336. Sutton, D. A.; Popik, V. V., Sequential Photochemistry of Dibenzo[a,e]dicyclopropa[c,g][8]annulene-1,6-dione: Selective Formation of Didehydrodibenzo[a,e][8]annulenes with Ultrafast SPAAC Reactivity. *J. Org. Chem.* **2016,** *81*, 8850-8857.

337. Kii, I.; Shiraishi, A.; Hiramatsu, T.; Matsushita, T.; Uekusa, H.; Yoshida, S.; Yamamoto, M.; Kudo, A.; Hagiwara, M.; Hosoya, T., Strain-promoted Double-click Reaction for Chemical Modification of Azido-biomolecules. *Org. Biomol. Chem.* **2010**, *8*, 4051-4055.

338. Smith, R. H.; Wladkowski, B. D.; Taylor, J. E.; Thompson, E. J.; Pruski, B.; Klose, J. R.; Andrews, A. W.; Michejda, C. J., Acid-catalyzed Decomposition of 1-Alkyltriazolines: A Mechanistic Study. *J. Org. Chem.* **1993,** *58*, 2097-2103.

339. Shea, K. J.; Kim, J. S., Influence of Strain on Chemical Reactivity. Relative Reactivity of Torsionally Strained Double Bonds in 1,3-Dipolar Cycloadditions. *J. Am. Chem. Soc.* **1992,** *114*, 4846-4855.

340. Gattner, M. J.; Ehrlich, M.; Vrabel, M., Sulfonyl Azide-Mediated Norbornene Aziridination for Orthogonal Peptide and Protein Labeling. *Chem. Commun.* **2014,** *50*, 12568-12571.

341. Margison, K. D.; Bilodeau, D. A.; Mahmoudi, F.; Pezacki, J. P., Cycloadditions of Trans-Cyclooctenes and Nitrones as Tools for Bioorthogonal Labelling. *ChemBioChem* **2020,** *21*, 948-951.

342. Gutsmiedl, K.; Wirges, C. T.; Ehmke, V.; Carell, T., Copper-Free "Click" Modification of DNA via Nitrile Oxide-norbornene 1,3-Dipolar Cycloaddition. *Org. Lett.* **2009,** *11*, 2405-2408.

343. Gutsmiedl, K.; Fazio, D.; Carell, T., High-density DNA Functionalization by a Combination of Cu-catalyzed and Cu-free Click Chemistry. *Chem. Eur. J.* **2010,** *16*, 6877-6883.

344. van Berkel, S. S.; Dirks, A. T.; Debets, M. F.; van Delft, F. L.; Cornelissen, J. J.; Nolte, R. J.; Rutjes, F. P., Metal-free Triazole Formation as a Tool for Bioconjugation. *ChemBioChem* **2007,** *8*, 1504-1508.

345. Hamzehloueian, M.; Hosseinzadeh, R.; Ghandiyar, S., A Theoretical Study on the Metal-free Triazole Formation through Tandem [3+2] Cycloaddition/Retro-Diels-Alder Reaction of Benzyl Azide and Oxanorbornadienedicarboxylate. *J. Mol. Graph. Model.* **2020,** *97*, 107552-107559.

346. Matikonda, S. S.; Orsi, D. L.; Staudacher, V.; Jenkins, I. A.; Fiedler, F.; Chen, J.; Gamble, A. B., Bioorthogonal Prodrug Activation Driven by a Strain-promoted 1,3-Dipolar Cycloaddition. *Chem. Sci.* **2015,** *6*, 1212-1218.

347. Carl, P. L.; Chakravarty, P. K.; Katzenellenbogen, J. A., A Novel Connector Linkage Applicable in Prodrug Design. *J. Med. Chem.* **1981,** *24*, 479-480.

348. Alouane, A.; Labruere, R.; Le Saux, T.; Schmidt, F.; Jullien, L., Self-immolative Spacers: Kinetic Aspects, Structure-Property Relationships, and Applications. *Angew. Chem., Int. Ed.* **2015,** *54*, 7492-7509.

349. Matikonda, S. S.; Fairhall, J. M.; Fiedler, F.; Sanhajariya, S.; Tucker, R. A. J.; Hook, S.; Garden, A. L.; Gamble, A. B., Mechanistic Evaluation of Bioorthogonal Decaging with trans-Cyclooctene: The Effect of Fluorine Substituents on Aryl Azide Reactivity and Decaging from the 1,2,3-Triazoline. *Bioconjugate Chem.* **2018,** *29*, 324-334.

350. Fairhall, J. M.; Murayasu, M.; Dadhwal, S.; Hook, S.; Gamble, A. B., Tuning activation and Self-immolative Properties of the Bioorthogonal Alkene-Azide Click-and-Release Strategy. *Org. Biomol. Chem.* **2020,** *18*, 4754-4762.

351. Mosey, R. A.; Floreancig, P. E., Versatile Approach to α-Alkoxy Carbamate Synthesis and Stimulus-responsive Alcohol Release. *Org. Biomol. Chem.* **2012,** *10*, 7980-7985.

352. Hay, M. P.; Sykes, B. M.; Denny, W. A.; O'Connor, C. J., Substituent Effects on the Kinetics of Reductively-initiated Fragmentation of Nitrobenzyl Carbamates Designed as Triggers for Bioreductive Prodrugs. *J. Chem. Soc. Perkin Trans. 1* **1999,** 2759-2770.

353. Hladikova, V.; Vana, J.; Hanusek, J., [3 + 2]-Cycloaddition Reaction of Sydnones with Alkynes. *Beilstein J. Org. Chem.* **2018,** *14*, 1317-1348.

354. Bernard, S.; Audisio, D.; Riomet, M.; Bregant, S.; Sallustrau, A.; Plougastel, L.; Decuypere, E.; Gabillet, S.; Kumar, R. A.; Elyian, J.; Trinh, M. N.; Koniev, O.; Wagner, A.; Kolodych, S.; Taran, F., Bioorthogonal Click and Release Reaction of Iminosydnones with Cycloalkynes. *Angew. Chem., Int. Ed.* **2017,** *56*, 15612-15616.

355. Riomet, M.; Decuypere, E.; Porte, K.; Bernard, S.; Plougastel, L.; Kolodych, S.; Audisio, D.; Taran, F., Design and Synthesis of Iminosydnones for Fast Click and Release Reactions with Cycloalkynes. *Chem. Eur. J.* **2018,** *24*, 8535-8541.

356. Shao, Z.; Liu, W.; Tao, H.; Liu, F.; Zeng, R.; Champagne, P. A.; Cao, Y.; Houk, K. N.; Liang, Y., Bioorthogonal Release of Sulfonamides and Mutually Orthogonal Liberation of Two Drugs. *Chem. Commun.* **2018,** *54*, 14089-14092.

357. Staudinger, H.; Meyer, J., Über neue organische Phosphorverbindungen III. Phosphinmethylenderivate und Phosphinimine. *Helv. Chim. Acta* **1919,** *2*, 635-646.

358. Palacios, F.; Alonso, C.; Aparicio, D.; Rubiales, G.; de los Santos, J. M., The aza-Wittig Reaction: an Efficient Tool for the Construction of Carbon–Nitrogen Double Bonds. *Tetrahedron* **2007,** *63*, 523-575.

359. Leffler, J. E.; Temple, R. D., Staudinger Reaction between Triarylphosphines and Azides. Mechanism. *J. Am. Chem. Soc.* **1967,** *89*, 5235-5246.

360. Pyun, S. Y.; Lee, Y.; Kim, T. R., Mechanism of the Hydrolysis of N-Aryliminotriphenylphosphoranes. *Kinet. Catal.* **2005,** *46*, 21-28.

361. Widauer, C.; Grutzmacher, H.; Shevchenko, I.; Gramlich, V., Insights into the Staudinger Reaction: Experimental and Theoretical Studies on the Stabilization of cis-Phosphazides. *Eur. J. Inorg. Chem.* **1999**, 1659-1664.

362. Alajarin, M.; Conesa, C.; Rzepa, H. S., Ab initio SCF-MO Study of the Staudinger Phosphorylation Reaction between a Phosphane and an Azide to form a Phosphazene. *J. Chem. Soc., Perkin Trans. 2* **1999**, 1811-1814.

363. Bebbington, M. W. P.; Bourissou, D., Stabilised Phosphazides. *Coord. Chem. Rev.* **2009,** *253*, 1248-1261.

364. Fortman, G. C.; Captain, B.; Hoff, C. D., Thermodynamic Investigations of the Staudinger Reaction of Trialkylphosphines with 1-Adamantyl Azide and the Isolation of an Unusual s-cis Phosphazide. *Inorg. Chem.* **2009,** *48*, 1808-1810.

365. Temple, R. D.; Leffler, J. E., The Dispersion of Substituent Effects in Organophosphorus Compounds. *Tetrahedron Lett.* **1968,** *15*, 1893-1898.

366. Gololobov, Y.; Kasukhin, L.; Ponomarchuk, M.; Klepa, T.; Yurchenko, R., Inductive and Steric Effects in the Staudinger Reaction. *Phosphorous Sulfur Rel. Elem.* **1981,** *10*, 339-341.

367. Maric, T.; Mikhaylov, G.; Khodakivskyi, P.; Bazhin, A.; Sinisi, R.; Bonhoure, N.; Yevtodiyenko, A.; Jones, A.; Muhunthan, V.; Abdelhady, G.; Shackelford, D.; Goun, E., Bioluminescent-based Imaging and Quantification of Glucose Uptake in vivo. *Nat. Methods* **2019,** *16*, 526-532.

368. Tsuno, Y.; Leffler, J. E., Some Decomposition Reactions of Acid Azides. *J. Org. Chem.* **1963,** *28*, 902-906.

369. Meguro, T.; Yoshida, S.; Hosoya, T., Aromatic Azido-selective Reduction via the Staudinger Reaction Using Tri-n-butylphosphonium Tetrafluoroborate with Triethylamine. *Chem. Lett.* **2017,** *46*, 473-476.

370. Vaultier, M.; Knouzi, N.; Carrie, R., Reduction d'azides en amines primaires par methode generale utilisant la reaction de Staudinger. *Tetrahedron Lett.* **1983,** *24*, 763-764.

371. Kohyama, A.; Koresawa, E.; Tsuge, K.; Matsuya, Y., Facile o-Quinodimethane Formation from Benzocyclobutenes Triggered by the Staudinger Reaction at Ambient Temperature. *Chem. Commun.* **2019,** *55*, 6205-6208.

372. Lin, F. L.; Hoyt, H. M.; van Halbeek, H.; Bergman, R. G.; Bertozzi, C. R., Mechanistic Investigation of the Staudinger Ligation. *J. Am. Chem. Soc.* **2005,** *127*, 2686-2695.

373. Stewart, B.; Harriman, A.; Higham, L. J., Predicting the Air Stability of Phosphines. *Organometallics* **2011,** *30*, 5338-5343.

374. Pianowski, Z.; Gorska, K.; Oswald, L.; Merten, C. A.; Winssinger, N., Imaging of mRNA in Live Cells Using Nucleic Acid-templated Reduction of Azidorhodamine Probes. *J. Am. Chem. Soc.* **2009,** *131*, 6492-6497.

375. Franzini, R. M.; Kool, E. T., Efficient Nucleic Acid Detection by Templated Reductive Quencher Release. *J. Am. Chem. Soc.* **2009,** *131*, 16021-16023.

376. Harcourt, E. M.; Kool, E. T., Amplified microRNA Detection by Templated Chemistry. *Nucleic Acids Res.* **2012,** *40*, e65.

377. Meguro, T.; Terashima, N.; Ito, H.; Koike, Y.; Kii, I.; Yoshida, S.; Hosoya, T., Staudinger Reaction Using 2,6-Dichlorophenyl Azide Derivatives for Robust aza-Ylide Formation Applicable to Bioconjugation in Living Cells. *Chem. Commun.* **2018,** *54*, 7904-7907.

378. Sundhoro, M.; Park, J.; Wu, B.; Yan, M., Synthesis of Polyphosphazenes by a Fast Perfluoroaryl Azide-mediated Staudinger Reaction. *Macromolecules* **2018,** *51*, 4532-4540.

379. Xie, Y.; Cheng, L.; Gao, Y.; Cai, X.; Yang, X.; Yi, L.; Xi, Z., Tetrafluorination of Aromatic Azide Yields a Highly Efficient Staudinger Reaction: Kinetics and Biolabeling. *Chem. Asian J.* **2018,** *13*, 1791-1796.

380. Zhang, J.; Gao, Y.; Kang, X.; Zhu, Z.; Wang, Z.; Xi, Z.; Yi, L., o,o-Difluorination of Aromatic Azide Yields a Fast-response Fluorescent Probe for H_2S Detection and for Improved Bioorthogonal Reactions. *Org. Biomol. Chem.* **2017,** *15*, 4212-4217.

381. Sundhoro, M.; Jeon, S.; Park, J.; Ramstrom, O.; Yan, M., Perfluoroaryl Azide Staudinger Reaction: A Fast and Bioorthogonal Reaction. *Angew. Chem., Int. Ed.* **2017,** *56*, 12117-12121.

382. Saito, F.; Noda, H.; Bode, J. W., Critical Evaluation and Rate Constants of Chemoselective Ligation Reactions for Stoichiometric Conjugations in Water. *ACS Chem. Biol.* **2015,** *10*, 1026-1033.

383. Cartwright, I. L.; Hutchinson, D. W.; Armstrong, V. W., The Reaction between Thiols and 8-Azidoadenosine Derivatives. *Nucleic Acids Res.* **1976,** *3*, 2331-2340.

384. Lin, V. S.; Chen, W.; Xian, M.; Chang, C. J., Chemical Probes for Molecular Imaging and Detection of Hydrogen Sulfide and Reactive Sulfur Species in Biological Systems. *Chem. Soc. Rev.* **2015,** *44*, 4596-4618.

385. Fang, Q.; Xiong, H.; Yang, L.; Wang, B.; Song, X., An Instantaneous Fluorescent Probe for Detecting Hydrogen Sulfide in Biological Systems. *New J. Chem.* **2019,** *43*, 13594-13599.

386. Gololobov, Y., Sixty Years of Staudinger Reaction. *Tetrahedron* **1981,** *37*, 437-472.

387. Molina, P.; Lopez-Leandro, C.; Llamas-Botia, J.; Foces-Foces, C.; Fernandez-Castano, C., Unexpected Staudinger Reaction of α-Azidoacetonitriles α-Phenyl Substituted with Triphenylphosphine. Preparation, X-ray Crystal and Molecular Structures of a Phosphazine, an Aminophosphonium Carbanion Salt and a Phosphazide, with (Z)-Configuration. *Tetrahedron* **1996,** *52*, 9629-9642.

388. Meguro, T.; Yoshida, S.; Igawa, K.; Tomooka, K.; Hosoya, T., Transient Protection of Organic Azides from Click Reactions with Alkynes by Phosphazide Formation. *Org. Lett.* **2018,** *20*, 4126-4130.

389. Li, H.; Franzini, R. M.; Bruner, C.; Kool, E. T., Templated Chemistry for Sequence-specific Fluorogenic Detection of Duplex DNA. *ChemBioChem* **2010,** *11*, 2132-2137.

390. Abe, H.; Wang, J.; Furukawa, K.; Oki, K.; Uda, M.; Tsuneda, S.; Ito, Y., A Reduction-triggered Fluorescence Probe for Sensing Nucleic Acids. *Bioconjugate Chem.* **2008,** *19*, 1219-1226.

391. Hansch, C.; Leo, A.; Taft, R. W., A Survey of Hammett Substituent Constants and Resonance and Field Parameters. *Chem. Rev.* **1991,** *91*, 165-195.

392. Shibata, A.; Abe, H.; Ito, Y., Oligonucleotide-templated Reactions for Sensing Nucleic Acids. *Molecules* **2012,** *17*, 2446-2463.

393. Sando, S.; Kool, E. T., Quencher as Leaving Group: Efficient Detection of DNA-joining Reactions. *J. Am. Chem. Soc.* **2002,** *124*, 2096-2097.

394. Abe, H.; Kool, E. T., Destabilizing Universal Linkers for Signal Amplification in Self-ligating Probes for RNA. *J. Am. Chem. Soc.* **2004,** *126*, 13980-13986.

395. Ackermann, M.; Pascariu, A.; Hocher, T.; Siehl, H. U.; Berger, S., Electronic Properties of Furyl Substituents at Phosphorus and their Influence on ^{31}P NMR Chemical Shifts. *J. Am. Chem. Soc.* **2006,** *128*, 8434-8440.

396. Baker, N. D.; Griffin, R. J.; Irwin, W. J.; Slack, J. A., The Reduction of Aryl Azides by Dithiothreitol: A Model for Bioreduction of Aromatic Azido-substituted Drugs. *Int. J. Pharmaceutics* **1989,** *52*, 231-238.

397. Getz, E. B.; Xiao, M.; Chakrabarty, T.; Cooke, R.; Selvin, P. R., A Comparison between the Sulfhydryl Reductants Tris(2-carboxyethyl)phosphine and Dithiothreitol for Use in Protein Biochemistry. *Anal. Biochem.* **1999,** *273*, 73-80.

398. Saneyoshi, H.; Ochikubo, T.; Mashimo, T.; Hatano, K.; Ito, Y.; Abe, H., Triphenylphosphinecarboxamide: An Effective Reagent for the Reduction of Azides and its Application to Nucleic Acid Detection. *Org. Lett.* **2014,** *16*, 30-33.

399. Xie, S.; Sundhoro, M.; Houk, K. N.; Yan, M., Electrophilic Azides for Materials Synthesis and Chemical Biology. *Acc. Chem. Res.* **2020,** *53*, 937-948.

400. Ma, D.; Kang, X.; Gao, Y.; Zhu, J.; Yi, L.; Xi, Z., Design and Synthesis of a Highly Efficient Labelling Reagent for Incorporation of Tetrafluorinated Aromatic Azide into Proteins. *Tetrahedron* **2019,** *75*, 888-893.

401. Cheng, L.; Kang, X.; Wang, D.; Gao, Y.; Yi, L.; Xi, Z., The One-pot Nonhydrolysis Staudinger Reaction and Staudinger or SPAAC Ligation. *Org. Biomol. Chem.* **2019,** *17*, 5675-5679.

402. Ndugire, W.; Wu, B.; Yan, M., Synthesis of Carbohydrate-Grafted Glycopolymers Using a Catalyst-Free, Perfluoroarylazide-Mediated Fast Staudinger Reaction. *Molecules* **2019,** *24*, 157-168.

403. Shalev, D. E.; Chiacchiera, S. M.; Radkowsky, A. E.; Kosower, E. M., Sequence of Reactant Combination Alters the Course of the Staudinger Reaction of Azides with Acyl Derivatives. Bimanes. *J. Org. Chem.* **1996,** *61*, 1689-1701.

404. Bures, J.; Martin, M.; Urpi, F.; Vilarrasa, J., Catalytic Staudinger-Vilarrasa Reaction for the Direct Ligation of Carboxylic Acids and Azides. *J. Org. Chem.* **2009,** *74*, 2203-2206.

405. Garcia, J.; Urpi, F.; Vilarrasa, J., New Synthetic "Tricks". Triphenylphosphine-mediated Amide Formation from Carboxylic Acids and Azides. *Tetrahedron Lett.* **1984,** *25*, 4841-4844.

406. Urpi, F.; Vilarrasa, J., New Synthetic 'Tricks'. Advantages of Using Triethylphosphine in some Phosphorus-based Reactions. *Tetrahedron Lett.* **1986,** *27*, 4623-4624.

407. Saxon, E.; Bertozzi, C. R., Cell Surface Engineering by a Modified Staudinger Reaction. *Science* **2000,** *287*, 2007-2010.

408. Saxon, E.; Luchansky, S. J.; Hang, H. C.; Yu, C.; Lee, S. C.; Bertozzi, C. R., Investigating Cellular Metabolism of Synthetic Azidosugars with the Staudinger Ligation. *J. Am. Chem. Soc.* **2002,** *124*, 14893-14902.

409. Prescher, J. A.; Dube, D. H.; Bertozzi, C. R., Chemical Remodelling of Cell Surfaces in Living Animals. *Nature* **2004,** *430*, 873-877.

410. Park, C. M.; Niu, W.; Liu, C.; Biggs, T. D.; Guo, J.; Xian, M., A Proline-based Phosphine Template for Staudinger Ligation. *Org. Lett.* **2012,** *14*, 4694-4697.

411. Ren, G.; Zheng, Q.; Wang, H., Aryl Fluorosulfate Trapped Staudinger Reduction. *Org. Lett.* **2017,** *19*, 1582-1585.

412. Restituyo, J. A.; Comstock, L. R.; Petersen, S. G.; Stringfellow, T.; Rajski, S. R., Conversion of Aryl Azides to O-Alkyl Imidates via Modified Staudinger Ligation. *Org. Lett.* **2003,** *5*, 4357-4360.

413. Soellner, M. B.; Nilsson, B. L.; Raines, R. T., Reaction Mechanism and Kinetics of the Traceless Staudinger Ligation. *J. Am. Chem. Soc.* **2006,** *128*, 8820-8828.

414. Back, J. W.; David, O.; Kramer, G.; Masson, G.; Kasper, P. T.; de Koning, L. J.; de Jong, L.; van Maarseveen, J. H.; de Koster, C. G., Mild and Chemoselective Peptide-bond Cleavage of Peptides and Proteins at Azido Homoalanine. *Angew. Chem., Int. Ed.* **2005,** *44*, 7946-7950.

415. Nilsson, B. L.; Soellner, M. B.; Raines, R. T., Chemical Synthesis of Proteins. *Annu. Rev. Biophys. Biomol. Struct.* **2005,** *34*, 91-118.

416. Nilsson, B. L.; Kiessling, L. L.; Raines, R. T., Staudinger Ligation: A Peptide from a Thioester and Azide. *Org. Lett.* **2000,** *2*, 1939-1941.

417. Nilsson, B. L.; Kiessling, L. L.; Raines, R. T., High-yielding Staudinger Ligation of a Phosphinothioester and Azide to form a Peptide. *Org. Lett.* **2001,** *3*, 9-12.

418. Saxon, E.; Armstrong, J. I.; Bertozzi, C. R., A "Traceless" Staudinger Ligation for the Chemoselective Synthesis of Amide Bonds. *Org. Lett.* **2000,** *2*, 2141-2143.

419. Tam, A.; Raines, R. T., Coulombic Effects on the Traceless Staudinger Ligation in Water. *Bioorg. Med. Chem.* **2009,** *17*, 1055-1063.

420. Tam, A.; Soellner, M. B.; Raines, R. T., Water-soluble Phosphinothiols for Traceless Staudinger Ligation and Integration with Expressed Protein Ligation. *J. Am. Chem. Soc.* **2007,** *129*, 11421-11430.

421. Tam, A.; Soellner, M. B.; Raines, R. T., Electronic and Steric Effects on the Rate of the Traceless Staudinger Ligation. *Org. Biomol. Chem.* **2008,** *6*, 1173-1175.

422. Nepomniaschiy, N.; Grimminger, V.; Cohen, A.; DiGiovanni, S.; Lashuel, H. A.; Brik, A., Switch Peptide via Staudinger Reaction. *Org. Lett.* **2008,** *10*, 5243-5246.

423. Lohani, C. R.; Soley, J.; Kralt, B.; Palmer, M.; Taylor, S. D., α-Azido Esters in Depsipeptide Synthesis: C-O Bond Cleavage during Azido Group Reduction. *J. Org. Chem.* **2016,** *81*, 11831-11840.

424. Taylor, S. D.; Lohani, C. R., A Fresh Look at the Staudinger Reaction on Azido Esters: Formation of 2H-1,2,3-Triazol-4-ols from alpha-Azido Esters Using Trialkyl Phosphines. *Org. Lett.* **2016,** *18*, 4412-4415.

425. Chou, H. H.; Raines, R. T., Conversion of Azides into Diazo Compounds in Water. *J. Am. Chem. Soc.* **2013,** *135*, 14936-14939.

426. Mix, K. A.; Aronoff, M. R.; Raines, R. T., Diazo Compounds: Versatile Tools for Chemical Biology. *ACS Chem. Biol.* **2016,** *11*, 3233-3244.

427. Chaturvedi, R. K.; Pletcher, T. C.; Zioudrou, C.; Schmir, G. L., The Hydrolysis of an Iminophosphorane. Evidence for an Intermediate. *Tetrahedron Lett.* **1970,** *11*, 4339-4342.

428. Serwa, R.; Wilkening, I.; Del Signore, G.; Muhlberg, M.; Claussnitzer, I.; Weise, C.; Gerrits, M.; Hackenberger, C. P., Chemoselective Staudinger-phosphite Reaction of Azides for the Phosphorylation of Proteins. *Angew. Chem., Int. Ed.* **2009,** *48*, 8234-8239.

429. Bohrsch, V.; Serwa, R.; Majkut, P.; Krause, E.; Hackenberger, C. P., Site-specific Functionalisation of Proteins by a Staudinger-type Reaction Using Unsymmetrical Phosphites. *Chem. Commun.* **2010,** *46*, 3176-3178.

430. Nischan, N.; Kasper, M. A.; Mathew, T.; Hackenberger, C. P., Bis(arylmethyl)-substituted Unsymmetrical Phosphites for the Synthesis of Lipidated Peptides via Staudinger-phosphite Reactions. *Org. Biomol. Chem.* **2016,** *14*, 7500-7508.

431. Vallee, M. R.; Majkut, P.; Krause, D.; Gerrits, M.; Hackenberger, C. P., Chemoselective Bioconjugation of Triazole Phosphonites in Aqueous Media. *Chem. Eur. J.* **2015,** *21*, 970-974.

432. Vallee, M. R.; Majkut, P.; Wilkening, I.; Weise, C.; Muller, G.; Hackenberger, C. P., Staudinger-phosphonite Reactions for the Chemoselective Transformation of Azido-containing Peptides and Proteins. *Org. Lett.* **2011,** *13*, 5440-5443.

433. Uzagare, M. C.; Claussnitzer, I.; Gerrits, M.; Bannwarth, W., A Novel Method for the Labelling of Peptides and Proteins through a Bioorthogonal Staudinger Reaction by Using 2-Cyanoethyl Phosphoramidites. *ChemBioChem* **2012,** *13*, 2204-2208.

434. Amyes, T. L.; Jencks, W. P., Lifetimes of Oxocarbenium Ions in Aqueous Solution from Common Ion Inhibition of the Solvolysis of α-Azido Ethers by Added Azide Ion. *J. Am. Chem. Soc.* **1989,** *111*, 7888-7900.

435. Loubinoux, B.; Tabbache, S.; Gerardin, P.; Miazimbakana, J., Protection des phenols par le groupement azidomethylene application a la synthese de phenols instables. *Tetrahedron* **1988,** *44*, 6055-6064.

436. Pothukanuri, S.; Winssinger, N., A Highly Efficient Azide-based Protecting Group for Amines and Alcohols. *Org. Lett.* **2007,** *9*, 2223-2225.

437. Li, H., Franzini, R. M., Bruner, C., Kool, E. T. Templated Chemistry for Sequence-Specific Fluorogenic Detection of Duplex DNA. *ChemBioChem* **2010,** *11*, 2132-2137.

438. Franzini, R. M.; Kool, E. T., Two Successive Reactions on a DNA Template: A Strategy for Improving Background Fluorescence and Specificity in Nucleic Acid Detection. *Chem. Eur. J.* **2011,** *17*, 2168-2175.

439. Griffin, R. J.; Evers, E.; Davison, R.; Gibson, A. E.; Layton, D.; Irwin, W. J., The 4-Azidobenzyloxycarbonyl Function; Application as a Novel Protecting Group and Potential Prodrug Modification for Amines. *J. Chem. Soc. Perkin Trans.* **1996,** 1205-1211.

440. Loubinoux, B.; Gerardin, P., Protection of Amines with the 4-Azidomethylenoxybenzyloxycarbonyl Group. *Tetrahedron Lett.* **1988,** *32*, 351-354.

441. Oppolzer, W., Intramolecular Cycloaddition Reactions of ortho-Quinodimethanes in Organic Synthesis. *Synthesis* **1978,** 793-802.

442. Azoulay, M.; Tuffin, G.; Sallem, W.; Florent, J. C., A New Drug-release Method Using the Staudinger Ligation. *Bioorg. Med. Chem. Lett.* **2006,** *16*, 3147-3149.

443. Balasubramanian, S., Sequencing Nucleic Acids: From Chemistry to Medicine. *Chem. Commun.* **2011,** *47*, 7281-7286.